Downloaded from orbit.dtu.dk on: Nov 08, 2017

Technical University of Denmark

Development and Operation of Decentralized Ventilation for Indoor Climate and Energy Performance

Smith, Kevin Michael; Svendsen, Svend

Publication date:
2015

Document Version
Publisher's PDF, also known as Version of record

Link back to DTU Orbit

Citation (APA):
Smith, K. M., & Svendsen, S. (2015). Development and Operation of Decentralized Ventilation for Indoor Climate and Energy Performance. Technical University of Denmark, Department of Civil Engineering.

DTU Library
Technical Information Center of Denmark

General rights
Copyright and moral rights for the publications made accessible in the public portal are retained by the authors and/or other copyright owners and it is a condition of accessing publications that users recognise and abide by the legal requirements associated with these rights.

- Users may download and print one copy of any publication from the public portal for the purpose of private study or research.
- You may not further distribute the material or use it for any profit-making activity or commercial gain
- You may freely distribute the URL identifying the publication in the public portal

If you believe that this document breaches copyright please contact us providing details, and we will remove access to the work immediately and investigate your claim.

Development and Operation of Decentralized Ventilation for Indoor Climate and Energy Performance

Kevin Michael Smith

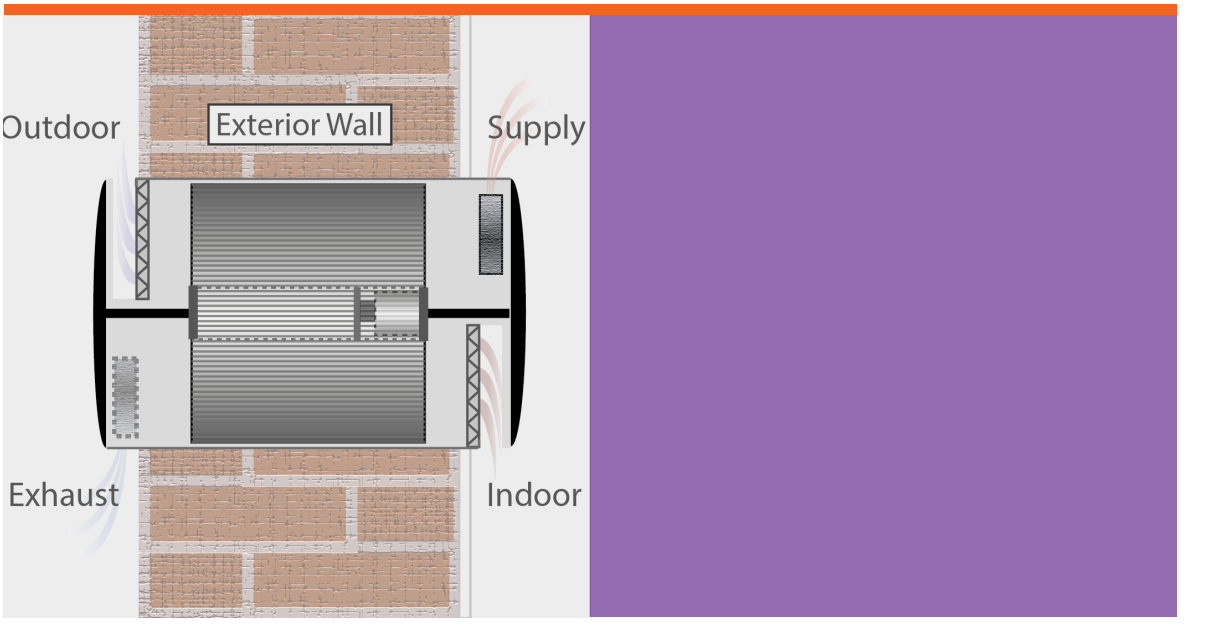

DTU Civil Engineering Report R-334

DTU Civil Engineering
Department of Civil Engineering

Development and Operation of Decentralized Ventilation for Indoor Climate and Energy Performance

Kevin Michael Smith

PhD Thesis

Department of Civil Engineering

2015

Supervisor:

Professor Svend Svendsen, Civil Engineering, DTU, Denmark

Assessment Committee:

Professor Toke R. Nielsen, Civil Engineering, DTU, Denmark

Associate Professor Dennis Johansson, Building Services Engineering, Lund University, Sweden

Christian Drivsholm, Energy Efficiency & Ventilation, Technological Institute, Denmark

Development and Operation of Decentralized Ventilation for Indoor Climate and Energy Performance

Copyright: © 2015 by Kevin Michael Smith

Publisher: Department of Civil Engineering,
Technical University of Denmark,
Brovej, building 118, 2800
Kgs. Lyngby, Denmark

ISBN: 9788778774286

ISSN: 1601-2917

Report: BYG R-334

Preface

This thesis is submitted as partial fulfilment of the requirements for a Doctorate of Philosophy at the Technical University of Denmark, Department of Civil Engineering. The thesis is the result of nearly four years of research on the development and implementation of room-based ventilation for renovated apartments in Denmark.

I would first like to thank my supervisor, Professor Svend Svendsen, for his extremely valuable guidance and expertise. His obvious concern for my best interests opened all lines of communication, and his faith in my abilities empowered me to persevere through every challenge and obstacle.

I would like to express my heartfelt thanks to my friend and colleague, Doctor Maria Harrestrup, who believed in me and supported me at every turn. Not enough can be said about the quality of friendship she provided, which helped me reach this point. This and her professional help were absolutely integral to the success of this PhD.

Of course this PhD study would not have been possible without partial funding from the Innovation Fund (Fornyelsesfonden) and the Technical University of Denmark, so I express my sincerest thanks for their enormous contributions. It was always a delight to work on this collaborative project, and I am grateful to everyone who participated. I would like to give special thanks to Christian Niepoort, Henning Solfeldt, Torben Kirkholt, Hasse Brønnum, and Anders L. Jansen.

I would also like to thank Doctor Michael Wetter for hosting me at Lawrence Berkeley National Laboratory and for his incredible insight into building simulation tools. It was inspiring to work with him.

I would like to thank all my colleagues for providing a friendly and productive atmosphere throughout my entire PhD study. Their cheerfulness was contagious.

I need to thank my dear friends, Gerard Baron, Tasja Buschhardt, and Laura McNair, for their endless support, generosity, insight, and warmth. I really cannot put into words how incredible they have been.

I unfortunately need to thank a bizarre cast of hapless misfits: Xavi, Nikos, Georgios, Dimitris, Ben, Rasmus, Gustav, JC, Lasse, Thomas, and Anton. Without them I might have finished sooner, but I am grateful for all the fond memories.

To my wonderful family, you led me to this moment. You inspired me to pursue my dream. It took me across the Atlantic and you never questioned it. You supported me every step of the way. When I fell on tough times, you encouraged me to push forward. You believed in me and gave me the power to believe in myself. I strive to emulate your strength, positivity, perspective, and sense of humor. You deserve a thesis more of acknowledgements, but this PhD is already proof of your love and support. This is dedicated to you.

Kevin Smith
Kgs. Lyngby, October 1st, 2015.

Abstract

The Danish government has targeted full reliance on renewable sources of energy for heating and electricity by 2035. Building renovations save energy and offset requirements for renewable supply. A Danish national action plan therefore expects to reduce heating consumption in existing buildings by at least 35% before 2050. Renovations improve airtightness and often require mechanical ventilation with heat recovery. The market will demand flexible cost-effective ventilation solutions and the knowledge and competence for proper implementation. Single-room ventilation provides simple installation, low fan power, and the potential for local heat recovery. This research developed, assessed, and investigated two single-room ventilation units. One development yielded a novel short plastic rotary heat exchanger and another yielded a novel spiral plastic recuperative heat exchanger. Thermal theory guided the selection of a polycarbonate honeycomb rotor with small circular channels for the former and the selection of rolled plastic sheets with planar channels for the latter. Equations predicted their performance with dimensionless groups. Experiments quantified flows and determined temperature efficiencies at several ventilation rates. The methods accounted for heat gains and air leakages with measurements and balance equations.

The measured and modelled temperature efficiencies showed adequate agreement for the rotary unit and exceeded 83% at 7.8 L/s. This result could not directly validate the model due to bypass leakage. All leakages were excessive and should be reduced with proper sealing. Experimental results demonstrated the option to reduce heat recovery by slowing rotational speed. Overall, the first development met preliminary objectives and provided a novel option for heat recovery. The development of the spiral recuperative heat exchanger provided encouraging first results. The heat exchanger provided a corrected supply temperature efficiency of 82.2% at 13.5 L/s. At this flow rate, the total measured pressure drop across the filter and heat exchanger was 40 Pa. The external and internal leakages were roughly 2.7% and 12.1%, respectively, so future prototypes should reduce internal leakage.

Numerical simulations investigated the impact of moisture transfer in the rotary unit. The investigation simulated moisture balance equations with simplified airflows in Matlab. Based on literature, the study assumed that all condensation in the exhaust evaporated into the supply. The simulations evaluated the risk of moisture issues and compared results to recuperative heat recovery and whole-dwelling ventilation. The simulations analyzed the sensitivity of results to moisture production, infiltration rate, heat recovery, and indoor temperature. With typical moisture production, the rotary heat exchanger recovered excessive moisture from kitchens and

bathrooms. The unit was only suitable for single-room ventilation of living rooms and bedrooms. The sensitivity analysis concluded that varying heat recovery or indoor temperature could limit indoor relative humidity in bedrooms and living rooms. The rotary heat exchanger also elevated the minimum relative humidity in each room, which could help to avoid negative health impacts from dryness. A discussion emphasized the potential benefits of selecting heat recovery to match the individual needs of each room.

Numerical simulations also investigated the annual impact of demand-controlled single-room ventilation with heat recovery on indoor climate and energy-use. The simulations used the expected efficiencies for the spiral recuperative unit based on anticipated improvements. Simulations of a renovated apartment in Denmark compared the demand-controlled single-room unit to a whole-dwelling unit. Convention and regulations determined the constant flow rates for the whole-dwelling system, whereas a controller determined flow rates in the single-room units based on sensed values of CO_2, relative humidity, and temperature. Both types of ventilation provided suitable indoor climate. In a comparison, the single-room unit improved or maintained air quality and thermal comfort while consuming less annual energy for fans and space heating. This provided relative savings of 74% and 4-6%, respectively. The results indicated that single-room ventilation with demand-control could provide a viable alternative for renovated apartments in Denmark.

In summation, the research used theory, literature, design criteria, rapid prototyping, and simulations to successfully develop and investigate single-room ventilation with heat recovery and demand control.

Resumé

Den danske regering har en målsætning om udelukkende at benytte vedvarende energiresurser til opvarmning og elforsyning af bygninger i 2035. Når en bygning energirenoveres reduceres energiforbruget, hvilket tilsvarende reducerer produktionen af vedvarende energi. I den danske handlingsplan er målsætningen at indføre besparelser af varmeforbruget i eksisterende bygninger svarende til mindst 35 % i 2050. Renoveringer forbedrer bygningens lufttæthed og kræver derfor ofte mekanisk ventilation med varmegenvinding. Markedet vil efterspørge fleksible kost-effektive ventilationsløsninger samt viden og erfaringer med rigtig implementering. Enkeltrums ventilation muliggør simpel installation, lavt elforbrug og mulighed for lokal varmegenvinding. Dette forskningsprojekt udviklede og analyserede to enkeltrums ventilationsenheder. Den ene med en ny kort roterende plastik varmeveksler, den anden med en ny oprullet (spiral) rekuperativ plastik varmeveksler. Den roterende varmeveksler blev designet med et polykarbonat mønster bestående af små cirkulære kanaler og den rekuperative varmeveksler blev designet med en oprullede plastik plade med plane kanaler. Begge design blev udviklet med udgangspunkt i termiske teorier. Temperaturvirkningsgraden blev bestemt ved forsøg ved forskellige luftstrømme. Metoderne inkluderede varmetilvækst og luftlækager.

De målte og modellerede temperaturvirkningsgrader viste god overensstemmelse for den roterende varmeveksler og havde en virkningsgrad på 83 % ved et flow på 7,8 L/s. Dette resultat kan dog ikke direkte validere modellen på grund af bypass-lækager. Alle lækager var meget store og bør reduceres med tætninger. De eksperimentelle resultater viste at når rotationshastigheden nedsættes reduceres varmegenvindingen. Samlet set opfyldte de første resultater de indledende kravspecifikationer til den nye opbygning af varmeveksleren. Udviklingen af spiral varmeveksleren viste lovende første resultater. Den målte temperaturvirkningsgrad var på 82,2 % ved et flow på 13,5 L/s. Ved samme flow var det totale målte tryktab over filteret og varmeveksleren 40 Pa. Den eksterne og interne lækage var henholdsvis 2,7 % og 12,1 %. Fremtidige prototyper bør reducere den interne lækage.

Påvirkningen af fugttransport i den roterende veksler blev analyseret med numeriske simuleringer. Simuleringerne af fugtbalancerne blev udført med simplificerede luftstrømme i Matlab. Baseret på et litteraturstudie blev det antaget at kondenseringen i udsugningen fordampede og blev optaget i indblæsningsluften. Risikoen for fugtproblemer blev evalueret og sammenlignet med resultater fra den rekuperative varmeveksler samt med ventilation på lejlighedsniveau. Resultaternes følsomhed overfor fugtproduktion, infiltration, varmegenvinding

og rumtemperatur blev analyseret. Ved typiske fugtproduktionsrater regenererede rotationsvarmeveksleren store mængder fugt fra køkken og bad. Ventilationsenheden var derfor kun velegnet til enkeltrumsventilation i opholdsrum og soveværelser. Følsomhedsanalysen konkluderede at varierende varmegenvinding og rumtemperatur kan begrænse relativ fugtighed i soveværelser og opholdsrum. Den roterende varmeveksler hævede derudover den laveste relative fugtighed i hvert rum, hvilket kan eliminere et for tørt indeklima og de relaterede negative sundhedspåvirkninger heraf. En diskussion understreger de potentielle fordele ved at udføre varmevinding på rumbasis.

Ved hjælp af simuleringer blev den årlige påvirkning af indeklimaet og energiforbrug ved behovstyret rumventilation med varmegenvinding analyseret. Simuleringerne blev udført med forventede virkningsgrader for spiral varmeveksleren baseret på forventede forbedringer. Derudover blev en renoveret lejlighed i Danmark simuleret med behovstyret rumventilation og sammenlignet med lejlighedsventilation. Lejlighedsventilation udføres oftest med konstante luftstrømme, hvorimod enkeltrumsventilationen muliggør behovstyret ventilation baseret på målte værdier for CO_2, relativ fugtighed og temperatur. Begge typer af ventilation resulterede i et godt indeklima. Enkeltrumsventilationen forbedrede eller vedligeholdte luftkvaliteten og den termiske komfort samtidig med at det årlige energiforbrug til ventilatorerne og rumvarmen blev reduceret. Dette resulterede i relative besparelser på henholdsvis 74 % og 4-6 %. Resultaterne indikerede at enkeltrumsventilation med behovstyring kan være et funktionsdygtigt alternativ til lejlighedsventilation i Danmark.

Nærværende afhandling har inkluderet teori, litteratur, design kriterier, hurtig udvikling af prototyper samt simuleringer for succesfuldt at kunne udvikle og analysere enkeltrumsventilation med varmegenvinding og behovstyring.

Table of contents

1 Introduction

This chapter provides an introduction to the research topics covered in this dissertation as well as the definition of its aim, scope, and hypotheses. It lastly provides the structure of this thesis.

1.1 Background

The background describes the context for research and development of room-based ventilation, including regulations, indoor air quality, potential efficiency and optimality, and barriers to implementation.

1.1.1 Danish energy targets

In an effort to mitigate anthropogenic climate change, many governments have targeted energy savings to reduce greenhouse gas emissions. The Danish government has targeted full reliance on renewable sources of energy for heating and electricity by 2035. This would stabilize energy prices and assist global efforts against anthropogenic climate change [1]. Building retrofits save energy and offset requirements for renewable supply. In 2012, heating in households accounted for 26% of final energy consumption in Denmark [2], so reduced heating could significantly contribute to energy savings. New construction represents less than 1% of the building stock annually in Europe [3], so it is important to retrofit existing buildings to meet future targets. A Danish national action plan [4] therefore expects to reduce heating consumption in existing buildings by at least 35% before 2050. An assessment by the Danish Building Research Institute provided the basis for these expectations. The assessment [5] also considered a scenario in which renovations improve airtightness and thus require mechanical ventilation with heat recovery. This would further decrease heating consumption and improve indoor climate. To achieve this scenario, the assessment emphasized the need for inexpensive and flexible ventilation systems with heat recovery as well as the necessary knowledge and competence for their proper implementation.

1.1.2 Renovation and air tightness

Building retrofits can improve heat retention by limiting thermal transmittance and air infiltration. Common measures include window replacement, sealing of cracks and orifices, added thermal insulation, and installation of ventilation with heat recovery. Many exhaust systems draw fresh air through the facade, so improved air-tightness leads to poor indoor air quality unless accompanied by mechanical air supply [6]. Ridley *et al.* [7] analyzed the impact of window replacement on the infiltration rate of dwellings and recommended controllable

ventilation to avoid moisture problems and comply with regulations. Some renovations provide fresh air through ducted vents in the façade, but this limits options for heat recovery. Controllable mechanical ventilation should utilize heat recovery to simultaneously improve air quality and reduce heat losses in temperate climates. The investment in heat recovery depends on cost-effectiveness, building regulations, and the extent of each renovation.

Air-to-air heat exchangers require a point of intersection between supply and exhaust, so renovations often mount supply ducts in limited space. Narrowing duct diameter exponentially increases frictional losses. Furthermore, renovations are unique, so the design and specification of ducts requires capital investment. The need to invest in planning before making an informed decision provides an early obstacle to renovation. Even after approval, installations may be labor intensive and temporarily displace occupants.

There are other inherent issues with centralized ventilation systems that do not relate to renovation. These issues include wasted energy from terminal reheating in constant air-volume (CAV) systems, non-optimal ventilation and diffusion determined by cooling load in variable air-volume (VAV) systems, excessive fan power requirements to force air across large pressure drops, duct air leakage and contamination, lack of flexibility for unoccupied zones, and the spread of smoke and other health hazards [8]. Methods for dealing with these issues can be improved, but there may be a limit to this improvement.

1.1.3 Room-based ventilation

To conserve space and reduce energy for ventilation, retrofits may install local ventilation units at the apartment level or in individual rooms. Unfortunately, the technology has not been established to the point of a commonly used name. A broad term for this technology is decentralized ventilation unit (DVU). In Paper 1, the term DVU specifically refers ventilation units for individual rooms. This thesis and Papers 2 and 3 use the terms single-room ventilation unit and room-based ventilation unit instead.

Single-room ventilation units occupy openings or drilled holes in the façade, which can minimize the necessary planning, labor, space, and frictional losses associated with duct installation. Reflecting the latter, the 2010 Danish building regulations set the maximum energy for ventilation at 1000 J/m^3 for single-dwelling systems and 1800 J/m^3 for systems serving multiple dwellings [9]. Single-room units can also limit issues with biological growth in ducts, spread of smoke and fire, and losses due to leakage and thermal transmittance through ducts.

Wulfinghoff argued many of these points in favor of single-room ventilation units and heavily focused on their potential optimality.

1.1.4 Demand Control

If these technologies develop to their potential, they may optimally match demand with supply in individual rooms. Detecting and matching demand is generally described as demand control. As renovations improve the thermal resistance and airtightness of building envelopes, indoor temperatures and pollutant concentrations become increasingly more sensitive to thermal gains and emissions, respectively. Rooms on opposite façades may have conflicting thermal demands, and rooms could have similarly diverse demands for fresh air. Every closed door increases this sensitivity, which incentivizes room-based demand-control. Installers could specify the ventilation units according to room type and size, while sensors and demand-control could ensure optimal comfort and air quality. Product designers could place wired sensors in the exhaust channels, which could allow their affordable usage.

1.1.5 Barriers for room-based ventilation

The implementation of room-based ventilation raises reasonable concerns. The technology is smaller and must provide for a range of conditions, which may yield potential barriers.

1.1.5.1 Efficiency

Many systems achieve efficiency gains from economies of scale. Larger components are typically less expensive to manufacture, assemble, and operate per unit of utility. System designers must weigh these efficiency gains against the potential advantages of decentralization, including optimal service delivery and reduced transmission losses. In renovated apartments, ventilation may exist on various levels. However existing research is inadequate to compare ventilation serving multiple dwellings, single dwellings, and single rooms.

1.1.5.2 Potential Moisture Issues

The basis for the Danish national energy efficiency action plan was a set of future scenarios that would reduce energy consumption of existing buildings. These scenarios assumed that renovations will replace worn out components with modern compliant components. The 2010 Danish building regulations require heat recovery with a temperature efficiency of 70% for ventilation of entire buildings and 80% for single dwellings [9]. The 2020 regulations will increase these requirements to 75% and 85%, respectively [10].

These regulations emphasize heat recovery, but they neglect the potential coupling of heat and moisture. They only discuss moisture transfer in heat exchangers when specifying conditions for testing. Similarly, a detailed guideline on indoor air quality from the World Health Organization recommended heat recovery to simultaneously retain heat and reduce indoor humidity, but it gave no further guidance on moisture transfer in heat exchangers [11]. In highly efficient heat recovery, the exhaust temperatures often decrease below the dew point temperatures of room air, so moisture condenses in the heat exchanger. If the amount of condensation is significant, it is important to know whether it will evaporate, drain, accumulate, or freeze, and the type of heat exchanger can influence this behavior.

There are two categories of air-to-air heat exchangers. These are regenerative and recuperative heat exchangers, which are known as regenerators and recuperators, respectively. Regenerators, such as rotary heat exchangers, intermittently expose airflows to the same medium to store and recover heat, whereas recuperators transfer heat through a membrane between airflows. A recuperator with an impermeable membrane does not transfer moisture. Any condensation on its surfaces must drain from the heat exchanger. Conversely, a regenerator exposes both airflows to the same heat transfer surface, so condensation from exhaust is likely to evaporate into the supply air [12].

Moisture removal is an important aspect of residential ventilation in humid temperate climates. According to the World Health Organization, excess indoor humidity can lead to health issues by promoting mold growth and proliferation of dust mites. It can also lead to structural issues by degrading building materials. Infiltration lowers indoor humidity during the heating season, but its heat loss is excessive, so renovations maximize air tightness. With minimal contributions from infiltration, mechanical ventilation must solely remove sufficient moisture.

In temperate humid climates, the outdoor air is nearly saturated with moisture throughout the heating season. For example, the average relative humidity is 86% from September 16th to May 15th in the 2013 Danish design reference year [13], and the maximum 30-day average is 94%. If a rotary heat exchanger transfers all condensation between airflows, its drying capacity is only the difference in moisture content between the nearly saturated outdoor air and the saturated exhaust air. At low temperatures, the relatively small difference in saturated moisture content may severely limit the drying capacity of mechanical ventilation with a rotary heat exchanger. Figure 1 demonstrates this behavior with psychrometric charts for an uncoated rotary heat exchanger with the average outdoor conditions of 86% relative humidity (RH) and 4°C during the heating season in Denmark. The uncoated rotary heat exchanger has a temperature efficiency of 85% and cools the exhaust air below its dew point temperature for each of the

three indoor relative humidities. If a single-room ventilation unit uses a rotary heat exchanger, it is therefore important to characterize its impact on indoor humidity to ensure its proper implementation.

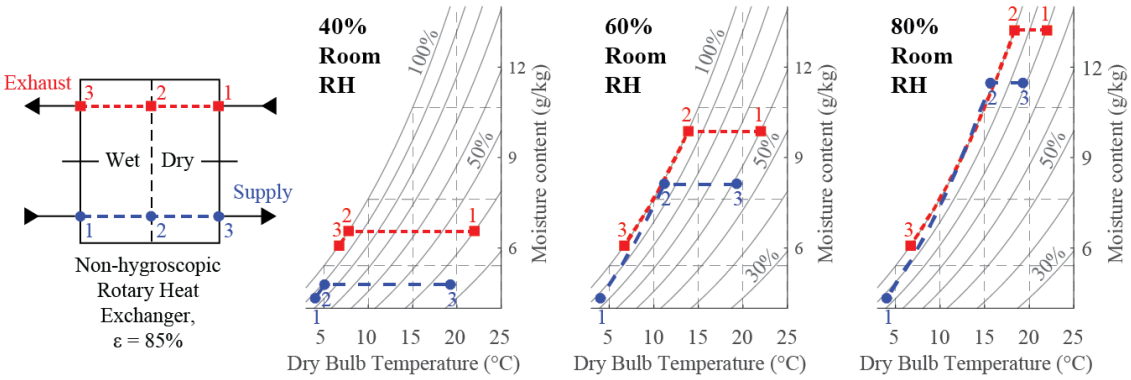

Figure 1. Supply and exhaust airflows through a heat exchanger with 85% temperature efficiency. Outdoor air is 4°C and 86% RH. Room air is 22 °C with three different relative humidities. The dew-point temperature of exhaust air is indicated by the red '2'.

1.2 Aim

This research aimed to develop room-based ventilation for use in renovated apartments in Denmark. Progressing towards effective room-based ventilation offered new opportunities for research that could not be applied to conventional systems. Modelling of unique centralized ventilation systems may be labor-intensive. In contrast, the model of each room-based ventilation unit encompassed all components and applied to all implementations. This provided clear requirements and development criteria for each. Matlab software was simple and flexible, which enabled the intended aims of rapid performance prediction, prototyping, and simplified numerical simulations of these units. Experiments aimed to validate models and expected performance, and simulation tools aimed to predict the impact of implementations in dwellings. An equation-based object-oriented modelling language suited these simulations due to its flexibility and ease of use. This flexibility allowed a simple simulation of a non-standard ventilation system. In contrast, many conventional building simulation tools assume centralized systems with standard heat recovery technologies. These monolithic programs have inflexible structures and cannot simulate innovative systems and controls, such as room-based ventilation with demand-control. This research aimed to demonstrate these capabilities and ultimately improve energy performance and indoor climate of buildings based on these developments and investigations.

1.3 Scope

The scope of this research was limited to early-stage development of room-based ventilation for renovated apartments in Denmark. This included an integrated design process that experimentally tested unit performance and identified potential effects of implementations using simulations. The research may apply to renovated buildings in other humid temperate climates, but this was not the aim of the research.

1.4 Hypotheses

This section provides the main hypothesis and four sub-hypotheses. The essential supposition of each hypothesis or sub-hypothesis is **bolded** for emphasis.

1.4.1 Main hypothesis

The development of decentralized HVAC systems allows cost-effective model-based implementation, including design, rapid prototyping, and advanced control for energy efficiency and indoor climate. This can be demonstrated through model construction and validation, which can then be applied throughout implementation while testing against standard performance benchmarks where applicable. Potential obstacles to implementation, such as excess leakage and moisture transfer, may be simulated to identify the extent of issues and facilitate improvements.

1.4.2 Sub-hypotheses

The research divided the hypothesis into four sub-hypotheses for greater detail and clarity.

1.4.2.1 1st Sub-Hypothesis

The system requirements of a decentralized HVAC unit, as well as its conceptual strengths and weaknesses, can guide an innovative and integrated design process from inception to completion, including multiple generations of prototypes. This is based on theory, regulations, a review of literature, and consideration for demand-control and continuous commissioning in the context of building renovations.

1.4.2.2 2nd Sub-Hypothesis

The modelled and expected performance of decentralized HVAC systems and their individual components can be validated through full-scale testing in a laboratory environment. This is facilitated by established developments that fulfil the 1st Sub-Hypothesis.

1.4.2.3 3rd Sub-Hypothesis

As regenerative heat recovery is commonly used in decentralized ventilation, there exists a knowledge gap regarding its impact on moisture conditions in low-energy residences in humid temperate climates. **Simulations can help to identify potential issues for a range of probable conditions, and a comparison with recuperative heat recovery can guide recommendations for future implementations.**

1.4.2.4 4th Sub-Hypothesis

Recent advances in building simulation tools allow greater abstraction and encapsulation of component models and processes. These tools are based on standardized equation-based object-oriented modelling languages, such as NMF in IDA-ICE or Modelica in Dymola. **This enables modelling of innovative systems, such as decentralized ventilation with heat recovery and advanced control, so simulations can predict and assess their potential.**

1.4.3 Research questions

The main hypothesis answers the following question: Can research guide the development and operation of decentralized ventilation toward future standards of energy efficiency and indoor climate? The research divided this into four separate questions, which corresponded to the four respective sub-hypotheses. Below are the four research questions.

1.4.3.1 1st research question

What set of criteria would guide integrated theoretical development of a room-based ventilation unit to ensure its adequate performance and regulatory compliance in the context of future systems?

1.4.3.2 2nd research question

What experimental methods are able to validate expected performance of room-based ventilation in the early stages of development?

1.4.3.3 3rd research question

Can simulations characterize and assess the impact of moisture transfer in new room-based ventilation units on issues related to indoor humidity?

1.4.3.4 4th research question

Can building simulation tools model innovative systems, such as room-based ventilation with advanced controls, to assess their performance with respect to indoor climate and energy?

1.4.4 Tested sub-hypotheses in papers

The appendices provided three papers that described tests of the sub-hypotheses. Paper 1 describes tests of the 1st and 2nd sub-hypotheses. Paper 2 describes tests of the 3rd sub-hypothesis. Paper 3 describes tests of the 2nd and 4th sub-hypotheses.

1.4.4.1 Paper 1

K.M. Smith, S. Svendsen, Development of a plastic rotary heat exchanger for room-based ventilation in existing apartments, *Energy Build*. 107 (2015) 1–10. doi:10.1016/j.enbuild.2015.07.061

Paper 1 documented the theoretical development of a room-based ventilation unit with a novel plastic rotary heat exchanger. The development determined that a plastic honeycomb with small circular channels provided the required heat transfer and limited longitudinal heat conduction through the unit. This tested the 1st sub-hypothesis, which posited that a set of non-mutually-exclusive criteria could guide a successful integrated design process. Paper 1 also documented the performance of the unit through experimental assessment. This tested the 2nd sub-hypothesis, which posited the ability of experiments to validate expected performance.

1.4.4.2 Paper 2

K.M. Smith, S. Svendsen, The effect of a rotary heat exchanger in room-based ventilation on indoor humidity in existing apartments in temperate climates, *Energy Build.* (Accepted with minor revisions).

Paper 2 investigated the moisture effects of a rotary heat exchanger in room-based ventilation on a renovated apartment in Denmark. Numerical simulations attempted to characterize the impact of moisture transfer on indoor relative humidity. The paper compared the moisture effects from single-room ventilation to whole-dwelling ventilation with two different types of heat recovery. The investigation tested the position of the 3rd sub-hypothesis by attempting to identify moisture-related issues.

1.4.4.3 Paper 3

K.M. Smith, A.L. Jansen, S. Svendsen, Assessment of a new demand-controlled room-based ventilation unit with heat recovery for existing apartments, *Energy Build*. (Awaiting decision)

Paper 3 documented an experimental assessment of a novel spiral recuperative heat exchanger for room-based ventilation. The author devised suitable experiments to assess the performance of the unit, which tested the 2nd sub-hypothesis. The paper also documented its potential with simulations of demand control. Simulations used the expected performance of the unit and predicted its effect on fan energy consumption and indoor climate. These simulations tested the position of the 4th sub-hypothesis, which posited that certain software tools enable modelling and assessment of innovative ventilation systems.

1.5 Structure of the thesis

This thesis contains seven main chapters and four reference chapters. Chapter 1 is an introduction to the study. Chapter 2 describes the furthest level of scientific achievement in each of the relevant research topics. Chapter 3 provides a summary of the applied methods for investigating the hypothesis and sub-hypotheses. Chapter 4 presents a summary of the results of each investigation. Chapter 5 discusses the context, accuracy, and implications of the results. Chapter 6 concludes on the hypothesis and sub-hypotheses based on the results of investigations. Chapter 7 provides the perspectives of the author as well as plans for relevant future work. Chapters 8 through 11 list the references, symbols, figures, and tables, respectively. Appendices A to C provide the three research papers that were co-written by the author. Appendix D provides the Matlab code for the calculation of predicted performance of the plastic rotary heat exchanger in Paper 1. Appendix E provides the Matlab code for the moisture simulations of Paper 2.

2 State of the art

The state of the art represents the furthest level of scientific achievement on the investigated topics. The following sections summarize the relevant publications.

2.1 Room-based ventilation

In early research on single-room ventilation, Manz *et al*. [14] experimentally tested and numerically simulated different units intended for cold climates to assess their performance with respect to ventilation efficiency, thermal comfort, heat recovery, electrical energy input, and acoustics. Sound pressure and sound reduction were their main issues and required further improvement. The lead authors published additional research that focused on unintentional flows of heat and air both inside and outside single-room ventilation [15]. Their model described these flows, and numerical examples showed considerable efficiency reductions unless unintended flows were limited to acceptable levels. Based on their results, the authors recommended greater focus on construction, manufacture, and installation. Single-room ventilation units are increasingly available commercially, but the work by Manz *et al.* is among limited published research investigating single-room ventilation for cold or temperate climates. Other published research documented the development and assessment of novel single-room ventilation units for warm and humid climates [16][17][18][19], but these units are generally not appropriate for temperate climates.

2.2 Moisture issues

Recent research has investigated intended moisture transfer in rotary heat exchangers [20][21][22]. These heat exchangers have hygroscopic surfaces to assist moisture transfer between airflows without the need for condensation. However the desirability of moisture transfer depends on context and may not be suitable for all applications. The research in this thesis specifically deals with the impacts of moisture transfer in non-hygroscopic heat exchangers with a focus on single-room ventilation in humid temperate climates. In the temperate zones of Sweden, non-hygroscopic rotary heat exchangers are often used in ventilation of entire dwellings, and limited research has indicated potential issues with excessive moisture recovery in certain contexts [23][24][25]. In other temperate climates, single-room ventilation units with various types of heat exchangers are increasingly installed through the façade of renovated buildings to supply fresh air and limit heat loss. Their impact on indoor humidity has not been adequately researched and compared to standard systems.

2.3 Demand Control

Recent research has investigated the benefits and risks of demand-controlled ventilation. Hesaraki and Holmberg [26] simulated demand-controlled ventilation in a new Swedish home and observed unsafe accumulation of volatile organic compounds unless ventilated prior to occupancy. The authors stated that the newly constructed building emitted pollutants at a relatively high rate and that existing buildings may not produce the same result. When safely ventilated, their results showed total potential energy savings for heating and fans of 16% compared to a CAV system. Cho *et al.* [27] performed simulations that offset fresh air demand with cleansed recirculated air in a Korean multi-residential building. The simulated system provided acceptable average air quality and potential energy savings of 20% compared to a CAV system. Laverge *et al.* [28] simulated four different demand-control strategies in a statistically-average detached Belgian home. They reported varied effects on indoor air quality, and their demand-control strategies reduced ventilation heat loss by 25%-60%. Morelli *et al.* [29] installed a whole-dwelling CAV ventilation unit in a renovated Danish apartment. The authors stated the need for demand-controlled ventilation due to the high incidence of open windows, which significantly lowered CO_2 concentrations. Mortensen *et al.* [30] assessed the impact of demand-controlled ventilation on occupant exposure to pollutants in residences by analyzing long-term exposure and peak exposure. Demand control reduced long-term exposure and increased peak exposure within safe limits.

3 Methods

This chapter provides the methods for the three main aspects of the research. The methods for theoretical development describe the integrated design process for two innovative ventilation units. The experimental methods describe the tests to validated modelled and expected performance. The simulation methods describe the steps to investigate implementation of the developed units and their potential impacts on a renovated apartment in Denmark.

3.1 Theoretical development

The research methods began with the theoretical development of room-based ventilation for temperate climates, which yielded two prototypes. These theoretical developments attempted to answer the first research question and investigate the first sub-hypothesis, which sought a set of criteria towards adequate performance and compliance in renovated buildings. The criteria formulated specific requirements towards successful development of room-based ventilation. Based on a broad review, the criteria targeted essential aspects. The review included theory, relevant research, building regulations, standards for indoor climate, and context for implementation of the units. The following criteria formed the basis of each development:

1. Provide an option to modulate bypass of heat recovery.
2. Provide greater than 80% supply temperature efficiency (η_{supply}) which is measured as

$$\eta_{supply} = \frac{(T_{supply} - T_{outdoor})}{(T_{indoor} - T_{outdoor})}$$

   where T_{supply}, $T_{outdoor}$, and T_{indoor} are the measured temperatures of supply air, outdoor air, and indoor air, respectively.
3. Devise a compact construction with inexpensive and durable materials.
4. Minimize air leakages.
5. Enable drill-hole installation through the façade.
6. Limit pressure drop to achieve an expected specific fan power of less than 800 J/m^3.

The following briefly justifies the selection of each criterion:

1. The variable demands for heating and cooling required the option for controllable bypass of heat recovery.
2. Danish building regulations require 80% temperature efficiency in new heat recovery ventilators.

3. The possibility to decentralize and broadly deploy ventilation required cost-effective solutions with simple manufacturing techniques, low material costs, and durable constructions.
4. Relevant research by Manz *et al.* [15] and Roulet *et al.* [31] recommended minimal air leakage.
5. Installation in existing brick-walled apartments demanded a simple solution that used drilled holes in the façade.
6. The future Danish building regulations will limit specific fan power to 800 J/m^3 in new installations that serve single dwellings.

The development criteria omitted several considerations for different reasons. Some required an unreasonable investment of resources to predict performance, so development used basic assumptions and planned iterative improvements for later stages. The basic assumptions included relationships to other criteria as well as obvious and straight-forward solutions.

Noise limits may have deserved their own criteria. When Manz *et al.* [14] tested single-room heat recovery ventilators, sound pressure and sound reduction were primary issues. However these quantities were difficult to model and predict in the early-stages of development. Rather than set limits to sound pressure levels, the development considered its relationship to other criteria. The sound power level from fans increases with fan power and static pressure. Therefore the requirements of low pressure drop and fan power implied less fan noise. Similarly, the sound power level from ducted flow mainly relates to air velocity. Frictional losses are proportional to the square of air velocity. To achieve low pressure drop, the development limited frictional losses by limiting air velocities. The indirect consequences of both considerations were less noise from fans and airflow, respectively.

The author believed that future development could iteratively reduce sound power levels if necessary. Development could add components to reflect or attenuate noise. This would add pressure losses, so development could benefit from acoustic and hydrodynamic simulations and optimizations. This would require a significant investment of resources so it was saved for later stages and not included in the criteria. Instead, the criteria guided development at an assumed nominal flow rate. Individual end-user priorities could lower maximum flow rates to reduce noise if necessary. This would not contradict the development criteria or the first sub-hypothesis, which posited an innovative, iterative, and integrated development process based on system requirements and conceptual strengths and weaknesses.

Sound reduction was a separate consideration. Each design prevented a direct line of sound transmission through the unit. This reflected a portion of sound back to the outdoors. Each heat exchanger provided some attenuation as well. Attenuation relates to surface area, which a separate criterion maximized to achieve the required heat transfer and temperature efficiency. This consideration did not require a separate criterion because the requirement was straight-forward and did not ensure adequate performance. Instead, later stages of development would require feedback from measurements to characterize necessary improvements.

The criteria did not explicitly state the need for a variable speed fan, but this was understood throughout development. The first sub-hypothesis considered demand-control as a potential system requirement. All developments assumed the use of variable speed fans for this purpose.

Each development must have satisfied these criteria to confirm the first sub-hypothesis. This was only feasible if all criteria were theoretically achievable and not mutually exclusive. The methods explain how each development targeted the criteria when not already obvious. Paper 1 and Paper 3 further demonstrate how the list of criteria guided the integrated design processes from inception to near-completion. Paper 1 listed Criteria 1 to 5 and described in detail how development targeted each criterion. The development in Paper 3 considered all six criteria but did not describe them in the paper.

3.1.1 Rotary unit

The following summarizes methods to develop the first prototype for room-based ventilation. Paper 1 describes each of these items in greater detail.

3.1.1.1 Description

As shown in Figure 2, development of the final prototype located fans on opposite ends to lower pressure gradients between airflows. Additive manufacturing minimized tolerances and air gaps. An inexpensive, rigid polycarbonate honeycomb of circular channels was suitable for a rotary heat exchanger. As shown in Figure 2, the circular channels of the honeycomb were 150 mm in length and 2.6 mm in diameter, and the channel walls were 0.2 mm thick. In this thesis, **the rotary unit** henceforth refers to a single-room ventilation unit with a rotary heat exchanger.

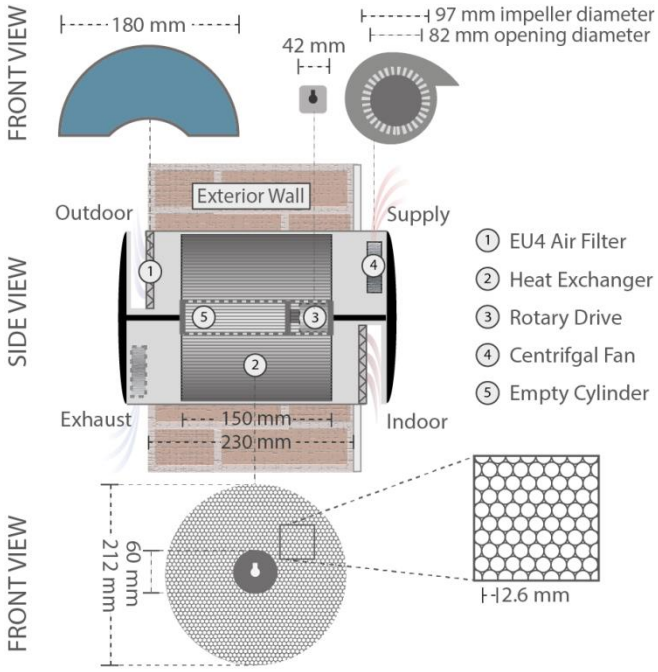

Figure 2. Detailed drawing of the developed rotary unit with a polycarbonate honeycomb rotary heat exchanger.

3.1.1.2 Bypass

Simple bypass helped to meet the requirements of Criterion 1. Rotary heat exchangers provide simple bypass by slowing their regenerative cycle. Experiments tested the final rotary unit at different cycling speeds to verify a reduction in heat recovery.

3.1.1.3 Temperature Efficiency

The ε-NTU_0 method predicted sensible effectiveness (ε) using dimensionless groups. The effectiveness and temperature efficiency were equal for case of the rotary unit. The modified number of transfer units (NTU_0) of a heat exchanger is the ratio of total thermal conductance to the smaller heat capacity rate of fluid flow (C_{min}). The subscript *0* indicates that NTU is modified for regenerative heat transfer. Shah and Sekulic [32] provided a ε-NTU_0 model:

$$\varphi = \left(\frac{\lambda NTU_0}{1 + \lambda\, NTU_0}\right)^{1/2} \quad for\ NTU_0 > 3,$$

$$C_\lambda = (1\ + NTU_0(1\ +\ \lambda\,\varphi)/(1\ +\ \lambda\, NTU_0))^{-1}\ -\ (1 +\ NTU_0)^{-1}$$

$$\varepsilon = \varepsilon_{\lambda=0}\left[1-\frac{C_\lambda}{2-C^*}\right] = \left[\frac{1-\left(-NTU_0(1-C^*)\right)exp}{1-C^*exp(-NTU_0(1-C^*)}\right]\cdot\left[1-\frac{1}{9(C_r{}^*)^{1.93}}\right]\cdot\left[1-\frac{C_\lambda}{2-C^*}\right]$$

where C^* is the ratios of heat capacity rates (C_{min}/C_{max}), Cr^* is the ratio of heat capacity rates of the rotor to airflow, C_λ is a coefficient to account for longitudinal heat conduction based on a conduction parameter (λ), φ is an intermediary parameter in the calculation of C_λ, and $\varepsilon_{\lambda=0}$ is the effectiveness with neglected longitudinal conduction. The conduction parameter (λ) is calculated as $\lambda=(k_{rotor}A_k)/(LC_{min})$, where k_{rotor} is the thermal conductivity of the rotor, A_k is the conductive cross-sectional area of the rotor, and L is the length of the rotor. This model assumed no leakage of unintended air flows. The model also assumed fully developed laminar flow, which allowed a simple determination of the convective heat transfer coefficient based on the geometry of the channels. Paper 1 describes this assumption and calculation in greater detail. Appendix D provides the Matlab code for performing the calculations.

3.1.1.4 Material Selection

The first prototype targeted a short heat exchanger to fit into the minimum thickness of a standard brick wall in Denmark. Longitudinal heat conduction can decrease the effectiveness of short regenerators. Low thermal conductivity limits longitudinal heat conduction, but it can negatively impact conductive and convective heat transfer. Based on simplified theory by Shah and Sekulic, the wall thermal resistance of a regenerator is $\delta/(3kA)$, where δ is the wall thickness, k is thermal conductivity, and A is the heat transfer surface area. The calculation of NTU_0 included this resistance to ensure that the heat exchanger material could be utilized. The thin walls of the plastic honeycomb ensured that conductive resistance was an order of magnitude less than convective resistance. The convective heat transfer is the same for all materials if channels are symmetric (i.e. circular or planar), so circular channels negated the impact of material choice. This solution limited longitudinal conduction and maximized effectiveness.

3.1.1.5 Air Leakage

The leakage paths around rotary heat exchangers fall into categories of pressure leakage (between airflows) and bypass leakage (between inlet and outlet). Leakage between airflows also occurs inside the rotary heat exchanger, known as carryover leakage.

Shah and Sekulic recommended the following model for pressure leakage through an orifice:

$$\dot{m}_{leak,press} = C_d A_o \sqrt{2\rho_{inlet}\Delta p}$$

where $\dot{m}$ is the mass flow rate and *leak,press* denotes pressure leakage, C_d is the coefficient of discharge, A_o is the orifice flow area, ρ_{inlet} is the density of the inlet air, and Δp is the pressure difference across the orifice.

The re-organized Darcy-Weisbach equation provided the approximate bypass flow as

$$Q_{leak,byp} = \left(\frac{(\Delta p)(D_h)^2 A}{48\mu L}\right)_{leak,byp}$$

where μ is the dynamic viscosity, Δp is the pressure drop through the bypass area, and A is the cross-sectional area of bypass flow around the heat exchanger for supply or exhaust.

Shah and Sekulic recommended a model for carryover leakage as

$$\dot{Q}_{leak,carry} = \pi(r^2 L\sigma N)_{rotor}$$

where r, σ, and N are the radius, void ratio, and cyclical speed of the rotor, respectively.

3.1.1.6 Installation

Criterion 5 required the possibility to install the single-room ventilation unit with drilled holes in the façade of an existing building. Criterion 5 sought a cylindrical-shaped heat exchanger to effectively utilize available space in a drilled hole. A rotary heat exchanger was suitable because its shape was inherently cylindrical.

3.1.1.7 Pressure drop

Shah and Sekulic provided a model of pressure drop through a heat exchanger as

$$\Delta p = \frac{u^2\rho}{2}\left[1 - \sigma^2 + K_{contract} + 2\left(\frac{\rho_{inlet}}{\rho_{outlet}} - 1\right) + f\frac{L}{D_h}\rho_{inlet}\left(\frac{1}{\rho}\right)_{mean} - \left(1 - \sigma^2 + K_{expand}\right)\frac{\rho_{inlet}}{\rho_{outlet}}\right] \quad (1)$$

where $K_{contract}$ and K_{expand} are the pressure loss coefficients for the entrance and exit effects, respectively. Shah and Sekulic provided a plot of these coefficients for a core of multiple circular tubes. The Fanning friction factor (f) for fully developed laminar flow in circular tubes is 16/Re, where Re is the Reynold number. Other values in Eq. (1) depend on the properties of flow, such as the velocity (u), the inlet and outlet density ($\rho_{inlet,outlet}$) and the ratio of matrix core flow area to face flow area (σ).

3.1.2 Spiral unit

The following describes the theoretical development of the second single-room ventilation unit with respect to the set of criteria. This development further investigated the first sub-hypothesis and helped to answer the first research question.

3.1.2.1 Description

Development yielded a 1.22-meter-long cylindrical counter-flow heat exchanger for a second room-based ventilation unit. Figure 3 depicts a cross-sectional view at either end. Its construction wrapped two 0.3 mm thick PVC sheets around a 3 mm thick PVC tube with 75 mm outer diameter. Narrow 3 mm thick spacers maintained the appropriate gap between sheets, and 3 mm rubber sealant blocked alternate layers at inlets and outlets. The two sheets simultaneously wrapped around the core and together created 26 channels from 13 full revolutions. A 3 mm thick PVC tube with 250 mm outer diameter enclosed the heat exchanger. The inner and outer tubes extended beyond the rolled sheets, and a plastic divider maintained separation between supply and exhaust. In this thesis, **the spiral unit** henceforth refers to a single-room ventilation unit with this recuperative heat exchanger.

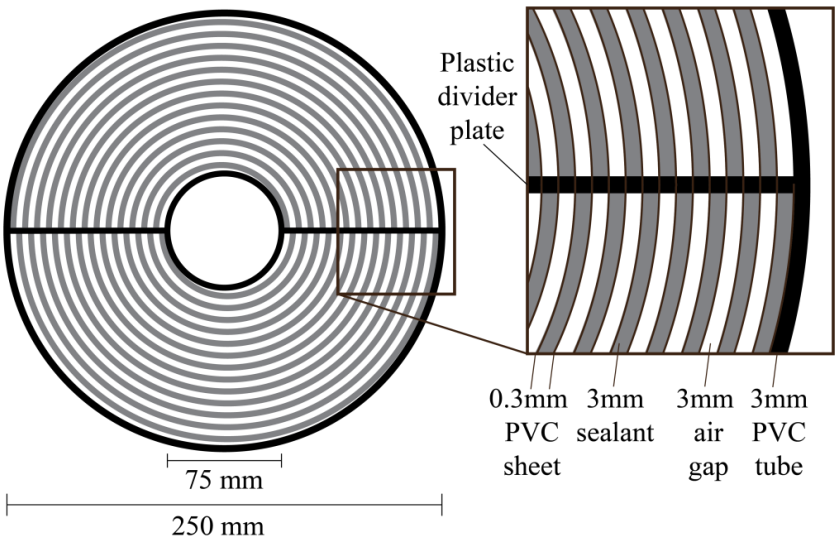

Figure 3. Face-view schematic of the developed heat exchanger for room-based ventilation. Its rolled construction facilitated manufacture and limited leakages.

3.1.2.2 Bypass

The inner tube of the ventilation unit provided a potential bypass of the heat exchanger in future prototypes. The unit could allow airflow through the inner tube in one direction to reduce heat transfer. Its development selected an appropriate diameter tube to provide much lower pressure

drop than the heat exchanger. This could allow full bypass with the opening of a valve, and a controller could modulate this valve to achieve partial bypass. This also made it easier to roll the PVC sheets at the beginning of its manufacturing process.

3.1.2.3 Temperature efficiency

The *NTU*-effectiveness method provided a means to predict temperature efficiency. With equal heat capacity rates of supply and exhaust, the *NTU*-effectiveness method predicted an *NTU* of 10.4 and a temperature efficiency of 93.2%, where *NTU* is the number of transfer units.

3.1.2.4 Material selection

Section 3.1.1.4 explains the benefits of plastic heat transfer surfaces with circular or planar channels. The low conductivity limits longitudinal heat conduction, and the geometry minimizes the impact of material choice on convective heat transfer. The difference with this development was transverse conduction through the heat transfer material. The spiral heat exchanger is recuperative, so the material transfers heat instead of storing it. The conductive resistance in a recuperative heat exchanger is $\delta/(kA)$, which is three times greater than the simplified conductive resistance in a regenerative heat exchanger. With the selected PVC sheets and dimensions, the conductive resistance was an order of magnitude less than the convective resistance, so the material and thickness did not limit heat transfer. Additionally, PVC sheets and tubes were inexpensive and durable items, which partially satisfied Criterion 3. This criterion also required compact construction, but compactness may exclude a low pressure drop system, which this development prioritized to limit fan energy and noise.

3.1.2.5 Pressure drop

The heat exchanger provided little resistance to flow. The Darcy-Weisbach equation predicted frictional losses of 25.2 Pa. Loss coefficients for respective contractions and expansions predicted pressure losses of 1.6 Pa at both the entrance and exit of the heat exchanger. The spacers between layers provided an additional expected pressure loss of 5.6 Pa. This included frictional losses from flow through the sinusoidal channels of the corrugated spacers as well as minor losses from each contraction and expansion at the spacer. In total, the heat exchanger provided a predicted pressure drop of 34.0 Pa at 15 L/s.

3.1.2.6 Leakage

The construction used two continuous PVC sheets to completely separate the two airflows inside the heat exchanger. Pieces of 3 mm thick butyl rubber tape with double-sided adhesive

provided airtight seals at either end of the heat exchanger. Alignment of the tape was a challenge, which may have provided leakage paths at the connections between the tape and the divider plates. Knowledge gained through the manufacturing experience could lead to better sealing in future prototypes.

3.1.2.7 Installation

The spiral unit placed the heat exchanger in the interior of the building. Installation of the unit required two holes with 100 mm diameter through the façade. This allowed drill-hole installation. It also limited the aesthetic interference on the exterior of the façade.

3.2 Experimental methods

Theoretical development resulted in the manufacture of two prototypes. Following this work, the methods reviewed, devised, and applied experimental tests to validate expected performance and investigate the second sub-hypothesis. The investigations first sought European or international standards with prescribed tests related to the listed criteria. These standards document established criteria, methods, practices and processes. Users may directly apply international standards or modify their contents to suit local conditions. Standards are often intended for conventional systems, but the developments in this research targeted novel solutions. The author therefore adjusted or disregarded prescribed methods as necessary.

3.2.1 Rotary unit

The available standards only focused on centralized ventilation systems during tests of the rotary unit. EN 308 provided test procedures for air-to-air heat recovery devices in ducted systems. The rotary unit had an irregular shape and was not compatible with these procedures. EN 308 also focused on final products and set small limits on leakages. For this reason, the author devised different methods to test the criteria under the assumption of significant leakages of airflows and substantial heat gains from components. The author derived energy and mass balance equations from first principles and combined these with measurements of tracer gas concentrations, energy and mass flows, and temperatures. The devised methods re-organized these equations into the required quantities of the development criteria. Paper 1 provides the full derivations for reference.

3.2.1.1 Flow and Leakage Determination

The experiments determined fan flow rates, ventilation rates, and approximate pressure leakages. Paper 1 provides figures of experimental setups and further details of test apparatuses.

3.2.1.1.1 Flow Rate Measurements

The author independently measured supply and exhaust flow rates by sealing the opposite flow direction. Due to its irregular shape, the rotary unit connected to a flow meter through a sealed box. The flow meter was a circular metal pipe that contained a pitot tube at its midpoint to measure the difference in static and total pressure. The probes connected to a low-range micromanometer. The measured pressure differences correlated to flow rates based on calibration data from the manufacturer.

3.2.1.1.2 Pressure Leakage Approximation

With the heat exchanger at rest, the rotary unit exchanged air between a warm chamber and a cold chamber. The flow through the fan included pressure leakage. A heat and mass balance with measured temperatures and fan powers determined the approximate pressure leakage for each set of flow rates.

A correction to the measured supply temperature accounted for heat gains from the fan as well as heat transferred through the divider plate. A mass balance demonstrated the relationship between temperature efficiency with a stationary rotor and the mass flow ratio of pressure leakage as

$$\frac{\dot{m}_{leak,press}}{\dot{m}_{supply}} = \frac{(T_{supply} - T_{outdoor})}{(T_{indoor} - T_{outdoor})} = \eta_{N=0}$$

where $\eta_{N=0}$ is the temperature efficiency with a stationary heat exchanger.

3.2.1.1.3 Direct ventilation rate measurement

Measurement of tracer gas decay determined ventilation rates in twin stainless-steel climate chambers, which were separated by an insulation panel. With an opening in the insulation panel sealed, the regression of Freon decay provided a baseline air change rate. With the rotary unit inserted, the fans provided balanced flow rates of 5, 10, and 15 L/s. The decay equation took the following form:

$$C(t)_{warm} - C(t)_{cold} = (C(0) - C(t)_{cold})e^{(-N_{meas}t)}$$

where *C(t)* is the tracer gas concentration at time *t* in the chamber specified by the subscript, *warm* or *cold*.

The ventilation rate, *Q*, was calculated as

$$Q = N_{vent} \cdot V_{warm} = (N_{meas} - N_{baseline}) \cdot V_{warm}$$

where V_{warm} is the warm chamber volume, and the ventilation air change rate (N_{vent}) is determined for each flow rate by subtracting the baseline air change rate ($N_{baseline}$) from the measured air change rate (N_{meas}). The subscript *vent* denotes fresh ventilation airflow.

3.2.1.2 Temperature efficiency measurements

Two measurement methods provided values of temperature efficiency.

3.2.1.2.1 Heat Input Method

In this experiment, the guarded hot box (GHB) measured the thermal transmittance through the rotary unit at different flow rates in order to calculate temperature efficiencies. A heat balance yielded the temperature efficiency of the rotary unit as

$$\eta_{vent.} = \frac{\left(\frac{P_{HEX}}{2} + P_{fan} + P_{heater}\right) - \left(\left(\left(A\frac{k}{\delta}\right)_{wall} + \left(A\frac{k}{\delta}\right)_{tube}\right)(T_{indoor} - T_{outdoor}) + \left(A\frac{k}{\delta}\right)_{box}(T_{box} - T_{outdoor})\right)}{(\dot{m}c_p)_{vent.}(T_{indoor} - T_{outdoor})}$$

where P_{HEX}, P_{fan}, and P_{heater} are the power demands from the heat exchanger drive, the supply fan, and the heater in the metering box, respectively. With respect to the designated heat transfer medium, A, k, and δ are the heat transfer area, thermal conductivity, and thickness, respectively. The subscripts *wall*, *box*, and *tube* denote the wall between chambers, the metering box, and the tube of the rotary unit, respectively.

3.2.1.2.2 Temperature Measurements

A similar experiment measured supply and exhaust temperatures at each inlet and outlet. This provided a calculation of temperature efficiencies for both supply and exhaust. Paper 1 describes the details and derivations. The measured temperatures were corrected for heat gains. The temperature efficiencies included pressure leakages, so the following correction yielded the temperature efficiency for only the ventilation flow:

$$\eta_{vent} = \frac{\eta_{supply} - \eta_{N=0}}{(1 - \eta_{N=0})} \quad (2)$$

3.2.2 Spiral unit

During development of the spiral unit, the European Committee for Standardization released standard EN 13141-8 [33], which prescribed methods to test single-room ventilation units with heat recovery. The standard focused on complete products, so the methods required some adjustment to accommodate early-stages of development. The author modified the methods to achieve similar conditions for testing. For example, prior to receiving the fans for the prototype,

the experiments used a vacuum cleaner to provide controllable flow through the heat exchanger. If strictly followed, standards allow reporting of performance without the need to document methods. Conversely, the modified tests demanded full documentation. The following gives a summary of methods, and Paper 3 provides the full details for reference.

3.2.2.1 Leakage

Experiments measured external and internal leakage. Paper 3 provides further details and figures to describe each experiment.

3.2.2.1.1 External Leakage

In a test of external leakage, a vacuum cleaner forced air into the heat exchanger. The regulator achieved interior pressures of 50 Pa and a gas meter measured the flow into the heat exchanger.

3.2.2.1.2 Internal Leakage

Internal leakage represents the airflow between supply and exhaust. The rolled sheets completely separated airflows inside the heat exchanger, so all internal leakage occurred at either end. The experiment first measured unblocked airflow through the ventilation unit with a vacuum cleaner at maximum power. The vacuum sucked air from the outlet duct at the cold end of the heat exchanger. The gas meter measured airflow, and the micromanometer measured the difference in pressure between the supply and exhaust airflows at either end of the heat exchanger. The experiment then blocked the airflow on the warm end of the heat exchanger. Regulation of the vacuum achieved the same average pressure difference between supply and exhaust, and the gas meter measured the flow rate of internal leakage. The internal leakage ratio (W) was $W=Q_{leak,int}/Q_{unsealed}$, where $Q_{leak,int}$ is the measured internal leakage and $Q_{unsealed}$ is the unblocked measured flow. This method was slightly different than the test described in EN 13141-8.

3.2.2.2 Flow Rate

The experiment connected supply and exhaust fans to the heat exchanger. A venturi meter on the supply fan measured flow rates at different fan speeds. The experiment determined flow rates at various fan speeds from 10% to 90% of capacity. The experiment repeated this procedure on the exhaust side to determine signal pairings for balanced flows. Standard EN 13141-8 offers a correction to flow rates based on measured leakages and mixing. The author calculated the real flow as $Q_{real}=Q_{meas}\cdot(1-(W-0.02))$, where Q_{real} is the actual flow through the heat exchanger in one flow direction, and Q_{meas} is the measured fan flow rate.

3.2.2.3 Temperature Efficiency

The GHB provided warm and cold chambers to measure temperature efficiencies. This experiment removed the metering box and only measured air temperatures. The temperatures of the warm and cold chambers were 5°C and 24°C, respectively. As recommended by EN 13141-8, the experiment measured air temperatures with at least four sensors in each inlet and outlet. The experiment measured fan powers at each flow rate and calculated the resulting change in temperatures. Both fans were on the cold side of the heat exchanger, so corrections added the heat gain to the measured cold chamber temperatures and subtracted it from the measured exhaust temperatures for each corrected flow rate. Since both fans were on the cold side of the heat exchanger, the calculations assumed all leakage on the cold side and negligible pressure difference on the warm side. Eq. (2) provided a correction to temperature efficiency based on a mass balance equation with leakage at one end of the heat exchanger.

3.3 Simulation methods

Steady state measurements were appropriate to assess the performance of the units with respect to the development criteria. In contrast, the operation and control of the single-room ventilation units as well as their context for implementation could significantly impact performance with respect to indoor conditions and energy-use. The indoor climate depends on the dynamic effects of occupant behavior, varying weather conditions, and adjustments to ventilation rates and heat recovery. Assessment of these effects requires dynamic simulations. The evaluation may depend on sustained or cumulative impacts. For this reason, numerical simulation investigated the dynamic effects of the developed ventilation units for the case of a renovated apartment in Denmark.

3.3.1 Moisture transfer simulation

The 3rd sub-hypothesis posited that simulations could help identify potential moisture issues with regenerative heat recovery in single-room ventilation. The rotary unit was the focus of this investigation. This represented one case of regenerative heat recovery. To investigate its potential moisture impacts, simulations applied moisture balance equations to simplified airflows in a renovated apartment in Denmark. Simulations compared the moisture effects from the developed rotary unit to a similar single-room unit with a recuperative heat exchanger. The simulations also compared with the effects of a whole-dwelling ventilation unit with either a recuperative or rotary heat exchanger. The simulations assumed that condensation in the rotary heat exchangers transferred entirely to the supply air, whereas the recuperative heat exchangers did not transfer moisture.

A review of literature revealed many knowledge gaps in existing research on moisture issues in residences. ASHRAE Standard 160 [34] provided criteria for moisture-control analysis in buildings. A review of the standard by one of its co-authors confirmed these knowledge gaps [35] as the standard based items on incomplete data or professional judgement. According to the review, development of the standard indicated the need for specific research in the areas of residential moisture generation, performance criteria, design weather data, and the effects of air flow. The following methods accounted for these uncertainties while investigating the third sub-hypothesis.

3.3.1.1 Apartment Description

The simulated apartment assumed new windows and improved sealing to obtain an infiltration air change rate of 0.05 h^{-1}. The gross area of the apartment was 77 m^2, and Table 1 lists individual room areas. The interior floor area was 67.5 m^2, and Figure 4 shows the floorplan based on an actual apartment. The rooms were 2.6 m in height. The layout of the apartment assumed that all rooms had access to the façade and that air movement between rooms was fully mixed in a central corridor. The average daily occupancy was 14.2 hours on weekdays, which compared to the recommended attendance time of 14 hours per day for Swedish apartments in Johansson *et al.* [36].

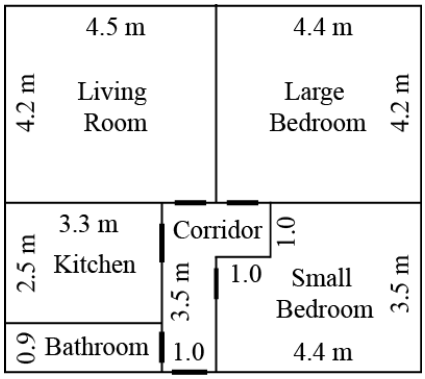

Figure 4. Floorplan of the simulated apartment with interior dimensions. The gross interior and exterior areas were 67.5 m2 and 77 m2, respectively. Room heights were 2.6 m.

Table 1. Room summary and occupancy profile for the assumed Danish apartment.

Room Type	Room Area m^2	Occupancy Schedule *Time interval*	Occupants *No. of adults*
Kitchen	8.3	7:00-8:00 12:00-13:00 17:00-20:00	1
Bathroom	3.0	7:00-9:00	1
Large Bedroom (adult couple)	18.5	22:00-7:00	2
Small Bedroom (child)	14.4	22:00-7:00	0.5
Living Room	18.9	16:00-22:00 (weekdays) 9:00-22:00 (weekends)	1
Corridor	4.4	-	0
Total	67.5	35.5 occupant-hours / weekday (59.2%) 42.5 occupant-hours / weekend day (70.8%)	

3.3.1.2 Moisture Production Schedule

Residential moisture generation provided a great deal of uncertainty towards identifying moisture issues and investigating the third sub-hypothesis. Many relevant standards list daily production rates without providing the source of measured data. This includes BS 5250 [37] and CIBSE Guide A [38]. Multiple studies have documented moisture production in greater detail. Angell and Olson [39] listed tabular data for individual sources, but many values originated from very old measurements on outdated appliances and practices. More recently, TenWolde and Pilon [40] collected and formulated rates, and Yik *et al.* [41] comprehensively measured rates for a household in Hong Kong. The section covering moisture production in Paper 2 describes these in greater detail.

Moisture release clearly varies with individual behavior and may vary with culture and location. For example, Yik *et al.* measured greater release from cooking a typical meal in Hong Kong compared to other studies. Further research and measurements would vastly improve certainty in this area, which would improve the characterization of moisture issues. In this investigation, the author tried to account for this uncertainty by testing an array of possible moisture production schedules. The author compiled three separate scenarios to reasonably represent the best-, typical-, and worst-case scenarios of moisture production. This involved a comprehensive literature review on limited research and data, which the methods of Paper 2 describe in detail. Moreover, the paper lists rates and assumptions by individual source and scenario.

3.3.1.2.1 Scenarios

The best-case scenario assumed the lowest estimated values from references, which often resulted from measures to control moisture sources. The typical scenario assumed common modern appliances, recently measured release rates, and common methods for source control.

The worst-case scenario mainly referenced standards and design guidelines. The assumed aggregate values for each scenario are listed in **Error! Reference source not found.**.

Table 2. Assumed aggregate values for the release of indoor moisture sources in the simulated apartment.

				Scenarios		
Activity	***Room***	**Frequency**	***Units***	**Best-case**	**Typical case**	**Worst-case**
Cooking method	*Kitchen*	-	-	Electric / Sealed-gas	Electric / Gas	Gas
Cooking load	*Kitchen*	-	*kg/day*	0.24	1.00 / 2.35	5.06
Dishwasher load	*Kitchen*	*daily*	*kg/day*	0.05	0.15	0.45
Cleaning	*All*	*weekly*	*kg/m2*	0.005	0.005	0.15
			kg/day	0.04	0.04	1.32
Shower load	*Bathroom*	3 *showers/day*	*kg/shower*	0.20	0.35	0.53
			kg/day	0.60	1.40	2.12
Clothes method	-	-	-	Dryer vented to outdoors	Fast spinning wash / Hang dry	Slow spinning wash / Hang dry
Clothes drying load	*Bathroom*	3 *loads/week*	*kg/load*	0	1.67	2.9
			kg/day	0	0.72	1.24
Plants	*Living*	*Continuous*	*kg/day*	0	0.06	0.45
Pets	*Living*	*Continuous*	*kg/day*	0	0.12	0.41

3.3.1.3 Moisture Limits

The author could not specify exact limits to prevent moisture issues due to the uncertainty regarding limits, surface temperatures, building materials, and cleanliness. The analysis instead used approximate limits and sought relative indicators of potential moisture issues. This extended analysis beyond sheer compliance or violation of limits in specific time steps.

3.3.1.3.1 Mold Growth

After a comprehensive study, Rowan *et al.* [42] recommended that local surface relative humidity be kept below 75% to limit fungal growth. Johansson *et al.* [43] provided a range of limits above 75% to account for material type and cleanliness. Vereecken and Roels [44] reviewed prediction models for mold growth and found that multiple models used a critical surface relative humidity (RH) of at least 80%. These studies demonstrated the variability of mold prediction and risk assessment.

With inexact limits on room RH, analyses can gauge relative mold risks with either the degree or the duration of violated limits. ASHRAE Standard 160:2009 attempts to evaluate both with one simple measure by limiting the maximum 30-day moving-average of surface relative humidities to 80% [34]. Surface temperatures depend on local effects, such as convective heat transfer coefficients, thermal transmittance of building components, and indoor and outdoor temperatures. Consequently, the minimum surface temperature in each room may be highly uncertain. During the heating season, a thermostat controls the average air temperature in each room, which increases its certainty. Simulations may assume fully mixed room air, which

enables a simple and accurate calculation of room RH for known air temperatures. To simplify analysis, this investigation estimated an approximate limit on room RH using an 80% limit on surface RH. The author assumed a 1.5°C temperature difference between the room air and the coldest interior surface. For fully mixed air, an increase in air temperature of 1.5°C roughly corresponds to a 10% decrease in RH, so the author estimated a limit of 70% for room RH. Analysis evaluated the 30-day moving-average of room RH against this limit. The results section displays the maximum annual value in each room during the heating season, which indicates a compliance or violation of this limit.

Maximum 30-day moving average RH may roughly correspond to a steady state. Figure 1 shows that indoor humidity does not affect the drying capacity of ventilation when the exhaust is saturated in an uncoated rotary heat exchanger, and all simulated airflows may be fairly constant. However steady state simulations cannot capture the effects of fluctuating indoor RH. Since mold only grows above critical limits, dynamic simulations can improve risk characterization by quantifying the total duration above limits. This ensures that results are not disproportionately influenced by warmer months with high outdoor moisture content. The duration above limits captured the cumulative risk for the whole heating season. This allowed a visual representation of the relative influence from varied parameters.

3.3.1.3.2 Dust Mites

An additional moisture issue is the growth of dust mites, which require relative humidity above 45%-50% and multiply faster at higher levels [45]. To completely avoid their proliferation, indoor air should be maintained below 50% during the heating season. This may be important in bedrooms and living rooms where carpets and furniture provide their habitat. This investigation did not analyze the issue of dust mites in detail, but the analysis includes relevant comments where appropriate.

3.3.1.3.3 Dryness

Reinikainen and Jaakkola [46] determined that low relative humidity can provoke skin symptoms, nasal dryness, and congestion. The standard EN 15251 [47] for indoor climate stated that less than 15%-20% RH can cause these symptoms. The standard recommended greater than 20% RH to achieve the minimum category of air quality and greater than 30% RH to achieve the best category. The analysis of results shows the minimum 1-day, 7-day, and 30-day moving-average RH for evaluations of sustained dryness.

3.3.1.4 Moisture Balance Equations

The investigation focused on room-based ventilation. The author assumed that closed interior doors provided a critical situation for indoor humidity with room-based ventilation because it minimized the diffusion of moisture to other rooms. This greatly simplified simulations of air movement in the apartment by allowing several key assumptions. In the case of room-based ventilation, air did not travel between rooms, so rooms were simulated individually. In the case of whole-dwelling ventilation, closed doors implied only one-way movement of air between rooms. For this case, the simulation assumed that airflow from the living room and bedrooms completely mixed in a central corridor before entering the kitchen and bathroom. These assumptions drastically reduced the complexity of calculations and enabled custom simulations in Matlab. The author derived many of the simulated balance equations, and Paper 2 provides their derivations. Paper 2 also includes a figure that shows the steps of the simulation and their associated equation numbers.

3.3.1.4.1 Ventilation

In the simulated apartment, the nominal infiltration rate was only 0.05 air changes per hour because renovations should significantly reduce infiltration to warrant investment in heat recovery [31]. The simulations assumed that the infiltration rate was constant and proportional to room volume. In reality, façade pressures and leakage areas would influence their actual values. When infiltration was low, its accuracy had less overall impact. However a sensitivity analysis increased infiltration to assess its influence on indoor humidity as described in Section 3.3.1.5. This increased the significance of simplified infiltration, and a more accurate simulation could take into account the dynamic effects of pressures and façade areas.

The minimum ventilation rate was 0.5 air changes per hour, as recommended in a multidisciplinary review of literature on ventilation and health by Sendell *et al.* based on limited data [48]. Simulations assumed exhaust capacities of 20 L/s and 15 L/s in kitchens and bathrooms, respectively, due to Danish regulations. The ventilation rate in kitchens and bathrooms underwent a controlled increased from minimum to maximum capacity based on indoor relative humidity. The proportional increase occurred from 50% to 70% RH. Simulations compared room-based ventilation to whole-dwelling ventilation to assess the impact of a rotary unit in each room.

3.3.1.4.2 Room-based ventilation

Room-based ventilation was balanced and assumed no exchange of air between rooms. Simulations applied the following iterations of discretized dynamic moisture balance equations for each room:

$$x_{room,i+1} = x_{room,i} + \frac{G_{room,i}}{(\rho V)_{room}} + N_{inf}\left(x_{amb,i} - min\{x_{room,i}, x_{sat,room}\}\right) + N_{vent,room,i}\left(x_{sup,room,i} - min\{x_{room,i}, x_{sat,room}\}\right) \quad (3)$$

where the subscripts *room*, *amb*, *sat*, *i*, *vent*, and *inf* denote room index, ambient, saturation, time step index, mechanical ventilation, and infiltration, respectively, $x_{room,i}$ is the moisture content in mass of water (i.e. vapor and condensation) per mass of dry air at the beginning of time step *i*, N_{inf} and $N_{vent,room,i}$ are the air change rates per time step, $x_{sat,room}$ is the saturation moisture content of room air, and G_i is moisture release in time step *i*. Infiltration air change rates were specified at dry air densities and indoor air temperatures.

3.3.1.4.3 Whole-dwelling ventilation

The term dry rooms may refer to living rooms and bedrooms, while the term wet rooms may refer to kitchens and bathrooms. The moisture balance equations for the whole-dwelling ventilation were similar to Eq. (3), but the exhaust from dry rooms mixed completely in the corridor and entered wet rooms as supply air. Simulations assumed that the flow rate from each dry room was proportional to its volume. In reality, ventilation demand is not always proportional to room volume, but this enabled a calculation of the mixed moisture content of exhaust from dry rooms at the beginning of each iteration as $x_{i,dmix}=\Sigma(V_{room} \cdot x_{i,room})/\Sigma(V_{room})$, where the subscript *dmix* denotes mixed exhaust from dry rooms. The simulations assumed that the minimum exhaust airflows from each wet room kept the same proportion as their maximum capacities. The whole-dwelling ventilation increased exhaust from the bathroom and kitchen up to their capacities based on relative humidity.

3.3.1.4.4 Variable calculations

The simulation imported hourly data from the 2013 Danish design reference year and copied it into 10 minutes intervals. The imported values included ambient air temperature, relative humidity, and pressure. At initialization, simulations calculated the partial pressures (*e*) for $e_{sat,room}$ and $e_{amb,i}$ at all time steps. Simulations also calculated the ambient moisture content ($x_{amb,i}$) for all time steps. Simulations then performed iterations for each time step. Each iteration calculated relative humidity from the moisture content of the previous iteration and limited it to 100%. Simulations then used temperature efficiency and temperature differential to calculate the exhaust temperature leaving the heat exchanger. Exhaust had a lower limit of 0.5°C.

Simulations of the rotary units assumed that all condensation evaporated into the supply air. Simulations of recuperative heat recovery assumed that all condensate drained from the heat exchanger. Paper 2 provides the individual formulae for variable calculations. Appendix E provides the Matlab code of the full simulation.

3.3.1.4.5 Heat recovery

The 2020 Danish building regulations will require 85% temperature efficiency for ventilation serving single dwellings. Experiments obtained similar efficiencies with the rotary unit at its nominal flow rate. To enable a comparison with whole dwelling ventilation, the temperature efficiency was set to 85% for all flow rates in both cases. Heat recovery only operated in the heating season, which ran from September 16th to May 15th in the simulation.

3.3.1.5 Parameter Variations

Simulations varied sensitive parameters to demonstrate the impact of different conditions. Based on the moisture balance equations, the author identified infiltration, heat exchanger efficiency, and room temperature as potentially influential parameters. In simulations, their standard values were 0.05 h^{-1}, 85%, and 22°C, respectively.

3.3.2 Demand control simulation

The 4th sub-hypothesis supposed that modelling and simulation of room-based ventilation and advanced controls could predict its potential. This work investigated the 4th sub-hypothesis using a simulation tool based on an object-oriented modelling language. The encapsulation and abstraction of component models allowed a simple re-structuring of the conventional building model to suit an innovative system with custom controls. The simulation tool IDA Indoor Climate & Energy (ICE) allowed the selection of different air handling units for each room, and each was customizable. A review of literature did not uncover documentation of a similar investigation.

3.3.2.1 Apartment Description

Simulations attempted to represent an actual case of a renovated apartment in Copenhagen with either whole-dwelling or room-based ventilation. The apartment in this investigation was different than the apartment described in Section 3.3.1.1.

3.3.2.1.1 Building Envelope

The apartment model used a modified floorplan of an existing apartment in Copenhagen, Denmark. Figure 5 shows the floorplan. The simulations assumed infiltration air change rates of 0.05 h^{-1}.

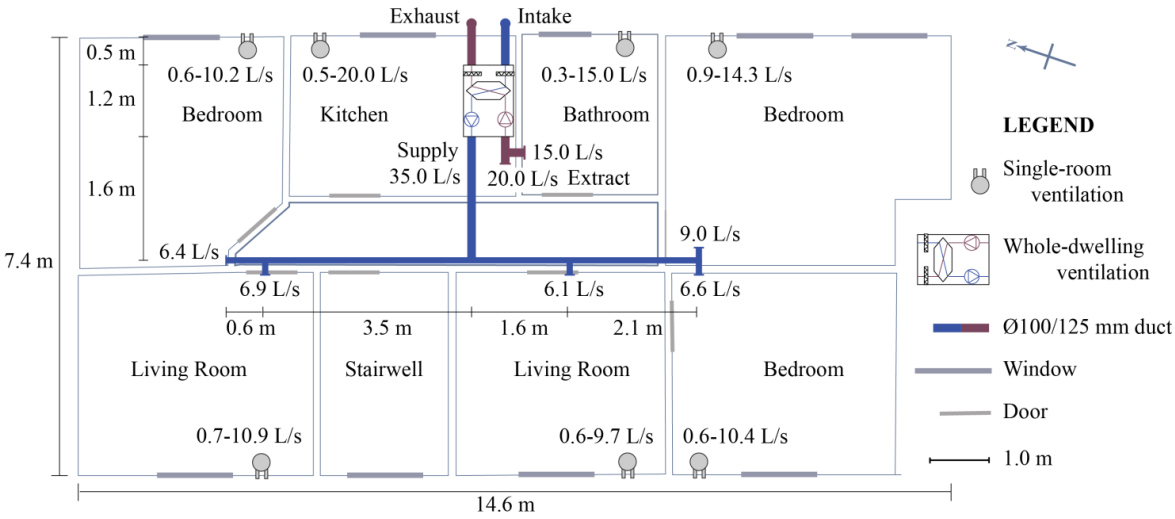

Figure 5. Floorplan of a renovated apartment with locations and airflows of the proposed ventilation systems.

3.3.2.1.2 Occupancy and Internal Loads

The software allowed scheduled releases of heat, moisture, and CO_2 from occupants and their activities, as well as heat from appliances and lighting. Table 3 lists the simulated schedules of occupancy, appliances, and vapor release. Each adult released CO_2, moisture, and heat according to equations from standard EN ISO 7730 [49].

Table 3. Occupancy and internal load schedule for simulations.

	Kitchen	**Bathroom**	**Living rooms**	**Adult bedroom**	**Child bedrooms**
Floor area [m^2]	10.4	6.3	12.2-13.6	17.9	12.8-13
Occupancy (Occ.)					
Average # *of adults*	1	0.8	1.2	2	0.6
Metabolic rate [MET]	1.4	1.2	1	0.9	0.9
Weekdays	7-8; 12-1; 18-20	7-8:30	16-22	22-7	22-7
Weekends	8-9; 12-1; 18-20	8-9:30	10-22	23-8	22-8
Appliances (App.)					
Schedule	7-7:30; 12-12:30; 18-19:30	-	Occ.	-	-
Heat gain [W]	220 (scheduled) 50 (constant)	-	40	-	-
Vapor					
Schedule	App.	Occ.	Occ.	Occ.	Occ.
Moisture gain [g/s]	0.11	0.30	Occ.	Occ.	Occ.

3.3.2.2 Ventilation Description

Simulations compared whole-dwelling ventilation to room-based ventilation with respect to indoor air quality and energy consumption.

3.3.2.2.1 Whole-dwelling CAV

Danish building regulations require maximum capacities of 15 L/s from bathrooms and 20 L/s from kitchens [9], so the simulated apartment required 35 L/s. A whole-dwelling ventilation system from *Airmaster A/S* (model CV200) provided suitable airflow and performance. At 35 L/s the whole-dwelling ventilation system had a dry temperature efficiency of 87% and a specific fan power (SFP) of 600 J/m^3 with 50 Pa of external resistance.

3.3.2.2.2 Single-room VAV

The single-room ventilation unit used demand-control based on three sensed variables. The controller used upper and lower limits for variables of air temperature and relative humidities and an upper limit for CO_2 concentration. In each room, the controller determined the required fan signal to meet the ventilation demands for each variable at each time step. The controller then assumed the maximum value. A proportional-integral (PI) controller set ventilation requirements with a CO_2 set-point of 750 ppm in each room. The controller also required lower outdoor absolute humidity and proportionally increased ventilation requirements between indoor absolute humidities of 6 g/kg to 12 g/kg. Temperature control set additional requirements for ventilation with a cooling set-point of 24°C on the extracted airflow.

Each single-room ventilation unit used a distinct range of potential ventilation rates. Danish building regulations determined the maximum ventilation rates in the kitchen and bathroom as 20 L/s and 15 L/s, respectively. Simulations set the maximum in bedrooms and living rooms to 0.8 L/sm^2. EN 15251 recommended minimum residential ventilation rates of 0.05-0.1 L/sm^2 when there is no demand. This study used 0.05 L/sm^2 because room-based demand-control quickly responded to occupancy. The limit for CO_2 was only 750 ppm, and occupants quickly elevated CO_2 concentrations, which increased ventilation demand.

The implementation of these controls required customization. This was straight-forward because the object-oriented modelling language allowed simple assembly of existing component models. The controls borrowed aspects from pre-defined demand-controls in the software and added additional ventilation requirements for humidity-based control.

The simulation tool also allowed specified performance of the heat exchanger and fans. The model of heat recovery received nominal inputs for flow rate and temperature efficiency. The

simulations assumed that future prototypes would achieve 90% efficiency at 15 L/s. The model used thermal theory to calculate part-load performance, and Paper 3 describes the derivation of the model. The fan models allowed custom inputs of specific fan power, efficiency, and coefficients for part-load performance. Customization of these components justified the use of this tool to investigate the 4th sub-hypothesis.

4 Results

The research tested aspects of the main hypothesis, which posited that development of room-based ventilation allows cost-effective model-based implementation for energy efficiency and indoor climate. The research divided the investigation into tests of different sub-hypotheses. This included experimental work as well as simulations of moisture transfer and demand control. The results of investigations provided preliminary evidence towards accepting or rejecting each sub-hypothesis and combined to evaluate the main hypothesis.

4.1 Experimental results

The experiments investigated the 1st sub-hypothesis and assessed the performance of the developed room-based ventilation units with respect to the specified criteria. The experiments also identified the existence of mutually exclusive criteria. Additionally, the experiments sought to investigate the 2nd sub-hypothesis and test the ability of the selected models to predict performance in the early stages of development. The analysis compared the predicted performance with measurements.

4.1.1 Rotary unit

Measurements on the rotary unit quantified airflows and determined temperature efficiencies.

4.1.1.1 Leakage Determination

Experiments determined fan flow rates, ventilation rates, and approximate pressure leakages.

4.1.1.1.1 Fan flow rates

Figure 6 shows the flow rates in the nominal range of operation from 5-15 L/s at various control signals. The flow rates increased linearly with fan speed, which adhered to fan affinity laws.

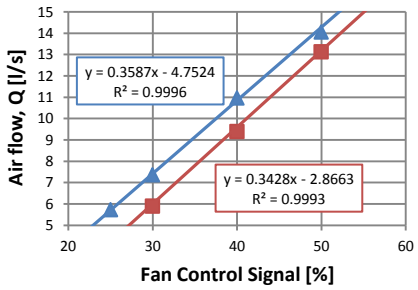

Figure 6. Independently measured flow rates in the rotary unit. The fan control signal was proportional to fan speed.

4.1.1.1.2 Pressure Leakage Approximation

Table 4 lists the results of pressure leakage approximations for three fan flow rates. The approximations used measurements and balance equations. The values were significantly greater than the modelled pressure leakages, which demonstrated a need to improve the models. Additionally, improved sealing may reduce pressure leakages to acceptable values.

Test	Expected fan flow rate, Q_{supply}	Stationary temperature efficiency, $\eta_{N=0}$		Modelled pressure leakage, $\dot{m}_{leak,press}/\dot{m}_{supply}$	
		Supply	Exhaust		
[Units]	*[L/s]*	*[%]*	*[%]*	*[%]*	*[L/s]*
24% supply, 27% exhaust	5	22	22	17	0.84
38% supply, 41% exhaust	10	17	19	12	1.19
52% supply, 55% exhaust	15	13	16	10	1.46

Table 4. Experimental results of temperature measurements on a stationary heat exchanger after accounting for heat gains. Modelled pressure leakages provide a comparison.

4.1.1.1.3 Direct Ventilation Rate Measurement

Table 5 shows the calculated ventilation rates from measurements with tracer gas, where Q_{fan} and Q_{vent} represent the fan flow rate and ventilation flow rate, respectively. Analysis compared measured ventilation rates to measured fan flow rates to estimate the percentage of recirculated air. This was nearly equivalent to pressure leakage, except that it also included short-circuiting of air outside the unit. Experiments helped to minimize short-circuiting by focusing circulation fans in the direction of the unit.

This experiment confirmed the need to reduce leakages with improved sealing. Measurements of fan powers and ventilation rates allowed calculations of specific fan powers, which are listed in Table 5. These values demonstrated low pressure drop through the unit, which satisfied Criterion 6.

Test	Measured fan flow rate, Q_{fan}	Air change rate	Corrected air change rate	Ventilation rate, $Q_{vent.}$		Recirculated air estimation, $1-(Q_{vent.}/Q_{fan})$	Specific fan power, *SFP*
[Units]	*[L/s]*	*[h^{-1}]*	*[h^{-1}]*	*[m3/h]*	*[L/s]*	*[%]*	*[J/m^3]*
0% supply, 0% exhaust	0	0.15	-	-	-	-	
24% supply 27% exhaust	5	0.60	0.45	14	3.9	22%	282
38% supply 41% exhaust	10	1.05	0.91	28	7.8	22%	282
52% supply 55% exhaust	15	1.63	1.48	46	12.8	15%	375

Table 5. Experimental results for the determination of ventilation rates and an estimation of pressure leakage.

4.1.1.2 Temperature Efficiency Measurements

A heat balance combined measurements of temperatures and heat gains to characterize the actual temperature efficiencies of the rotary unit at several ventilation rates.

4.1.1.2.1 Heat Input Method

Table 6 lists the measured temperature efficiencies based on delivered heat to the metering box. The table also lists measured and modelled ventilation rates as well as the modelled efficiencies, which accounted for 6% bypass leakage. The measured and modelled temperature efficiencies showed good agreement for the two largest flow rates and somewhat poor agreement for the smallest flow rate.

Test	HEX Drive Power	Fan Power	Heater Power	Heat Loss	Measured Fan Flow Rate	Measured Ventilation Rate	Measured Efficiency	Modelled Ventilation Rate	Modelled Efficiency
[Units]	*W*	*W*	W	W	*[L/s]*	*[L/s]*	[%]	*[L/s]*	[%]
24% sup. 27% exh.	5.2	1.1	20.7	6.4	5	3.9	83	3.6	90
38% sup. 41% exh.	5.2	2.2	33.8	5.8	10	7.8	83	8.2	84
52% sup. 55% exh.	5.2	4.8	64.8	5.9	15	12.8	79	13.0	78

Table 6. Experimental results from a heat balance to determine temperature efficiencies of the heat exchanger, and a comparison with modelled efficiency. The terms sup and exh represent fan signals for supply and exhaust airflows, respectively.

4.1.1.2.2 Temperature Measurements

Table 7 lists the temperature efficiencies based on measured temperatures after adjusting for heat gains. For the two largest flow rates, the average of these temperature efficiencies showed good agreement with modelled values. They also agreed with measured efficiencies using the heat input method. However, the supply and exhaust temperature efficiencies were dissimilar at all flow rates, which implied an un-centered heat exchanger or misallocated heat gains.

Test	Measured fan flow rate, Q_{fan}	Raw measured temperature efficiency		Temperature efficiency (corrected)			Modelled efficiency (corrected), η
		Supply, η_{supply}	Exhaust, $\eta_{exhaust}$	Supply, η_{supply}	Exhaust, $\eta_{exhaust}$	Average, $\eta_{average}$	
[Units]	*[L/s]*	*[%]*	*[%]*	*[%]*	*[%]*	*[%]*	*[%]*
24% sup. 27% exh.	5	96	95	91	97	94	90
38% sup. 41% exh.	10	86	88	81	87	84	84
52% sup. 55% exh.	15	79	80	74	78	76	78

Table 7. Experimental results with temperature measurements to determine temperature efficiencies of the heat exchanger, and a comparison with modelled results.

Figure 7 demonstrated that slowing rotational speeds provided decreased temperature efficiencies, which met the requirement of Criterion 1.

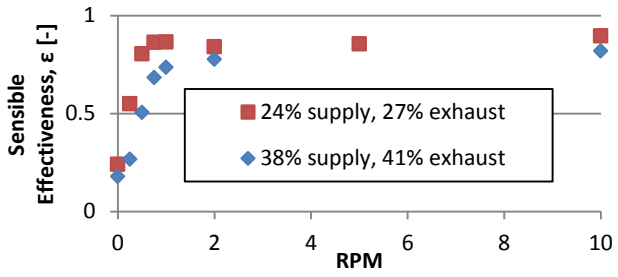

Figure 7. Experimental results of temperature efficiency for various rotational speeds.

4.1.2 Spiral unit

Experiments assessed the preliminary performance of the spiral unit.

4.1.2.1 Leakage

Experiments measured the external leakage as 0.53 L/s at 50 Pa, which equates to 2.7% of maximum flow. A modified experiment measured the ratio of internal leakage (W) as 12.1% of ventilation flow. This development attempted to minimize air leakages and did not predict their values. The external leakage met the aims of the development, but the internal leakage was excessive and should be reduced in future prototypes. Since this was a novel construction, the leakage measurements were a promising first result.

4.1.2.2 Flow Rates

Figure 8 shows the results of measured flow rates. The supply fan required twice the fan speed to achieve similar flow. The internal leakage ratio corrected the ventilation rates with the equation $Q_{real}=Q_{meas}\cdot(1-(0.12-0.02))=0.9\cdot Q_{meas}$, where *real* denotes the corrected value. Table 8 lists the corrected flow rates.

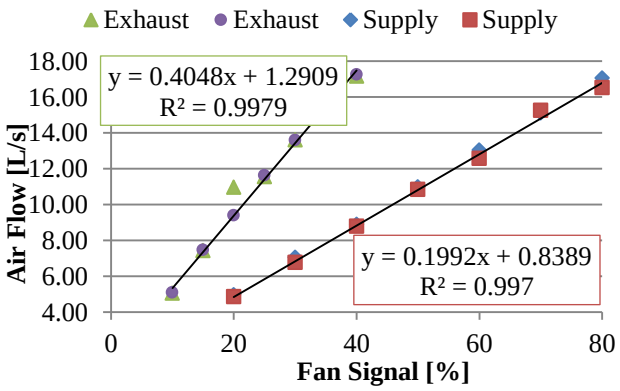

Figure 8. Measured fan flow rates at different fan signals for supply and exhaust in the developed single-room ventilation unit.

4.1.2.3 Temperature Efficiency

Table 8 lists the raw and corrected temperature efficiencies. The temperature efficiency at the maximum corrected flow rate was 82.2%. The efficiency remained stable for all flow rates, which may have implied a physical limit or measurement error. This was less than the predicted efficiency of 93.2%, but it was a promising first result for the novel heat exchanger.

Table 8. Measured and corrected ventilation rates and temperature efficiencies for the developed heat exchanger. The corrected flow rates account for internal leakage. The corrected supply temperature efficiencies account for heat gains from fans. The corrected exhaust temperature efficiencies account for both leakage and heat gains from fans.

Measured flow rate *L/s*	Corrected flow rate *L/s*	Measured $\eta_{exhaust}$ *%*	Corrected $\eta_{exhaust}$ *%*	Measured η_{supply} *%*	Corrected η_{supply} *%*	Simulated η_{supply} *%*	Measured $(SFP)_{supply}$ *J/m³*	Measured $(SFP)_{exhaust}$ *J/m³*	Simulated *SFP* *J/m³*
15	13.5	77.4	80.9	83.1	82.2	90.0	1148	378	300
12.5	11.25	80.2	83.3	82.5	81.8	91.5	987	347	217
10	9	78.0	79.8	83.2	82.6	93.1	856	311	147
7.5	6.75	78.8	79.7	81.4	80.8	94.7	690	249	90
5	4.5	70.9	69.6	75.8	75.3	96.4	458	229	45

4.1.2.4 Pressure Drop and SFP

Experiments also measured the approximate differences in static pressures across the heat exchanger and filter at balanced flow rates. At a corrected flow of 13.5 L/s, the measured pressure drop was 37 Pa across the heat exchanger and 3 Pa across the filter. This showed reasonable agreement with the predicted pressure drop of 34 Pa at 15 L/s across the heat exchanger. The measured fan powers and flow rates also allowed a calculation of SFP for each fan, which are shown in Table 8. The fan powers implied low pressure drop through the exhaust side of the unit, which satisfied Criterion 6. This also indicated the potential to decrease losses in the supply airflow of future prototypes.

4.2 Simulation results

The simulations of moisture transfer investigated the 3rd sub-hypothesis and tested the potential to identify moisture issues in room-based ventilation. The simulations of demand control investigated the 4th sub-hypothesis and tested the capability of a building simulation tool to enable modelling and performance prediction of an innovative system.

4.2.1 Moisture transfer

The reference case simulated recuperative heat recovery with the typical moisture production scenario. The test cases simulated the rotary unit with each of the moisture production scenarios. All simulated cases compared single-room and whole-dwelling ventilation.

4.2.1.1 Recuperative Heat Recovery

With the typical moisture production scenario, **Error! Reference source not found.** shows the minimum moving-average relative humidities for ventilation serving single-rooms or whole-dwellings. The table compares these values to the recommended design minimum in standard EN 15251 of 15%-20%. The results indicate that the relative humidity in the living room and bedrooms may be insufficient for short durations with recuperative heat recovery.

Table 9. Minimum moving-average relative humidities with the standard simulation parameters and recuperative heat recovery.

			Minimum moving average RH in heating season [%]				
Ventilation type	**EN 15251 Annex B.3 Criteria**	**Minimum moving average**	**Kitchen**	**Bathroom**	**Large bedroom**	**Small bedroom**	**Living room**
Single-room	> 15-20%	1-day	26	16	19	13	15
		7-day	28	26	22	16	18
		30-day	32	30	26	21	23
Whole-dwelling	> 15-20%	1-day	20	16	12	11	11
		7-day	22	23	15	14	14
		30-day	27	28	20	19	19

Error! Reference source not found. shows that the maximum 30-day moving averages did not exceed 60% RH. All values were less than the estimated limit of 70% room RH, which implied minimal mold risk. Figure 9 shows the percentage of time steps with greater than 70% RH for each ventilated zone with the typical moisture production scenario. Ventilation with recuperative heat recovery adequately removed moisture from all rooms for both ventilation types. In terms of the varied parameters, temperature efficiency did not influence indoor relative humidity, and infiltration had a very minor effect over the simulated range. Cooler room temperatures provided slightly higher relative humidities, but none of the simulated cases provided 30-day moving-averages greater than 70% room RH.

Table 10. Maximum 30-day moving-average relative humidities with standard simulation parameters and recuperative heat recovery.

Ventilation Type	**Maximum Moving Average**	**ASHRAE Surface Limit**	**Adjusted Room Limit**	**Kitchen [%]**	**Bathroom [%]**	**Large Bedroom [%]**	**Small Bedroom [%]**	**Living Room [%]**
Single-room	30-day	< 80%	< 70%	57	56	56	51	53
Whole-dwelling	30-day	< 80%	< 70%	57	57	49	48	49

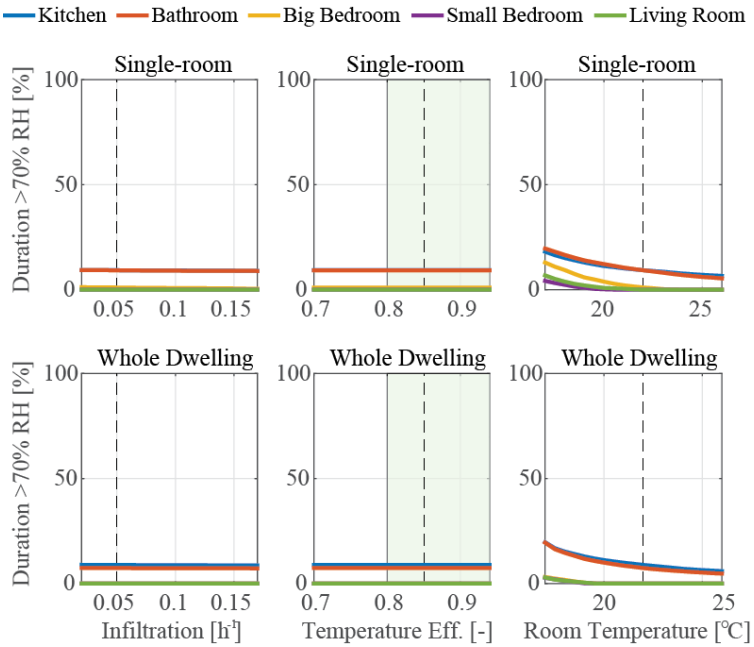

Figure 9. Recuperative heat recovery. Duration curves for the percentage of time with greater than 70% room RH for simulations with varied parameters.

4.2.1.2 Rotary unit

Results compared the rotary unit to the reference case.

4.2.1.2.1 Best case scenario

At the nominal conditions in this scenario, the moving average relative humidities never exceeded the limits of ASHRAE 160 for any of the simulated cases. Figure 10 presents the results of simulations for single-room ventilation and whole-dwelling ventilation with the best-case moisture scenario. Only the bathroom and large bedroom provided potential concerns. As described in Section 3.3.1.3.2, dust mites proliferate in fabrics at relative humidities greater than 50%, whereas the interior surfaces of bathrooms may be resistant to mold growth, which raises their critical humidity. As such, the high humidity in bedrooms was more concerning.

Figure 10 also presents the results of a rotary heat exchanger with the whole-dwelling ventilation system. The results were similar to the reference case with recuperative heat recovery. In this system, moisture transfer applied to the bulk properties of the mixed supply and exhaust airflows so recovered moisture was distributed more evenly throughout the dwelling.

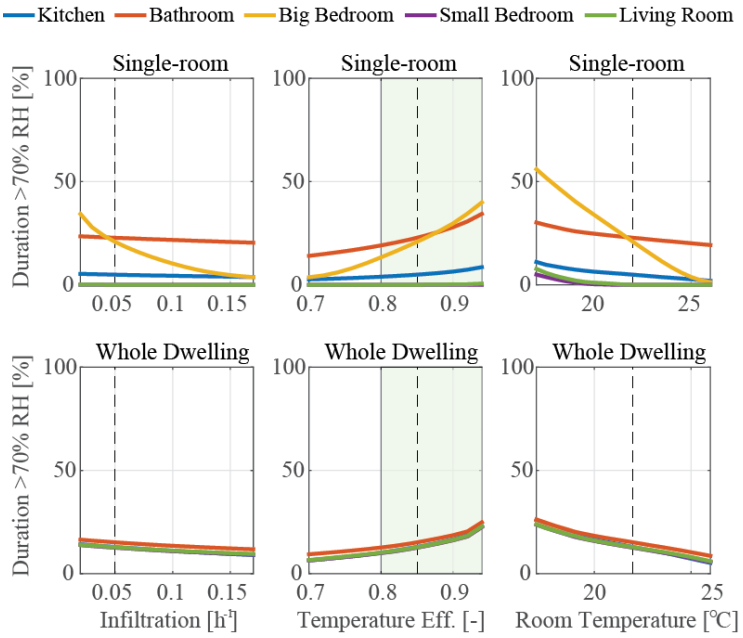

Figure 10. Simulation of regenerative heat recovery with the best-case moisture production scenario. Duration curves for percentage of time with greater than 70% room RH for simulations with varied parameters.

4.2.1.2.2 Typical scenario

With the typical moisture production scenario, Table 11 shows the minimum moving-average relative humidities for ventilation serving single-rooms or whole-dwellings with a rotary heat exchanger. Compared to the reference case with recuperative heat recovery, nearly all simulations provided better categories of relative humidity according to standard EN 15251. This demonstrates the potential benefit of moisture recovery to reduce dryness.

Table 11. Minimum moving-average relative humidities with the standard simulation parameters and a rotary heat exchanger.

			Minimum moving average RH in heating season [%]				
Ventilation type	**EN 15251 Annex B.3 Criteria**	**Minimum moving average**	**Kitchen**	**Bathroom**	**Large bedroom**	**Small bedroom**	**Living room**
Single-room	1-day	> 20%	43	40	27	13	15
	7-day		48	51	32	16	19
	30-day		53	53	42	21	25
Whole-dwelling	1-day	> 20%	40	39	33	32	33
	7-day		47	47	40	39	39
	30-day		57	57	50	49	50

Table 12 compares the maximum 30-day moving averages to the adjusted ASHRAE limits to predict mold growth at nominal conditions. The single-room ventilation did not violate limits in any dry rooms, while the kitchen and bathroom violated the limit to different degrees. The whole-dwelling ventilation produced excessive moisture risk in all rooms.

Table 12. Maximum 30-day moving-average relative humidities with standard simulation parameters and a rotary heat exchanger.

Ventilation Type	Maximum Moving Average	ASHRAE Surface Limit	Adjusted Room Limit	Kitchen [%]	Bathroom [%]	Large Bedroom [%]	Small Bedroom [%]	Living Room [%]
Single-room	30-day	< 80%	< 70%	87	94	64	51	53
Whole-dwelling	30-day	< 80%	< 70%	97	97	91	90	90

Figure 11 shows that all simulations of single-room ventilation, including parameter variations, provided excessive humidity in kitchens and bathrooms with this moisture scenario. The kitchen and large bedroom had similar profiles, but only the kitchen violated the ASHRAE limit with nominal parameters. Therefore a shift in parameters could result in a violation for the large bedroom as well.

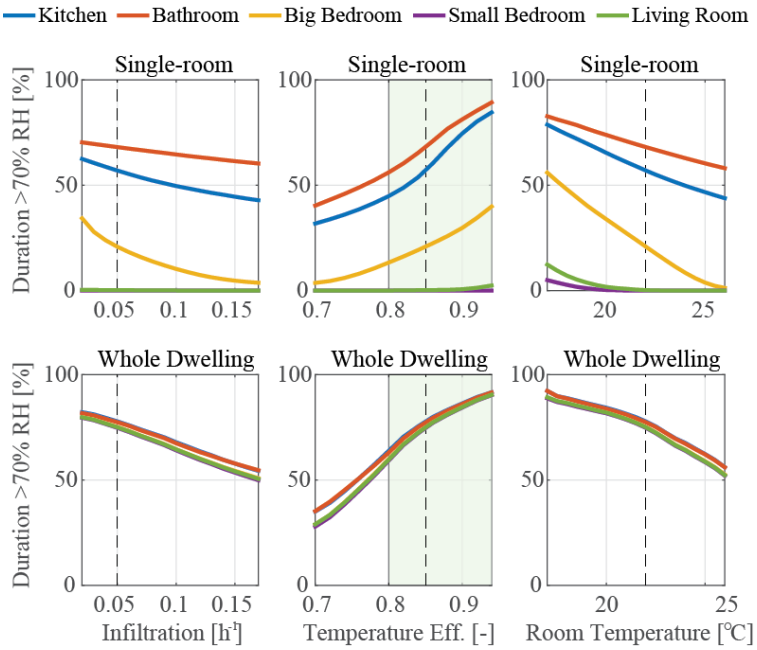

Figure 11. Simulation of regenerative heat recovery with the typical moisture production scenario. Duration curves for percentage of time with greater than 70% room RH for simulations with varied parameters.

Figure 12 shows the cumulative distribution curve for indoor RH during representative months to assess seasonal differences. A rightward or downward shift provided an unfavorable change in RH. The curves are relatively similar in all the displayed months. However January provided the least favorable conditions for the kitchen and bathroom and the most favorable conditions for the small bedroom and living room. Humidity in the adult bedrooms was the most critical in October.

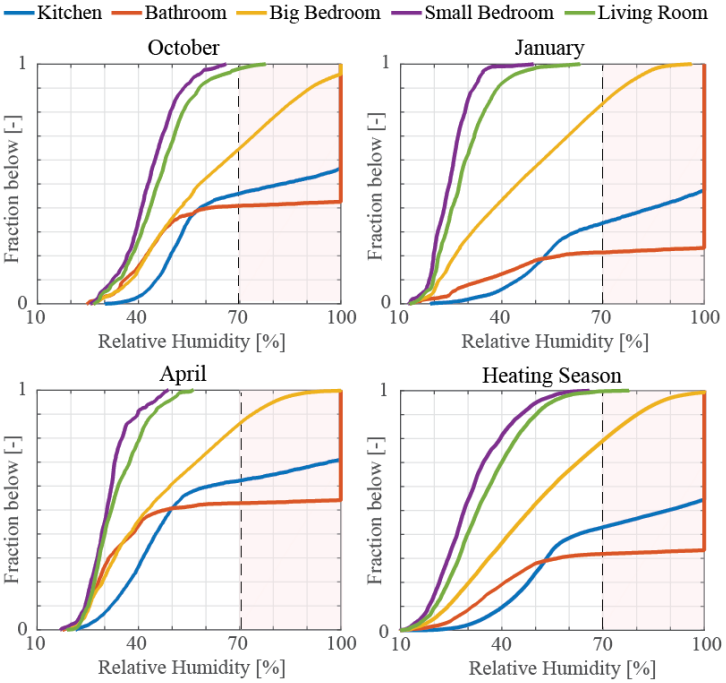

Figure 12. Cumulative distribution function of indoor relative humidities in each room during the months of October, January, April, and the whole heating season with a rotary heat exchanger in single-room ventilation and the typical moisture production scenario.

4.2.1.2.3 Worst-case scenario

With the worst-case moisture scenario, Figure 13 shows that ventilation serving only wet rooms provided an extremely high mold risk, but ventilation serving dry rooms yielded a moderate risk. With nominal parameters in the worst-case scenario, all 30-day moving averages exceeded the limits from ASHRAE 160 except for the case of the living room and bedrooms with single-room ventilation, which exceeded none. Whole-dwelling ventilation with a rotary heat exchanger yielded excessive relative humidity for the majority of the heating season in all the simulated rooms for all the parameter variations.

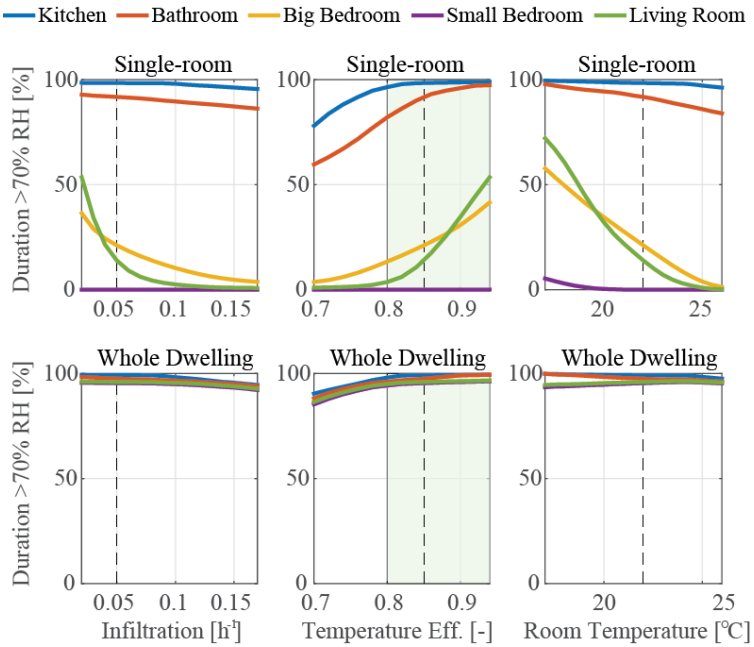

Figure 13. Simulation of regenerative heat recovery with the worst-case moisture production scenario. Duration curves for percentage of time with greater than 70% room RH for simulations with varied parameters.

4.2.2 Demand Control

Simulations compared single-room ventilation with demand control to whole-dwelling ventilation with constant flow. Both ventilation systems employed recuperative heat recovery. The simulated single-room ventilation unit represented the spiral unit with expected improvements. The simulated whole-dwelling unit represented a commercially available product. The results refer to categories from EN 15251 to characterize indoor climate.

4.2.2.1 Air quality

Simulations compared whole-dwelling ventilation to single-room ventilation with all doors either fully opened or fully closed.

4.2.2.1.1 CO_2 and Relative humidity

The simulations predicted relative humidities and CO_2 concentrations in each room. Table 13 lists the percentage of hours in category II or IV for each air quality indicator, ventilation type, and room with fully closed doors. Table 14 lists the same quantities from simulations with fully opened doors. Overall, the air quality analysis indicated that the developed single-room ventilation with demand-control could potentially achieve equal or better air quality as compared to a standard whole-dwelling ventilation system.

Table 13. Always open doors. Percentage of evaluated hours belonging to category II and IV for indoor relative humidity and CO_2 concentration with each ventilation type.

OPEN DOORS	Category II				Category IV			
	Duration below 60% RH		Duration below 900 ppm		Duration above 70% RH		Duration above 1200 ppm	
Room type	Whole-dwelling	Single-room	Whole-dwelling	Single-room	Whole-dwelling	Single-room	Whole-dwelling	Single-room
Kitchen	97	97	100	100	0	0	0	0
Bathroom	93	91	100	100	3	4	0	0
Living room	99	98	92-100	99	0	0	0	0
Adult bedroom	98	98	87	99	0	0	0	0
Child bedroom	99	98	100	100	0	0	0	0

Table 14. Always closed doors. Percentage of evaluated hours belonging to category II and IV for indoor relative humidity and CO_2 concentration with each ventilation type.

CLOSED DOORS	Category II				Category IV			
	Duration below 60% RH		Duration below 900 ppm		Duration above 70% RH		Duration above 1200 ppm	
Room type	Whole-dwelling	Single-room	Whole-dwelling	Single-room	Whole-dwelling	Single-room	Whole-dwelling	Single-room
Kitchen	97	94	96	100	0	1	0	0
Bathroom	82	82	100	100	17	17	0	0
Living room	98-99	99	66-76	68-72	0	0	0-23	0
Adult bedroom	98	99	67	71	0	0	21	0
Child bedroom	99	99	100	100	0	0	0	0

4.2.2.1.2 Average age of air

Table 15 reports the average age of air in each zone to cover a broader range of pollutants.

Table 15. Average age of air in each room with either whole-dwelling or single-room ventilation.

		Average age of air during occupied hours [h]					
Ventilation Type	Doors	Kitchen	Bath	Living	Adult	Child	**Total**
Whole-dwelling ventilation	Open	1.9	1.8	1.5-1.6	1.6	1.5-1.6	1.6
	Closed	1.9	1.8	1.4	1.4	1.4	1.5
Single-room ventilation	Open	2.13	1.9	1.8	1.7	1.8-2.0	1.9
	Closed	2.65	2.1	1.2-1.3	1.2	2.2	1.8

Table 16 shows the peak values for all time steps, which mainly occurred as the occupant entered a zone. Performance criteria for residential ventilation may specify limits for peak exposures to pollutants [50]. The peak concentration of pollutants would depend on the constant rate of emission a given zone. A room with highly polluting materials may cause an issue due to the increase in peak age of air. It was therefore difficult to conclude on its impact. Additionally, it was evident that open doors distributed air and provided less variance.

Table 16. Peak age of air in each room with demand-controlled single-room ventilation.

Peak age of air during all hours [h]						
Doors	Kitchen	Bath	Living	Adult	Child	**Total**
Open	4.9	5.0	4.5-4.6	4.5	4.7-5.4	4.8
Closed	6.8	8.3	6.8	7.4	7.5	7.2

4.2.2.2 Thermal Comfort

Table 17 lists the percentage of hours with operative temperatures in categories II and IV for each room and ventilation type. None of the simulated cases experienced temperatures below 18°C, which would also produce category IV thermal comfort. The single-room ventilation unit improved or maintained thermal comfort in all rooms.

Table 17. Percentage of hours with thermal comfort in categories II and IV for each room and ventilation type.

	OPEN DOORS				**CLOSED DOORS**			
	Category II		Category IV		Category II		Category IV	
	20°C to 25°C [%]		Above 27°C [%]		20°C to 25°C [%]		Above 27°C [%]	
Room type	Whole-dwelling	Single-room	Whole-dwelling	Single-room	Whole-dwelling	Single-room	Whole-dwelling	Single-room
Kitchen	92	96	2	0	88	95	4	0
Bathroom	95	98	1	0	95	99	1	0
Living room	92-93	92-93	2	1	88-89	89-90	3	1-2
Adult bedroom	94	96	1	0	95	96	0	0
Child bedroom	94-95	94-96	1	0	94-95	95-97	0-1	0
Average	**93.6**	**95.5**	**1.4**	**0.2**	**92.2**	**95.1**	**1.7**	**0.3**

4.2.2.3 Energy

Table 18 lists the annual delivered energy per unit floor area for ventilation and space heating as well as the total recovered heat. The whole-dwelling ventilation unit consumed 3.9 kWh/m^2 while the simulated single-room ventilation units together consumed 1.0 kWh/m^2 towards relative savings of 74%. Space heating consumed 78.4 kWh/m^2 to 79.0 kWh/m^2 using the whole-dwelling ventilation and 74.0 kWh/m^2 to 75.2 kWh/m2 using the single-room ventilation for relative savings of 4% to 6%. The recovered heat was similar for both ventilation types with opened doors, while the single-room ventilation units recovered roughly 8% less heat with closed doors.

Table 18. Simulated annual energy with each ventilation type and open or closed doors.

		Simulated annual energy [kWh/m^2]		
	Doors	**Ventilation**	**Space Heating**	**Heat Recovery**
Whole-dwelling	Open	3.9	78.4	45.1
	Closed	3.9	79.0	45.3
Single-room	Open	1.0	75.2	45.0
	Closed	1.0	74.0	41.6

4.2.2.3.1 Test Cases

In a simple test case, the measured exhaust fan powers provided coefficients for part-load performance of the simulated single-room ventilation units. The resulting fan energy consumption was 12% higher at 1.1 kWh/m^2. This demonstrated that the assumed SFPs and part-load coefficients were somewhat reasonable.

Another test case assessed the impact of window openings on the energy consumption of demand-controlled single-room ventilation. The simulation opened windows to one-quarter their potential during occupied hours of the cooling season. The resulting fan energy consumption was 22% less at 0.8 kWh/m^2. This demonstrated a response to decreased ventilation demand.

5 Discussion

This research investigated the theoretical development, performance prediction and validation, and implementation of room-based ventilation for renovated apartments. The following provides context for the results and describes their relevance. The discussion also provides a critique of methods and assumptions as well as a description of the potential impacts on future work.

5.1 Theoretical development

Theoretical development led to the construction of two room-based ventilation units.

5.1.1 Rotary unit

The first sub-hypothesis supposed that a set of development criteria could guide an integrated design process of room-based ventilation. The first development of a single-room ventilation unit produced a novel rotary heat exchanger with an inexpensive plastic honeycomb rotor. Theoretical development targeted high temperature efficiencies for a short heat exchanger, and plastic material limited efficiency reductions from longitudinal heat conduction. Continuous circular channels allowed excellent convective heat transfer and pressure efficiency for laminar flow, and high cycling speeds (i.e. up to 10 rpm) negated poor heat conduction. Based on predicted performance, a ceramic fixed-matrix heat exchanger is able to provide similarly high temperature efficiencies, but they operate in pairs, require greater heat transfer surface area, provide varying supply temperatures, and are widely available commercially. The development therefore produced a novel solution for a growing market with a thorough description of its theoretical background. Paper 1 documented this contribution to research.

Thermal design theory justified the use of a plastic rotary heat exchanger with small circular channels, but the construction of a mechanically functional single-room rotary unit proved difficult. Seals and mechanical components occupy space, so the development condensed the design into a smaller form by removing seals and placing the motor inside the heat exchanger. This required low tolerances in construction, which had negative consequences. The low tolerances insufficiently sealed against leakage flows. They also obstructed rotation, which demanded a larger motor and multiple re-alignments of the heat exchanger. Placement of the motor inside the heat exchanger also contributed to alignment issues. Criterion 3 required a compact construction with durable materials, but a better criterion would ensure durable and robust operation of the unit. The development could determine which designs are mechanically

feasible. This would limit the compactness of the unit. Placing the motor outside the heat exchanger would increase the length of the unit, and adding proper seals would increase its diameter. Both measures may be necessary to ensure robust its operation. Future theoretical developments would emphasize this point as a criterion.

5.1.2 Spiral unit

Development of the spiral recuperative unit targeted the same criteria with a single exception. The development did not require the heat exchanger to fit inside a single drilled hole in the façade. Instead, the unit occupied space inside the building and connected to the exterior through two smaller, less obtrusive holes. This resulted from a prioritization of low pressure drop at high nominal flow rates. The purpose was lower sound pressures and less fan power. Whereas the development of the rotary heat exchanger emphasized compactness, the spiral unit emphasized low pressure drop. A rotary heat exchanger can provide less resistance to flow because its rotation transfers heat between flows. Conversely, a recuperative heat exchanger must divide flows to run adjacently and directly transfer heat. This often results in added pressure drop from contractions and expansions of airflow, but the spiral unit construction maintained low pressure drop with the developed unit. The successful production of a novel low-pressure recuperative heat exchanger demonstrated the efficacy of the development criteria to guide an integrated design process based on theory. It also contributed to society and ongoing research with an inexpensive heat exchanger design for ventilation applications.

There was an obvious difference in size between the developed heat exchangers. Due to its placement inside the building, the spiral heat exchanger required a layer of insulation to prevent condensation on its exterior surface. This added size to the unit, and occupants may find its overall presence obtrusive. This demonstrated some mutual exclusivity between development criteria. If the unit is developed further, its success will depend on consumer demand, and its size may discourage potential buyers. Future versions may attempt to scale the spiral unit to a smaller size. This will compromise on other objectives, such as low pressure drop, so development must achieve a balance between criteria.

5.2 Performance and validation

Models enabled performance prediction where appropriate and experiments attempted to validate expected performance.

5.2.1 Rotary unit

Experiments assessed the performance of the rotary unit. After deducting heat gains and accounting for leakages, two measurement methods yielded temperature efficiencies greater than 83% for a flow rate of 7.8 L/s. Measurements confirmed that development met its intended aims for early stages of development, but the results carried uncertainties due to key assumptions.

For a nominal flow rate of 8 L/s, the plastic rotary heat exchanger provided a modelled temperature efficiency of 89%, but this neglected bypass leakage around the rotor. The corrected model accounted for 6% bypass leakage based on pressure loss equations, which yielded 84% temperature efficiency. The equation for bypass leakage showed a strong influence on temperature efficiency from fine changes to tolerance. The unit used low tolerances as seals, but this created unbalanced and directly unmeasurable leakages. The author did not conceive a method to quantify bypass leakage, so the validation of temperature efficiency models carried uncertainty.

With the expectation of considerable leakages, the experiments utilized temperature measurements and balance equations to determine actual temperature efficiencies. A motor inside the cylindrical axle of the heat exchanger drove its rotation, so its heat gains could not be accurately allocated. In the assumed heat balance, supply and exhaust evenly shared the contribution of 5.2 W. This provided a significant source of error, especially for low flow rates. The errors from unpredictable bypass leakage and misallocation of heat gains implied that the results could neither fully validate nor fully reject the model. Instead, the comparison between the results and the model provided a preliminary indication of its validity.

Additionally, the model for the ratio of pressure leakage predicted 12% leakage at the nominal flow rate for a 2 mm gap. One method to determine pressure leakage used balance equations and measurements, while another method subtracted ventilation rates from measured fan flow rates. These methods provided uncertainty since they combined multiple measurement techniques to indirectly determine leakage. Paper 3 describes the error of each measurement and none individually disrupted the result, but their compounded errors may have had an impact.

The discussion in Section 5.1.1 recommended placement of the motor outside the heat exchanger to improve its alignment and rotation. Moving the motor to a distinct and open section of the unit would also improve allocation of heat gains in measurements. Moreover, prior to implementation in a ventilation unit, an experimental setup could isolate the heat exchanger in a separate assembly with optimal sealing and minimal heat gains. This could

minimize leakages and improve validation of the regenerator effectiveness model. With known temperature efficiencies of the heat exchanger and properly allocated heat gains, the applied methods would accurately determine leakages and overall performance of the actual unit.

5.2.2 Spiral unit

The experimental tests provided a preliminary indication of the potential performance of the spiral heat exchanger. The unit requires further development to limit internal leakage and achieve targeted efficiencies and fan powers, but the initial results were promising. In particular, the development targeted low pressures to negate the impacts of smaller, less-efficient fans. The measured pressure drop through the heat exchanger was only 37 Pa at 13.5 L/s. As a result, the measured SFPs of the supply and exhaust fans at 15 L/s were 1148 J/m^3 and 378 J/m^3, respectively. The heat exchanger was symmetrical, so the low SFP of the exhaust fan represented the potential for improved airflow on the supply side of future prototypes. The exhaust SFP compared very well to other heat recovery ventilators. Roulet *et al.* audited thirteen units and the average SFP of ten centralized ventilation units was 1267 J/m^3. Despite lower fan efficiencies, the three single-room ventilation units had low SFPs that ranged from 720 J/m^3 to 864 J/m^3. Therefore, measurements on the spiral unit provided further evidence that low pressure drop can negate smaller fan efficiencies.

The model of temperature efficiency predicted increasing efficiencies at lower flow rates, as shown in Table 8. However the measured temperature efficiencies were similar at all flow rates. It is possible that the flows were not completely counter-current to each other and provided a physical limit on efficiency. Cross- and parallel-flow heat exchangers provide similar limits. However, the ratio of channel length to width ranged from roughly 10:1 to 3:1, which implied counter-current flows. As this was only a preliminary study, future tests should attempt to diagnose the cause of this limit and fix the issue. This would also help to validate the model of temperature efficiency and improve performance prediction.

5.2.3 Test apparatuses

In some cases, the availability of test apparatuses governed the selection of methods for experiments. In comparison with the standards, this either improved or reduced measurement certainty. For example, the methods in the first development used an apparatus that accurately measured thermal transmittance through a test element. An international standard would not assume the availability of this apparatus, so the applied methods improved upon the accuracy of the standardized methods. Similarly, the second development did not include access to tracer

gas, which the first development used to directly measure ventilation rates. Instead, the second development only measured fan flow rates and subtracted the measured leakage. The leakage test included significant assumptions and carried uncertainty. This uncertainty propagated to the calculated ventilation rates, so the author preferred direct measurement with a tracer gas. In this way, better apparatuses improved measurement certainty and added greater support to the second sub-hypothesis. This sub-hypothesis only states that experiments can validate modelled performance, so this could assume access to appropriate apparatuses.

5.3 Implementation

Simulations provided a means to investigate implementations of the developed units and their impacts on moisture effects, indoor climate, and energy consumption.

5.3.1 Simulation of moisture transfer

Simulations investigated the impacts on indoor humidity of regenerative and recuperative heat recovery in a specific set of conditions. In the simulations of single-room ventilation, the regenerator represented the rotary unit and the recuperator represented the spiral unit.

5.3.1.1 Rotary unit

The results indicated that highly efficient rotary heat exchangers were unsuitable for wet rooms under the assumed conditions due to excessive moisture recovery. The results also indicated that rotary heat exchangers may provide low to moderate mold risk with single-room ventilation of dry rooms for a range of probably conditions. These results guided recommendations for future implementations as posited by the 3rd sub-hypothesis. The author proposed that an adequate solution could implement rotary units in dry rooms and recuperators in wet rooms. A rotary heat exchanger transfers condensation to the supply air, so it does not require drainage. It may also prevent negative health impacts from dryness as indicated by **Error! Reference source not found.**. Recuperators require drainage, and installation in kitchens and bathrooms would allow easier access to plumbing. This combination utilizes the inherent advantages of each heat exchanger for the specific demands of individual rooms.

The moisture production schedule in dry rooms was similar for all three scenarios, so the rotary units consistently provided low to moderate mold risk. This could allow fine adjustments to control indoor humidity and minimize mold risk. The figures in Section 4.2.1.2 demonstrated the clear influence of varied parameters on the duration of excess relative humidity. Interestingly, two of the varied parameters are controllable during operation. This offers options

to adjust relative humidity in dry rooms to maintain appropriate levels. A rotary heat exchanger relies on cyclical regeneration, so a controller could reduce its cyclical speed to reduce heat transfer. Less heat transfer implies greater exhaust temperatures and drying capacities. Similarly, higher room temperatures result in lower relative humidities and mold risks, so a controller could maintain sufficient room temperatures to avoid risk. Both options could negatively affect occupant thermal comfort. The former option could generate local discomfort due to cool draughts from lower supply temperatures, while the latter could affect whole-body comfort with changes in room temperatures. However Figure 11 indicates that the required reductions in heat recovery or increases in room temperatures may be small to limit relative humidities to acceptable levels.

This investigation simplified implementation with many assumptions. Simulations did not account for moisture buffering from walls, which could dampen variations on indoor humidity and reduce the duration of exceeded limits. Salonvaara *et al.* [51] and Mortensen *et al.* [52] determined that typical interior paints can act as vapor barriers and effectively limit moisture transfer between construction materials and room air, so this assumption was reasonable. However, the simulation did not account for dampening from furniture, books, and textiles, and Svennberg *et al.* [53] measured a reduced daily peak of 10% RH and an increased daily trough of 5% RH after fully furnishing a room.Additionally, the simulations did not distinguish between interior surface materials, which provide different resistances to mold growth and different critical humidities. The investigation also assumed approximate surface temperatures, which highly influence surface relative humidities. Greater knowledge of the average Danish apartment could therefore improve the assessment of mold risk with these ventilation systems.

This study also assumed that rotary heat exchangers transfer all condensation in the exhaust to the supply air. This point is commonly advertised by manufacturers to emphasize that drainage is unnecessary. However, Holmberg [54] presents the possibility of excess moisture in a rotary heat exchanger. If cold outdoor air is nearly saturated upon entry to the heat exchanger then condensation may not be able to completely evaporate. This small longitudinal region would then accumulate moisture and its movement would be difficult to predict. This study assumed that any accumulated moisture moved to a warmer section of the heat exchanger and evaporated into the supply air. This can only be confirmed experimentally.

This investigation relied on simulations. Future work could attempt to validate these findings with experiments and real implementations. More specifically, future experiments could test the impacts of excess condensation and moisture transfer in the rotary unit. If developed sufficiently, the rotary and spiral units could be installed in the manner proposed above to assess

their combined impact in an actual renovated apartment. The use of temperature and humidity sensors in controls could help to validate performance.

5.3.1.2 Spiral Heat Exchanger

Simulations compared moisture impacts of both rotary and recuperative heat exchangers for a specific set of conditions. The simulated units had similar sizes and efficiencies to the developed units. The simulations used nominal temperature efficiencies of 85%, and the spiral unit provided a temperature efficiency of 82.2% at 13.5 L/s. It is therefore reasonable to equate the simulations of recuperative heat recovery in the single-room ventilation to future prototypes of the spiral unit. The simulations implied that the spiral unit may be effective at limiting indoor humidity, but it may also produce dry conditions over short durations in living rooms and bedrooms. These findings assumed that all condensation drained from the unit and did not obstruct airflow. If the spiral unit drains all condensation, simulations could predict the amount of condensate collected from the heat exchanger in each scenario. This could provide a useful tool for future development and dimensioning of condensate removal systems.

5.3.2 Simulation of demand-control

Simulations investigated the potential impacts of the developed spiral unit with demand control on indoor climate and energy consumption. The assessment compared its performance to a whole-dwelling ventilation system.

5.3.2.1 Rotary unit

The investigation of demand-control focused on the spiral unit, which could potentially provide a solution for all rooms in a renovated apartment. Conversely, the simulations of moisture transfer in the rotary unit indicated that it was likely unsuitable for wet rooms. Its potential suitability for dry rooms could lead to simulations with demand-control for improved performance. The author attempted to modify the recuperative heat exchanger model in IDA-ICE to represent the rotary unit and transfer condensation. The author used the IDA translator to convert the model from Neutral Model Formal to importable files. However, the modified model produced an error in the numerical solver of IDA-ICE, which could not factorize a singular matrix. Future work will attempt to correct this issue and assess the impact of a combined solution with rotary units in dry rooms and spiral units in wet rooms, as discussed in Section 5.3.1.1. This would expand the tests of the 4th sub-hypothesis to include user-modified component models.

5.3.2.2 Spiral heat exchanger

The software tool IDA-ICE provided a simulation environment to investigate the expected performance of the spiral unit. The simulation tool allowed performance specification of the fans and heat exchanger in distinct air handling units for each room. The tool also allowed changes and additions to pre-defined demand-controls through the use of a graphical user-interface. This enabled easy assembly and rapid simulation of an innovative room-based ventilation unit with demand-control, as posited by the 4th sub-hypothesis. The simulated single-room ventilation unit provided equivalent air quality and thermal comfort with less total fan energy. This demonstrated the potential of the developed unit.

Several key assumptions warrant further investigation. The minimum airflow rates of individual rooms ranged from 0.3 L/s to 0.9 L/s in simulations. This may be difficult to achieve in practice since many fans have built-in minimum fan speeds. Oscillations between on/off flow could produce this minimum on average, but sensors in the exhaust would be slower to detect increased concentrations of pollutants. Instead it may be necessary to increase the minimum ventilation rates in simulation, which would likely increase annual fan energy consumption. Additionally, the audit by Roulet *et al.* demonstrated that short-circuiting of airflow is a significant concern in single-room ventilation units. The simulations assumed that extracted air accurately represented the bulk properties of mixed air in each room, but short-circuiting could influence sensor readings in the exhaust. Short-circuiting could also reduce ventilation effectiveness. It is therefore important that future prototypes ensure adequate separation between the supply and exhaust airflows to limit short-circuiting.

6 Conclusions

This chapter concludes on the validity of the four sub-hypotheses based on the investigations. These four conclusions then provide the basis for a conclusion on the main hypothesis.

6.1 Theoretical development

Two theoretical developments resulted in two prototypes of single-room ventilation units with heat recovery. These developments investigated the 1st sub-hypothesis.

6.1.1 1st sub-hypothesis

Sub-hypothesis: The system requirements of a decentralized HVAC unit, as well as its conceptual strengths and weaknesses, can guide an innovative and integrated design process from inception to completion, including multiple generations of prototypes.

Evaluation: The 1st sub-hypothesis is true. Theory, literature, regulations, and context for implementation all contributed towards a set of development criteria, which guided successful development of two innovative prototypes for room-based ventilation with heat recovery.

The first development yielded a novel application of an inexpensive plastic honeycomb as a short rotary heat exchanger. Using thermal theory, an integrated design process guided the selection of an appropriate material and technology. This resulted in a plastic rotary heat exchanger with circular channels, which could effectively limit longitudinal conduction and maintain high rates of heat transfer. Models predicted temperature efficiencies and pressure losses that met the development criteria. Since a criterion required compactness, the prototype compromised robustness toward compact design. The author improved criteria for future prototypes with a prioritized requirement for robust operation. This provided a path to completion of the unit.

The second development yielded an inexpensive recuperative heat exchanger for ventilation applications. This development of the spiral unit targeted the same criteria with one exception. The development prioritized low pressure drop in a recuperative heat exchanger at high flow rates. The successful production of a novel low-pressure heat exchanger demonstrated the efficacy of criteria. The low pressure heat exchanger demanded a large construction, and occupants may find its overall presence obtrusive. This demonstrated some mutual exclusivity between development criteria, but this was not enough to reject the 1st sub-hypothesis.

6.2 Performance and validation

Experiments attempted to validate the modelled and expected performance of the two developed room-based ventilation units to investigate the 2nd sub-hypothesis.

6.2.1 2nd sub-hypothesis

Sub-hypothesis: The modelled and expected performance of decentralized HVAC systems and their individual components can be validated through full-scale testing in a laboratory environment.

Evaluation: The 2nd sub-hypothesis is mostly true. The measured performance of two prototypes showed reasonable agreement with modelled and expected performance at early stages of development, but experiments had difficulty isolating several quantities.

Experimental methods combined measurements and balance equations to determine temperature efficiencies and pressure leakages. The experiments did not isolate and measure bypass leakage. Instead the experiments validated the combined model of effectiveness and bypass leakage. Measurements on the rotary unit agreed with modelled performance and provided a temperature efficiency of 83-84% at 7.8 L/s after accounting for leakages and heat gains. The efficiency at the lowest flow rate showed less agreement. The single-room ventilation unit met the development criteria, but measurements showed excessive pressure leakage, which future improvements should limit. The actual pressure leakage was 18%, which was greater than expected. The author was satisfied with the methods to predict and measure performance. The experience provided a path to improve experiment by isolating components and known heat gains.

A single-room ventilation unit with a spiral heat exchanger performed reasonably well in experiments. The heat exchanger had a supply temperature efficiency of 82.2% and pressure drop of 37 Pa at 13.5 L/s. In comparison, the modelled efficiency and pressure drop were 93.2% and 34 Pa, respectively, at 15 L/s. The external and internal leakages were approximately 2.7% and 12.1% of flow, respectively. The author expected less internal leakage because two rolled sheets provided continuous separation between flows. Future prototypes should focus on the seals and connections at each end to limit leakage. Overall, these experiments provided promising first results.

The experiments measured performance and allowed a comparison to modelled and expected performance. Based on the results, the author identified improvements for individual aspects of each prototype, which may guide future development.

6.3 Implementation

Simulations implemented the developed ventilation units in renovated apartments in Denmark to test the 3rd and 4th sub-hypotheses through impacts on moisture issues, indoor climate, and energy-use.

6.3.1 3rd sub-hypothesis

Sub-hypothesis: Simulations can help to identify potential moisture issues for a range of probable conditions, and a comparison with recuperative heat recovery can guide recommendations for future implementations.

Evaluation: The 3rd sub-hypothesis is true. The simulations helped to identify potential moisture issues for a range of probable conditions with either of the developed prototypes, and the results guided recommendations for future implementations.

The investigation constructed and simulated moisture balance equations for the rotary unit. Its assessment focused on its moisture impacts in a typical renovated apartment in a humid temperate climate. The rotary unit recovered excess moisture in kitchens and bathrooms and provided a serious mold risk. The rotary unit was only suitable for ventilation of dry rooms, such as living rooms and bedrooms. In these rooms, the risk depended on moisture production. The sensitivity analysis concluded that varying heat recovery or indoor temperature could limit indoor relative humidity in dry rooms when a moderate mold risk was present. The rotary unit also elevated the minimum moving-average relative humidities, which may help to avoid negative health impacts from dry air. Simulations of recuperative heat recovery provided a baseline for comparison and characterized potential moisture effects of the spiral unit. The spiral unit may be effective at limiting indoor humidity, but it may also produce dry conditions over short durations in living rooms and bedrooms. These results guided recommendations for future implementations, including a proposed solution that matches the type of heat recovery to the needs of individual rooms.

6.3.2 4th sub-hypothesis

Sub-hypothesis: Recent advances in building simulation tools enable modelling of innovative systems, such as decentralized ventilation with heat recovery and advanced control, so simulations can predict and assess their potential.

Evaluation: The 4th sub-hypothesis is true. A building simulation tool enabled modelling and performance prediction of room-based ventilation units with heat recovery and user-defined demand-based controls in a renovated apartment in Denmark.

The software tool IDA-ICE provided a simulation environment to investigate the expected performance of the spiral unit. Simulations assumed improvements to the prototype, including adequate separation of supply and exhaust airflows and higher temperature efficiencies. The tool allowed performance specification of the fans and heat exchanger in separate air handling units for each room. The tool also allowed custom assembly of demand-controls through a graphical user-interface. This enabled rapid modelling and simulation of an innovative ventilation unit. Simulations compared the single-room demand-controlled unit to a commercially available whole-dwelling CAV unit. The simulation of whole-dwelling ventilation re-used the apartment model, re-assigned rooms to a single air-handling unit, and altered component specifications and room set-points. Both units ventilated a residential apartment in annual simulations and provided suitable indoor climate. In this comparison, the single-room units improved or maintained air quality and thermal comfort and consumed less annual fan energy. The analysis assumed that sensed values in the exhaust represented the fully-mixed room air, which provided idealized results for room-based ventilation. The results demonstrated the potential of single-room ventilation units to provide a viable alternative for renovated apartments through the inclusion of demand control. It also demonstrated capabilities for rapid modelling and simulation of an innovative ventilation unit.

The author attempted to modify the heat exchanger model in IDA-ICE to represent the rotary unit with moisture transfer. Implementing a user-modified component introduced an issue in the numerical solver, which requires further work. This did not reject the 4th sub-hypothesis as this investigation focused on the spiral unit, and efforts to model the rotary unit were not complete.

6.4 Main hypothesis

Main hypothesis: The development of decentralized HVAC systems allows cost-effective model-based implementation, including design, rapid prototyping, and advanced control for energy efficiency and indoor climate.

Evaluation: Based on the sub-hypotheses, the main hypothesis is true. Cost-effective development of decentralized HVAC systems, such as room-based ventilation with heat recovery and demand control, applied design criteria, rapid prototyping, experimentation, and model-based implementation (i.e. simulations) towards improvements in energy efficiency and indoor climate.

7 Perspectives and future work

This dissertation presented work in three main parts related to the development and operation of room-based ventilation for renovated apartments in Denmark. The first part was a theoretical development of prototypes. The second part investigated their performance. The third part simulated their impact on moisture effects, indoor climate, and energy-use.

7.1 Theoretical development

The methods for theoretical development were fairly specific to the context of renovated apartments in Denmark. However, the criteria and documented experiences may guide similarly successful developments in the future. These developments may also scale the novel heat exchangers to a larger size for use in whole-dwelling ventilation or other applications altogether. Both of the room-based ventilation units will be developed to completion in planned projects. Real implementations will test their actual performance before commercialization.

7.2 Performance and validation

The devised methods to test performance and validate models were mostly specific to the developed units and depended on the availability of apparatuses. However, the experiments demonstrated that modifications based on available measurements and balance equations could characterize performance in the early stages of development. Future developments may replicate these processes to create specific tests for novel ventilation units. These methods provided enough information to roughly verify expected performance and guide planned improvements. These development projects will perform planned improvements and use similar procedures to test the results. After completion of the units, the projects will use standardized testing, such as EN 13141-8, to report performance for commercialization.

7.3 Implementation

The methods to test implementation of the developed units used two different simulation techniques. The simulations to test the moisture effects of heat recovery used procedural code devised by the author to iteratively calculate moisture transfer. The simulations assumed closed doors to simplify equations for airflow. In contrast, the simulations of demand control used a flexible object-oriented modelling environment that allowed specification of components and multi-zonal airflow. Both methods were useful for their respective purposes, and future work may replicate and build upon these methods. Experimental data could improve the model of

moisture transfer in the rotary unit, and successful modification of the heat exchanger model in IDA-ICE would allow simulations of demand control.

8 References

[1] The Danish Government, The Danish Ministry of Climate, Energy and Buildings, Our Energy Future, 2011, Retrieved from http://www.ens.dk/ sites/ens.dk/files/policy/danish-climate-energy-policy/our future energy. pdf

[2] Energi Styrelsen, Energistatistik 2012 (2012), Retrieved from http://www.ens.dk/info/tal-kort/statistik-nogletal/arlig-energistatistik

[3] C.-H. Baek, S.-H. Park, Changes in renovation policies in the era of sustainability, Energy Build. 47 (2012) 485–496, http://dx.doi.org/10.1016/j. enbuild.2011.12.028

[4] Danish Energy Agency, Denmark's National Energy Efficiency Action Plan, Copenhagen, 2014, Retrieved from https://ec.europa.eu/energy/sites/ener/files/documents/2014_neeap_en_denmark.pdf

[5] Dansk Klima-, Energi- og Bygningsministeriet, Strategi for energirenovering af bygninger [Strategy for energy renovation of buildings], Copenhagen, 2014, Retrieved from http://www.ens.dk/sites/ens.dk/files/byggeri/Strategi-for-energirenovering-af-bygninger/strategi-for-energirenovering-af-bygninger-web-050514.pdf

[6] G. Villi, C. Peretti, S. Graci, M. De Carli, Building leakage analysis and infiltration modelling for an Italian multi-family building, J. Building Perform. Simul. 6 (2013) 98–118, http://dx.doi.org/10.1080/19401493.2012.699981

[7] I. Ridley, J. Fox, T. Oreszczyn, S. Hong, The impact of replacement windows on air infiltration and indoor air quality in dwellings, Int. J. Vent. 1 (2003) 209–218, Retrieved from http://discovery.ucl.ac.uk/2259/

[8] D.R. Wulfinghoff, Multiple-zone HVAC: an obsolete template, Energy Eng. 108 (2) (2011) 44–56, http://dx.doi.org/10.1080/01998595.2011.10389019

[9] Energi Styrelsen, Build. Regul. (2010), Retrieved from http://bygningsreglementet.dk/file/155699/BR10 ENGLISH.pdf

[10] Energi Styrelsen, Fælles bestemmelser for bygninger omfattet af bygningsklasse 2020 [Provisions common to buildings covered by the class of 2020] (2010), Retrieved from http://bygningsreglementet.dk/br10_05_id5181/0/42

[11] WHO Regional Office for Europe, WHO guidelines for indoor air quality: Dampness and mold, World Health Organization, Geneva, 2009, Retrieved from – http://www.euro.who.int/__data/assets/pdf_file/0017/43325/E92645.pdf

[12] R.B. Holmberg, Heat and mass transfer in rotary heat exchangers with nonhygroscopic rotor materials, J. Heat Transf. ASME. 99 (1977) 196–202.

[13] P.G. Wang, M. Scharling, K.P. Nielsen, 2001-2010 Design Reference Year for Denmark, Technical report 12-17, Danish Meteorological Institute, Copenhagen, 2012, Retrieved from – http://www.dmi.dk/fileadmin/Rapporter/TR/tr12-17.pdf

[14] H. Manz, H. Huber, A. Schalin, A. Weber, M. Ferrazzini, M. Studer, Performance of single room ventilation units with recuperative or regenerative heat recovery, Energy Build. 31 (2000) 37–47, http://dx.doi.org/10.1016/S0378- 7788(98)00077-2

[15] H. Manz, H. Huber, D. Helfenfinger, Impact of air leakages and short circuits in ventilation units with heat recovery on ventilation efficiency and energy requirements for heating, Energy Build. 33 (2001) 133–139, http://dx.doi.org/ 10.1016/S0378-7788(00)00077-3

[16] L. Baldini, M.K. Kim, H. Leibundgut, Decentralized cooling and dehumidification with a 3 stage LowEx heat exchanger for free reheating, Energy Build. 76 (2014) 270–277, http://dx.doi.org/10.1016/j.enbuild.2014. 02.021

[17] F. Meggers, J. Pantelic, L. Baldini, Evaluating and adapting low exergy systems with decentralized ventilation for tropical climates, Energy Build. 67 (2013) 559–567, http://dx.doi.org/10.1016/j.enbuild.2014.05.009

[18] M.K. Kim, H. Leibundgut, J.-H. Choi, Energy and exergy analyses of advanced decentralized ventilation system compared with centralized cooling and air ventilation systems in the hot and humid climate, Energy Build. 79 (2014) 212–222, http://dx.doi.org/10.1016/j.enbuild.2014.05.009

[19] R.S. Iyengar, E. Saber, F. Meggers, The feasibility of performing high-temperature radiant cooling in tropical buildings when coupled with a decentralized ventilation system, HVAC&R Res. 19 (2013) 992–1000, http:// dx.doi.org/10.1080/10789669.2013.826065

[20] C.J. Simonson, R.W. Besant, Heat and moisture transfer in energy wheels during sorption, condensation, and frosting conditions, J. Heat Transfer. 120 (1998) 699. doi:10.1115/1.2824339.

[21] W. Ruan, M. Qu, W.T. Horton, Modeling analysis of an enthalpy recovery wheel with purge air, Int. J. Heat Mass Transf. 55 (2012) 4665–4672. doi:10.1016/j.ijheatmasstransfer.2012.04.025.

[22] S. De Antonellis, M. Intini, C.M. Joppolo, F. Pedranzini, Experimental analysis and practical effectiveness correlations of enthalpy wheels, Energy Build. 84 (2014) 316–323. doi:10.1016/j.enbuild.2014.08.001.

[23] L. Jensen, Fuktöverföring vid regenerativ värmeväxling [Moisture transfer in regenerative heat exchange], Lund University, Lund, 2010, Retrieved from – http://www.lunduniversity.lu.se/lup/publication/3290479

[24] L. Jensen, Fukttillskott i frånluft [Excess moisture in exhaust air], Lund University, Lund, 2010, Retrieved from – http://www.lunduniversity.lu.se/lup/publication/3290476

[25] D. Malm, Fuktåterföring i roterande värmeväxlare [Moisture transfer in rotary heat exchangers] (Master's Thesis), Royal Institute of Technology, Stockholm, 2012, Retrieved from – http://kth.diva-portal.org/smash/get/diva2:550959/FULLTEXT01.pdf

[26] A. Hesaraki, S. Holmberg, Demand-controlled ventilation in new residential buildings: Consequences on indoor air quality and energy savings, Indoor Built Environ. 24 (2013) 162–173. doi:10.1177/1420326X13508565.

[27] W. Cho, D. Song, S. Hwang, S. Yun, Energy-efficient ventilation with air-cleaning mode and demand control in a multi-residential building, Energy Build. 90 (2015) 6–14. doi:10.1016/j.enbuild.2015.01.002.

[28] J. Laverge, N. Van Den Bossche, N. Heijmans, A. Janssens, Energy saving potential and repercussions on indoor air quality of demand controlled residential ventilation strategies, Build. Environ. 46 (2011) 1497–1503. doi:10.1016/j.buildenv.2011.01.023.

[29] M. Morelli, L. Rønby, S.E. Mikkelsen, M.G. Minzari, T. Kildemoes, H.M. Tommerup, Energy retrofitting of a typical old Danish multi-family building to a "nearly-zero" energy building based on experiences from a test apartment, Energy Build. 54 (2012) 395–406. doi:10.1016/j.enbuild.2012.07.046.

[30] D.K Mortensen, I. Walker, M. Sherman, Optimization of Occupancy Based Demand Controlled Ventilation in Residences, Int J Vent. 10 (2011) 49–60. Retrieved from http://eetd.lbl.gov/sites/all/files/publications/20-optimization-2011.pdf

[31] C.A. Roulet, F.D. Heidt, F. Foradini, M.C. Pibiri, Real heat recovery with air handling units, Energy Build. 33 (2001) 495–502. doi:10.1016/S0378-7788(00)00104-3.

[32] R.K. Shah, D.P. Sekulic, Fundamentals of Heat Exchanger Design, John Wiley & Sons, Hoboken, NJ, 2003, http://dx.doi.org/10.1002/9780470172605

[33] European Committee for Standardization, Ventilation for buildings – Performance testing of components/products for residential ventilation – Part 8: Performance testing of un-ducted mechanical supply and exhaust ventilation units (including heat recovery) for mechanical ventilation systems intended for a single room, EN 13141-8:2014, Authors, Brussels, Belgium, 2014.

[34] ASHRAE Standing Standard Project Committee 160, Addendum A to ANSI/ASHRAE Standard 160-2009, American Society of Heating, Refrigerating and Air-Conditioning

Engineers, Atlanta, 2011, Retrieved from – https://www.ashrae.org/File%20Library/docLib/StdsAddenda/160_2009_a_COMPLETE.pdf

[35] A. Tenwolde, A review of ASHRA standard 160 - Criteria for moisture controle design analysis in buildings, J. Test. Eval. 39 (2011) 1–5. doi:10.1520/jte102896.

[36] D. Johansson, H. Bagge, L. Lindstrii, Measurements of occupancy levels in multi-family dwellings - Application to demand controlled ventilation, Energy Build. 43 (2011) 2449–2455. doi:10.1016/j.enbuild.2011.05.031.

[37] British Standard Institution, Code of practice for control of condensation in buildings, BS 5250, Authors, London, 1989.

[38] Chartered Institution of Building Services Engineers, CIBSE Guide A – Environmental Design. Authors, London, 1999.

[39] W.J. Angell, W.W. Olson, Moisture sources associated with potential damage in cold climate housing, Minnesota Extension Service, University of Minnesota (1988) 1-8.

[40] A. TenWolde, C.L. Pilon, The effect of indoor humidity on water vapor release in homes, Therm. Perform. Exter. Envel. Whole Build. X Int. Conf. (2007) 1–9. Retrieved from – http://www.fpl.fs.fed.us/documnts/pdf2007/fpl_2007_tenwolde001.pdf

[41] F.W.H. Yik, P.S.K. Sat, J.L. Niu, Moisture generation through Chinese household activities, Indoor Built Environ. 13 (2004) 115–131. doi:10.1177/1420326X04040909.

[42] N.J. Rowan, C.M. Johnstone, R.C. McLean, J.G. Anderson, J. a Clarke, Prediction of toxigenic fungal growth in buildings by using a novel modelling system., Appl. Environ. Microbiol. 65 (1999) 4814–21. Retrieved from – http://www.pubmedcentral.nih.gov/articlerender.fcgi?artid=91649&tool=pmcentrez&rendertype=abstract.

[43] P. Johansson, I. Samuelson, A. Ekstrand-Tobin, K. Mjörnell, P.I. Sandberg, E. Sikander, Extracts from Microbiological growth on building materials: Critical moisture levels - State of the art, SP Technical Research Institute of Sweden, Borås, 2005, Retrieved from – http://www.kuleuven.be/bwf/projects/annex41/protected/data/SP%20Oct%202005%20Paper%20A41-T4-S-05-3.pdf

[44] E. Vereecken, S. Roels, Review of mould prediction models and their influence on mould risk evaluation, Build. Environ. 51 (2012) 296–310. doi:10.1016/j.buildenv.2011.11.003.

[45] L.G. Arlian, Water balance and humidity requirements of house dust mites, Exp. Appl. Acarol. 16 (1992) 15–35. doi:10.1007/BF01201490.

[46] L.M. Reinikainen, J.J.K. Jaakkola, Significance of humidity and temperature on skin and upper airway symptoms, Indoor Air. 13 (2003) 344–352. doi:10.1111/j.1600-0668.2003.00155.x.

[47] European Committee for Standardization, Indoor environmental input parameters for design and assessment of energy performance of buildings addressing indoor air quality, thermal environment, lighting and acoustics, EN 15251:2007, Authors, Brussels, Belgium, 2007.

[48] J. Sundell, H. Levin, W.W. Nazaroff, W.S. Cain, W.J. Fisk, D.T. Grimsrud, et al., Ventilation rates and health: Multidisciplinary review of the scientific literature, Indoor Air. 21 (2011) 191–204. doi:10.1111/j.1600-0668.2010.00703.x.

[49] International Organization for Standardization, Ergonomics of the thermal environment -- Analytical determination and interpretation of thermal comfort using calculation of the PMV and PPD indices and local thermal comfort criteria, EN ISO 7730:2006, European Committee for Standardization, Brussels, Belgium, 2006.

[50] European Committee for Standardization, Ventilation for buildings. Determining performance criteria for residential ventilation systems, EN 15665:2009, Authors, Brussels, Belgium, 2009.

[51] M. Salonvaara, T. Ojanen, A. Holm, H. Kunzel, A. Karagiozis, Moisture buffering effects on indoor air quality – experimental and simulation results, Proc. Perform. Exter. Envel. Whole Build. IX (2004) 1–11.

[52] L.H. Mortensen, C. Rode, R. Peuhkuri, Full scale tests of moisture buffer capacity of wall materials, Proc. 7th Symp. Build. Phys. Nord. Ctries. (2005) 662–669.

[53] K. Svennberg, L.G. Hedegaard, C. Røde, Moisture buffer performance of a fully furnished room, Proc. Perform. Exter. Envel. Whole Build. IX (2004) 1–11.

[54] R.B. Holmberg, Prediction of condensation and frosting limits in rotary wheels for heat recovery in buildings, ASHRAE Transactions. 95 (1989) 64-69.

List of Symbols

Latin

A	Heat transfer surface area [m^2]
A_k	Cross-sectional area perpendicular to the direction of thermal conductivity [m^2]
A_o	Orifice area [m^2]
c_p	Specific heat capacity [J/kgK]
C_d	Coefficient of discharge [-]
C	Heat capacity rate [W/K]
C^*	Ratio of minimum to maximum heat capacity rates [-]
C_r^*	Ratio of rotor to minimum heat capacity rates [-]
$C(t)$	Tracer gas concentration at time, t [ppm]
CAV	Constant air-volume
D_h	Hydraulic diameter [m]
DVU	Decentralized ventilation unit
e	Partial pressure of water vapor in air [hPa]
f	Fanning friction factor [-]
G_i	Moisture release in time step i [g]
h	Convective heat transfer coefficient [W/m^2K]
k	Thermal conductivity [W/mK]
K	Pressure loss coefficient [-] or calculation parameter [L/s]
L	Length [m]
$\dot{m}$	Mass flow rate [g] [kg/s]
N	Rotational speed [rev/s] or air changes rate [dt^{-1}][h^{-1}]
NTU	Number of transfer units [-]
NTU_0	Modified number of transfer units [-]
Nu	Nusselt Number, [-]
p	Barometric pressure [hPa]
P	Power demand [W]
Q	Volumetric flow rate [m^3/s]
r	Radius [m]
Re	Reynold's number [-]
SFP	Specific fan power
t	Elapsed time [h]
T	Temperature [°C]
u	Velocity [m/s]
U	Total heat transfer coefficient [W/m^2K]
V	Volume [m^3]
VAV	Variable air-volume
W	Internal leakage ratio [-]
x	Moisture content in mass of water per mass of dry [g/kg]

Greek

δ	Thickness [m]
Δp	Pressure difference [Pa]

ε	Effectiveness [-]
λ	Dimensionless parameter for longitudinal heat conduction [-]
μ	Dynamic viscosity [Pa·s]
$\eta_{supply/exhaust}$	Temperature efficiency of supply or exhaust [-]
φ	intermediary parameter in the calculation of C_λ [-]
ρ	Density [kg/m^2]
σ	Ratio of rotor void area to face flow area [-]

Subscripts

amb	Ambient air
byp	Bypass leakage around a heat exchanger
carry	Carryover leakage between flows
cold	Cold chamber in an experiment
contract	Entrance / contraction
divider	Plate dividing supply and exhaust flows
dmix	Mixed exhaust from dry rooms
dry	Dry air
exh	Flow direction
expand	Exit/expansion
heater	Property of the heater in the metering box
HEX	Heat exchanger
fan	Property of the fan
i	Time step index
indoor	Property of warm/indoor air
inlet	Property at the inlet
inf	Infiltration air
leak	Air leakage
int	Internal leakage
max	Maximum
mean	Mean value
meas.	Measured
min	Minimum
N=0	Stationary heat exchanger
outdoor	Property of cold/outdoor air
outlet	Property at the outlet
press	Pressure leakage between flows
real	Corrected value
room	Room index
rotor	Property of the rotary heat exchanger
sat	Saturation
sup	Flow direction or point of supply
unsealed	Unblocked airflow
vent	Fresh ventilation without recirculated air
warm	Warm chamber in an experiment
λ=0	Longitudinal conductive resistance is zero

List of Figures

List of Tables

Appendix A – Paper 1

K.M. Smith, S. Svendsen,

Development of a plastic rotary heat exchanger for room-based ventilation in existing apartments,

Energy Build. 107 (2015) 1–10.

doi:10.1016/j.enbuild.2015.07.061

Energy and Buildings 107 (2015) 1–10

Contents lists available at ScienceDirect

Energy and Buildings

journal homepage: www.elsevier.com/locate/enbuild

Development of a plastic rotary heat exchanger for room-based ventilation in existing apartments

Kevin Michael Smith*, Svend Svendsen

Department of Civil Engineering, Technical University of Denmark, DTU Byg, Building 118, Brovej, Kgs. Lyngby 2800, Denmark

ARTICLE INFO

Article history:
Received 19 March 2015
Received in revised form 9 July 2015
Accepted 24 July 2015
Available online 1 August 2015

Keywords:
Decentralized ventilation
Single room ventilation
Heat recovery ventilator
Rotary heat exchanger
Energy retrofit

ABSTRACT

The existing building stock will likely undergo widespread energy renovations to meet future emissions targets. Single-room ventilation may enable the process due to its simple installation, low fan power, and potential for local heat recovery. A short plastic rotary heat exchanger is developed for single-room ventilation based on thermal design theory. Performance is predicted from correlations of dimensionless groups for regenerative heat exchangers, and this guides the selection of a polycarbonate honeycomb with small circular channels. Experiments quantify flows and determine temperature efficiencies at several ventilation rates while accounting for heat gains from motors and air leakage. The measured and modelled temperature efficiencies show adequate agreement and exceed 80% for a balanced nominal ventilation rate of 28 m^3/h. This result meets the development criteria but cannot validate the model due to the presence of unmeasurable bypass leakage. All leakages are slightly excessive and should be reduced with proper sealing. Experimental results demonstrate the potential to reduce heat recovery by slowing rotational speed, which is required to prevent frost accumulation. Overall, the development meets objectives and provides a novel and efficient option for ventilation heat recovery.

© 2015 Elsevier B.V. All rights reserved.

1. Introduction

The Danish government has targeted full reliance on renewable sources of energy for heating and electricity by 2035. This would stabilize energy prices and assist global efforts against anthropogenic climate change [1]. Building retrofits save energy and offset requirements for renewable supply. In 2012, heating in households accounted for 26% of final energy consumption in Denmark [2], so reduced heating could significantly contribute to energy savings. New construction represents less than 1% of the building stock annually in Europe [3], so buildings that exist at present will likely consume a significant share of energy in 2035. It is therefore important to retrofit these buildings to meet future targets.

Building retrofits can improve heat retention by limiting thermal transmittance and air infiltration. Common measures include window replacement, sealing of cracks and orifices, added thermal insulation, and installation of ventilation with heat recovery. Many exhaust systems draw fresh air through the facade, so improved airtightness leads to poor indoor air quality unless accompanied by mechanical supply [4]. Ridley et al. analyzed the impact of window replacement on the infiltration rate of dwellings and recommended controllable ventilation to avoid moisture problems and comply with regulations [5]. Controllable mechanical ventilation should utilize heat recovery to simultaneously improve air quality and reduce heat losses in temperate climates. The investment in heat recovery depends on cost-effectiveness, building regulations, and the extent of each renovation.

Many existing apartments use mechanical exhaust and lack available space for supply ducts and central heat recovery. Even with available space, installation may be labor intensive and temporarily displace occupants. Installation of supply ducts also implies greater frictional losses and fan power. To reflect this, the 2010 Danish building regulations set the maximum energy for ventilation at 1000 J/m^3 for single-dwelling systems and 1800 J/m^3 for systems serving multiple dwellings [6]. To conserve space and reduce energy for ventilation, retrofits may install supply and exhaust in the façade of each room. This minimizes frictional losses, facilitates installation, and allows local heat recovery [7]. A broad term for this technology is “decentralized ventilation unit” (DVU), which may refer to units that serve single rooms or individual dwellings. This article specifically deals with DVUs for single rooms.

This work aims to develop a short, novel heat exchanger for single-room ventilation that would meet future building regulations and to experimentally validate its performance. In early research on DVUs, Manz et al. [8] experimentally tested and numerically simulated different types intended for cold climates

* Corresponding author. Tel.: +45 45 25 50 34.
E-mail address: kevs@byg.dtu.dk (K.M. Smith).

http://dx.doi.org/10.1016/j.enbuild.2015.07.061
0378-7788/© 2015 Elsevier B.V. All rights reserved.

Nomenclature

Latin

A	heat transfer surface area [m^2]
A_k	cross-sectional area perpendicular to the direction of thermal conductivity [m^2]
A_o	orifice area [m^2]
c_p	specific heat capacity [J/kg K]
C_d	coefficient of discharge [–]
C_{min}	minimum heat capacity rate [W/K]
C_{max}	maximum heat capacity rate [W/K]
C^*	ratio of minimum to maximum heat capacity rates [–]
C_{rotor}	rotor heat capacity rate [W/K]
C^*_{rotor}	ratio of rotor to minimum heat capacity rates [–]
$C(t)$	tracer gas concentration at time, t [ppm]
D_h	hydraulic diameter [m]
f	fanning friction factor [–]
h	convective heat transfer coefficient [W/m^2 K]
k	thermal conductivity [W/m K]
$K_{contract}$	pressure loss coefficient for entrance/contraction [–]
K_{expand}	pressure loss coefficient for exit/expansion [–]
L	length [m]
M	mass [kg]
$\dot{m}$	mass flow rate [kg/s]
N	rotational speed [rev/s]
NTU_0	number of transfer units [–]
Nu	Nusselt number [–]
P	power demand [W]
Q	volumetric flow rate [m^3/s]
r	radius [m]
Re	Reynold's number [–]
T	temperature [°C]
u	velocity [m/s]

Greek

δ	thickness [m]
λ	dimensionless parameter for longitudinal heat conduction [–]
Δp	pressure difference [Pa]
$\eta_{supply/exhaust}$	temperature efficiency of supply or exhaust [–]
ρ	density [kg/m^2]
σ	ratio of rotor void area to face flow area [–]
τ	period or cycle length [s]
ε	effectiveness [–]

Subscripts

supply	flow direction or point of supply
exhaust	flow direction or point of exhaust
indoor	property of warm/indoor air
outdoor	property of cold/outdoor air
vent	fresh ventilation without recirculated air
leak	air leakage
pressure	pressure leakage between flows
carry	carryover leakage between flows
bypass	bypass leakage around a heat exchanger
rotor	property of the rotary heat exchanger
$\lambda = 0$	longitudinal conductive resistance is zero
$N = 0$	stationary heat exchanger
divider	plate dividing supply and exhaust flows
HEX	heat exchanger

to assess their performance with respect to ventilation efficiency, thermal comfort, heat recovery, electrical energy input, and acoustics. Sound pressure and sound reduction were the main issues with DVUs and required further improvement. The lead authors published additional research that focused on unintentional flows of heat and air both inside and outside DVUs [9]. Their model described these flows, and numerical examples showed considerable efficiency reductions unless unintended flows were limited to acceptable levels. Based on their results, the authors recommended greater focus on construction, manufacture, and installation. DVUs are increasingly available commercially, but the work by Manz et al. is among limited published research investigating DVUs for cold or temperate climates. Other published research documented the development and assessment of novel DVUs for warm and humid climates [10–13], but these DVUs are generally not appropriate for temperate climates.

2. Theoretical development

This work seeks to develop a heat exchanger for a single-room DVU in a temperate climate. Its design is based on the following list of criteria for a nominal ventilation flow of 8 L/s:

1. Provide option to modulate bypass of heat recovery.
2. Provide greater than 80% supply temperature efficiency, η_{supply}, which is measured as:

$$\eta_{supply} = \frac{\left(T_{supply} - T_{outdoor}\right)}{\left(T_{indoor} - T_{outdoor}\right)} \quad (1)$$

   where T_{supply}, $T_{outdoor}$, and T_{indoor} are the measured temperatures of supply air, outdoor air, and indoor air, respectively.
3. Devise a compact construction with inexpensive and durable materials.
4. Minimize air leakages.
5. Fit the heat exchanger into a short cylindrical tube for drill-hole installation.

2.1. Bypass

Criterion 1 requires the option to reduce sensible heat recovery during operation. This option serves several purposes. Slight reductions prevent frost accumulation in the exhaust by maintaining sufficient outlet temperatures. Moderate reductions control supply air temperatures and maintain stable indoor air temperature. Full reductions combine with increased ventilation rates to provide cooling since ambient temperatures in Denmark rarely exceed 26 °C. These requirements are especially important in deeply renovated buildings which experience shorter heating seasons and greater response to heat gains. The final DVU will include sensors and advanced controls to facilitate these functions in later work.

This development considers both regenerative and recuperative heat exchangers, which are known as regenerators and recuperators, respectively. Regenerators intermittently expose flows to a medium to store and recover heat, while recuperators provide heat transfer through a solid medium between flows. In regenerators, slower cycle speeds reduce sensible heat recovery without requiring additional space and mechanisms for bypass air flow. Simple bypass helps to meet the requirements of Criterion 1, so this development prioritizes regenerators. Section 3.2.2 reports on experiments which test the final DVU at different cycling speeds to verify a reduction in heat recovery.

2.2. Temperature efficiency

Criterion 2 constrains the type of heat exchanger to be used. Only counter-flow heat exchangers provide temperature efficiencies

greater than 80% for balanced flow. Options exist for both regenerative (e.g. rotary; fixed-matrix) and recuperative (e.g. parallel plate; shell-and-tube) heat exchangers. This development prioritizes a theoretical investigation of regenerators based on Criterion 1.

2.2.1. Regenerator model: ε-NTU$_0$ method

The ε-NTU$_0$ method predicts sensible effectiveness, ε, of regenerators using dimensionless groups. This development considers both rotary and fixed-matrix heat exchangers. Heat capacity rates are roughly similar for balanced airflows, so the designs of rotary and fixed-matrix heat exchangers has equal heat transfer surface areas and periods, respectively. Based on these assumptions, the following dimensionless groups apply:

$$C_{\min} = \left(\dot{m}c_p\right)_{\min} \tag{2}$$

$$\mathrm{NTU}_0 = \left(\frac{C_{\min}}{2/\mathrm{h}\quad \mathrm{A}+\delta/3\quad \mathrm{kA}}\right)^{-1} \tag{3}$$

$$C^* = \frac{C_{\min}}{C_{\max}} \tag{4}$$

$$C^*_{\mathrm{rotor}} = \frac{\left(Mc_pN\right)_{\mathrm{rotor}}}{C_{\min}} \tag{5}$$

where C is the heat capacity rate of supply or exhaust airflows, $\dot{m}$ is the mass flow rate, c_p is the specific heat capacity, NTU$_0$ is the modified number of transfer units for a regenerator, h is the convective heat transfer coefficient, A is the heat transfer surface area, δ is the minimum wall thickness between channels, k is the thermal conductivity, C^* is the ratio of heat capacity rates of airflows, C^*_{rotor} is the ratio of the rotor heat capacity rate to the minimum airflow heat capacity rate, and M and N are the total mass and cyclical speed of the rotor, respectively.

Based on simplified theory by Shah and Sekulic [15], the wall thermal resistance of a regenerator is $\delta/3$ kA. Eq. (3) includes this resistance in the calculation of NTU$_0$ to ensure that the heat exchanger material can be utilized.

A calculation of the convective heat transfer coefficient, h, for this development yields

$$h = \frac{Nu\cdot k_{\mathrm{air}}}{D_h} = \frac{436\cdot 0.025\quad \mathrm{W/(m\quad K)}}{0.0026\quad \mathrm{m}} = 42.0\quad \mathrm{W/\left(m^2\quad K\right)} \tag{6}$$

where k_{air} is the thermal conductivity of air, and D_h is the hydraulic diameter of channel flow, and Nu is the Nusselt number, which represents the ratio of convective to conductive heat transfer. Shah and London [14] list the Nusselt number for fully developed laminar flow through continuous circular channels as 4.36. The velocity profile may nearly fully develop before the thermal profile starts developing, and both profiles have an associated entrance length. The sum of entrance lengths provides the maximum length of the developing region. Shah and Sekulic [15] provide equations for the maximum hydrodynamic and thermal entrance lengths for laminar flow in circular channels. The hydrodynamic entrance length, L_{hy}, is given as

$$L_{hy} = 0.056\cdot Re\cdot D_h \tag{7}$$

The dimensionless Reynolds number, Re, in Eq. (7) is expressed by

$$Re = \frac{\rho\cdot u\cdot D_h}{\mu} \tag{8}$$

where ρ is the fluid density, u is the mean fluid velocity, and μ is the dynamic viscosity.

The thermal entrance length, L_{th}, for a fully developed velocity profile is given as

$$L_{\mathrm{th}} = 0.0431\cdot Re\cdot Pr\cdot D_h \tag{9}$$

where the Prandtl number, Pr, is the ratio of kinematic viscosity to thermal diffusivity and is roughly equal to 0.7 for air. At a nominal flow rate of 8 L/s in this development, the predicted Reynold number is less than 130 in the considered heat exchangers, which ensures laminar flow (i.e. $Re < 2000$). Therefore the maximum expected entrance length was calculated by:

$$\begin{aligned} L_{\mathrm{entrance}} &= L_{hy} + L_{th} = Re\cdot D_h\cdot(0.056 + 0.0431\cdot Pr) \\ &= 130\cdot 0.0026\quad \mathrm{m}\cdot 0.086 \approx 0.03\quad \mathrm{m} \end{aligned} \tag{10}$$

The Nusselt number is greatest in the entrance region, and the maximum entrance length of 0.03 m is short relative to the nominal heat exchanger length of 0.15 m. Therefore the assumption of all fully developed flow is slightly conservative in estimating convective heat transfer.

Lambertson [16] used the finite difference method to determine regenerator effectiveness and correlated results to the dimensionless groups. The applicable ranges were $3 \le \mathrm{NTU}_0 \le 9$, $0.90 \le C^* \le 1$, and $1.25 \le C^*_{\mathrm{rotor}} \le 5$. Kays and London [17] adjusted the correlation, which agreed within ±1% of effectiveness. The correlation for effectiveness assumes no longitudinal heat conduction:

$$\varepsilon = \left[\frac{1-\exp\left[-\mathrm{NTU}_0\left(1-C^*\right)\right]}{1-C^*\exp\left[-\mathrm{NTU}_0\left(1-C^*\right)\right]}\right]\cdot\left[1-\frac{1}{9(C^*_r)^{1.93}}\right] \tag{11}$$

Longitudinal heat conduction decreases sensible effectiveness in thermally conductive regenerators [15]. Bahnke and Howard [18] used the finite difference method to calculate effectiveness and the influence of longitudinal conduction over a range of dimensionless groups. They created an additional dimensionless group, λ, as a conduction parameter. It is given by

$$\lambda = \frac{k_{\mathrm{rotor}}\cdot A_k}{L\cdot C_{\min}} \tag{12}$$

where k_{rotor} is the thermal conductivity of the rotor, A_k is the conductive cross-sectional area of the rotor, and L is the length of the rotor.

Shah [19] correlated the results of Bahnke and Howard with the dimensionless groups and modified the model in Eq. (11) to be the following:

$$\varphi = \left(\frac{\lambda\mathrm{NTU}_0}{1+\lambda\mathrm{NTU}_0}\right)^{1/2} \text{ for } \mathrm{NTU}_0 > 3, \tag{13}$$

$$C_\lambda = \left(1+\mathrm{NTU}_0\left(1+\lambda\varphi\right)/\left(1+\lambda\mathrm{NTU}_0\right)\right)^{-1} - \left(1+\mathrm{NTU}_0\right)^{-1} \tag{14}$$

$$\begin{aligned} \varepsilon = \varepsilon_{\lambda=0}1 - \frac{C_\lambda}{2-C^*} &= \left[\frac{1-(-\mathrm{NTU}_0\left(1-C^*\right))\exp}{1-C^*\exp(-\mathrm{NTU}_0\left(1-C^*\right)}\right] \\ &\quad\cdot\left[1-\frac{1}{9(C^*_r)^{1.93}}\right]\cdot\left[1-\frac{C_\lambda}{2-C^*}\right] \end{aligned} \tag{15}$$

where C_λ is a coefficient to account for longitudinal heat conduction based on the conduction parameter, λ, and φ is an intermediary parameter in the calculation of C_λ. This model assumes no leakage of unintended air flows. Section 2.4 describes leakages, which are taken into account in final calculations of effectiveness.

The sensible effectiveness, ε, compares the actual transfer of sensible heat to its thermodynamically limited maximum. The temperature efficiency, η, compares the actual temperature change to its maximum. Therefore the supply temperature efficiency, η_{supply}, relates to the supply effectiveness, $\varepsilon_{\mathrm{supply}}$, by the equation:

$$\varepsilon_{\mathrm{supply}} = \frac{C_{\mathrm{supply}}\left(T_{\mathrm{supply}}-T_{\mathrm{outdoor}}\right)}{C_{\min}\left(T_{\mathrm{indoor}}-T_{\mathrm{outdoor}}\right)} = \frac{C_{\mathrm{supply}}}{C_{\min}}\cdot\eta_{\mathrm{supply}} \tag{16}$$

If C_{supply} is less than $C_{exhaust}$, the supply effectiveness is equal to the supply temperature efficiency.

2.3. Material selection

Criterion 3 requires inexpensive and durable materials in a simple and compact construction. The DVU should fit into the minimum thickness of a standard brick wall in Denmark, but longitudinal heat conduction can decrease the effectiveness of short regenerators. For example, a calculation of λ for a small rotary heat exchanger made of aluminum foil demonstrates significant influence:

$$\lambda = \frac{k_{aluminium} \cdot A_k}{L \cdot C_{min}} = \frac{159 \ \text{W/m K} \cdot 0.003 \ \text{m}^2}{0.2 \ \text{m} \cdot \left(0.01 \ \text{m}^3/\text{s} \cdot 1.2 \ \text{kg/m}^3 \cdot 1005 \ \text{J/kg K}\right)} = 0.25[-] \quad (17)$$

According to measurements on regenerators by Kays and London [17], the reduction in effectiveness is greater than 10% for all $\lambda > 0.08$ where $NTU_0 < 15$ and $C^* = 0.95$, which applies to this development.

Low thermal conductivity limits longitudinal heat conduction, but it can also negatively impact the thermal boundary condition for convective heat transfer. In this regard, the shape of continuous channels for laminar flow is significant. Certain shapes provide asymmetrical resistance to flow, which results in stagnant zones. Highly conductive materials compensate for stagnant zones by conducting heat peripherally around channel walls. Less conductive materials offer greater resistance to peripheral heat conduction, so heat capacity is underutilized near stagnant zones. If the shape of the channel is symmetric (i.e. circular or infinitely parallel), stagnant zones are minimized and all materials experience the same convective heat transfer. For example, the Nusselt number for circular channels is 4.36 for all materials. Comparatively, the Nusselt number for equilateral triangular channels is 3.11 for highly conductive materials (e.g. metals) and 1.89 for less conductive materials (e.g. plastics).

It is also necessary to limit the impact of thermal resistance by the channel wall. In the regenerative heat exchanger model of Section 2.2, $\delta/3k$ and $2/h$ represent conductive and convective resistance, respectively. In this development the selected wall thickness, δ, ensures that conductive resistance is an order of magnitude less than convective resistance, so convection is the limiting form of heat transfer. The selection of a thin wall implies less heat capacity and determines the appropriate mechanism for cycling.

This development considers two appropriate materials. An inexpensive, rigid polycarbonate honeycomb of circular channels is considered for a rotary heat exchanger. Polycarbonate is light (1.2 g/cm^3) and the void ratio of the honeycomb is greater than 0.7, so a small electric motor can rotate it. The specific heat capacity of polycarbonate (1.2–1.3 J/g K) is greater than aluminum (0.9 J/g K) and mullite ceramic (0.95 J/g K), which partially compensates for its low density. Furthermore, the fast cycling speeds in rotary heat exchangers reduce the necessary heat capacity. As shown in Fig. 1, the circular channels of the honeycomb are 150 mm in length and 2.6 mm in diameter, and the channel walls are 0.2 mm thick. The convective resistance (5×10^{-2} m^2 K/W) is two orders of magnitude greater than the conductive resistance (3×10^{-4} m^2 K/W), so conduction does not limit heat transfer.

The development considers an inexpensive mullite ceramic honeycomb for testing as a fixed-matrix heat exchanger. The material is denser and has slightly thicker walls, so its total heat capacity

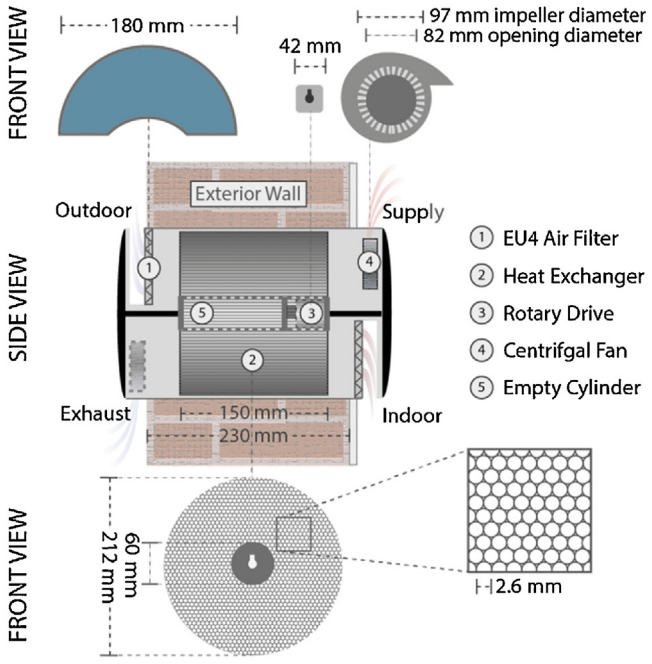

Fig. 1. Detailed drawing of the developed DVU prototype with a polycarbonate honeycomb rotary heat exchanger.

is 84% greater per volume of honeycomb than the polycarbonate (i.e. 944 kJ/m^3 K versus 514 kJ/m^3 K). Its greater mass and total heat capacity make it suitable for a fixed-matrix heat exchanger. These heat exchangers depend on large capacities to enable slow cycling speeds since their airflow typically reverses direction every 60–70 s. This limits losses due to flow reversal. However, Criterion 1 requires the option to reduce heat recovery by slowing cycling speeds. In fixed-matrix heat exchangers, this lowers the average supply air temperature and increases its variance. This could cause discomfort at the occupant as the supply air approaches outdoor temperatures in each cycle. Additionally, many DVUs with ceramic fixed-matrix heat exchangers are commercially available, and this development seeks a novel solution. Therefore, the development focuses on the rotary heat exchanger made of polycarbonate honeycomb. This holds the advantage of stable supply air temperatures at slow cycling speeds, which facilitates experimental validation.

2.4. Air leakage

Criterion 4 targets acceptably low air leakage in the heat exchanger. The leakage paths around rotary heat exchangers fall into categories of pressure leakage (between airflows) and bypass leakage (between inlet and outlet). The first prototype of a rotary heat exchanger had excessive pressure leakage because construction tolerances were poor and the fans were on the same end of the heat exchanger. This resulted in unbalanced flow and unacceptable ratios of heat capacity rates, C_{min}/C_{max}. As shown in Fig. 1, the final prototype locates fans on opposite ends to lower pressure gradients between airflows, while the use of additive manufacturing minimizes tolerances and air gaps.

Shah and Sekulic [15] recommend the following model for pressure leakage through an orifice:

$$\dot{m}_{leak,pressure} = C_d A_o \sqrt{2\rho_{inlet}\Delta p} \quad (18)$$

where C_d is the coefficient of discharge assumed to be 0.8, A_o is the orifice flow area, and Δp is the pressure difference across the orifice. Both air inlets are nearly symmetrical about the center point of the DVU, so the pressure at entry to the heat exchanger is

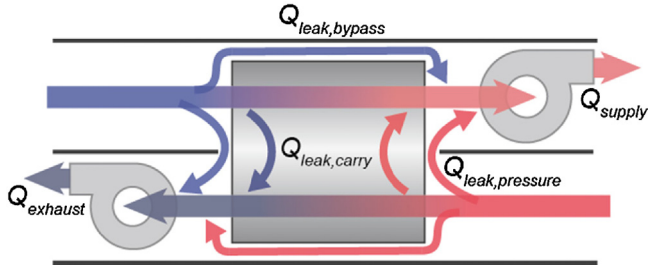

Fig. 2. Schematic of air flows for a rotary heat exchanger in a DVU.

approximately equal for supply and exhaust. Based on this assumption, the pressure difference across the orifice is equal to the pressure drop through the heat exchanger. Shah and Sekulic [15] provide the following model of pressure drop through a heat exchanger:

$$\Delta p = \frac{u^2\rho}{2}\left[1-\sigma^2+K_{\text{contract}}+2\left(\frac{\rho_{\text{inlet}}}{\rho_{\text{outlet}}}-1\right) + f\frac{L}{D_h}\rho_{\text{inlet}}\left(\frac{1}{\rho}\right)_{\text{mean}}-\left(1-\sigma^2+K_{\text{expand}}\right)\frac{\rho_{\text{inlet}}}{\rho_{\text{outlet}}}\right] \quad (19)$$

In Eq. (19), K_{contract} and K_{expand} are the pressure loss coefficients for the entrance and exit effects, respectively. Shah and Sekulic [15] provide a plot of these coefficients for a core of multiple circular tubes. The Fanning friction factor, f, for fully developed laminar flow in circular tubes is $16/Re$, and other values in Eq. (19) depend on the properties of flow, such as inlet and outlet density, $\rho_{\text{inlet,outlet}}$, and the ratio of matrix core flow area to face flow area, σ.

In centralized ventilation units, rotary heat exchangers may include a purge section and greater supply side pressures to reduce the risk of contamination from exhaust air. The purge flow is often constant and excessive. Since DVUs serve a single room, contamination is not an issue and pressure leakage may be beneficial. As long as the percentage of total air flow is small, re-circulated indoor air prevents cool draughts by raising supply air temperatures. Additionally, recirculated outdoor air reduces the relative humidity of exhaust air below its saturation point, which limits the risk of condensation on exterior surfaces. In an evaluation of acceptable leakage, the benefits of recirculated air weigh against the costs of additional fan power or reduced fresh air supply.

Leakage between airflows also occurs inside a rotary heat exchanger, known as carryover leakage. Rotation across the divider plate causes air to reverse flow direction in channels. Shah and Sekulic [15] recommend a model for carryover leakage, which yields the following calculation for this development:

$$\dot{Q}_{\text{leak,carry}} = \pi\left(r^2 L\sigma N\right)_{\text{rotor}} = 3.14\cdot(0.106\ \text{m}-0.030\ \text{m})^2 \cdot 0.150\ \text{m}\cdot 0.7\cdot 10\ \text{m}^{-1}\cdot 60\ \text{m/h} = 2.0\ \text{m}^3/\text{h} \quad (20)$$

where σ and N are the void ratio and cyclical speed of the rotor, respectively.

As shown in Fig. 2, the flow model approximates ventilation rates, $Q_{\text{vent.}}$, by the equation:

$$Q_{\text{vent.}} = Q_{\text{supply}} - Q_{\text{leak,carry}} - Q_{\text{leak,pressure}} \quad (21)$$

where Q_{supply} is the flow rate through the supply fan, and $Q_{\text{leak,pressure}}$ and $Q_{\text{leak,carry}}$, are the leakages due to pressure and carryover, respectively.

The thin tolerance between the heat exchanger and its encasing tube acts as a bypass seal for the system, which allows a prediction of bypass leakage. The equation for frictional pressure loss, Δp, in laminar flow is

$$\Delta p = \rho f\frac{4L}{D_h}\frac{u^2}{2} \quad (22)$$

where ρ and u are the mean density and mean velocity of fluid flow, respectively, and f is the Fanning Friction factor. Shah and London [14] list the Fanning friction factor for fully developed laminar flow between two parallel surfaces as:

$$f = \frac{24}{Re}\frac{24}{\rho u D_h/\mu} \quad (23)$$

By inserting Eq. (23) into Eq. (22) and isolating velocity, u, the following equation approximates the bypass flow:

$$Q_{\text{leak,bypass}} = (uA)_{\text{leak,bypass}} = \left(\frac{(\Delta p)(D_h)^2 A}{48\ \mu L}\right)_{\text{leak,bypass}} \quad (24)$$

where A is the cross-sectional area of bypass flow around the heat exchanger for supply or exhaust and Δp is the pressure drop through the bypass area, which is equal to the pressure drop through the heat exchanger from Eq. (19).

2.5. Installation

Criterion 5 requires the possibility to install the DVU into a drilled hole in the façade of an existing building. Placement of the heat exchanger inside the facade minimizes obtrusiveness and moves the cold side of the heat exchanger toward the exterior surface of the façade, where condensation poses less of a risk to building materials. To minimize the required diameter for drilling, Criterion 5 seeks a cylindrical-shaped heat exchanger to effectively utilize available space in a drilled hole. The rotary heat exchanger is suitable because its shape is inherently cylindrical.

3. Experimental assessment

Experimental work attempted to validate the modelled performance of the heat exchanger. All experiments were performed in test facilities at the Technical University of Denmark (DTU).

3.1. Flow and leakage determination

The experiments determined fan flow rates, ventilation rates, and approximate pressure leakages.

3.1.1. Flow rate measurements

The outlets of the DVU are asymmetrical about its center point, so pressure loss through the supply and exhaust are unequal. The authors independently measured supply and exhaust flow rates by sealing the opposite flow direction. Due to its irregular shape, the DVU connected to a flow meter through a sealed 160 Liter box, which added unknown pressure loss. The flow meter is a circular metal pipe from *Veab Elmicro* with dimensions of 0.1 m inner diameter and 1.0 m length. The pipe contains a pitot tube at its midpoint that measures the difference in static and total pressure. The pipe provides a straight length of five diameters before the pitot tube, which satisfies typical recommendations for measurements. Pitot tubes can achieve accuracies better than 1% for ideal flow, so the experiment conservatively assumes 2% accuracy. The probes of the flow meter connected to a low-range micromanometer from *Furness Controls* (model FCO510), which measured the pressure difference with an error of 0.06 Pa. The measured pressure differences correlate to flow rates based on calibration data for the flow meter. Fig. 3 shows the measured flow rates in the nominal range of operation from 5 to 15 L/s. The control signal of the fans ranges from 0 to

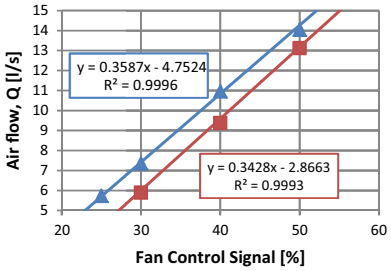

Fig. 3. Independently measured flow rates in the DVU.

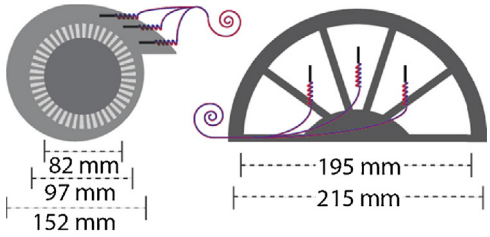

Fig. 4. Thermocouple locations for air temperature measurements at outlets (left) and inlets (right) for supply and exhaust.

10 V and corresponds directly to fan speed. The flow rates increase linearly with fan speed, which adheres to the affinity laws for fans.

3.1.2. Pressure leakage approximation

With the heat exchanger at rest, the DVU exchanged air between a warm chamber at 25 °C and a cold chamber at 12 °C. The dew point of fresh ventilation air was below 6 °C, which ensured dry conditions for testing. The ventilation system of each chamber uses a differential pressure transmitter from *Dwyer* (model 603A) to maintain specified pressures in the chamber by controlling exhaust airflow. A separate micromanometer from *Furness Controls* (model FCO510) confirmed negligible pressure differences between chambers throughout the experiments.

The flow through the fan includes pressure leakage, as depicted in Fig. 2. A heat and mass balance with measured temperatures and fan powers yields the approximate pressure leakage for each set of flow rates. Three evenly spaced T-type thermocouples measured temperatures at each inlet and outlet with a precision of ±0.5 °C. A data-logger from *Agilent Technologies* (model 34970A) recorded temperatures every 10 s to obtain averages for each location. The thermocouples at the outlets were downstream of the fans to ensure mixing, as shown in Fig. 4.

A correction to the measured supply temperature accounts for heat gains from the fan as well as heat transferred through the divider plate, as shown in Eq. (25). The data-logger also recorded the voltage across a 1 Ω shunt resistor connected in series to the fan. This data yields a calculation of the fan power with an accuracy of ±1%. The Dittus–Boelter correlation roughly predicts convective heat transfer coefficients at the divider plate. The heat capacity rates in Section 3.1.1 are used to calculate temperature increases, ΔT, from heat gains. The following equation gives the corrected supply temperature:

$$T_{\text{supply}} = T_{\text{meas.,supply}} - \Delta T_{\text{fan}} - \Delta T_{\text{divider}} = T_{\text{meas.,supply}} - \frac{P_{\text{fan}}}{(\dot{m}c_p)_{\text{supply}}} - \frac{(UA)_{\text{divider}}\left(T_{\text{indoor}} - T_{\text{supply}}\right)}{(\dot{m}c_p)_{\text{supply}}} \quad (25)$$

where $T_{\text{meas.,supply}}$ is the measured supply temperature, ΔT_{fan} is the temperature increase due to the fan, $\Delta T_{\text{divider}}$ is the temperature increase due to heat transfer through the divider plate, and P_{fan} is the measured power to the fan. Inserting T_{supply} from Eq. (25) into Eq. (1) yielded the supply temperature efficiency.

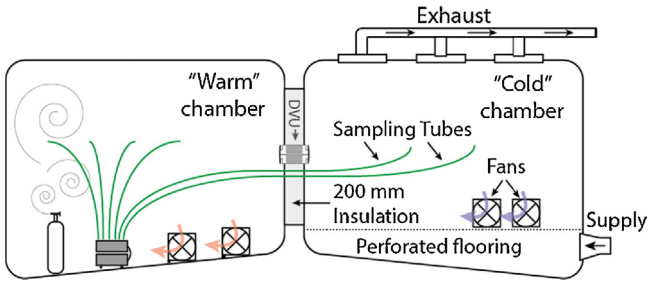

Fig. 5. Schematic of the experimental setup in twin climate chambers.

To demonstrate the relationship between temperature efficiency with a stationary rotor and the mass flow ratio of pressure leakage, a heat balance is formulated with outdoor temperature as a reference:

$$\dot{m}_{\text{vent}}c_p\left(T_{\text{vent}} - T_{\text{outdoor}}\right) + \dot{m}_{\text{leak,pressure}}c_p\left(T_{\text{indoor}} - T_{\text{outdoor}}\right) = \dot{m}_{\text{supply}}c_p\left(T_{\text{supply}} - T_{\text{outdoor}}\right) \quad (26)$$

where $\dot{m}_{\text{vent}}$ and T_{vent} are the mass flow rate and temperature, respectively, of ventilation exiting the rotor. With a stationary rotor T_{vent} is equal to the outdoor temperature, T_{outdoor}. Re-arranging the mass balance in Eq. (26) yields:

$$\frac{\dot{m}_{\text{leak,pressure}}}{\dot{m}_{\text{supply}}} = \frac{\left(T_{\text{supply}} - T_{\text{outdoor}}\right)}{\left(T_{\text{indoor}} - T_{\text{outdoor}}\right)} = \eta_{N=0} \quad (27)$$

where $\dot{m}_{\text{leak,pressure}}$ is the mass flow rate of pressure leakage and $\eta_{N=0}$ is the temperature efficiency with a stationary heat exchanger. These values provide an indication of leakage in the prototype. Table 1 lists the results for three flow rates. The measured pressure leakage from the balance equations is significantly greater than the modelled pressure leakage. This is not attributable to pressure differences between flows, as the modelled values from Section 2.4 (6, 12, 20 Pa) are greater than the measured values (4, 10, 17 Pa). The measurements of pressure difference used the same micromanometer as described in Section 3.1.3 and 8 mm polyethylene tubes. The tubes were perpendicular to airflow to sample static pressure, which added uncertainty due to potentially disturbed flow. Additionally, the discrepancy between measured and modelled values may be due to greater orifice leakage area, since the modelled value only considers the 2 mm gap at the divider plate.

3.1.3. Direct ventilation rate measurement

Measurement of tracer gas decay determined ventilation rates in twin stainless-steel climate chambers, as depicted in Fig. 5. The chambers share a steel door that was replaced by a 200 mm polystyrene insulation panel with an opening for the DVU. The chambers open to the exterior through a pressurized door. Each chamber has its own air handling unit to control temperature and flow rate, but ventilation dampers for the warm side were closed for this experiment. A manually controlled valve dosed the warm chamber with Freon R134a gas ($C_2H_2F_4$) up to a fully mixed concentration greater than 40 ppm. A multi-point sampler (model Innova 1303) and multi-gas monitor (model Innova 1312) from Brüel & Kjær measured and recorded concentrations during the decay of the tracer gas for each set of balanced flow rates. The processed data is shown in Fig. 6. The sampling tubes are 3 mm in diameter and no cracks or leaks were visible in the tubes. The precision of measured concentrations by the multi-gas monitor is ±1%. The heat exchanger rotated at a nominal rate of 10 rpm. The exhaust fan of the cold chamber maintained approximately zero pressure difference between chambers.

With the opening of the insulation panel sealed, the regression of Freon decay provided a baseline air change rate. With the DVU

Table 1
Experimental results of temperature measurements on a stationary heat exchanger after accounting for heat gains, and a comparison to modelled pressure leakage.

Test	Expected fan flow rate, Q_{supply}	Stationary temperature efficiency, $\eta_{N=0}$		Modelled pressure leakage, $\dot{m}_{leak,pressure}/\dot{m}_{supply}$	
		Supply	Exhaust		
[Units]	[L/s]	[%]	[%]	[%]	[L/s]
24% Supply, 27% exhaust	5	22	22	17	0.84
38% Supply, 41% exhaust	10	17	19	12	1.19
52% Supply, 55% exhaust	15	13	16	10	1.46

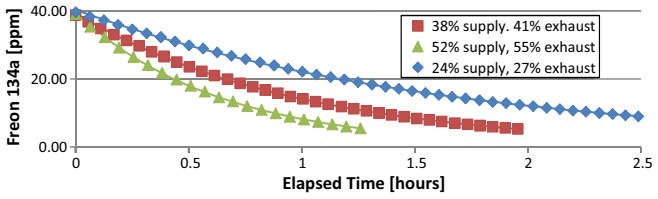

Fig. 6. Decay of Freon concentration to determine ventilation rates through the DVU for specified fan settings.

inserted, the fans provided balanced flow rates of 5, 10, and 15 L/s based on the measurements described in Section 3.1.1. The decay equation takes the following form:

$$C(t)_{warm} - C(t)_{cold} = (C(0) - C(t)_{cold})\, e^{(-n_{measured}t)} \quad (28)$$

where $C(t)$ is the tracer gas concentration at time t in the chamber specified by the subscript, *warm* or *cold*.

The ventilation rate, Q, is calculated as

$$Q = n_{ventilation} \cdot V_{warm\,chamber} = (n_{measured} - n_{baseline}) \cdot V_{warm\,chamber} \quad (29)$$

where $V_{warm\ chamber}$ is the warm chamber volume, and the ventilation air change rate, $n_{ventilation}$, is determined for each flow rate by subtracting the baseline air change rate, $n_{baseline}$, from the measured air change rate, $n_{measured}$. This assumes that the cold chamber supplied all ventilation air and that its concentration, $C(t)_{cold}$, remained stable.

Table 2 shows the calculated ventilation rates. The pressure leakages from both experimental methods are in reasonable agreement, but neither validates the theoretical model in Section 2.4, which predicts less pressure leakage.

3.2. Temperature efficiency measurements

A heat balance combines measurements of temperatures and heat gains to characterize actual temperature efficiencies of the DVU.

$$\eta_{vent.} = \frac{(T_{vent} - T_{outdoor})}{(T_{indoor} - T_{outdoor})} = \frac{(q_{gains} - q_{losses})/C_{vent.}}{T_{indoor} - T_{outdoor}} = \frac{\left(\left(P_{HEX}/2\right) + P_{fan} + P_{heater}\right) - (q_{wall} + q_{box} + q_{tube})}{C_{vent.}\,(T_{indoor} - T_{outdoor})}$$
$$= \frac{\left(\left(P_{HEX}/2\right) + P_{fan} + P_{heater}\right) - \left(\left(\left(A\left(k/\delta\right)\right)_{wall} + \left(A\left(k/\delta\right)\right)_{tube}\right)(T_{indoor} - T_{outdoor}) + \left(A\left(k/\delta\right)\right)_{box}(T_{box} - T_{outdoor})\right)}{\left(\dot{m}c_p\right)_{vent.}(T_{indoor} - T_{outdoor})} \quad (30)$$

3.2.1. Heat input method

A guarded hot box (GHB) provides calibrated measurements of thermal transmittance, as in Standard EN ISO 8990 [20], and may be used to measure heat recovery at low ventilation rates [21]. A GHB contains a thick insulated wall between two temperature controlled chambers. The wall contains an opening for a test element, which is surrounded by a tightly-sealed five-panel metering box in the warm chamber. The metering box contains a heating element, and a closed-loop control system maintains the same temperature in the metering box as the surrounding warm chamber. This minimizes heat loss through the panels of the metering box. According to the standard, at least nine shielded T-type thermocouples measure temperatures in each chamber and the metering box. A data acquisition system logs average temperatures as well as the power input to the heating element in the metering box.

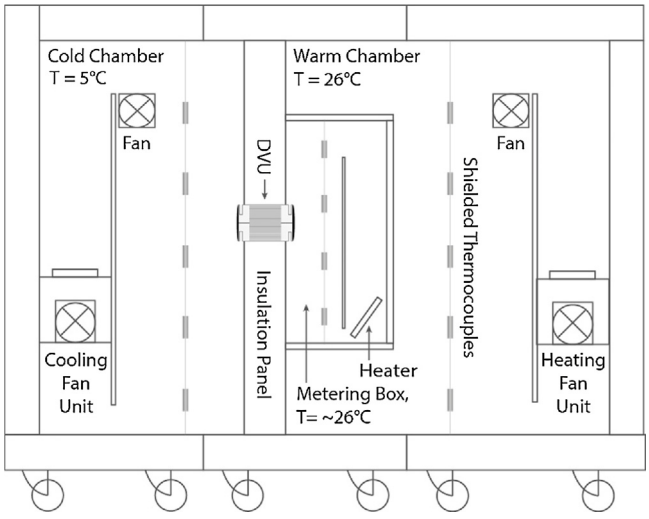

Fig. 7. Experimental setup in the Guarded Hot Box to measure temperature efficiency of the DVU.

In this experiment, the guarded hot box (GHB) measured the total thermal transmittance through the DVU at different flow rates in order to calculate temperature efficiencies. The temperatures of the warm and cold chambers were 26 °C and 5 °C, respectively. The experimental setup is shown in Fig. 7. A heat balance yields the temperature efficiency of the DVU as

where P_{HEX}, P_{fan}, and P_{heater} are the power demands from the heat exchanger drive, the supply fan, and the heater in the metering box, respectively, and q_{wall}, q_{box}, and q_{tube} are a heat transfer rates through the wall between chambers, the metering box, and the DVU tube, respectively. With respect to the designated heat transfer medium, A, k, and δ are the heat transfer area, thermal conductivity, and thickness, respectively. The experiment described in Section 3.1.3 provides mass flow rates, $\dot{m}_{vent.}$.

Table 2
Experimental results for the determination of ventilation rates and an estimation of leakage.

Test	Measured fan flow rate, Q_{flow}	Air change rate	Corrected air change rate	Ventilation rate, $Q_{vent.}$		Recirculated air estimation, $1-(Q_{vent.}/Q_{flow})$
[Units]	[L/s]	[h^{-1}]	[h^{-1}]	[m^3/h]	[L/s]	[%]
0% Supply, 0% exhaust	0	0.15	–	–	–	–
24% Supply 27% exhaust	5	0.60	0.45	14	3.9	22
38% Supply 41% exhaust	10	1.05	0.91	28	7.8	22
52% Supply 55% exhaust	15	1.63	1.48	46	12.8	15

An oversized motor ensures rotation of the heat exchanger. However, the motor demands 5.2 W and a significant assumption is the location of these heat gains. Heat gains are evenly allocated to supply and exhaust in the heat balance equation because the motor is located in the cylindrical axle of the heat exchanger, and this provides a significant source of error.

Table 3 lists modelled temperature efficiencies, which are produced by the model of regenerator effectiveness described in Section 2.2. During nominal operation of the DVU, the volumetric flows through the fans are equal. Since the fans are located at the outlets of the DVU, the supply side has a lower heat capacity rate due to lower air density. It follows from Eq. (16) that supply temperature efficiency, η_{supply}, is equal to sensible effectiveness, ε, since $C_{supply} = C_{min}$. Therefore the model for regenerator effectiveness directly yields temperature efficiencies for this development.

Table 3 also lists the modelled ventilation rates, which are calculated as the measured fan flow rates minus the modelled leakages due to pressure and carryover. Table 1 provides the modelled pressure leakages, and Eq. (20) provides the carryover leakage. The modelled efficiency includes the bypass leakage from Eq. (24), which is approximately 6% of airflow. The measured and modelled flow rates and temperature efficiencies show good agreement for the two largest flow rates and poor agreement for the smallest flow rate.

The predicted efficiency for the lowest flow rate may be prone to error since the heat gains and losses are relatively large compared to the heat capacity rates of airflows. It is possible that the heat exchanger was not centered during measurements, which provides another source of error. A non-centered heat exchanger would lead to unequal temperature efficiencies for supply and exhaust, yet the metering box only measured supply temperature efficiency. In contrast, the temperature measurements described in Section 3.2.2 allow a comparison of supply and exhaust temperature efficiencies.

3.2.2. Temperature measurements

Instead of logging the heat input to the metering box, a similar experiment measured supply and exhaust temperatures at each inlet and outlet. This provides data to calculate of temperature efficiencies for both supply and exhaust. The previous section describes the setup of the GHB, and Section 3.1.2 describes sensor placement and data acquisition. As in Section 3.2.1, the measured temperatures are corrected for heat gains from the fans and the heat exchanger drive. The resulting temperature efficiencies include pressure leakages, which are deducted in the following balance equations for heat and mass flows:

$$\dot{m}_{vent} = \dot{m}_{supply} - \dot{m}_{pressure} \tag{31}$$

$$\dot{m}_{vent} c_p (T_{vent.} - T_{outdoor}) = \dot{m}_{supply} c_p \times \left(T_{supply} - T_{outdoor}\right) - \dot{m}_{pressure} c_p (T_{indoor} - T_{outdoor}) \tag{32}$$

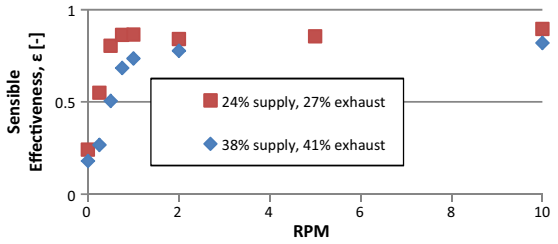

Fig. 8. Experimental results of temperature efficiency for various rotational speeds.

Substituting Eq. (31) into Eq. (32) and dividing by $c_p\left(\dot{m}_{supply}\right)(\Delta T_{indoor\text{-}outdoor})$ yields:

$$\frac{\left(\dot{m}_{supply} - \dot{m}_{pressure}\right)}{\left(\dot{m}_{supply}\right)} \frac{(T_{vent.} - T_{outdoor})}{(T_{indoor} - T_{outdoor})} = \frac{\left(T_{supply} - T_{outdoor}\right)}{(T_{indoor} - T_{outdoor})} - \frac{\dot{m}_{pressure}}{\left(\dot{m}_{supply}\right)} \tag{33}$$

Then substituting Eq. (27) in Eq. (33) yields the temperature efficiency for only the ventilation flow:

$$(1 - \eta_{N=0})\,\eta_{vent} = \eta_{supply} - \eta_{N=0} \tag{34}$$

$$\eta_{vent} = \frac{\eta_{supply} - \eta_{N=0}}{(1 - \eta_{N=0})} \tag{35}$$

In the above formulation, the exhaust subscript is substituted for supply to determine exhaust temperature efficiencies. Table 4 lists the results of the calculations. The results show some agreement with modelled and measured temperature efficiencies reported in Section 3.2.1. However, after deducting heat gains from outlet temperatures and correcting temperature efficiencies for leakage, the supply and exhaust temperature efficiencies are dissimilar. This implies that the heat exchanger was not centered in its encasing tube in the experiments or that heat gains are misallocated in balance equations.

The model for bypass leakage in Section 2.4 assumes an average gap of 1.5 mm around the entire circumference of the heat exchanger based on measurements. For this sized gap, the model predicts 6% bypass leakage or approximately 5% reduced temperature efficiency, and values are very sensitive to peripheral tolerance around the heat exchanger. A reduction to 1 mm yields modelled efficiencies 2–3% higher for the same ventilation rates, and an increase to 2 mm decreases modelled efficiencies by 5%. Despite the strong impact of bypass leakage, there is no simple method to isolate and measure it.

To assess the DVU with respect to Criterion 1, experiments used the same method as above to determine the temperature efficiency for varying rotational speeds. The experiment varied the rotational speed of the heat exchanger from 0 to 10 RPM. As shown in Fig. 8, slowing rotational speeds provides decreased temperature efficiency, which meets the requirement of Criterion 1.

Table 3
Experimental results from a heat balance to determine temperature efficiencies of the heat exchanger, and a comparison with modelled efficiency.

Test [Units]	HEX drive power [W]	Fan power [W]	Heater power [W]	Total heat loss, q_{losses} [W]	Measured fan flow rate [L/s]	Measured ventilation rate [L/s]	Measured efficiency [%]	Modelled ventilation rate [L/s]	Modelled efficiency [%]
24% Supply 27% exhaust	5.2	1.1	20.7	6.4	5	3.9	83	3.6	90
38% Supply 41% exhaust	5.2	2.2	33.8	5.8	10	7.8	83	8.2	84
52% Supply 55% exhaust	5.2	4.8	64.8	5.9	15	12.8	79	13.0	78

Table 4
Experimental results of temperature measurements to determine temperature efficiencies of the heat exchanger, and a comparison with modelled results.

Test	Measured fan flow rate, Q_{flow}	Raw measured temperature efficiency		Temperature efficiency (corrected)			Modelled efficiency (corrected), η
[Units]	[L/s]	Supply, η_{supply} [%]	Exhaust, $\eta_{exhaust}$ [%]	Supply, η_{supply} [%]	Exhaust, $\eta_{exhaust}$ [%]	Average, $\eta_{average}$ [%]	[%]
24% Supply 27% exhaust	5	96	95	91	97	94	90
38% Supply 41% exhaust	10	86	88	81	87	84	84
52% Supply 55% exhaust	15	79	80	74	78	76	78

4. Discussion

For the purpose of single-room ventilation units, this development uses an inexpensive plastic honeycomb rotor as a novel rotary heat exchanger. Its theoretical development targets high temperature efficiencies for a short heat exchanger, and plastic material limits efficiency reductions from longitudinal heat conduction. Continuous circular channels allow excellent convective heat transfer and pressure efficiency for laminar flow, and high cycling speeds (up to 10 RPM) negate poor heat conduction. Based on predicted performance, a ceramic fixed-matrix heat exchanger is able to provide similarly high temperature efficiencies, but they operate in pairs, require greater heat transfer surface area, provide varying supply temperatures, and are widely available commercially.

For a nominal flow rate of 8 L/s, the developed plastic rotary heat exchanger provides a modelled temperature efficiency of 89% based on correlations of dimensionless values, but this neglects bypass leakage around the rotor. The corrected model accounts for 6% bypass leakage based on pressure loss equations, which yields 84% temperature efficiency. As intended in the design, low tolerances provide sealing around the heat exchanger in a compact construction. However this technique provides bypass leakage that is unbalanced and difficult to quantify. Similarly low tolerances between the rotor and the divider plate provide a seal against pressure leakage. The predicted pressure leakage ratio is 12% of nominal flow for a 2 mm gap, which may be regarded as acceptable for re-circulated air. However a heat balance with measured temperatures and heat gains determine the pressure leakage to be 18% of nominal flow. These techniques provide acceptable accuracy to measure all flows except bypass leakage. Low tolerances do not provide adequate sealing in the developed DVU, and the authors recommend that future prototypes of this kind use proper seals even in compact low-tolerance constructions.

In the described experiments, two measurement methods yield temperature efficiencies greater than 80% for a nominal flow rate of 8 L/s after deducting heat gains and accounting for leakages. The developed heat exchanger met its intended aims, but the conclusion carries uncertainty due to key assumptions. The irregular form of the DVU does not permit the use of standards to measure temperature efficiencies, such as EN 308 [22], so experiments may utilize temperature measurements and heat balance equations instead. A motor inside the cylindrical axle of the heat exchanger drives its rotation, so its heat gains can not be accurately allocated. In the assumed heat balance, supply and exhaust evenly shared the contribution of 5.2 W, which provides a significant source of error, especially for low flow rates. Moving the motor to a distinct and open section of the DVU would improve allocation of heat gains. Furthermore, isolating the rotor in a separate assembly would improve validation of the regenerator effectiveness model. With known temperature efficiencies through the heat exchanger and the appropriate allocation of heat gains, the method in this paper would accurately characterize leakage and overall performance of the DVU. Similarly, future measurement standards should accommodate irregular systems such as DVUs to be certain that their performance is reported accurately.

5. Conclusion

Based on thermal design theory, a novel rotary heat exchanger uses a short inexpensive plastic honeycomb. Based on dimensionless groups, the predicted temperature efficiency of the heat exchanger is 89% for a flow rate 8 L/s, but this excludes leakages. After accounting for modelled bypass leakages, the predicted temperature efficiency lower to 84%. This shows good agreement with measured efficiencies of 83–84%% for 7.8 L/s from two experimental methods. The available measurement standards did not suit this application, so the performed experiments combine thermal measurements and heat balance equations to determine temperature efficiencies and pressure leakages. Pressure leakage reduces ventilation and increases recirculated air, and bypass leakage reduces temperature efficiencies. The measured pressure leakage is 18%, so fan flow rates must be increased accordingly to meet ventilation requirements. Despite significant leakage, the single-room ventilation unit meets the development criteria and achieves greater than 80% temperature efficiency for a balanced nominal ventilation rate of 8 L/s. Additionally, lower rotational speeds decrease heat recovery in order to modulate supply and exhaust temperatures, and the compact and inexpensive heat exchanger fits appropriately into a cylindrical tube.

Grayscale Images (Color is not required in print.)

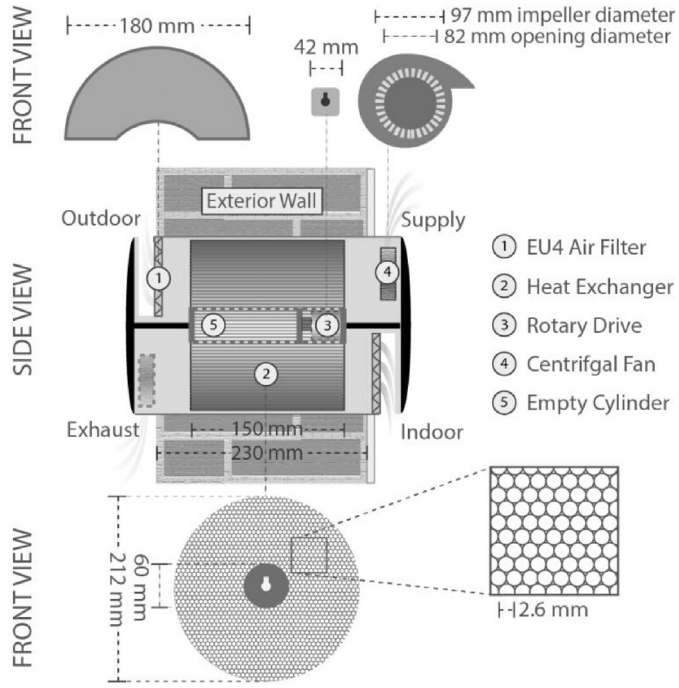

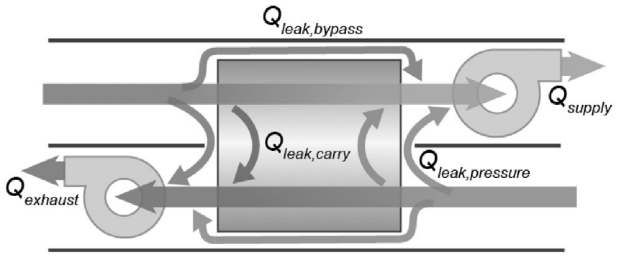

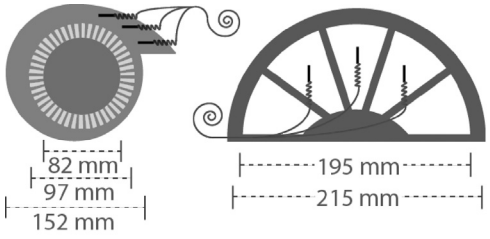

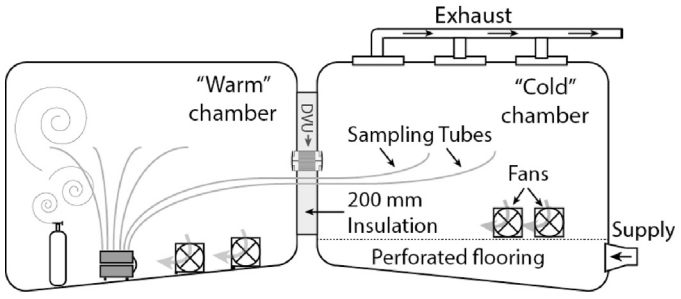

Acknowledgements

This research was funded by the Technical University of Denmark and the Innovation Fund (Fornyelsesfonden) as part of a collaborative project to research and develop decentralized ventilation for existing residential apartments. Partners included Christian Niepoort of Smith Innovation, Henning Solfeldt of PLH Architects, Torben Kirkholt of EBM Papst, Hasse Brønnum of Brønnum Plast, and Anders L. Jansen of the Technical University of Denmark.

References

[1] The Danish Government, The Danish Ministry of Climate, Energy and Buildings, Our Energy Future, 2011, Retrieved from ⟨http://www.ens.dk/sites/ens.dk/files/policy/danish-climate-energy-policy/our_future_energy.pdf⟩.
[2] Energi Styrelsen, Energistatistik 2012 (2012), Retrieved from ⟨http://www.ens.dk/info/tal-kort/statistik-nogletal/arlig-energistatistik⟩.
[3] C.-H. Baek, S.-H. Park, Changes in renovation policies in the era of sustainability, Energy Build. 47 (2012) 485–496, http://dx.doi.org/10.1016/j.enbuild.2011.12.028
[4] G. Villi, C. Peretti, S. Graci, M. De Carli, Building leakage analysis and infiltration modelling for an Italian multi-family building, J. Building Perform. Simul. 6 (2013) 98–118, http://dx.doi.org/10.1080/19401493.2012.699981
[5] I. Ridley, J. Fox, T. Oreszczyn, S. Hong, The impact of replacement windows on air infiltration and indoor air quality in dwellings, Int. J. Vent. 1 (2003) 209–218, Retrieved from: ⟨http://discovery.ucl.ac.uk/2259/⟩.
[6] Energi Styrelsen, Build. Regul. (2010), Retrieved from ⟨http://bygningsreglementet.dk/file/155699/BR10_ENGLISH.pdf⟩.
[7] D.R. Wulfinghoff, Multiple-zone HVAC: an obsolete template, Energy Eng. 108 (2) (2011) 44–56, http://dx.doi.org/10.1080/01998595.2011.10389019
[8] H. Manz, H. Huber, A. Schalin, A. Weber, M. Ferrazzini, M. Studer, Performance of single room ventilation units with recuperative or regenerative heat recovery, Energy Build. 31 (2000) 37–47, http://dx.doi.org/10.1016/S0378-7788(98)00077-2
[9] H. Manz, H. Huber, D. Helfenfinger, Impact of air leakages and short circuits in ventilation units with heat recovery on ventilation efficiency and energy requirements for heating, Energy Build. 33 (2001) 133–139, http://dx.doi.org/10.1016/S0378-7788(00)00077-3
[10] L. Baldini, M.K. Kim, H. Leibundgut, Decentralized cooling and dehumidification with a 3 stage LowEx heat exchanger for free reheating, Energy Build. 76 (2014) 270–277, http://dx.doi.org/10.1016/j.enbuild.2014.02.021
[11] F. Meggers, J. Pantelic, L. Baldini, Evaluating and adapting low exergy systems with decentralized ventilation for tropical climates, Energy Build. 67 (2013) 559–567, http://dx.doi.org/10.1016/j.enbuild.2014.05.009
[12] M.K. Kim, H. Leibundgut, J.-H. Choi, Energy and exergy analyses of advanced decentralized ventilation system compared with centralized cooling and air ventilation systems in the hot and humid climate, Energy Build. 79 (2014) 212–222, http://dx.doi.org/10.1016/j.enbuild.2014.05.009
[13] R.S. Iyengar, E. Saber, F. Meggers, The feasibility of performing high-temperature radiant cooling in tropical buildings when coupled with a decentralized ventilation system, HVAC&R Res. 19 (2013) 992–1000, http://dx.doi.org/10.1080/10789669.2013.826065
[14] R.K. Shah, A.L. London, Laminar flow Forced Convection in Ducts. Supplement 1 to Advances in Heat Transfer, Academic Press, New York, NY, 1978.
[15] R.K. Shah, D.P. Sekulic, Fundamentals of Heat Exchanger Design, John Wiley & Sons, Hoboken, NJ, 2003, http://dx.doi.org/10.1002/9780470172605
[16] T.J. Lambertson, Performance factors of periodic-flow heat exchanger, Am. Soc. Mech. Eng. Trans. 80 (1957) 586–592.
[17] W.M. Kays, A.L. London, Compact Heat Exchangers, third ed., McGraw-Hill, New York, NY, 1984.
[18] G.D. Bahnke, C.P. Howard, Effect of longitudinal heat conduction on periodic-flow heat exchanger performance, J. Eng. Power 86 (1964) 105–120, http://dx.doi.org/10.1115/1.3677551
[19] R.K. Shah, A correlation for longitudinal heat conduction effects in periodic-flow heat exchangers, J. Eng. Power 97 (1975) 453–454, http://dx.doi.org/10.1115/1.3446030
[20] International Organization for Standardization, EN ISO 8990: 1996 – Thermal Insulation – Determination of Steady-state Thermal Transmission Properties—Calibrated and Guarded Hot Box, European Committee for Standardisation, Brussels, 1997.
[21] D. Appelfeld, S. Svendsen, Experimental analysis of energy performance of a ventilated window for heat recovery under controlled conditions, Energy Build. 43 (2011) 3200–3207, http://dx.doi.org/10.1016/j.enbuild.2011.08.018
[22] European Committee for Standardisation, EN 308:1997 – Heat Exchangers – Test Procedures for Establishing Performance of Air to Air Flue Gases Heat Recovery Devices, Authors, Brussels, 1997.

Appendix B - Paper 2

K.M. Smith, S. Svendsen,

The effect of a rotary heat exchanger in room-based ventilation on indoor humidity in existing apartments in temperate climates,

Energy Build. (Accepted with minor revisions – Resubmitted and awaiting decision).

The effect of a rotary heat exchanger in room-based ventilation on indoor humidity in existing apartments in temperate climates

Authors: Kevin Michael Smith*, Svend Svendsen

Department of Civil Engineering, Technical University of Denmark, Building 118, Brovej, Kgs. Lyngby 2800, Denmark.

*Corresponding author. Tel.: +45 45 25 50 34. Email: kevs@byg.dtu.dk (K. Smith).

Abstract

The investigation constructed and simulated moisture balance equations for single-room ventilation with a non-hygroscopic rotary heat exchanger. Based on literature, the study assumed that all condensed moisture in the exhaust subsequently evaporated into the supply. Simulations evaluated the potential for moisture issues and compared results with recuperative heat recovery and whole-dwelling ventilation systems. To assess the sensitivity of results, the simulations used three moisture production schedules to represent possible conditions based on literature. The study also analyzed the sensitivity to influential parameters, such as infiltration rate, heat recovery, and indoor temperature. With a typical moisture production schedule, the rotary heat exchanger recovered excessive moisture from kitchens and bathrooms, which provided a mold risk. The rotary heat exchanger was only suitable for single-room ventilation of dry rooms, such as living rooms and bedrooms. The sensitivity analysis concluded that varying heat recovery or indoor temperature could limit indoor relative humidity in dry rooms when a moderate risk was present. The rotary heat exchanger also elevated the minimum relative humidity in each room, which could help to avoid negative health impacts. A discussion emphasized the potential benefits of selecting heat recovery to match the individual needs of each room.

Keywords

Decentralized ventilation; single-room ventilation; room-based ventilation; rotary heat exchanger; moisture issues; mold risk; renovated buildings; energy retrofit; temperate climate.

Highlights

- The simulated rotary heat exchanger provided moisture concerns in several rooms.
- The rotary heat exchanger was only suitable for ventilation of so-called dry rooms.
- Varying heat recovery or temperature can limit indoor relative humidity in dry rooms.
- Single-room ventilation allows selection of heat recovery to match the needs of rooms.

Nomenclature

Latin		**Subscripts**	
e	partial pressure of water vapor in air [hPa]	*amb*	ambient air
$G(t)$	mass flows of moisture at time t [g/h]	*dmix*	mixed dry room exhaust
G_i	moisture release in time step i [g]	*dp*	dew-point
m	mass [g][kg]	*dry*	subset of dry rooms
M	molar mass [g/mol]	*exh*	exhaust air
N	air changes rate [dt^{-1}][h^{-1}]	i	time step index
p	total barometric pressure [hPa]	*in,out*	direction of flow
R	universal gas constant [J/mol·K]	*inf*	infiltration air
T	air temperature [°C]	*max*	maximum
V	volume [m^3]	*min*	minimum
x	moisture content in mass of water per mass of dry [g/kg]	*room*	room index
		sat	saturation
Greek		*sources*	indoor sources
ρ	density [kg/m3]	*sup*	supply air
η	temperature efficiency [-][%]	*vent*	ventilation air
φ	relative humidity [%]	*wet*	subset of wet rooms
		wmix	mixed wet room exhaust

1 Introduction

In an effort to mitigate anthropogenic climate change, many governments have targeted energy savings to reduce greenhouse gas emissions. In the temperate climate of Denmark, heating in buildings is responsible for 25% of final energy consumption [1], so renovations provide obvious potential for savings. A Danish national action plan [2] therefore expects to reduce heating consumption in existing buildings by at least 35% before 2050. An assessment by the Danish Building Research Institute provided the basis for these expectations. The assessment [3] also considered a scenario in which renovations improve airtightness and thus require mechanical ventilation with heat recovery. This would further decrease heating consumption and improve indoor climate. To achieve this scenario, the assessment emphasized the need for inexpensive and flexible ventilation systems with heat recovery as well as the necessary knowledge and competence for proper implementation. For that purpose, Smith and Svendsen [4] described a collaborative development of a

rotary heat exchanger for room-based ventilation in existing apartments. The development of that prototype led to the current investigation, which simulated its impacts on indoor humidity to obtain knowledge for proper implementation.

The above scenarios assumed that renovations will replace worn out components with new components that that comply with building regulations. The 2010 Danish building regulations require heat recovery with a temperature efficiency of 70% for ventilation of entire buildings and 80% for single dwellings [5]. The 2020 regulations will increase these requirements to 75% and 85%, respectively [6], and the aforementioned prototype targeted the latter value. These regulations emphasize heat recovery, but they neglect the potential coupling of heat and moisture. They only discuss moisture transfer in heat exchangers when specifying conditions for testing. Similarly, a detailed guideline on indoor air quality from the World Health Organization recommended heat recovery to simultaneously retain heat and reduce indoor humidity, but it gave no further guidance on moisture transfer in heat exchangers [7]. In highly efficient heat recovery, the exhaust temperature often decreases below its dew point, so moisture condenses in the heat exchanger. If the amount of condensation is significant, it is important to know whether it will evaporate, drain, accumulate, or freeze, and the type of heat exchanger can influence this behavior.

There are two categories of air-to-air heat exchangers. Regenerators, such as rotary exchangers, intermittently expose airflows to the same medium to store and recover heat, whereas recuperators transfer heat through a membrane between airflows. A recuperator with an impermeable membrane does not transfer moisture. Any condensation on its surfaces must drain from the heat exchanger. Conversely, a regenerator exposes both airflows to the same heat transfer surface, so condensation from exhaust is likely to evaporate into the supply air [8]. This investigation focused on the latter to assess the impact of moisture transfer in a single-room rotary heat exchanger on indoor humidity and moisture issues for different room types.

Moisture removal is an important aspect of residential ventilation in humid temperate climates. According to the World Health Organization, excess indoor humidity can lead to health issues by promoting mold growth and proliferation of dust mites. It can also lead to structural issues by degrading building materials.

Infiltration lowers indoor humidity during the heating season, but its heat loss is excessive, so renovations maximize air tightness. With minimal contributions from infiltration, mechanical ventilation must solely remove sufficient moisture.

In temperate humid climates, the outdoor air is nearly saturated with moisture throughout the heating season. For example, the average relative humidity is 86% from September 16th to May 15th in the 2013 Danish design reference year [9], and the maximum 30-day average is 94%. If a rotary heat exchanger transfers all condensation between airflows, its drying capacity is only the difference in moisture content between the nearly saturated outdoor air and the saturated exhaust air. At low temperatures, the relatively small difference in saturated moisture content may severely limit the drying capacity of mechanical ventilation with a rotary heat exchanger. Figure 1 demonstrates this behavior with psychrometric charts for an uncoated rotary heat exchanger with the average outdoor conditions of 86% relative humidity (RH) and 4°C during the heating season in Denmark. The uncoated rotary heat exchanger has a temperature efficiency of 85% and cools the exhaust air below its dew point temperature for each of the three indoor relative humidities.

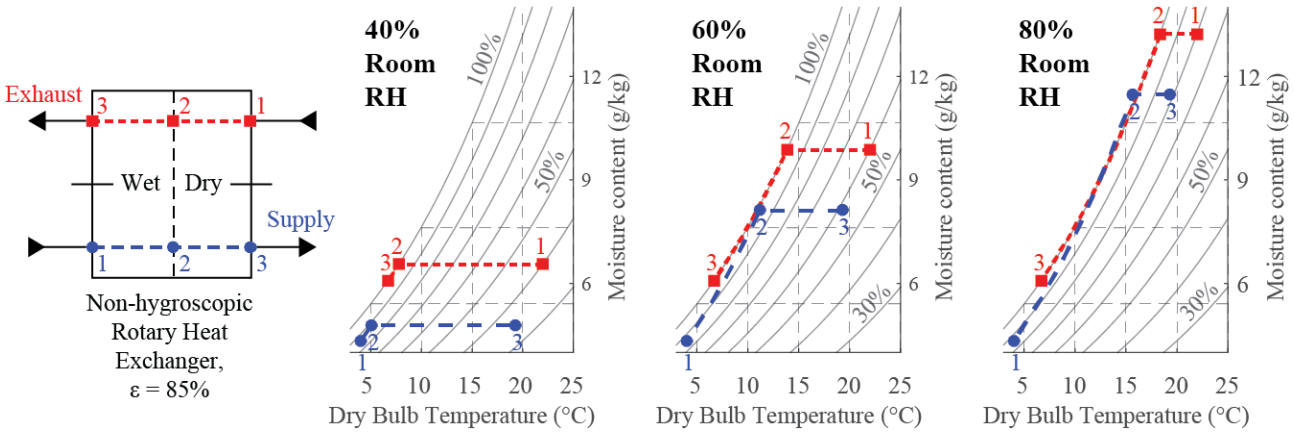

Figure 1. Supply and exhaust airflows through a heat exchanger with 85% temperature efficiency. Outdoor air is 4°C and 86% RH. Room air is 22 °C with three different relative humidities. The dew-point temperature of exhaust air is indicated by the red '2'.

In contrast, a desiccant-coated rotary heat exchanger that is "fully hygroscopic" may produce outlet conditions that are on a straight line between inlet conditions on a psychrometric chart, as shown in Figure 2. The term "fully hygroscopic" refers to a rotor with sufficiently high moisture capacity and sufficiently low diffusion resistance such that the moisture transfer efficiency is as high as the temperature efficiency [10].

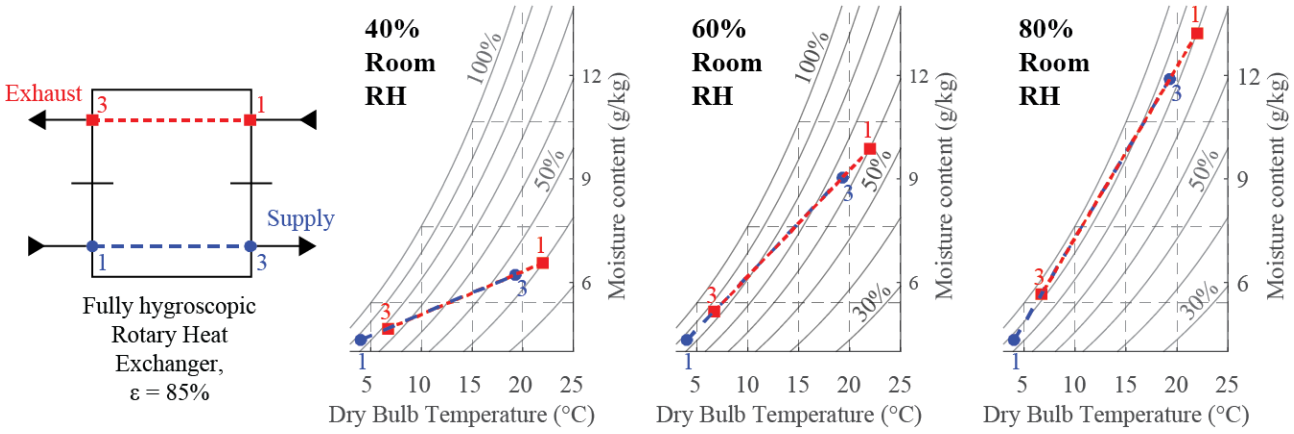

Figure 2. Example of a fully hygroscopic rotary heat exchanger with temperature and moisture efficiencies of 85%. The term "fully hygroscopic" refers to a rotor with sufficiently high moisture capacity and sufficiently low diffusion resistance such that moisture transfer efficiency may equal temperature efficiency.

Recent research has investigated intended moisture transfer in rotary heat exchangers [11][12][13]. These heat exchangers have hygroscopic surfaces to assist moisture transfer between airflows without the need for condensation. However the desirability of moisture transfer depends on context and may not be suitable for all applications. The current study specifically deals with the impacts of moisture transfer in non-hygroscopic heat exchangers with a focus on single-room ventilation in humid temperate climates. In the temperate zones of Sweden, non-hygroscopic rotary heat exchangers are often used in ventilation of entire dwellings, and limited research has indicated potential issues with excessive moisture recovery in certain contexts [14][15][16]. In other temperate climates, single-room ventilation units with various types of heat exchangers are increasingly installed through the façade of renovated buildings to supply fresh air and limit heat loss. These units provide simple installation and inherent advantages in potential efficiency [17], but their impact on indoor humidity has not been adequately researched and compared to standard systems.

This paper presents a preliminary assessment of the moisture impacts from a single-room ventilation unit with a non-hygroscopic rotary heat exchanger in a renovated Danish apartment. The schedule and rates of residential moisture production are clearly influential, so available literature was reviewed to identify suitable schedules. Using moisture balance equations, simulations yielded the sensitivities of indoor humidity to varying levels of moisture production, infiltration, heat exchanger efficiency, and room temperature for ventilation units serving individual rooms or whole dwellings. Since the focus was primarily

single-room ventilation, the results compared the rotary heat exchanger to recuperative heat exchangers that do not transfer moisture. If the single-room rotary unit could not meet requirements for temperature efficiency and avoid moisture issues, then the results favored recuperative heat recovery instead.

2 Methods

Simulations applied moisture balance equations to simplified airflows in a renovated apartment in Denmark. The simulations sought to determine the impact on indoor moisture conditions of single-room ventilation with a non-hygroscopic rotary heat exchanger.

2.1 Apartment Description

The simulated apartment assumed new windows and improved sealing to obtain an infiltration air change rate of 0.05 h^{-1}. The gross area of the apartment was 77 m^2, which is the average for low-rise social housing in Denmark [18]. Social housing comprises the largest share of multi-story dwellings in Denmark. Simulated rooms were 2.6 m in height, and Table 1 lists individual room areas. The interior floor area was 67.5 m^2, and Figure 3 shows the floorplan based on an actual apartment. The layout of the apartment assumed that all rooms had access to the façade and that air movement between rooms was fully mixed in a central corridor. The average daily occupancy was 14.2 hours on weekdays, which compared to the recommended attendance time of 14 hours per day for Swedish apartments in Johansson *et al.* [19].

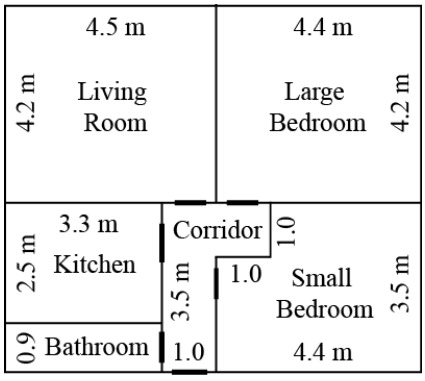

Figure 3. Floorplan of the simulated apartment with interior dimensions. The gross interior and exterior areas were 67.5 m^2 and 77 m^2, respectively. Room heights were 2.6 m.

Table 1. Room summary and occupancy profile for the assumed Danish apartment.

Room Type	Room Area *m^2*	Occupancy Schedule *Time interval*	Occupants *No. of adults*
Kitchen	8.3	7:00-8:00 12:00-13:00 17:00-20:00	1
Bathroom	3.0	7:00-9:00	1
Large Bedroom (adult couple)	18.5	22:00-7:00	2
Small Bedroom (child)	14.4	22:00-7:00	0.5
Living Room	18.9	16:00-22:00 (weekdays) 9:00-22:00 (weekends)	1
Corridor	4.4	-	0
Total	67.5	35.5 occupant-hours / weekday (59.2%) 42.5 occupant-hours / weekend day (70.8%)	

2.2 Moisture Production Schedule

Standards and guidelines provide design values for indoor moisture production. This investigation referenced data from BS 5250: Code of practice for control of condensation in buildings [20] and CIBSE Guide A: Environmental Design [21]. However the origins of this data were unclear. Multiple studies have documented moisture production in greater detail. Angell and Olson [22] listed tabular data for individual sources, but some values originated from a study published in 1948 that may be outdated. More recently, TenWolde and Pilon [23] collected and formulated rates and Yik *et al.* [24] comprehensively measured rates for a household in Hong Kong. Reported values have varied substantially, so simulations used three different scenarios to cover greater possibilities.

2.2.1 Scenarios

The best-case scenario assumed the lowest estimated values from references, which often resulted from measures to control moisture sources. This included venting of the washer/dryer to the outdoors, cooking with an electric stove, drying inside a dishwasher, and maximum drainage while showering. The typical scenario assumed common modern appliances, recently measured release rates, and common methods for source control. The worst-case scenario mainly referenced standards and design guidelines. It described a scenario with gas stoves, steam-intensive meals, older appliances, wet mopping, and lengthy showers. The assumed aggregate values for each scenario are listed in Table 2.

Table 2. Assumed aggregate values for the release of indoor moisture sources in the simulated apartment.

				Scenarios		
Activity	***Room***	**Frequency**	***Units***	**Best-case**	**Typical case**	**Worst-case**
Cooking method	*Kitchen*	-	-	Electric / Sealed-gas	Electric / Gas	Gas
Cooking load	*Kitchen*	-	*kg/day*	0.24	1.00 / 2.35	5.06
Dishwasher load	*Kitchen*	*daily*	*kg/day*	0.05	0.15	0.45
Cleaning	*All*	*weekly*	*kg/m2*	0.005	0.005	0.15
			kg/day	0.04	0.04	1.32
Shower load	*Bathroom*	3 *showers/day*	*kg/shower*	0.20	0.35	0.53
			kg/day	0.60	1.40	2.12
Clothes method	-	-	-	Dryer vented to outdoors	Fast spinning wash / Hang dry	Slow spinning wash / Hang dry
Clothes drying load	*Bathroom*	3 *loads/week*	*kg/load*	0	1.67	2.9
			kg/day	0	0.72	1.24
Plants	*Living*	*Continuous*	*kg/day*	0	0.06	0.45
Pets	*Living*	*Continuous*	*kg/day*	0	0.12	0.41

2.2.2 Cooking

Cooking on a gas stove releases approximately 0.45 kg/h from combustion [23][24] unless it is sealed and vented to the outdoors. The best-case scenario assumed negligible release from breakfast and lunch and 0.24 kg from a warm dinner cooked with an electric stove. TenWolde and Pilon proposed this dinner using data measured by Yik *et al.*. This scenario also assumed negligible release from an electric kettle. The typical scenario applied data from Hite and Bray [25] that listed loads from three meals as 0.17 kg, 0.25kg, and 0.58 kg, plus 0.28 kg, 0.32 kg, and 0.75 kg from gas combustion. The study noted the wide variability of moisture loads from different meals. The worst-case scenario used measured moisture loads by Yik *et al.* for a family of four in Hong Kong. The loads were approximately 0.25 kg, 0.95 kg, and 3.8 kg for three meals, which included gas combustion.

2.2.3 Dishwashing

Modern washers heat dishes to evaporate moisture and allow vapor to condense on interior surfaces. They include a sensor to indicate complete drying, so minimal moisture remains. The best-case scenario assumed 0.05 kg release from dishwashing. The typical scenario assumed a release of 0.15 kg/day, which agreed with the measured value for hand-washing and drying of 0.144 kg/day by Yik *et al.* as well as the recommended minimum of 0.15 kg/day in CIBSE Guide A. The worst-case scenario assumed 0.45 kg/day, which the CIBSE guide provided as a maximum.

2.2.4 Cleaning

Yik *et al.* measured a release rate from mopping of only 5 g/m^2. Modern mops use microfiber pads and deposit minimal moisture, so the best-case and typical scenarios assumed 5 g/m^2 once per week. The worst-case scenario assumed a value 150 g/m^2 as reported by Hite & Bray and repeated in BS 5250. Simulations assumed that carpets and furniture covered 20% of the floor area.

2.2.5 Showering

Angell and Olson referred to a study from 1985 that estimated the moisture release from a 5 minute shower as 0.25 kg. The estimate did not seem to include all drying, including towels, spillage, bath mats, or hair drying. A study by Unilever N.V. in 2011 determined the average shower length in the UK to be 8 minutes using embedded sensors in shower heads [26]. Yik *et al.* calculated the moisture release from a shower to be 0.53 kg based on ventilation rate, sensor data, and a moisture balance, and their surveyed respondents reported an average shower length of 18 minutes.

In the simulated apartment, the best case scenario assumed 0.25 kg per shower based on the load for a 5-minute shower cited by Angel & Olson. The typical case scenario estimated 0.40 kg per shower based on the same rate over an 8-minute shower as measured by Unilever. The worst case scenario assumed the rate of 0.53 kg per shower as measured by Yik *et al.*.

2.2.6 Washing and drying of clothes

CIBSE Guide A provided outdated release rates of 0.5-1.8 kg for clothes washing and 5-14 kg for drying. Yik *et al.* measured undrained moisture in a clothes washer and regarded it as negligible, so this investigation only considered drying. Hite and Bray reported hand-wringing laundry and measured 12 kg of moisture in a single load. Improvements to washing machines have allowed faster speeds and greater drying. Angell and Olson reported 2.2-2.95 kg per load in 1988 and Yik *et al.* measured 1.66 kg per load in 2004, which may reflect these improvements. Apartments often lack space for a dryer, so Yik *et al.* hung their clothes to dry and measured the release rate over time.

The moisture release from drying laundry depends on the method applied. In this investigation, the best-case scenario assumed full source control and no moisture release. The typical scenario used the total release from Yik *et al.* and assumed similar rates that decreased linearly over 10 hours, as shown in Figure 4. The worst case scenario assumed hang-drying of a wetter load that released 2.9 kg over the same time span.

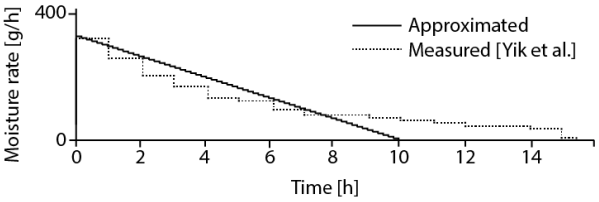

Figure 4. The simulated release of 1.66 kg of moisture from a load of laundry hung to dry based on measurements by Yik et al..

2.2.7 Plants

The best case scenario assumed that the apartment did not contain plants. The typical scenario assumed three plants at 2.5 g/h per plant based on the explanation by TenWolde and Pilon. The worst case scenario assumed seven average sized plants and a total release of 20 g/h as listed by Angell & Olson.

2.2.8 People and pets

TenWolde and Pilon calculated moisture release from an adult person as 0.03 to 0.07 kg/h. This agreed with other reported rates, including 0.04-0.1 kg/h in Yik *et al.* and CIBSE Guide A as well as 0.04 to 0.055 kg/h in BS 5250. For all scenarios, this investigation assumed that an adult of 70 kg released 0.06 kg/h and a child released half this rate. The release for pets was constant and assumed the same release per mass as adults. Their masses were 0 kg, 6 kg, and 20 kg in the best-case, typical, and worst-case scenarios, respectively.

2.3 Moisture Limits

The authors could not specify exact limits to prevent moisture issues due to uncertainty regarding surface temperatures, building materials, and cleanliness. The analysis instead used standards and approximate limits.

2.3.1 Dryness

Reinikainen and Jaakkola [27] studied the impact of relative humidity on human health and determined that low relative humidity can provoke skin symptoms, nasal dryness, and congestion. The standard EN 15251 for indoor climate stated that less than 15%-20% RH can cause these symptoms. The standard recommended greater than 20% RH to achieve the minimum category of air quality and greater than 30% RH to achieve the best category.

2.3.2 Mold Growth

After a comprehensive study, Rowan *et al.* [28] recommended that local surface relative humidity be kept below 75% to limit fungal growth. Johansson *et al.* [29] provided a range of limits above 75% to account for material type and cleanliness. Vereecken & Roels [30] reviewed prediction models for mold growth and found that multiple models used a critical surface RH of at least 80%. These studies demonstrated the variability of mold prediction and risk assessment.

With inexact limits on room RH, analyses can gauge relative mold risks with either the degree or the duration of violated limits. ASHRAE Standard 160:2009 attempts to evaluate both with one simple measure by limiting the maximum 30-day moving-average of surface relative humidities to 80% [31]. Surface temperatures depend on local effects, such as convective heat transfer coefficients, thermal transmittance of building components, and indoor and outdoor temperatures. Consequently, the minimum surface temperature in each room may be highly uncertain. During the heating season, a thermostat controls the average air temperature in each room, which increases its certainty. Simulations may assume fully mixed room air, which enables a simple and accurate calculation of room RH for known air temperatures. To simplify analysis, this investigation estimated an approximate limit on room RH using an 80% limit on surface RH. The author assumed a 1.5°C temperature difference between the room air and the coldest interior surface. For fully mixed air, an increase in air temperature of 1.5°C roughly corresponds to a 10% decrease in RH, so the author estimated a limit of 70% for room RH. Analysis evaluated the 30-day moving-average of room RH against this limit. The results section displays the maximum annual value in each room during the heating season, which indicates a compliance or violation of this limit.

The evaluation only considered surface relative humidities in the heating season since the summer period provides uncertain conditions. Most Danish apartment buildings turn off space heating in summer periods and do not use active cooling, so a lack of thermostatic control provides varying indoor air temperatures. Additionally, higher outdoor temperatures result in warmer interior surfaces, which also depend on the thermal inertia of the building construction. Lastly, the outdoor moisture content is high in summer and may dominate other influences. Many occupants open their windows in the summer period, which increases this effect.

Maximum 30-day moving average RH may roughly correspond to a steady state. Figure 1 shows that indoor humidity does not affect the drying capacity of ventilation when the exhaust is saturated in an uncoated rotary heat exchanger, and all simulated airflows may be fairly constant. However steady state simulations cannot capture the effects of fluctuating indoor RH, and Section 2.2 showed that indoor moisture sources vary over time. Since mold only grows above critical limits, dynamic simulations can improve risk characterization by quantifying the total duration above limits. This ensures that results are not disproportionately influenced by warmer months with high outdoor moisture content. Simulations of these months carry the greatest uncertainty due to the aforementioned issues in the summer period. The duration above limits captured the cumulative risk for the whole heating season. This allowed a visual representation of the relative influence from varied parameters.

2.3.3 Dust Mites

Dust mites require relative humidity above 45%-50% and multiply faster at higher levels [32]. They feed on dust that is abundantly available in beds and carpets, so relative humidity is the primary factor driving their growth [7]. As a result, indoor air should be maintained below 50% during the heating season, particularly in bedrooms and living rooms.

2.4 Moisture Balance Equations

The authors derived and simulated balance equations to describe the properties and dynamics of moisture flows in a renovated Danish apartment. Simulations used Matlab software to perform calculations with time steps of 10 minutes. Figure 5 shows the steps of the simulation and their associated equation numbers.

2.4.1 Weather data

The simulation imported hourly data from the 2013 Danish design reference year and copied it into 10 minutes intervals to capture the dynamic effects from short and intense moisture sources. The imported values included ambient air temperature, relative humidity, and pressure. Table 3 shows the quartiles of hourly values of temperature and relative humidity for the months of January, April, July, and October.

	Temperature					Relative Humidity				
Month	**Min.**	**25%**	**50%**	**75%**	**Max.**	**Min.**	**25%**	**50%**	**75%**	**Max.**
January	-8	0	1	3	5	58	84	91	96	100
April	0	4	7	10	20	34	67	78	87	100
July	9	15	18	20	28	38	63	79	91	98
October	1	8	10	12	16	62	82	89	94	100

Table 3. The minimum, 1st quartile, median, 3rd quartile, and maximum of hourly values of temperature and relative humidity in the Danish design reference year for the months of January, April, July, and October.

2.4.2 Infiltration

In the simulated apartment, the nominal infiltration rate was only 0.05 air changes per hour since infiltration should be minimized to warrant investment in heat recovery [33]. This assumed that infiltration rate was constant and proportional to room volume. In reality, various factors influence infiltration, such as wind pressure, indoor temperature, ventilation flows, and leakage in the building envelope [34], so it may not be uniformly distributed.

2.4.3 Ventilation requirements

The minimum ventilation rate was 0.5 air changes per hour, as recommended in a multidisciplinary review of literature on ventilation and health by Sendell *et al.* based on limited data [35]. Danish regulations require exhaust capacity in kitchens and bathrooms of 20 L/s and 15 L/s respectively, so simulations assumed these maximum rates. The ventilation rate in kitchens and bathrooms underwent a controlled increased from

minimum to maximum capacity based on indoor relative humidity. The proportional increase occurred from 50% to 70% RH, which took the following form in simulations:

$$N_{vent,room,i} = N_{vent,room,min} + \left[\left(N_{vent,room,max} - N_{vent,room,min}\right) \cdot min\{1, max\{\varphi_{room,i} - 50\%, 0\}/(70\% - 50\%)\}\right] \quad (1)$$

where $\varphi_{room,i}$ is the relatively humidity of the *room* at time step *i*, and $N_{vent,room}$ is the minimum, maximum, or variable ventilation air change rate in *room* denoted by *min*, *max*, and *i*, respectively. Simulations compared room-based ventilation to whole-dwelling ventilation to assess the impact of a local rotary heat exchanger in each room.

2.4.4 Room-based ventilation

Room-based ventilation was balanced and assumed no exchange of air between rooms. Simulations applied the following moisture balance equations for each room:

$$\left[m\frac{dx}{dt}\right]_{room} = G_{sources}(t) + G_{in}(t) - G_{out}(t) \quad (2)$$

where *m* is the mass of dry air, *x* is the moisture content per mass of dry air, *G(t)* are mass flows of moisture at time *t*, *in* and *out* denote inward and outward airflows respectively, and the subscript *sources* denotes moisture from indoor sources. Expanding Eq. (2) yielded

$$(\rho V)_{room}\frac{dx}{dt} = G_{sources}(t) + N_{inf}(\rho V)_{room}[x_{amb}(t) - x_{room}(t)] + N_{vent,room}(t)(\rho V)_{room}\left[x_{sup}(t) - x_{room}(t)\right] \quad (3)$$

where ρ and *V* are the dry air density and volume respectively, N_{inf} is the air change rates per time increment *dt* from infiltration, and the subscripts *amb* and *sup* denote ambient air and supply air respectively. Eq. (3) was discretized and took the following form for simulated iterations:

$$x_{room,i+1} = x_{room,i} + \frac{G_{room,i}}{(\rho V)_{room}} + N_{inf}\left(x_{amb,i} - min\{x_{room,i}, x_{sat,room}\}\right) + N_{vent,room,i}\left(x_{sup,room,i} - min\{x_{room,i}, x_{sat,room}\}\right) \quad (4)$$

where $x_{room,i}$ is the moisture content in mass of water (i.e. vapor and condensation) per mass of dry air at the start of time step *i*, N_{inf} and $N_{vent,room,i}$ are the air change rates per time step, $x_{sat,room}$ is the saturation moisture

content of room air, and $G_{room,i}$ is moisture release in *room* during time step *i*. Infiltration air change rates were specified at dry air densities and indoor air temperatures.

2.4.5 Whole-dwelling ventilation

For ventilation of whole-dwellings, the term *dry rooms* describes bedrooms and living rooms while *wet rooms* describes kitchens and bathrooms. Fresh air enters dry rooms and exhaust exits from wet rooms. The moisture balance equations for the whole-dwelling were similar to Eq. (4), but the exhaust from dry rooms mixed completely in the corridor and entered wet rooms as supply air. Simulations assumed that the flow rate from each dry room was proportional to its volume, which took the form of

$$N_{vent,room,i} = \frac{V_{room}}{\sum V_{dry}} \cdot \sum N_{vent,wet,i} \;\; \forall \, room \subset dry \qquad (5)$$

where *dry* and *wet* denote subsets of dry and wet rooms respectively. This enabled a calculation of the moisture content of the mixed exhaust from dry rooms, $x_{dmix,i}$, at the beginning of each iteration as

$$x_{dmix,i} = \frac{\sum(V_{room} \cdot x_{room,i})}{\sum V_{room}} \;\; \forall \, room \subset dry \qquad (6)$$

The equation for the moisture content of the supply air to wet rooms followed as $x_{sup,wet,i} = x_{dmix,i}$. The exhaust flows from wet rooms provided a combined minimum air change rate of 0.5 h^{-1} for the entire apartment. The simulation assumed that the minimum exhaust airflows from each wet room kept the same proportion as their maximum capacities. Therefore the 107.8 m^3/h divided into minimum rates, $N_{vent,wet,min}$, of 46.2 m^3/h and 61.6 m^3/h for the bathroom and kitchen respectively. Similar to the room-based ventilation, the whole-dwelling ventilation increased exhaust from the bathroom and kitchen up to their capacities, $N_{vent,wet,max}$, based on relative humidity. Moisture and sensible heat were transferred from mixed exhaust to mixed supply. The equation for the moisture content of mixed wet room exhaust, $x_{wmix,i}$, took the form:

$$x_{wmix,i} = \sum(N_{vent,wet,i} \cdot x_{wet,i}) \,/\, \sum N_{vent,wet,i} \qquad (7)$$

2.4.6 Variable calculations

The August-Roche-Magnus formula calculates the saturation vapor pressure of air as

$$e_{sat} = C_1 exp\left(\frac{A_1 T}{B_1 + T}\right) = 610.94\ Pa \times exp\left(\frac{17.625T}{243.04°C + T}\right) \quad (8)$$

where T is air temperature, e is the partial pressure of water vapor in air, and the subscript *sat* denotes saturation. Alduchov and Eskridge [36] suggested coefficients of A_1 = 17.625, B_1 = 243.04°C, C_1 = 610.94 Pa, which provide accuracy within 0.4% over the range -40°C to 50°C.

The equation $\varphi = 100 \cdot e/e_{sat}$ relates relative humidity, φ, to partial vapor pressure. Inserting Eq. (8) yielded:

$$e = e_{sat} \frac{\varphi}{100} = 610.94\ Pa \times exp\left(\frac{17.625T}{243.04°C + T}\right) \times \frac{\varphi}{100} \quad (9)$$

At initialization, simulations calculated $e_{sat,room}$ and $e_{amb,i}$ for all time steps. Simulations also calculated the ambient moisture content, $x_{amb,i}$, for all time steps. The moisture content, x, is the mass ratio of water vapor to dry air given by

$$x = \frac{M_{H_2O}}{M_{dry\ air}} = \frac{18.0\ g/mol \cdot \frac{e}{RT}}{29.0\ g/mol \cdot \frac{p-e}{RT}} = 0.622 \frac{e}{p-e} \quad (10)$$

where M is the molar mass, p is the total barometric pressure, e is the vapor pressure as calculated above, and R is the universal gas constant.

Simulations then performed iterations for each time step of ten minutes. The indoor moisture content, $x_{room,i}$, was allowed to exceed saturation, and the surplus moisture represented condensation on surfaces that immediately evaporated when possible. The simulation used moisture content from the previous iteration and limited relative humidity to 100%. Each iteration calculated relative humidity from the moisture content with the following equation:

$$\varphi_{room,i} = min\{x_{room,i}/x_{sat,room}, 100\} \quad (11)$$

Simulations then used the following formula from Lawrence [37] to calculate the dew point in each room, $T_{dp,room,i}$:

$$T_{dp,room,i} = \frac{B_1 ln\left(\frac{e_{room,i}}{C_1}\right)}{A_1 - ln\left(\frac{e_{room,i}}{C_1}\right)} = \frac{B_1 \left[ln\left(\frac{\varphi_{room,i}}{100}\right) + \frac{A_1 T_{room}}{B_1 + T_{room}}\right]}{A_1 - ln\left(\frac{\varphi_{room,i}}{100}\right) - \frac{A_1 T_{room}}{B_1 + T_{room}}} = \frac{243.04°C \left[ln\left(\frac{\varphi_{room,i}}{100}\right) + \frac{17.625\ T_{room}}{243.04°C + T_{room}}\right]}{17.625 - ln\left(\frac{\varphi_{room,i}}{100}\right) - \frac{17.625\ T_{room}}{243.04°C + T_{room}}} \quad (12)$$

where $\varphi_{room,i}$ and T_{room} are the relative humidity and temperature in the room respectively.

Simulations then used temperature efficiency and temperature differential to calculate the exhaust temperature leaving the heat exchanger. Exhaust had a lower limit of 0.5°C to avoid freezing inside the heat exchanger. Additionally, the exhaust temperature could not exceed the indoor room temperature, so it was determined by

$$T_{exh,i} = min\left\{T_{room}, max\left\{T_{room} - \eta_{exh}\left(T_{room} - T_{amb,i}\right), 0.5℃\right\}\right\} \quad (13)$$

where $\underline{\eta_{exh}}$ is the exhaust temperature efficiency, which was assumed to be equal to the supply temperature efficiency**.**

If the exhaust was warmer than the dew point temperature inside the room, heat recovery was a dry process. If the exhaust was colder, then it was saturated and vapor condensed inside the heat exchanger. Simulations of the rotary heat exchangers assumed that all condensation evaporated into the supply air, and equations for moisture content were

$$x_{exh,room,i} = \begin{cases} x_{sat,exh,i} = 0.622\frac{e_{sat,exh,i}}{p_{atm} - e_{sat,exh,i}}, & T_{exh,i} \le T_{dp,room,i} \\ min\left\{x_{room,i}, x_{sat,room}\right\}, & T_{exh,i} > T_{dp,room,i} \end{cases} \quad (14)$$

$$x_{sup,room,i} = \begin{cases} x_{amb,i} + min\left\{x_{room,i}, x_{sat,room}\right\} - x_{exh,room,i}, & T_{exh,i} \le T_{dp,room,i} \\ x_{amb,i}, & T_{exh,i} > T_{dp,room,i} \end{cases} \quad (15)$$

where the subscripts *exh*, *sup*, and *amb* denoted exhaust, supply, and ambient air respectively.

Simulations of recuperative heat recovery assumed that all condensate drained from the heat exchanger. Therefore the equations for moisture content of exhaust were the same as Eq. (14) and (15), except that the supply air had $x_{sup,i} = x_{amb,i} \; \forall \; T_{exh,i}$.

For both types of heat recovery, each iteration lastly updated moisture content according to Eq. (4).

SIMULATION STEPS

Parameters $G_{room,i}$ T_{room} η N_{inf} $T_{amb,i}$ $\varphi_{amb,i}$ V_{room} $N_{vent,room,min/max}$

Variables $\varphi_{room,i}$ $e_{room,i}$ $x_{room,i}$ $T_{dp,room,i}$ $x_{exh,room,i}$ $x_{sup,room,i}$ $N_{vent,room,i}$ $e_{exh,room,i}$ $x_{dmix,i}$ $x_{wmix,i}$ $\varphi_{wmix,i}$ $T_{dp,wmix,i}$

Initial equations **Eq. #**

1: $\{T_{room}\ \varphi_{room,1}\} \rightarrow e_{room,1}$ (9)

2: $e_{room,1} \rightarrow x_{room,1}$ (10)

3: $T_{room} \rightarrow e_{sat,room} \rightarrow x_{sat,room}$ (8,10)

4: $\{T_{room}\ T_{amb,i}\ \eta\} \rightarrow T_{exh,i} \forall\ i$ (13)

5: $T_{exh,i} \rightarrow e_{sat,exh,i} \forall\ i$ (8)

6: $\{T\ \varphi\}_{amb,i} \rightarrow e_{amb,i} \rightarrow x_{amb,i} \forall\ i$ (9,10)

Single-room vent. iteration **Eq. #**

1: $x_{room,i} \rightarrow \varphi_{room,i} \rightarrow T_{dp,room,i}$ (11,12)

2: $T_{exh,i} < T_{dp,room,i} \rightarrow x_{exh,room,i}, x_{sup,room,i}$ (14,15)

3: *Wet room iteration* $\{room \subset wet\}$

$\varphi_{room,i} \rightarrow N_{vent,room,i}$ (1)

4: $\{x\ G\ N_{vent}\ x_{sup}\}_{room,i} \rightarrow x_{room,i+1}$ (4)

Whole-dwelling vent. iter. **Eq. #**

1: $x_{room,i} \rightarrow \varphi_{room,i}$ (11)

2: *Mixed dry room exhaust*

$x_{room,i} \rightarrow x_{dmix,i} \forall\ room \subset dry$ (6)

3: *Wet room iteration* $\{room \subset wet\}$

$\varphi_{room,i} \rightarrow T_{dp,room,i}$ (12)

$\varphi_{room,i} \rightarrow N_{vent,room,i}$ (1)

$x_{dmix,i} = x_{sup,room,i}$

4: *Mixed wet room exhaust*

$\{N_{vent}\ x\}_{wet,i} \rightarrow x_{wmix,i}$ (7)

$x_{wmix,i} \rightarrow \varphi_{wmix,i} \rightarrow T_{dp,wmix,i}$ (11,12)

$T_{exh,i} < T_{dp,wmix,i} \rightarrow x_{wmix,i}$ (14)

5: *Dry room iteration* $\{room \subset dry\}$

$T_{exh,i} < T_{dp,wmix,i} \rightarrow x_{sup,room,i}$ (15)

$N_{vent,wet,i} \rightarrow N_{vent,room,i}$ (5)

6: $\{x\ G\ N_{vent}\ x_{sup}\}_{room,i} \rightarrow x_{room,i+1}$ (4)

Figure 5. Schematic of simulation steps, including equation numbers for reference. The simulation declared variables for all time steps *i*, specified parameters, calculated the initial equations, and then performed the iterations. The iterations only show variables.

2.4.7 Heat recovery

The 2020 Danish building regulations will require 85% temperature efficiency for ventilation serving single dwellings. The authors obtained similar efficiencies for a range of flow rates using a prototype single-room ventilator with a rotary heat exchanger intended for use in existing apartments [4]. Its modelled temperature efficiency accounted for leakage and predicted 90% to 78% for balanced flow rates of 3.6 L/s to 13.0 L/s respectively, and experiments agreed adequately despite some uncertainty.

To enable a comparison with whole dwelling ventilation, the temperature efficiency was set to 85% for all flow rates in both cases. In reality, higher flow rates result in decreased temperature efficiencies and even

greater drying capacity. In this investigation, only the kitchens and bathrooms allowed variable fan flow. With whole-dwelling ventilation, the allowable range of flow rates was much smaller because 0.5 h^{-1} applied to the whole apartment and required at least 30 L/s. Conversely, the minimum flow rates with single-room ventilation were much smaller as the air change rate applied to each room. To further simplify analysis, heat recovery only operated in the heating season, which ran from September 16th to May 15th in the simulation.

2.5 Parameter Variations

Simulations varied sensitive parameters to demonstrate the impact of different conditions. Based on the moisture balance equations, the authors identified infiltration, heat exchanger efficiency, and room temperature as three potentially influential parameters. Their standard values were 0.05 h^{-1}, 85%, and 22°C, respectively. Variable moisture sources were also influential, but their influence was assessed through the three scenarios described in Section 2.2.1.

3 Results

The following section shows the results of the reference case, which simulated recuperative heat recovery with the typical moisture production scenario. The subsequent section shows the results of the test case, which simulated a rotary heat exchanger with all moisture production scenarios. In all figures the dashed lines represents the standard case as listed in Section 2.5, which is used with other parameter variations.

3.1 Recuperative Heat Recovery

Ventilation with recuperative heat recovery provided the reference case for comparison. With the typical moisture production scenario, Table 4 shows the minimum moving-average relative humidities for ventilation serving single-rooms or whole-dwellings. The table compares these values to the recommended design minimum in standard EN 15251 of 15%-20%. The data represents the standard simulation with 85% temperature efficiency, an infiltration rate of 0.05 h^{-1}, and an indoor temperature of 22°C. The results indicate that the relative humidity in the living room and bedrooms may be insufficient for short durations with recuperative heat recovery.

Table 4. Minimum moving-average relative humidities with the standard simulation parameters and recuperative heat recovery.

			Minimum moving average RH in heating season [%]				
Ventilation type	**EN 15251 Annex B.3 Criteria**	**Minimum moving average**	**Kitchen**	**Bathroom**	**Large bedroom**	**Small bedroom**	**Living room**
Single-room	> 15-20%	1-day	26	16	19	13	15
		7-day	28	26	22	16	18
		30-day	32	30	26	21	23
Whole-dwelling	> 15-20%	1-day	20	16	12	11	11
		7-day	22	23	15	14	14
		30-day	27	28	20	19	19

With the standard simulation parameters, Table 5 shows that the maximum 30-day moving averages did not exceed 60% RH. All values were less than the estimated limit of 70% room RH, which implied that mold risk was not an issue. As described in Section 2.3, the authors assumed equivalence between this room air RH limit and the 80% surface RH specified in ASHRAE 160. Figure 6 shows the percentage of time steps with greater than 70% RH for each ventilated zone with the typical moisture production scenario. Ventilation with recuperative heat recovery adequately removed moisture from all rooms for both ventilation types. In terms of varied parameters, temperature efficiency did not influence indoor relative humidity, and infiltration had a very minor effect over the simulated range. Cooler room temperatures provided slightly higher relative humidities, but none of the simulated cases provided 30-day moving-averages greater than 70% room RH.

Table 5. Maximum 30-day moving-average relative humidities with standard simulation parameters and recuperative heat recovery.

Ventilation Type	**Maximum Moving Average**	**ASHRAE Surface Limit**	**Adjusted Room Limit**	**Kitchen [%]**	**Bathroom [%]**	**Large Bedroom [%]**	**Small Bedroom [%]**	**Living Room [%]**
Single-room	30-day	< 80%	< 70%	57	56	56	51	53
Whole-dwelling	30-day	< 80%	< 70%	57	57	49	48	49

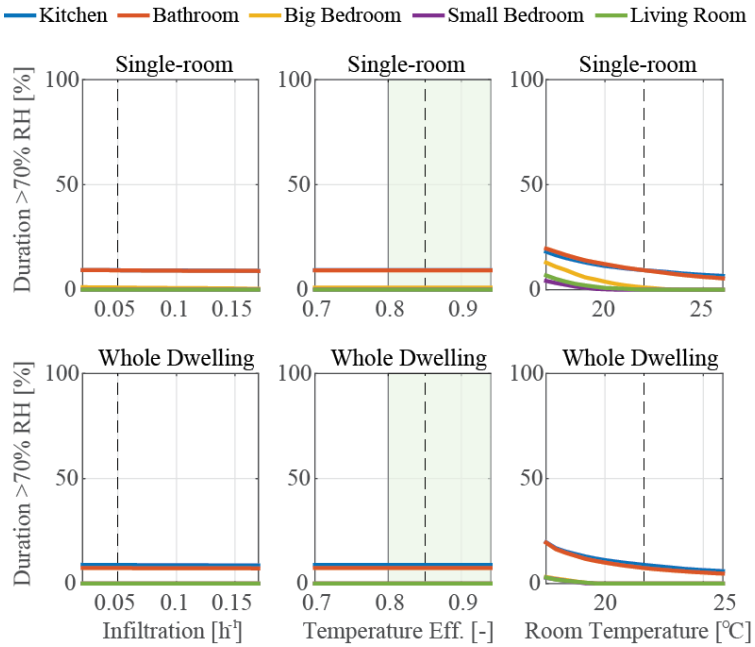

Figure 6. Recuperative heat recovery. Duration curves for the percentage of time steps with greater than 70% room RH for simulations with varied parameters.

3.2 Rotary Heat Exchanger

Results compared single-room ventilation with a rotary heat exchanger to the reference case. The results include simulations of whole-dwelling ventilation with a rotary heat exchanger for supplemental reference.

3.2.1 Best case scenario

At the nominal conditions in this scenario, the moving average relative humidities never exceeded the limits of ASHRAE 160 for any of the simulated cases, even after applying the 10% deduction described in Section 2.3.2. This standard protects against mold growth [38], so any concerns about dust mites still applied.

Figure 7 presents the results of simulations for single-room ventilation with the best-case moisture scenario. Air did not mix between rooms, so results were distinct. Only the bathroom and large bedroom provided potential concerns. In reality these two rooms have very different critical humidities, so they cannot be directly compared using this evaluation. As described in Section 2.3, dust mites proliferate in fabrics at relative humidities greater than 50%, whereas the interior surfaces of bathrooms may be resistant to mold growth, which raises their critical humidity. As such, the high humidity in bedrooms was more concerning.

Figure 7 also presents the results of rotary heat exchanger with the whole-dwelling ventilation system. The results were similar to the reference case with recuperative heat recovery. In this system, moisture transfer applied to the bulk properties of the mixed supply and exhaust airflows so recovered moisture was distributed evenly throughout the dwelling.

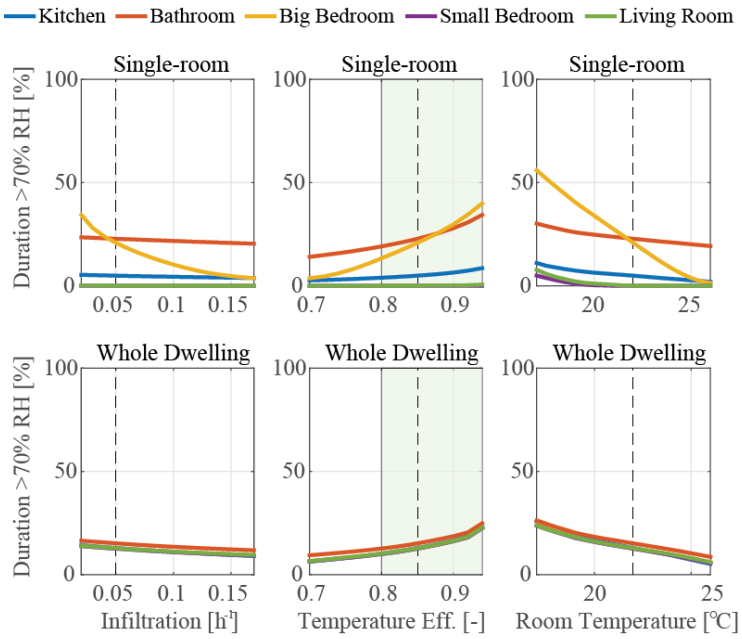

Figure 7. Simulation of regenerative heat recovery with the best-case moisture production scenario. Duration curves for percentage of time steps with greater than 70% room RH for simulations with varied parameters.

3.2.2 Typical scenario

With the typical moisture production scenario, Table 6 shows the minimum moving-average relative humidities for ventilation serving single-rooms or whole-dwellings with a rotary heat exchanger. Compared to the reference case with recuperative heat recovery, nearly all simulations provided better categories of relative humidity according to standard EN 15251. This demonstrates a potential benefit of moisture recovery.

Table 6. Minimum moving-average relative humidities with the standard simulation parameters and a rotary heat exchanger.

			Minimum moving average RH in heating season [%]				
Ventilation type	**EN 15251 Annex B.3 Criteria**	**Minimum moving average**	**Kitchen**	**Bathroom**	**Large bedroom**	**Small bedroom**	**Living room**
Single-room	1-day	> 20%	43	40	27	13	15
	7-day		48	51	32	16	19
	30-day		53	53	42	21	25
Whole-dwelling	1-day	> 20%	40	39	33	32	33
	7-day		47	47	40	39	39
	30-day		57	57	50	49	50

Table 7 compares the maximum 30-day moving averages to the adjusted ASHRAE limits to predict mold growth at nominal conditions. The single-room ventilation did not violate limits in any dry rooms.

Table 7. Maximum 30-day moving-average relative humidities with standard simulation parameters and a rotary heat exchanger.

Ventilation Type	**Maximum Moving Average**	**ASHRAE Surface Limit**	**Adjusted Room Limit**	**Kitchen [%]**	**Bathroom [%]**	**Large Bedroom [%]**	**Small Bedroom [%]**	**Living Room [%]**
Single-room	30-day	< 80%	< 70%	87	94	64	51	53
Whole-dwelling	30-day	< 80%	< 70%	97	97	91	90	90

Figure 8 shows that all simulations of single-room ventilation, including parameter variations, provided excessive humidity in kitchens and bathrooms with this moisture scenario.

In the best-case scenario reported above, whole-dwelling ventilation provided less risk of excessive humidity by combining airflows and evenly distributing recovered moisture to all rooms. In the typical scenario, the same mixing recovered moisture to all rooms, but the contributions from wet rooms were much more significant.

Figure 9 shows the cumulative distribution curve for indoor RH during representative months to assess seasonal differences. A rightward or downward shift provided an unfavorable change in RH. The curves are relatively similar in all the displayed months. However January provided the least favorable conditions for the kitchen and bathroom and the most favorable conditions for the small bedroom and living room. Humidity in the adult bedrooms was the most critical in October.

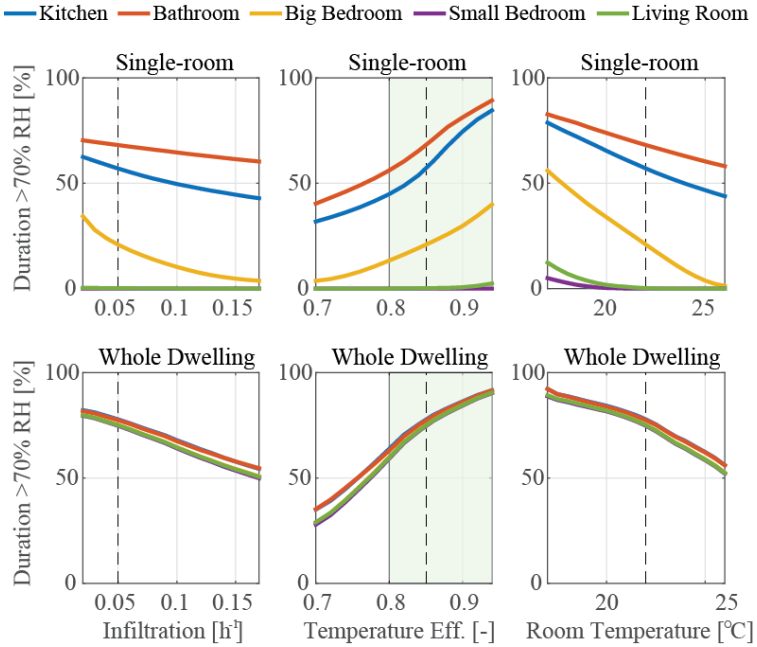

Figure 8. Simulation of regenerative heat recovery with the typical moisture production scenario. Duration curves for percentage of time steps with greater than 70% room RH for simulations with varied parameters.

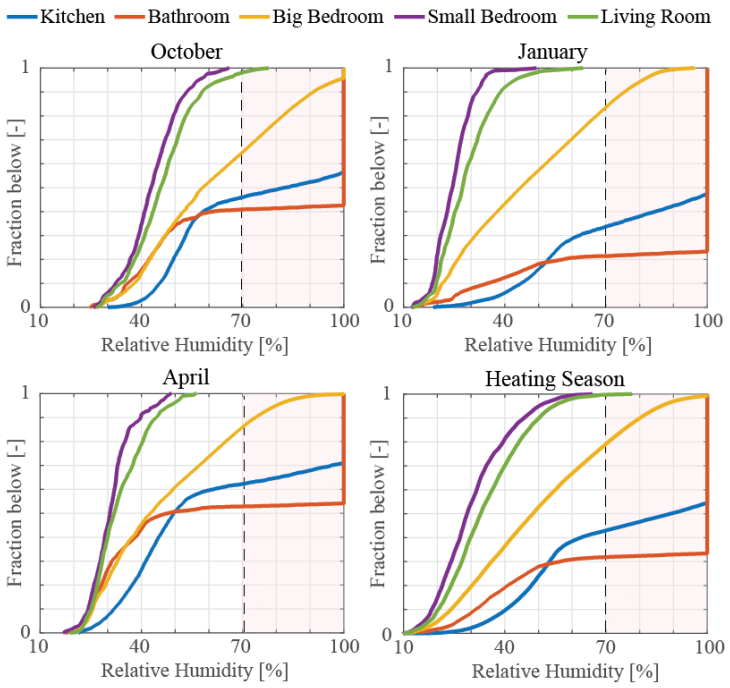

Figure 9. Cumulative distribution function of indoor relative humidities in each room during the months of October, January, April, and the whole heating season with a rotary heat exchanger in single-room ventilation and the typical moisture production scenario.

3.2.3 Worst-case scenario

With the worst-case moisture scenario, Figure 10 shows that ventilation serving only wet rooms provided an extremely high mold risk, but ventilation serving dry rooms yielded a moderate risk. With nominal

parameters in the worst-case scenario, all 30-day moving averages exceeded the limits from ASHRAE 160 except for the case of the living room and bedrooms with single-room ventilation, which exceeded none. Whole-dwelling ventilation with a rotary heat exchanger yielded excessive relative humidity for the majority of the heating season in all simulated rooms for all parameter variations.

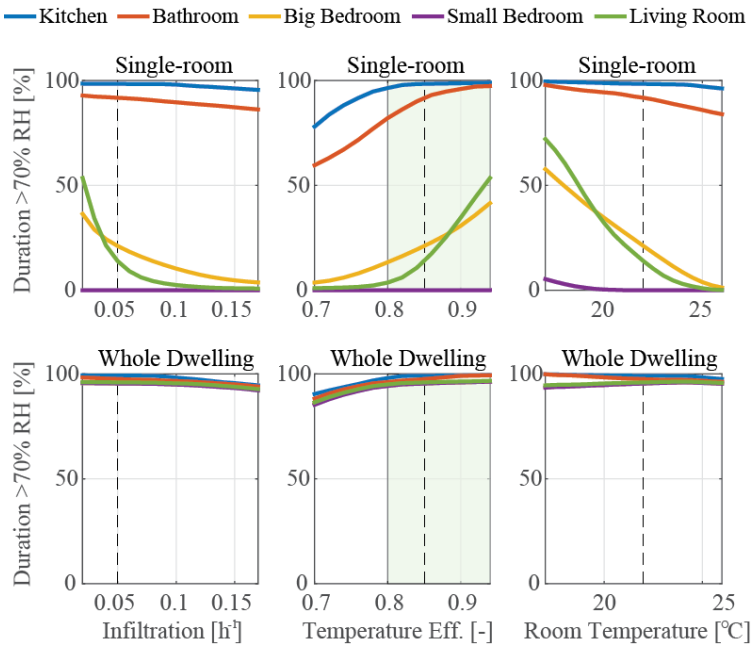

Figure 10. Simulation of regenerative heat recovery with the worst-case moisture production scenario. Duration curves for percentage of time steps with greater than 70% room RH for simulations with varied parameters.

4 Discussion

The results indicated that highly efficient rotary heat exchangers were unsuitable for wet rooms under the assumed conditions due to excessive moisture recovery. The results also indicated that rotary heat exchangers may provide low to moderate mold risk with single-room ventilation of dry rooms for a range of probable conditions.

The authors speculate that an adequate solution could include rotary heat exchangers in dry rooms and recuperative heat exchangers in wet rooms. A rotary heat exchanger transfers condensation to the supply air, so it does not require drainage. It may also prevent negative health impacts from dryness, as indicated by Table 6. Recuperative heat exchangers require drainage, and installation in kitchens and bathrooms would

allow easier access to plumbing. This combination utilizes the inherent advantages of each heat exchanger for the specific demands of individual rooms.

The moisture production schedule in dry rooms was similar for all three scenarios, so the rotary heat exchanger consistently provided a low to moderate mold risk with single-room ventilation. This could allow finer adjustments to minimize mold risk. The figures in Section 3.2 demonstrated the clear influence of varied parameters on the duration of excess relative humidity. Interestingly, two of the varied parameters are controllable during operation. This realization yields potential options to adjust relative humidity in dry rooms to maintain appropriate levels. A rotary heat exchanger relies on cyclical regeneration, so a controller could reduce its cyclical speed to reduce heat transfer. Less heat transfer implies greater exhaust temperatures and drying capacity. Similarly, higher room temperatures result in lower relative humidities and mold risk, so a controller could maintain sufficient room temperatures to avoid risk. Both options could negatively affect occupant thermal comfort. The former option could generate local discomfort due to cool draughts from lower supply temperatures, while the latter could affect whole-body comfort with changes in room temperature. However Figure 10 indicates that the required reduction in heat recovery or increase in room temperature may be small to limit relative humidities to acceptable levels.

This paper focused on single-room ventilation, but the same concerns may apply to whole-dwelling ventilation that extracts exhaust from wet rooms. The whole-dwelling simulation included many significant assumptions regarding air flows. It also assumed ambitious infiltration rates and temperature efficiencies, so the results are not conclusive. The results merely suggest that whole-dwelling ventilation with a highly efficient rotary heat exchanger should be researched in greater detail to assess potential issues from moisture recovery.

This investigation simplified implementation with many assumptions. Simulations did not account for moisture buffering from walls, which could dampen variations on indoor humidity and reduce the duration of exceeded limits. Salonvaara *et al.* [39] and Mortensen *et al.* [40] determined that typical interior paints can act as vapor barriers and effectively limit moisture transfer between construction materials and room air, so

this assumption was reasonable. However, the simulation did not account for dampening from furniture, books, and textiles, and Svennberg *et al.* [41] measured a reduced daily peak of 10% RH and an increased daily trough of 5% RH after fully furnishing a room. Additionally, simulations did not distinguish between interior surface materials, which provide different resistances to mold growth and different critical humidities. The investigation also assumed approximate surface temperatures, which highly influence surface relative humidities. Greater knowledge of the average Danish apartment could therefore improve the assessment of mold risk with these ventilation systems.

This study also assumed that rotary heat exchangers transfer all condensation in the exhaust to the supply air. This point is commonly advertised by manufacturers to emphasize that drainage is not required. However, Holmberg [10] presents the possibility of excess moisture in the heat exchanger. If cold outdoor air is nearly saturated upon entry to the heat exchanger then condensation may not be able to completely evaporate. This small longitudinal region would then accumulate moisture and its movement is difficult to predict. This study assumed that any accumulated moisture moved to a warmer section of the heat exchanger and evaporated into the supply air. This can only be confirmed experimentally.

5 Conclusion

The investigation constructed and simulated moisture balance equations for a single-room ventilation unit with a non-hygroscopic rotary heat exchanger. Its assessment focused on its moisture impacts in a typical renovated apartment in a humid temperate climate. The rotary heat exchanger recovered excess moisture in kitchens and bathrooms and provided a serious mold risk. The rotary heat exchanger was only suitable for single-room ventilation of dry rooms, such as living rooms and bedrooms. In these rooms, the risk of mold depended on moisture production. The sensitivity analysis concluded that varying heat recovery or indoor temperature could limit indoor relative humidity in dry rooms when a moderate risk was present. The rotary heat exchanger also elevated the minimum moving-average relative humidities, which may help to avoid negative health impacts from dry air. A discussion emphasized the potential benefits of selecting heat recovery to match the needs of individual rooms.

Acknowledgements

This research was funded by the Technical University of Denmark and the Innovation Fund (Fornyelsesfonden) as part of a collaborative project to research and develop decentralized ventilation for existing residential apartments. Partners included Christian Niepoort of Smith Innovation, Henning Solfeldt of PLH Architects, Torben Kirkholt of EBM Papst, Hasse Brønnum of Brønnum Plast, and Anders L. Jansen of the Technical University of Denmark.

References

[1] Energi Styrelsen, Energistatistik 2014 [Energy statistics 2014], Copenhagen, 2014. http://www.ens.dk/sites/ens.dk/files/info/tal-kort/statistik-noegletal/aarlig-energistatistik/energistatistik_2014.pdf.

[2] Danish Energy Agency, Denmark's National Energy Efficiency Action Plan, Copenhagen, 2014. https://ec.europa.eu/energy/sites/ener/files/documents/2014_neeap_en_denmark.pdf

[3] Dansk Klima-, Energi- og Bygningsministeriet, Strategi for energirenovering af bygninger [Strategy for energy renovation of buildings], Copenhagen, 2014. http://www.ens.dk/sites/ens.dk/files/byggeri/Strategi-for-energirenovering-af-bygninger/strategi-for-energirenovering-af-bygninger-web-050514.pdf

[4] K.M. Smith, S. Svendsen, Development of a plastic rotary heat exchanger for room-based ventilation in existing apartments, Energy Build. 107 (2015) 1–10. doi:10.1016/j.enbuild.2015.07.061.

[5] Danish Energy Agency, Building Regulations, Copenhagen, 2010. http://bygningsreglementet.dk/file/155699/BR10_ENGLISH.pdf

[6] Energi Styrelsen, Fælles bestemmelser for bygninger omfattet af bygningsklasse 2020 [Provisions common to buildings covered by the class of 2020] (2010). http://bygningsreglementet.dk/br10_05_id5181/0/42

[7] WHO Regional Office for Europe, WHO guidelines for indoor air quality: Dampness and mold, World Health Organization, Geneva, 2009. http://www.euro.who.int/__data/assets/pdf_file/0017/43325/E92645.pdf

[8] R.B. Holmberg, Heat and mass transfer in rotary heat exchangers with nonhygroscopic rotor materials, J. Heat Transf. ASME. 99 (1977) 196–202.

[9] P.G. Wang, M. Scharling, K.P. Nielsen, 2001-2010 Design Reference Year for Denmark, Technical report 12-17, Danish Meteorological Institute, Copenhagen, 2012. http://www.dmi.dk/fileadmin/Rapporter/TR/tr12-17.pdf

[10] R.B. Holmberg, Prediction of condensation and frosting limits in rotary wheels for heat recovery in buildings, ASHRAE Transactions. 95 (1989) 64-69.

[11] C.J. Simonson, R.W. Besant, Heat and moisture transfer in energy wheels during sorption, condensation, and frosting conditions, J. Heat Transfer. 120 (1998) 699. doi:10.1115/1.2824339.

[12] W. Ruan, M. Qu, W.T. Horton, Modeling analysis of an enthalpy recovery wheel with purge air, Int. J. Heat Mass Transf. 55 (2012) 4665–4672. doi:10.1016/j.ijheatmasstransfer.2012.04.025.

[13] S. De Antonellis, M. Intini, C.M. Joppolo, F. Pedranzini, Experimental analysis and practical effectiveness correlations of enthalpy wheels, Energy Build. 84 (2014) 316–323. doi:10.1016/j.enbuild.2014.08.001.

[14] L. Jensen, Fuktöverföring vid regenerativ värmeväxling [Moisture transfer in regenerative heat exchange], Lund University, Lund, 2010. http://www.lunduniversity.lu.se/lup/publication/3290479

[15] L. Jensen, Fukttillskott i frånluft [Excess moisture in exhaust air], Lund University, Lund, 2010. http://www.lunduniversity.lu.se/lup/publication/3290476

[16] D. Malm, Fuktåterföring i roterande värmeväxlare [Moisture transfer in rotary heat exchangers] (Master's Thesis), Royal Institute of Technology, Stockholm, 2012. http://kth.diva-portal.org/smash/get/diva2:550959/FULLTEXT01.pdf

[17] D.R. Wulfinghoff, Multiple-zone HVAC: An obsolete template, World Energy Eng. Congr. 2009, WEEC 2009. 2 (2008) 762–768. doi:10.1080/01998595.2011.10389019.

[18] H. Kristensen, Housing in Denmark, Realdania Research, Copenhagen, 2007. http://boligforskning.dk/sites/default/files/Housing_130907.pdf

[19] D. Johansson, H. Bagge, L. Lindstrii, Measurements of occupancy levels in multi-family dwellings - Application to demand controlled ventilation, Energy Build. 43 (2011) 2449–2455. doi:10.1016/j.enbuild.2011.05.031.

[20] British Standard Institution, Code of practice for control of condensation in buildings, BS 5250, Authors, London, 1989.

[21] Chartered Institution of Building Services Engineers, CIBSE Guide A – Environmental Design. Authors, London, 1999.

[22] W.J. Angell, W.W. Olson, Moisture sources associated with potential damage in cold climate housing, Minnesota Extension Service, University of Minnesota (1988) 1-8.

[23] A. TenWolde, C.L. Pilon, The effect of indoor humidity on water vapor release in homes, Therm. Perform. Exter. Envel. Whole Build. X Int. Conf. (2007) 1–9. http://www.fpl.fs.fed.us/documnts/pdf2007/fpl_2007_tenwolde001.pdf

[24] F.W.H. Yik, P.S.K. Sat, J.L. Niu, Moisture generation through Chinese household activities, Indoor Built Environ. 13 (2004) 115–131. doi:10.1177/1420326X04040909.

[25] S.C. Hite, J.L. Bray, Research in home humidity control, Engineering Experiment Station, Research Series No. 106 (1948).

[26] Unilever, Sustainable Shower Study (2011). http://www.unilever.co.uk/media-centre/pressreleases/2011/sustainableshowerstudy.aspx

[27] L.M. Reinikainen, J.J.K. Jaakkola, Significance of humidity and temperature on skin and upper airway symptoms, Indoor Air. 13 (2003) 344–352. doi:10.1111/j.1600-0668.2003.00155.x.

[28] N.J. Rowan, C.M. Johnstone, R.C. McLean, J.G. Anderson, J. a Clarke, Prediction of toxigenic fungal growth in buildings by using a novel modelling system., Appl. Environ. Microbiol. 65 (1999) 4814–21. http://www.pubmedcentral.nih.gov/articlerender.fcgi?artid=91649&tool=pmcentrez&rendertype=abstract.

[29] P. Johansson, I. Samuelson, A. Ekstrand-Tobin, K. Mjörnell, P.I. Sandberg, E. Sikander, Extracts from Microbiological growth on building materials: Critical moisture levels - State of the art, SP Technical Research Institute of Sweden, Borås, 2005. http://www.kuleuven.be/bwf/projects/annex41/protected/data/SP%20Oct%202005%20Paper%20A41-T4-S-05-3.pdf

[30] E. Vereecken, S. Roels, Review of mould prediction models and their influence on mould risk evaluation, Build. Environ. 51 (2012) 296–310. doi:10.1016/j.buildenv.2011.11.003.

[31] ASHRAE Standing Standard Project Committee 160, Addendum A to ANSI/ASHRAE Standard 160-2009, American Society of Heating, Refrigerating and Air-Conditioning Engineers, Atlanta, 2011. https://www.ashrae.org/File%20Library/docLib/StdsAddenda/160_2009_a_COMPLETE.pdf

[32] L.G. Arlian, Water balance and humidity requirements of house dust mites, Exp. Appl. Acarol. 16 (1992) 15–35. doi:10.1007/BF01201490.

[33] C.A. Roulet, F.D. Heidt, F. Foradini, M.C. Pibiri, Real heat recovery with air handling units, Energy Build. 33 (2001) 495–502. doi:10.1016/S0378-7788(00)00104-3.

[34] C. Younes, C. a. Shdid, G. Bitsuamlak, Air infiltration through building envelopes: A review, J. Build. Phys. 35 (2012) 267–302. doi:10.1177/1744259111423085.

[35] J. Sundell, H. Levin, W.W. Nazaroff, W.S. Cain, W.J. Fisk, D.T. Grimsrud, et al., Ventilation rates and health: Multidisciplinary review of the scientific literature, Indoor Air. 21 (2011) 191–204. doi:10.1111/j.1600-0668.2010.00703.x.

[36] O.A. Alduchov, R.E. Eskridge, Improved Magnus form approximation of saturation vapor pressure, J. Appl. Meteorol. 35 (1996) 601–609. doi:10.1175/1520-0450(1996)035<0601:IMFAOS>2.0.CO;2.

[37] M.G. Lawrence, The relationship between relative humidity and the dewpoint temperature in moist air: A simple conversion and applications, Bull. Am. Meteorol. Soc. 86 (2005) 225–233. doi:10.1175/BAMS-86-2-225.

[38] A. Tenwolde, A review of ASHRA standard 160 - Criteria for moisture controle design analysis in buildings, J. Test. Eval. 39 (2011) 1–5. doi:10.1520/jte102896.

[39] M. Salonvaara, T. Ojanen, A. Holm, H. Kunzel, A. Karagiozis, Moisture buffering effects on indoor air quality – experimental and simulation results, Proc. Perform. Exter. Envel. Whole Build. IX (2004) 1–11.

[40] L.H. Mortensen, C. Rode, R. Peuhkuri, Full scale tests of moisture buffer capacity of wall materials, Proc. 7th Symp. Build. Phys. Nord. Ctries. (2005) 662–669.

[41] K. Svennberg, L.G. Hedegaard, C. Røde, Moisture buffer performance of a fully furnished room, Proc. Perform. Exter. Envel. Whole Build. IX (2004) 1–11.

Appendix C - Paper 3

K.M. Smith, A.L. Jansen, S. Svendsen,

Assessment of a new demand-controlled room-based ventilation unit with heat recovery for existing apartments,

Energy Build. (Awaiting decision)

Assessment of a new demand-controlled room-based ventilation unit with heat recovery for existing apartments

Authors: Kevin Michael Smith*, Anders Lund Jansen, Svend Svendsen

Department of Civil Engineering, Technical University of Denmark, Building 118, Brovej, Kgs. Lyngby 2800, Denmark.

*Corresponding author. Tel.: +45 45 25 50 34. Email: kevs@byg.dtu.dk (K. Smith).

Abstract

A novel heat exchanger made of rolled plastic sheets provided encouraging results in a single-room ventilation unit. The heat exchanger provided a corrected supply temperature efficiency of 82.2% at a balanced ventilation rate of 13.5 L/s. At this flow rate, the total measured pressure drop across the filter and heat exchanger was 40 Pa. The external and internal leakages were approximately 2.7% and 12.1%, respectively. The authors simulated annual performance with predicted temperature efficiencies based on anticipated improvements. Simulations compared the single-room unit with variable-flow to a commercially available whole-dwelling unit with constant airflow. Both units ventilated a renovated residential apartment in Denmark in annual simulations. National regulations dictated the flow rates for the whole-dwelling system, while a controller determined flow rates in the single-room units based on sensed values of CO_2, relative humidity, and temperature in the extracted air. Both types of ventilation provided suitable indoor climate. Compared to the whole-dwelling unit, the single-room unit improved or maintained air quality and thermal comfort in simulations. The single-room unit also consumed less annual energy for fans and space heating with savings of 74% and 4-6%, respectively. The results indicated that single-room ventilation using demand control could provide a viable alternative for renovated apartments in Denmark.

Keywords

Decentralized ventilation; single-room ventilation; room-based ventilation; demand-control ventilation; air-to-air heat exchanger; ventilation heat recovery; renovated buildings; energy retrofit.

Nomenclature

Latin

C	Heat capacity rate [W/K]
c_p	Specific heat capacity [J/gK]
K	Calculation parameter [L/s]
NTU	Number of transfer units [-]
Q	Flow rate [L/s]
Re	Reynold number [-]
W	Internal leakage ratio [-]

Greek

ρ	density [kg/m^3]
η	temperature efficiency [%]

Subscripts

leak,int	Internal leakage
max	Maximum
meas.	Measured
min	Minimum
nom	Nominal value
Q	At flow rate, Q
real	Corrected value
unsealed	Unblocked airflow

1 Introduction

Many governments have targeted energy savings to reduce greenhouse gas emissions and limit anthropogenic climate change. In Denmark, heating in buildings is responsible for 26% of final energy consumption [1], and renovations could provide significant savings [2]. A Danish national action plan therefore expects to reduce heating consumption in the current building stock by at least 35% before 2050 [3]. Many existing apartments rely on mechanical exhaust to draw fresh air through cracks and orifices in the building envelope. Renovations improve airtightness [4] and require new supply points to maintain adequate air quality [5]. Some renovations provide fresh air through ducted vents in the façade, but this limits options for heat recovery. Air-to-air heat exchangers require a point of intersection between supply and exhaust, so renovations often mount supply ducts in limited space. Narrowing duct diameter exponentially increases frictional losses. Furthermore, renovations are unique, so the design and specification of ducts requires investment. The need to invest in planning before making an informed decision provides an early obstacle to renovation. Even after approval, installations may be labor intensive and temporarily displace occupants. A renovation with room-based ventilation aims to minimize these negatives. Single-room units occupy drilled holes in the façade, which can minimize the necessary planning, labor, space, and frictional losses associated with duct installation. Single-room units can also limit issues with biological growth in ducts, spread of smoke and fire, and losses due to leakage and thermal transmittance. Wulfinghoff [6] argued many of these points in favor of single-zone HVAC and heavily focused on its potential optimality.

If these technologies develop to their potential, they could optimally match demand with supply in individual rooms. As renovations improve the thermal resistance and airtightness of building envelopes, indoor temperatures and pollutant concentrations become increasingly more sensitive to thermal gains and emissions, respectively. Rooms on opposite façades may have conflicting thermal demands, and rooms could have similarly diverse demands for fresh air. Every closed door increases this sensitivity, which incentivizes room-based demand-control. Installers could specify the units according to room type and size, while sensors and demand-control could ensure optimal comfort and air quality. Product designers could place wired sensors in exhaust channels, which could allow their affordable usage.

Many systems achieve efficiency gains from economies of scale. Larger components are typically less expensive to manufacture, assemble, and operate per unit of utility. System designers must weigh these efficiency gains against the potential advantages of decentralization, including optimal service delivery and reduced transmission losses. In renovated apartments, ventilation may exist on various levels. However existing research is inadequate to compare ventilation serving multiple dwellings, whole dwellings, and single rooms. A more helpful comparison could include demand-control to represent future systems.

Recent research has investigated the benefits and risks of demand-controlled ventilation. Hesaraki and Holmberg [7] simulated demand-controlled ventilation in a new Swedish home and observed unsafe accumulation of volatile organic compounds unless ventilated prior to occupancy. When safely ventilated, their results showed total potential energy savings for heating and fans of 16% compared to a constant air volume (CAV) system. Cho *et al.* [8] performed simulations that offset fresh air demand with cleansed recirculated air in a Korean multi-residential building. Their results indicated acceptable average air quality and potential energy savings of 20% compared to a CAV system. Laverge *et al.* [9] simulated four different demand-control strategies in a statistically-average detached Belgian home. They reported varied effects on indoor air quality (IAQ), and their demand-control strategies reduced ventilation heat loss by 25%-60%. Morelli *et al.* [2] installed a whole-dwelling CAV ventilation unit in a renovated Danish apartment. The authors stated the need for demand-controlled ventilation due to high incidences of open windows, which significantly lowered CO_2 concentrations. Mortensen et al. [10] assessed the impact of demand-controlled

ventilation on occupant exposure to pollutants in residences by analyzing long-term exposure and peak exposure. Demand control reduced long-term exposure and increased peak exposure within safe limits.

As part of a collaborative development project for room-based ventilation, the authors tested a novel heat exchanger made of rolled polyvinyl chloride (PVC) sheets. Its measured and anticipated performance provided input data for simulations. The simulated single-room ventilation unit used demand-control based on CO2, temperature, and humidity. Analysis compared its performance to whole-dwelling ventilation. Many building simulation programs lack modularity, which hinders their ability to simulate innovative systems [11]. The platform IDA Indoor Climate and Energy (ICE) provided the necessary user-interface and modularity of components to model and simulate decentralized ventilation systems. The authors assembled suitable models of air handling units (AHU) for each ventilation type to resemble the actual systems. The authors simulated their impact on a renovated apartment in Denmark. The subsequent analysis reviewed performance with respect to energy and indoor air quality.

2 Methods

Experiments measured the performance of a novel heat exchanger for room-based ventilation. The results guided input data for simulations, which compared its implementation to a whole-dwelling system.

2.1 Heat Exchanger Performance

Standard EN 13141-8 [12] provides test methods to measure leakages and supply-temperature ratios for single-room ventilation systems, and experiments applied similar methods to a novel heat exchanger for single-room ventilation. Separate experiments measured approximate flow rates at different fan speeds.

2.1.1 Description

A collaborative development yielded a 1.22-meter-long cylindrical counter-flow heat exchanger. Figure 1 depicts a cross-sectional view at either end. Its construction wrapped two 0.3 mm thick PVC sheets around a 3 mm thick PVC tube with 75 mm outer diameter. Narrow 3 mm thick spacers maintained the appropriate gap between sheets, and 3 mm rubber sealant blocked alternate layers at inlets and outlets. The two sheets

simultaneously wrapped around the core and together created 26 channels from 13 full revolutions. A 3 mm thick PVC tube with 250 mm outer diameter enclosed the heat exchanger. The inner and outer tubes extended beyond the rolled sheets, and a plastic divider maintained separation between supply and exhaust.

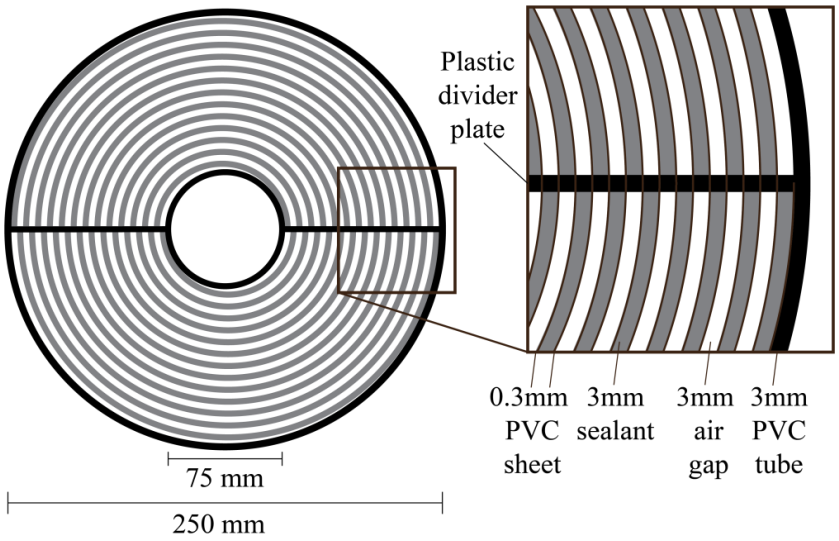

Figure 1. Face-view schematic of the developed heat exchanger for room-based ventilation. Its rolled construction facilitated manufacture and limited leakages.

The heat exchanger provided little resistance to flow. The nominal flow rate of 15 L/s corresponded to a velocity of 0.88 m /s. With a hydraulic diameter of approximately 3 mm, the Reynold number (*Re*) predicted laminar flow. For laminar planar flow, Shah and Sekulic [13] listed the Darcy friction factor as 96/*Re*. The Darcy-Weisbach equation predicted frictional losses of 25.2 Pa. Contractions and expansions with respective loss coefficients of 0.68 and 0.25 provided additional pressure losses of 1.6 Pa at both the entrance and exit of the heat exchanger. The spacers between layers provided additional expected pressure losses of 5.6 Pa for a total of 34.0 Pa.

The NTU-effectiveness method predicted heat transfer. The number of transfer units (NTU) of a heat exchanger is the ratio of total thermal conductance to the smaller heat capacity rate of fluid flow (C_{min}). For laminar planar flow, Shah and Sekulic listed a Nusselt number of 8.24, which is the ratio of convective to conductive heat transfer. The thermal conductivity and thickness of the heat transfer material were 0.20 W/mK and 0.3 mm, respectively. This provided a total heat transfer coefficient of 35 W/m^{2}K over a heat

transfer surface of approximately 13.5 m^2. Due to the expected presence of dead zones adjacent to seals, the authors estimated the effective heat transfer surface as 80% of the total. The supply and exhaust fans were on the same side of the heat exchanger and provided equal flow rates at similar temperatures, so their capacity rates were equal (i.e. $C_{min}=C_{max}$). Effectiveness compares the real transfer of sensible heat to its thermodynamically limited maximum. Temperature efficiency (η) compares the real temperature change to its maximum. With equal heat capacity rates of supply and exhaust, the temperature efficiency and effectiveness were equal. These conditions provided an NTU of 10.4 and a predicted efficiency of 93.2%.

2.1.2 Leakage

Experiments measured external and internal leakage. Before testing temperature efficiency, standard EN 13141-8 recommended that both leakages be less than 10% of the maximum flow rate during operation.

2.1.2.1 External Leakage

A PID/XP multi-function regulator controlled flow through a vacuum cleaner, which provided the desired pressures inside the heat exchanger. Figure 2 shows the experimental setup. In the first test, the vacuum forced air into the heat exchanger, and a low-range micromanometer from Furness Controls (model FCO510) measured gauge pressure inside the enclosed unit with an error of 0.06 Pa. The regulator achieved the desired interior pressure of 50 Pa, and a K-type gas meter of unknown brand measured the flow into the heat exchanger.

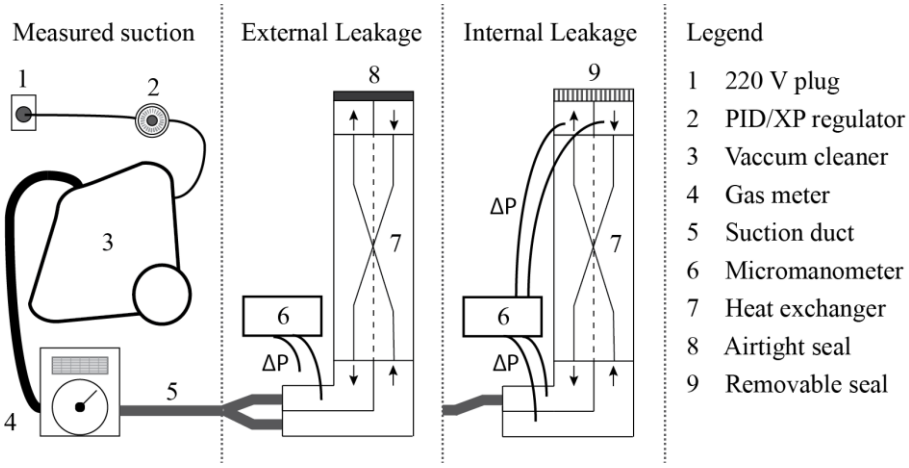

Figure 2. Experimental setup for internal and external leakage measurements of the developed heat exchanger.

2.1.2.2 Internal Leakage

Internal leakage represents the flow between supply and exhaust. The rolled sheets completely separated airflows inside the heat exchanger, so all internal leakage occurred at either end. Figure 2 shows the experimental setup to measure internal leakage. The experiment first measured unblocked airflow through the ventilation unit with the vacuum at maximum power. The gas meter measured airflow, and the micromanometer measured the difference in pressure between supply and exhaust at either end of the heat exchanger. The experiment then blocked airflow at one end and regulated the vacuum to achieve the same average pressure difference between supply and exhaust at either end. The gas meter measured the flow rate of internal leakage. The ratio of measured flows was $W=Q_{leak,int}/Q_{unsealed}$, where $Q_{leak,int}$ is the measured internal leakage and $Q_{unsealed}$ is the unblocked measured flow. This method was slightly different than the test described in EN 13141-8, which uses two fans and encourages the use of tracer gas.

2.1.3 Flow Rate

The experiment connected supply and exhaust fans to the heat exchanger as shown in Figure 3. The fans were DC axial fans from *EBM Papst* (model 3254 J/2 H3P). A venturi meter on the supply fan measured flow rates at different fan speeds. The venturi meter was a 1 meter long circular metal pipe from *Veab Elmicro* with 100 mm diameter. Its mid-section contained a pitot probe that measured the dynamic pressure as the difference in static and total pressure. This correlated to volume flow rates based on calibration data from the manufacturer. The measured flows were at the lower end of the calibrated range and provided uncertainty. The experiment widened the calibrated range by connecting it to a venturi meter with a 50 mm contraction. The narrow meter was more accurate over the tested range and provided flow rate data to calibrate the 100 mm venturi meter. The narrow meter was not used in experiments due to excessive pressure loss. Both venturi meters provided a straight length of five pipe diameters before the pitot probe, which satisfied typical recommendations for ideal flow in measurements. Pitot probes can achieve accuracies of less than 1% with these conditions. The control signal to the fans ranged from 0 to 10 Volts and corresponded directly to fan speed. The experiment determined flow rates at various fan speeds from 10% to 90% of capacity. The experiment repeated this procedure on the exhaust side to determine signal pairings for

balanced flows. At 15 L/s the venturi meter provided frictional losses of 6 Pa. The experiment removed the venturi meter for temperature efficiency measurements, which introduced a potential source of error.

Standard EN 13141-8 offers a correction to flow rates based on measured leakages and mixing. Only the correction for internal leakage applied in this experiment. The authors calculated the real flow as $Q_{real}=Q_{meas}\cdot(1-(W-0.02))$, where Q_{real} is the actual flow through the heat exchanger in one flow direction, Q_{meas} is the measured fan flow rate, and W is ratio of internal leakage from Section 2.1.2.2.

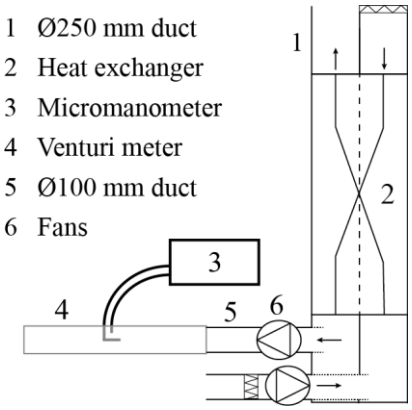

Figure 3. Schematic of experimental setup for flow rate measurements with attached fans on the developed heat exchanger.

2.1.4 Temperature Efficiency

An insulated apparatus provided warm and cold chambers to measure temperature efficiency. Figure 4 shows the experimental setup. The apparatus separated two temperature controlled chambers with a thick insulated wall. The wall contained an opening for the test element. The temperatures of the warm and cold chambers were 5°C and 24°C, respectively. Standard EN 308 [14] recommends 5°C for supply inlet air and 25°C for exhaust inlet air when testing air-to-air heat exchangers, so temperatures followed the standard. Additionally, the average outdoor temperature is 4°C in the heating season of the Danish design reference year [15]. As recommended by EN 13141-8, the experiment measured air temperatures with at least four sensors in each inlet and outlet. The sensors were T-type thermocouples with a precision of ±0.5°C. A data acquisition system from *Agilent Technologies* (model 34970A) recorded temperatures every 10 seconds to obtain averages for each location. Figure 4 and Figure 5 show the placement of sensors inside the unit. Two layers of 10 mm thick Aerogel insulation wrapped the heat exchanger and air ducts to minimize external heat

transfer and prevent condensation on its exterior. The experiment measured fan powers at each flow rate and calculated the resulting change in temperatures. Both fans were on the cold side of the heat exchanger, so corrections added the heat gain to the measured cold chamber temperature and subtracted it from the measured exhaust temperature. Calculations used the heat capacity rates of the corrected flow rates.

Both fans were on the cold side of the heat exchanger, so calculations assumed all leakage on the cold side and negligible pressure difference on the warm side. Smith and Svendsen [16] provided a correction to temperature efficiency based on a mass balance equation and leakage at one end of a heat exchanger. The expression was $\eta_{corrected}=(\eta_{measured}-W)/(1-W)$, where $\eta_{corrected}$ *and* $\eta_{measured}$ are the corrected and measured temperature efficiencies, respectively. The expression assumed constant air density.

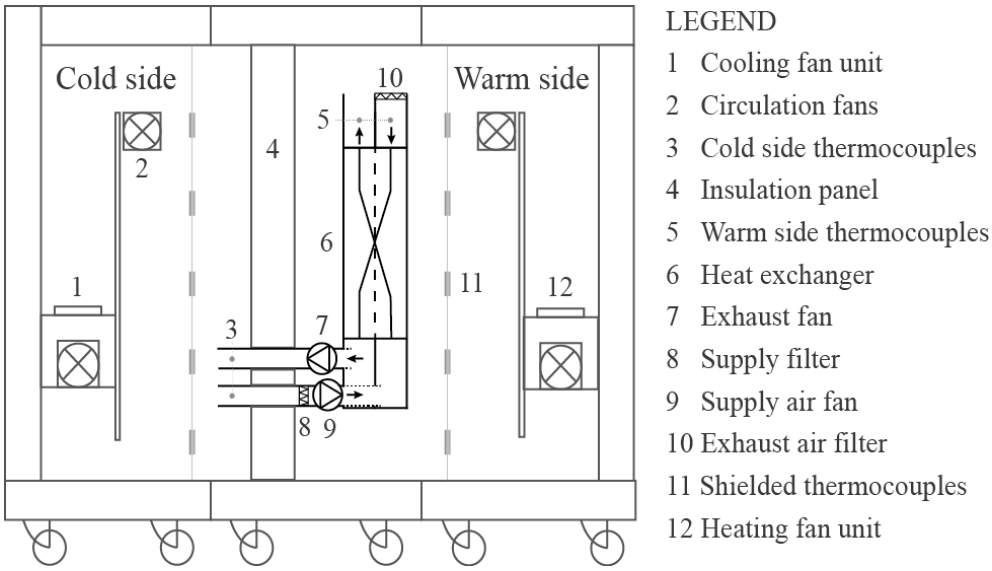

Figure 4. Test apparatus with warm and cold chambers for temperature efficiency measurements of the single-room ventilation unit.

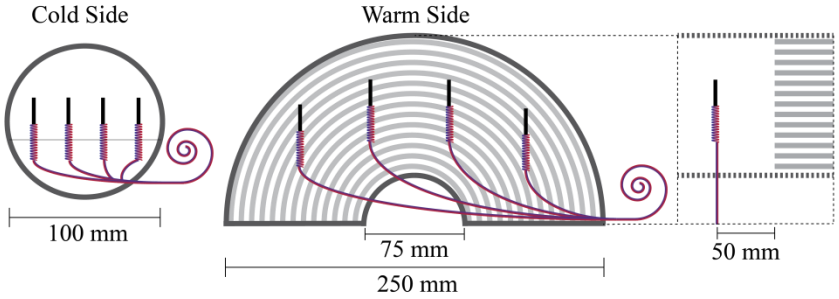

Figure 5. Schematic of thermocouple placement at each inlet and outlet in temperature efficiency measurements of the developed heat exchanger.

2.2 Apartment Description

Simulations attempted to represent an actual case of a renovated apartment in Copenhagen with either whole-dwelling or room-based ventilation.

2.2.1 Building Envelope

The apartment model used a modified floorplan of an existing apartment in Copenhagen, Denmark. Figure 6 shows the floorplan, which had a total interior floor area 93.3 m^2, excluding the stairwell. Construction materials included brick for exterior walls, gypsum boards for interior walls, and concrete for flooring and ceiling. The renovated apartment used new windows with a U-value of 0.5 W/m^2K. The simulations assumed infiltration air change rates of 0.05 h^{-1} due to window replacement.

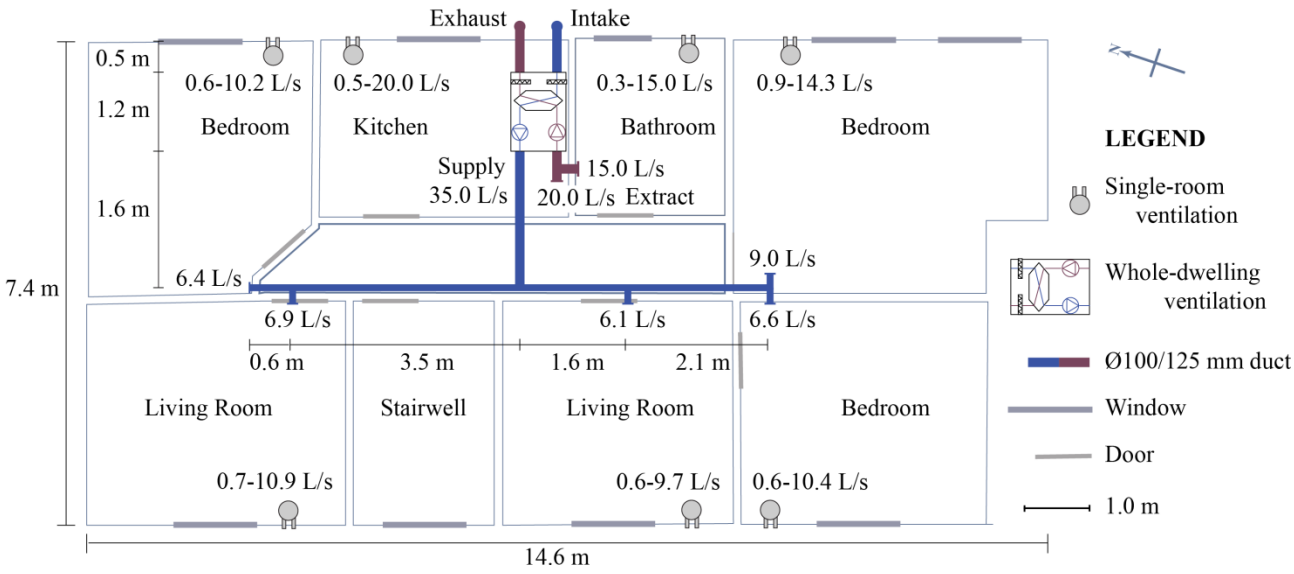

Figure 6. Floorplan of a renovated apartment with locations and airflows of the proposed ventilation systems.

2.2.2 Occupancy and Internal Loads

Table 1 lists the simulated schedules of occupancy, lighting, appliances, and vapor release. Each adult released CO_2, moisture, and heat according to equations from standard EN ISO 7730 [17]. Each child represented the equivalent of 0.6 adults. The moisture gain from cooking corresponded to 0.2 kg per 30 minutes. Breakfast and lunch released 0.2 kg and dinner released 0.6 kg. Hite and Bray [18] listed similar moisture gains from breakfast, lunch, and dinner as 0.17 kg, 0.25kg, and 0.58 kg, respectively, if cooked with an electric element. The total daily moisture gain from showering was 1.6 kg based on measured data

by Yik *et al.* [19]. Their study calculated the moisture release from a shower to be 0.53 kg based on ventilation rate, sensor data, and a moisture balance. Simulations neglected all other moisture sources. Simulations assumed sensible heat gains of 220 W during 2.5 hours of cooking per day and a constant gain of 50 W from a refrigerator based on US housing simulation protocols [20]. Simulations assumed heat gains of 40 W from electronics in living rooms during occupied hours.

Table 1. Occupancy and internal load schedule for simulations.

	Kitchen	**Bathroom**	**Living rooms**	**Adult bedroom**	**Child bedrooms**
Floor area [m^2]	10.4	6.3	12.2-13.6	17.9	12.8-13
Occupancy (Occ.)					
Average *# of adults*	1	0.8	1.2	2	0.6
Metabolic rate [MET]	1.4	1.2	1	0.9	0.9
Weekdays	7-8; 12-1; 18-20	7-8:30	16-22	22-7	22-7
Weekends	8-9; 12-1; 18-20	8-9:30	10-22	23-8	22-8
Lighting					
Schedule	7-10; 17-22	Occ.	7-10; 17-22	7-9; 21-23	7-9; 21-23
# of 10 W LEDs	3	3	3	2	1
Appliances (App.)					
Schedule	7-7:30; 12-12:30; 18-19:30	-	Occ.	-	-
Heat gain [W]	220 (scheduled) 50 (constant)	-	40	-	-
Vapor					
Schedule	App.	Occ.	Occ.	Occ.	Occ.
Moisture gain [g/s]	0.11	0.30	Occ.	Occ.	Occ.

2.3 Ventilation Description

Simulations compared whole-dwelling ventilation to room-based ventilation with respect to indoor air quality and energy consumption.

2.3.1 Whole-dwelling AHU

Danish building regulations require maximum capacities of 15 L/s from bathrooms and 20 L/s from kitchens [21], so the simulated apartment required 35 L/s. Sendell *et al.* reviewed literature on ventilation and health and recommended at least 0.5 air changes per hour based on limited data [22]. The ventilated floor area was 93.3 m^2 and the room height was 2.7 m, so an air change rate of 0.5 h^{-1} equaled the required capacity of 35 L/s. The whole-dwelling AHU extracted constant flow from the kitchen and bathroom and supplied constant flow to living rooms and bedrooms, as shown in Figure 6. The distribution of supply air was directly proportional to the floor area of each room. A real installation in an existing apartment provided the basis for

selection of components. A whole-dwelling ventilation system from *Airmaster A/S* (model CV200) provided suitable airflow and performance, so simulations used data from the manufacturer. Based on the ventilation design in Figure 6, the pressure drop across the supply system was approximately 50 Pa at 35 L/s. The duct diameters ranged from 100 to 125 mm, and adjustable diffusers provided resistances to achieve the desired flow. At 35 L/s and 50 Pa total external resistance, the whole-dwelling ventilation system had specific fan power (SFP) of 600 J/m^3 and dry temperature efficiency of 87%.

2.3.2 Single-room AHU

Simulations of the single-room AHU used measured and expected data as input parameters. As shown by Figure 6, the single-room unit provided balanced controllable ventilation in each room, which allowed demand-control based on sensors in the exhaust of each unit. Danish building regulations require at least 0.3 L/sm^2 at all times in residences. However standard EN 15251 [23] recommends minimum residential ventilation rates of 0.05 L/sm^2 to 0.1 L/sm^2 when there is no demand. This study used 0.05 L/sm^2 because room-based demand-control quickly responded to occupancy. The lower limit for CO_2 was only 500 ppm, or 100 ppm above ambient levels, so an occupant generating approximately 0.25 L/min [24] quickly elevated CO_2 concentrations, which increased ventilation rates. The upper limit for CO_2 was only 750 ppm to assess the potential for optimal air quality. Danish building regulations determined the maximum ventilation rates in the kitchen and bathroom as 20 L/s and 15 L/s, respectively. Simulations set the maximum in bedrooms and living rooms to 0.8 L/sm^2. The central corridor did not contain a ventilation unit.

Table 2 lists upper and lower limits for temperature, CO2, and relative humidity. A proportional-integral (PI) controller set ventilation requirements to limit CO_2 in each room. The bathroom and kitchen had non-occupant sources of moisture, and EN 15251 recommends limits on indoor absolute humidity of 12 g/kg. As such, the controller also set ventilation requirements to limit humidity. The controller required lower outdoor absolute humidity and proportionally increased ventilation rates between indoor absolute humidities of 6 g/kg to 12 g/kg. Temperature control set additional requirements for ventilation. The controller ensured cooling capacity by comparing the supply temperature to room temperature, and it set the required flow with

a PI controller and a cooling set-point of 24°C on the extracted airflow. The signals to the fans assumed the maximum ventilation requirements of each room.

Table 2. Simulated limits for demand-controlled ventilation of individual rooms.

Variable	Carbon Dioxide	Temperature	Absolute Humidity
Units	*ppm*	*°C*	*g/kg*
Lower limit	500	21	6
Upper limit	750	24	12

2.3.2.1 Heat Exchanger Model

The simulation software only allowed input of temperature efficiency at one flow rate. With this data point, simulations used the NTU-effectiveness model to approximate the change in temperature efficiency for a change in balanced flow rates. The simulated temperature efficiency of the single-room heat exchanger was 90% at a nominal ventilation rate of 15 L/s. This was slightly less than the expected performance from Section 2.1.1. The NTU-effectiveness model assumes $\eta=NTU/(1+NTU)$ for balanced heat recovery, so simulations calculated an initial parameter (K_{nom}) as

$$K_{nom} = (Q_{nom})(NTU_{nom}) = (Q_{nom})\left(\frac{\eta_{nom}}{1-\eta_{nom}}\right) = 15\frac{L}{s}\cdot\left(\frac{0.9}{1-0.90}\right) = 135\ L/s$$

where the subscript *nom* indicates nominal values. The NTU-effectiveness model assumes constant total thermal conductance for all flow rates, so $NTU \cdot C_{min}$ is constant. Furthermore C_{min} *equals* $\rho \cdot Q \cdot c_p$, where density (ρ) and specific heat capacity (c_p) are constant for all flow rates. Therefore $(NTU \cdot Q)_{nom}$ *equals* $(NTU \cdot Q)_Q$, where the subscript Q denotes a non-nominal flow rate. This yielded an approximation of temperature efficiency at decreased flow rates (η_Q) as

$$\eta_Q = \frac{NTU_Q}{(1+NTU_Q)} = \frac{1}{(1+1/NTU_Q)} = \frac{1}{\left(1+\frac{Q}{(Q_{nom})(NTU_{nom})}\right)} = \frac{1}{\left(1+\frac{Q}{K_{nom}}\right)} = \frac{1}{\left(1+\frac{Q}{135\ L/s}\right)}$$

3 Results

The results compared simulations of the developed demand-controlled single-room ventilation unit to a commercially available whole-dwelling ventilation unit.

3.1 Heat Exchanger Performance

Experiments assessed the preliminary performance of a single-room ventilator with a novel heat exchanger.

3.1.1 Leakage

EN 13141-8 suggests methods to measure internal and external leakages. Experiments measured the external leakage as 0.53 L/s at 50 Pa, which equates to 2.7% of maximum flow. The first class limit is 2% in the standard. A modified experiment measured the ratio of internal leakage (W) as 12.1% of ventilation flow. This did not satisfy the 10% limit, but the authors continued with planned experiments.

3.1.2 Flow Rates

The fan signals for equal flow rates were different for supply and exhaust. Figure 7 shows the results of measurements. The supply fan required twice the fan speed to achieve similar flow. Future prototypes will place greater focus on improving airflow on the supply air side. The internal leakage ratio allowed corrections to ventilation rates with the expression $Q_{real}=Q_{meas}\cdot(1-(0.12-0.02))=0.9\cdot Q_{meas}$. Table 3 lists the corrected flow rates.

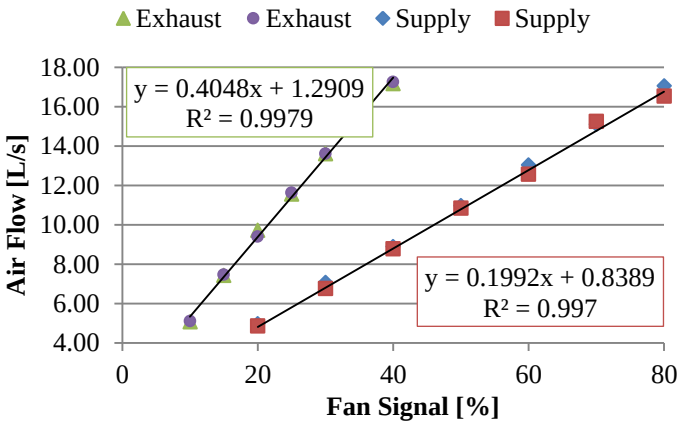

Figure 7. Measured fan flow rates at different fan signals for supply and exhaust in the developed single-room ventilation unit.

3.1.3 Temperature Efficiency

Table 3 lists the raw and corrected temperature efficiencies. Due to the location of sensors, the temperature corrections strongly influenced exhaust efficiencies despite smaller heat gains from the exhaust fan. The leakage corrections negated this influence, and the results were slight increases and reductions in exhaust and

supply temperature efficiencies, respectively. The corrected efficiencies for supply and exhaust were roughly equal, which indicated balanced flow. The temperature efficiency at the maximum corrected flow rate was 82.2%. The NTU-effectiveness method predicted 93% at 15 L/s in Section 2.1.1, so the experiment provided a promising first result at this early stage of development. The efficiency remained stable for all flow rates, which may have implied a physical limit.

The simulations assumed that future prototypes would improve overall quality and achieve 90% at 15 L/s. The simulations also assumed complete counter-current flow and increased temperature efficiencies at lower flow rates. Table 3 lists these efficiencies based on the model in Section 2.3.2.1.

Table 3. Measured and corrected ventilation rates and temperature efficiencies for the developed heat exchanger. The corrected flow rates account for internal leakage. The corrected supply temperature efficiencies account for heat gains from fans. The corrected exhaust temperature efficiencies account for both leakage and heat gains from fans.

Measured flow rate *L/s*	Corrected flow rate *L/s*	Measured $\eta_{exhaust}$ *%*	Corrected $\eta_{exhaust}$ *%*	Measured η_{supply} *%*	Corrected η_{supply} *%*	Simulated η_{supply} *%*	Measured $(SFP)_{supply}$ *J/m³*	Measured $(SFP)_{exhaust}$ *J/m³*	Simulated *SFP* *J/m³*
15	13.5	77.4	80.9	83.1	82.2	90.0	1148	378	300
12.5	11.25	80.2	83.3	82.5	81.8	91.5	987	347	217
10	9	78.0	79.8	83.2	82.6	93.1	856	311	147
7.5	6.75	78.8	79.7	81.4	80.8	94.7	690	249	90
5	4.5	70.9	69.6	75.8	75.3	96.4	458	229	45

3.1.4 Specific Fan Power

Experiments also measured the approximate difference in static pressure across the heat exchanger and filter at balanced flow rates. The experiment inserted probes perpendicular to flow at 1 cm depths before and after the heat exchanger and filter. The probes measured at equal cross-sections to roughly negate dynamic pressure. At a corrected flow of 13.5 L/s, the measured pressure drop was 37 Pa across the heat exchanger and 3 Pa across the filter.

Simulations assumed only 20 Pa pressure drop in the duct design of future prototypes for a total of 60 Pa. The simulations assumed fan efficiencies of 20% toward a specific fan power of 300 J/m^3 at 15 L/s. Appendix G in ASHRAE Standard 90.1 provides polynomial coefficients to predict part load performance of fans. The simulations used the ASHRAE calculation, and Table 3 shows the simulated SFP values at smaller flow rates. The measured SFPs are comparatively higher than the simulated values, and the ASHRAE calculation may have underestimated part-load power. The affinity laws of fans state that fan power is

proportional to the cube of flow rate, which would have provided higher simulated SFPs. This added uncertainty to simulations.

3.2 Air quality

Simulations compared whole-dwelling ventilation to single-room ventilation with all doors either fully opened or fully closed. This provided a range of potential outcomes.

3.2.1 CO_2 and Relative humidity

The simulations predicted relative humidities and CO_2 concentrations in each room. EN 15251 describes category II as the normal level of expectation that should be used for all new and renovated buildings. Category IV is only acceptable for a limited part of the year. Table 4 lists the percentage of hours in each category for each IAQ indicator, ventilation type, and room with fully closed doors. Table 5 lists the same quantities from simulations with fully opened doors. The evaluation only considered relative humidities during the heating season from September 16th to May 15th since outdoor absolute humidity often exceeded indoor humidity in the cooling season.

With fully opened doors, the duration with category II relative humidity was greater than 90% of the heating season for both ventilation types. The bathroom was the only room to experience category IV relative humidity but for only 3%-4% of the simulated hours. CO_2 concentrations never exceeded 1200 ppm and rarely exceeded 900 ppm for both ventilation types. Additionally, single-room demand-control provided near-continuous category II CO_2concentrations. With fully closed doors, the effect was higher CO_2 concentrations in individual rooms, and the whole-dwelling system provided instances above 1200 ppm. Overall, the IAQ analysis indicated that the developed single-room ventilation with demand-control could potentially achieve equal or better air quality as compared to a standard whole-dwelling ventilation system.

Table 4. Always open doors. Percentage of evaluated hours belonging to category II and IV for indoor relative humidity and CO_2 concentration with each ventilation type.

OPEN DOORS	Category II				Category IV			
	Duration below 60% RH		Duration below 900 ppm		Duration above 70% RH		Duration above 1200 ppm	
Room type	Whole-dwelling	Single-room	Whole-dwelling	Single-room	Whole-dwelling	Single-room	Whole-dwelling	Single-room
Kitchen	97	97	100	100	0	0	0	0
Bathroom	93	91	100	100	3	4	0	0
Living room	99	98	92-100	99	0	0	0	0
Adult bedroom	98	98	87	99	0	0	0	0
Child bedroom	99	98	100	100	0	0	0	0

Table 5. Always closed doors. Percentage of evaluated hours belonging to category II and IV for indoor relative humidity and CO_2 concentration with each ventilation type.

CLOSED DOORS	Category II				Category IV			
	Duration below 60% RH		Duration below 900 ppm		Duration above 70% RH		Duration above 1200 ppm	
Room type	Whole-dwelling	Single-room	Whole-dwelling	Single-room	Whole-dwelling	Single-room	Whole-dwelling	Single-room
Kitchen	97	94	96	100	0	1	0	0
Bathroom	82	82	100	100	17	17	0	0
Living room	98-99	99	66-76	68-72	0	0	0-23	0
Adult bedroom	98	99	67	71	0	0	21	0
Child bedroom	99	99	100	100	0	0	0	0

3.2.2 Average age of air

CO_2 and relative humidity cannot indicate levels of constantly emitted pollutants, such as volatile organic compounds, as well as some activity-based emissions, such as odours. Table 6 reports the average age of air in each zone to cover a broader range of pollutants. The whole-dwelling ventilation used a CAV system that yielded a constant age of air in each zone. The single-room units provided VAV flow, so results reported averages during occupancy. The average age of air using the two ventilation types were similar in the bathroom, living room, and adult bedroom. With closed doors, the air in the kitchen and small bedrooms had longer dwell times due to lower emissions of moisture and CO_2. Table 7 shows the peak values for all hours, which mainly occurred as the occupant entered a zone. Performance criteria for residential ventilation may specify limits for peak and accumulated exposures to pollutants [25]. If the peak age of air is excessive, the controller might use a higher minimum ventilation rate or implement some form of occupancy prediction. It was evident that open doors distributed air and provided less variance.

Table 6. Average age of air in each room with either whole-dwelling or single-room ventilation.

		Average age of air during occupied hours [h]					
Ventilation Type	Doors	Kitchen	Bath	Living	Adult	Child	**Total**
Whole-dwelling ventilation	Open	1.9	1.8	1.5-1.6	1.6	1.5-1.6	1.6
	Closed	1.9	1.8	1.4	1.4	1.4	1.5
Single-room ventilation	Open	2.13	1.9	1.8	1.7	1.8-2.0	1.9
	Closed	2.65	2.1	1.2-1.3	1.2	2.2	1.8

Table 7. Peak age of air in each room with demand-controlled single-room ventilation.

Peak age of air during all hours [h]						
Doors	Kitchen	Bath	Living	Adult	Child	**Total**
Open	4.9	5.0	4.5-4.6	4.5	4.7-5.4	4.8
Closed	6.8	8.3	6.8	7.4	7.5	7.2

3.3 Thermal Comfort

Table 8 lists the percentage of hours with operative temperatures in categories II and IV for each room and ventilation type. None of the simulated cases experienced temperatures below 18°C, which would produce category IV. The single-room ventilation unit improved or maintained thermal comfort in all rooms.

Table 8. Percentage of hours with thermal comfort in categories II and IV for each room and ventilation type.

	OPEN DOORS				CLOSED DOORS			
	Category II		Category IV		Category II		Category IV	
	20°C to 25°C [%]		Above 27°C [%]		20°C to 25°C [%]		Above 27°C [%]	
Room type	Whole-dwelling	Single-room	Whole-dwelling	Single-room	Whole-dwelling	Single-room	Whole-dwelling	Single-room
Kitchen	92	96	2	0	88	95	4	0
Bathroom	95	98	1	0	95	99	1	0
Living room	92-93	92-93	2	1	88-89	89-90	3	1-2
Adult bedroom	94	96	1	0	95	96	0	0
Child bedroom	94-95	94-96	1	0	94-95	95-97	0-1	0
Average	**93.6**	**95.5**	**1.4**	**0.2**	**92.2**	**95.1**	**1.7**	**0.3**

3.4 Energy

Table 9 lists the annual delivered energy per unit floor area for ventilation and space heating as well as the total recovered heat. The whole-dwelling ventilation unit consumed 3.9 kWh/m^2 while the simulated single-room ventilation units together consumed 1.0 kWh/m^2 towards relative savings of 74%. Space heating consumed 78.4-79.0 kWh/m^2 using the whole-dwelling ventilation and 74.0-75.2 kWh/m^2 using the single-room ventilation for relative savings of 4% to 6%. The recovered heat was similar for both ventilation types with opened doors, while the single room units recovered roughly 8% less heat with closed doors.

Table 9. Simulated annual energy with each ventilation type and open or closed doors.

		Simulated annual energy [kWh/m^2]		
	Doors	**Ventilation**	**Space Heating**	**Heat Recovery**
Whole-dwelling	Open	3.9	78.4	45.1
	Closed	3.9	79.0	45.3
Single-room	Open	1.0	75.2	45.0
	Closed	1.0	74.0	41.6

3.4.1 Test Cases

In a simple test case, the measured exhaust fan powers provided coefficients for part-load performance of the simulated single-room ventilation units. The resulting fan energy consumption was 12% higher at 1.1 kWh/m^2. This demonstrated that the assumed SFPs and part-load coefficients had limited impact.

Another test case assessed the impact of window openings on the energy consumption of demand-controlled single-room ventilation. The simulation opened windows to one-quarter their potential during occupied hours of the cooling season. The resulting fan energy consumption was 22% less at 0.8 kWh/m^2. This demonstrated a significant response to decreased ventilation demand.

4 Discussion

The experimental tests provided a preliminary indication of the potential performance of a novel counter-flow heat exchanger for single-room ventilation. The results of experiments were promising, but the unit requires further development to limit internal leakage and achieve targeted efficiencies and fan powers.

Roulet *et al. [26]* audited 13 heat recovery ventilators and measured relatively low fan efficiencies in three single-room ventilation units. In general, fan efficiencies decreased with rated capacity. However the single-room units provided far less pressure drop and demanded lower SFP, which ranged from 720 J/m^3 to 864 J/m^3. The average SFP of the 10 largest heat recovery ventilators was 1267 J/m^3 for comparison. In our investigation, the measured SFP of the exhaust fan was only 378 J/m^3 at maximum capacity. This reflected the potential for especially low SFP in future prototypes.

The simulated single-room ventilation unit provided equivalent air quality and thermal comfort with less total fan energy. It achieved this performance with demand-controlled variable air-volume flow and low pressure drop through a wide construction. The low pressure drop likely provided additional benefits with

respect to noise. Manz *et al.* [27] experimentally tested single-room heat recovery ventilators to assess their performance, and sound pressure was a primary issue. The sound power level from a fan increases with fan power and static pressure, so lower pressure drop and SFP imply less fan noise. Similarly, the sound power level from ducted flow increases with air velocity and cross-sectional area, so wider ducts and channels imply less noise from airflow. Therefore the low operating pressure of the unit may allow increased flow rates with respect to noise while improving air quality.

Several key assumptions warrant further investigation. The minimum airflow rates of individual rooms ranged from 0.3 L/s to 0.9 L/s in simulations. This may be difficult to achieve in practice. Oscillations between on/off flow could produce this minimum, but sensors in the exhaust would be slower to detect increased concentrations of pollutants. Instead it may be necessary to increase the minimum ventilation rates. The audit by Roulet *et al.* demonstrated that short-circuiting of airflow is a significant concern. The simulations assumed that extracted air accurately represented the bulk air properties in each room, but short-circuiting could influence sensor readings in the exhaust. It could also reduce ventilation rates. It is therefore important that future prototypes ensure adequate separation between the supply and exhaust airflows.

5 Conclusion

A single-room ventilation unit with a novel heat exchanger performed well in experiments. The heat exchanger provided a supply temperature efficiency of 82.2% at a balanced ventilation rate of 13.5 L/s. The total measured pressure drop across the heat exchanger and filter was 40 Pa at this flow. The external and internal leakages were approximately 2.7% and 12.1% of flow, respectively. Simulations compared a demand-controlled single-room ventilation unit with predicted performance to a commercially available whole-dwelling ventilation unit with constant airflow. Both units ventilated a residential apartment in annual simulations and provided suitable indoor climate. In this comparison, the single-room units improved or maintained air quality and thermal comfort. They also consumed less annual energy for fans at 1.0 kWh/m^2 and for heating at 74.0-75.2 kWh/m^2 towards energy savings of 74% and 4-6%, respectively. This

demonstrated the potential of single-room ventilation units to provide a viable alternative for renovated apartments through the inclusion of demand control.

6 Acknowledgements

This research was funded by ELFORSK and the Technical University of Denmark to research and develop a novel heat exchanger for decentralized ventilation in existing residential apartments.

7 References

[1] Danish Energy Agency, Energistatistik 2012 (2012). Retrieved from http://www.ens.dk/info/tal-kort/statistik-nogletal/arlig-energistatistik.

[2] M. Morelli, L. Rønby, S.E. Mikkelsen, M.G. Minzari, T. Kildemoes, H.M. Tommerup, Energy retrofitting of a typical old Danish multi-family building to a "nearly-zero" energy building based on experiences from a test apartment, Energy Build. 54 (2012) 395–406. doi:10.1016/j.enbuild.2012.07.046.

[3] Danish Energy Agency, Denmark's National Energy Efficiency Action Plan (2014). Retrieved from https://ec.europa.eu/energy/sites/ener/files/documents/2014_neeap_en_denmark.pdf

[4] I. Ridley, J. Fox, T. Oreszczyn, S. Hong, The Impact of Replacement Windows on Air Infiltration and Indoor Air Quality in Dwellings, (2003). Retrieved from http://discovery.ucl.ac.uk/2259/.

[5] G. Villi, C. Peretti, S. Graci, M. De Carli, Building leakage analysis and infiltration modelling for an Italian multi-family building, J. Build. Perform. Simul. (2012) 1–21. doi:10.1080/19401493.2012.699981.

[6] D.R. Wulfinghoff, Multiple-zone HVAC: An obsolete template, World Energy Eng. Congr. 2009, WEEC 2009. 2 (2008) 762–768. doi:10.1080/01998595.2011.10389019.

[7] A. Hesaraki, S. Holmberg, Demand-controlled ventilation in new residential buildings: Consequences on indoor air quality and energy savings, Indoor Built Environ. 24 (2013) 162–173. doi:10.1177/1420326X13508565.

[8] W. Cho, D. Song, S. Hwang, S. Yun, Energy-efficient ventilation with air-cleaning mode and demand control in a multi-residential building, Energy Build. 90 (2015) 6–14. doi:10.1016/j.enbuild.2015.01.002.

[9] J. Laverge, N. Van Den Bossche, N. Heijmans, A. Janssens, Energy saving potential and repercussions on indoor air quality of demand controlled residential ventilation strategies, Build. Environ. 46 (2011) 1497–1503. doi:10.1016/j.buildenv.2011.01.023.

[10] D.K Mortensen, I. Walker, M. Sherman, Optimization of Occupancy Based Demand Controlled Ventilation in Residences, Int J Vent. 10 (2011) 49–60. Retrieved from http://eetd.lbl.gov/sites/all/files/publications/20-optimization-2011.pdf

[11] M. Wetter, A view on future building system modeling and simulation, Chapter in: Building performance simulation for design and operation, J.L.M. Hensen, R. Lamberts (editors), Routledge, UK, 2011. Retrieved from http://architecture.mit.edu/pdfs/lecturereadings/f13/future.pdf

[12] European Committee for Standardization, Ventilation for buildings – Performance testing of components/products for residential ventilation – Part 8: Performance testing of un-ducted mechanical supply and exhaust ventilation units (including heat recovery) for mechanical ventilation systems intended for a single room, EN 13141-8:2014, Authors, Brussels, Belgium, 2014.

[13] R.K. Shah, Fundamentals of heat exchanger design, John Wiley & Sons, Hoboken, NJ, 2003. doi: 10.1002/9780470172605

[14] European Committee for Standardization, Heat exchangers – Test procedures for establishing performance of air to air flue gases heat recovery devices, EN 308:1997, Authors, Brussels, Belgium, 1997.

[15] P.G. Wang, M. Scharling, K.P. Nielsen, 2001 – 2010 Design Reference Year for Denmark, Danish Meteorological Institute, Teknisk Rapport 12-17 (2012). Retrieved from http://www.dmi.dk/fileadmin/Rapporter/TR/tr12-17.pdf

[16] K.M. Smith, S. Svendsen, Development of a plastic rotary heat exchanger for room-based ventilation in existing apartments, Energy Build. 107 (2015) 1–10. doi:10.1016/j.enbuild.2015.07.061.

[17] International Organization for Standardization, Ergonomics of the thermal environment -- Analytical determination and interpretation of thermal comfort using calculation of the PMV and PPD indices and local thermal comfort criteria, EN ISO 7730:2006, European Committee for Standardization, Brussels, Belgium, 2006.

[18] S.C. Hite, J.L. Bray, Research in Home Humidity Control, Engineering Experiment Station, Research Series No. 106 (1948).

[19] F.W.H. Yik, P.S.K. Sat, J.L. Niu, Moisture Generation through Chinese Household Activities, Indoor Built Environ. 13 (2004) 115–131. doi:10.1177/1420326X04040909.

[20] E. Wilson, C.. Engebrecht Metzger, S. Horowitz, R. Hendron, 2014 Building America House Simulation Protocols (NREL/TP-5500-60988), (2014). Retrieved from http://energy.gov/sites/prod/files/2014/03/f13/house_simulation_protocols_2014.pdf

[21] Danish Energy Agency. Building Regulations (2010). Retrieved from http://bygningsreglementet.dk/file/155699/BR10_ENGLISH.pdf

[22] J. Sundell, H. Levin, W.W. Nazaroff, W.S. Cain, W.J. Fisk, D.T. Grimsrud, et al., Ventilation rates and health: Multidisciplinary review of the scientific literature, Indoor Air. 21 (2011) 191–204. doi:10.1111/j.1600-0668.2010.00703.x.

[23] European Committee for Standardization, Indoor environmental input parameters for design and assessment of energy performance of buildings addressing indoor air quality, thermal environment, lighting and acoustics, EN 15251:2007, Authors, Brussels, Belgium, 2007.

[24] D.S. Dougan, CO2-based demand control ventilation: Do risks outweigh potential rewards?, Ashrae J. 46 (2004) 47 – 54. Retrieved from https://www.ashrae.org/File%20Library/docLib/Public/ASHRAE-D-22751-20040930.pdf

[25] European Committee for Standardization, Ventilation for buildings. Determining performance criteria for residential ventilation systems, EN 15665:2009, Authors, Brussels, Belgium, 2009.

[26] C.-A. Roulet, F.D. Heidt, F. Foradini, M.C. Pibiri, Real heat recovery with air handling units, Energy Build. 33 (2001) 495–502. doi:10.1016/S0378-7788(00)00104-3.

[27] H. Manz, H. Huber, a. Schälin, a. Weber, M. Ferrazzini, M. Studer, Performance of single room ventilation units with recuperative or regenerative heat recovery, Energy Build. 31 (2000) 37–47. doi:10.1016/S0378-7788(98)00077-2.

Appendix D – Heat exchanger calculations

K.M. Smith,

Matlab calculations of temperature efficiency, pressure leakage, bypass leakage, and pressure drop for a rotary heat exchanger with small circular plastic channels,

Matlab Code

```
% Calculations of temperature efficiency, pressure leakage, bypass
 leakage, and pressure drop for a rotary heat exchanger with circular
 plastic channels

% Written by Kevin Michael Smith

% Please see Shah and Sekulic (2003) or Smith and Svendsen (2015) for
 reference of equations

clc, clear

% Conditions
To = 5; % outdoor temperature
Ti = 26; % indoor temperature
rpm = 10; % rotor RPM
q = [3.9 8.8 12.8].*3.6; % Actual flows due to measures pressure
 leakage
q_flow = [5 10 15]*3.6; % Expected flows based on fan flow rates
dPmeas = [4 10.2 17]; % Measured pressure difference across heat
 exchanger
omega = rpm*2*pi/60; % angular velocity in [rad/s]

% Placeholders
N = length(q);
eff = zeros(1,N);
q_real = zeros(1,N);
dP = zeros(1,N);
deltaT = length(q);

% Fluid constants
h2s = 1/3600; % hours to seconds coef
rho5 = 1.269; % density of air at 5dC
rho20 = 1.205; % density of air at 20dC
rho = (rho5+rho20)/2; % average density
kAir = 0.025; % thermal conductivity of air
cp = 1005; % specific heat [J/kgK]
mu = 1.81e-5; % dynamic viscosity of air [Pa.s]

% Honeycomb data - polycarbonate http://en.wikipedia.org/wiki/
Polycarbonate
rhoRot = 1210; % density
cpRot = 1250; % specific heat
kRot = 0.2; % thermal conductivity
dRot = 0.0001; % wall thickness for single channel, delta/2

% Heat exchanger constants
rChan = 0.0013; % radius of a straw
rTubeOuter = 0.106; % Outer radius of the heat exchanger
rTubeInner = 0.03; % Inner radius of the heat exchanger
L = 0.15; % straw length
nChan = round(0.82*(rTubeOuter^2-rTubeInner^2)/(rChan+dRot)^2); %
 number of straws based on a void fraction of 18%
```

```
Dh = 2*rChan; % hydraulic diameter, and I guessed 0.95 modifier to
 account for deformation from circular
SA = 2*pi*rChan*L*nChan/2; % heat transfer surface area in one half
Nu = 4.364; % Nusselts number
h = Nu*kAir/Dh; % heat transfer coef, fully developed laminar [W/m2K]

% Straw calculations
C = pi*((rChan+dRot)^2-rChan^2)*L*rhoRot*cpRot*nChan; % total heat
 capacity of the entire matrix
CRot = C*(rpm/60); % Capacity ratio of rotor according to Shah and
 Sekulic

for i = 1:N % Calculate for N number of flow rates
u = q(i)*h2s /((nChan*pi*rChan^2)/2); % average velocity assuming only
 inner flow (based on void fraction)
Re = rho*u*Dh/mu; % Reynold's number
C1 = q(i)*rho20*cp*h2s; % Capacity rate of airflow
C2 = q(i)*rho5*cp*h2s;
CMin = min(C1,C2);
CMax = max(C1,C2);
NTU0(i) = SA/(2/h+2*dRot/(3*kRot))/CMin; % NTU with wall resistance

% Axial conduction correction
cross_area = (pi*(rChan+dRot)^2-pi*rChan^2)*nChan;
lambda = kRot*cross_area/(L*CMin); % As defined in Shah and Sekulic

% Capacity Ratios
Z = CMin/CMax;
ZRot = CRot/CMin;
ZRotM = 2*ZRot*Z/(1+Z); % Denoted C*_r in Shah and Sekulic

% Error in written method in Shah and Sekulic (2003), see Smith and
 Svendsen (2015) for fixed equations.
% Erroneous formulas included in comments of steps 2-4
NTU0M = 2*NTU0(i)*Z/(1+Z);
epsCF = NTU0M/(1+NTU0M);
modRot = 1-1/(9*((ZRotM)^(1.93)));
epsR = epsCF*modRot;

%2
phi = sqrt(lambda*NTU0M/(1+lambda*NTU0M));
CLambda = ((1+NTU0M)/NTU0M)*(1-1/(1+NTU0M*(1+lambda*phi)/
(1+lambda*NTU0M)));
% CLambda = (1+NTU0M*(1+lambda*phi)/(1+lambda*NTU0M))^(-1)-
(1+NTU0M)^(-1);

%3
epsRWithLambda = epsR*CLambda;
% epsRWithLambda = epsR*(1-CLambda/(2-Z));

%4
epsExp = exp(epsRWithLambda*(Z^2-1)/(2*Z*(1-epsRWithLambda)));
eps = (1-epsExp)/(1-Z*epsExp);
eff(i) = eps;
```

```
% epsExp = exp(epsR*(Z^2-1)/(2*Z*(1-epsR)));

% Flow carryover correction
porosity = nChan*(rChan^2)/(rTubeOuter^2-rTubeInner^2);
correction_omega = 1-(porosity*omega*L/(pi*u));
q_real(i) = q(i)*(correction_omega);

% Pressure drop calculations (simplified forumlae for pressure
 prediction)
% A more detailed calculation is further down
dP_minor = 3*rho*(u^2)/(2*9.81);
dP_major = 32*mu*L*u/(Dh)^2;
dP(i) = dP_major + dP_minor;

% Estimate of average change in heat exchanger material temperature
 per cycle
Qdot = q(i)*rho20*cp*h2s*(Ti-To)*eff(i); % average heat transfer rate
 to HE matrix
deltaT(i) = (30/rpm)*Qdot/(C/2); %946.00 kg/m³ time for one-half
 rotation X heat flux / heat capacity

% Bypass flow prediction
tol = 0.0015; % Radial tolerance around the heat exchanger
A_per = tol*pi*rTubeOuter;
P_per = 2*pi*rTubeOuter+2*tol;
Dh_per = 4*A_per/P_per; % Hydraulic diameter through bypass gap
u_p(i) = dP(i)*(Dh_per)^2/(48*mu*L); % Bypass gap velocity
q_per(i) = u_p(i)*A_per*3600; % Flow rate

% Implementation pressure equation for heat exchanger flow from Shah
 (2003)
rho_inlet = rho20; % Exhaust flow inlet density
rho_outlet = rho5;
rho_inverse = 0.5*(1/rho_inlet+1/rho_outlet);
Kc = 0.79; % From table in Shah and Sekulic (2003) p386
Ke = -0.38;
f = 16/Re;
gc = 1; % gravitational constant
sigmaA = porosity;
G = rho20*u;
dP2(i) = G^2/(2*gc*rho_inlet)*(1-sigmaA^2+Kc+2*(rho_inlet/
rho_outlet-1)+...
    f*L/(Dh/4)*rho_inlet*rho_inverse-(1-sigmaA^2-Ke)*rho_inlet/
rho_outlet);

% Pressure leakage prediction
w_gap_press = 0.002;
L_gap_press = 2*(tol+rTubeOuter-rTubeInner);
mdot_press_leak(i) =
 0.8*(L_gap_press*w_gap_press)*sqrt(2*rho20*dP(i))*3600;
press_leak(i) = mdot_press_leak(i)/rho20;

% Compare with flow rates from measured pressure difference
```

```
press_leak_meas(i) =
 0.8*(L_gap_press*w_gap_press)*sqrt(2*rho20*dPmeas(i))*3600/rho20;
end

% Calculate pressure leakage ratios
press_leak_ratio = press_leak./q_flow;
meas_press_leak_ratio = press_leak_meas./q_flow;

% Calculate real efficiencies accounting for bypass leakage
realeff = eff.*(1-q_per./q);
```

Published with MATLAB® R2015a

Appendix E – Simulation

K.M. Smith,

Numerical simulation of moisture flows in ventilation with heat recovery,

Matlab Code

```
% Simplified simulation of moisture balance equations in an apartment
% Written by Kevin Michael Smith
% Please see Paper 2 by Smith and Svendsen for reference of methods
 and equations

clear, clc

% Parameters definitions and variable declarations

% Scenarios
scen = 2; % 1:best 2:typical 3:worst case scenario
rh_limit = 70;

% Read weather data
[hr,day,dayhr,minute,rh_amb,t_amb,press] =
 read_weather('DenmarkDRY.txt');
time_step = (1:size(hr,1))'; % column vector with time_steps
length_ts = minute(2)-minute(1); % time step length in minutes
dayofweek = mod(day,7)+1;
i_wkday = dayofweek <= 5; % index weekdays
i_wkend = dayofweek >= 6; % index weekends
N_day = (24*60)/length_ts; % number of time steps in a day
N_year = 365*N_day-1; % number of time steps in year

% General
family = 3; % family size
rooms = {'Kitchen' 'Bathroom' 'Bedroom1' 'Bedroom2' 'Living'};
a_room = [8.25 2.97 18.48 14.40 18.90 4.5]; % room area, m2
h_room = 2.6; % room height, m
t_room = 22; % indoor room temperature, dC
rh_room_init = 50; % initial indoor relative humidity, %
rho_room = 1.225; % indoor air density, kg/m3
rh_Pctrl_low = 50;
rh_Pctrl_high = 70;
vol_room = a_room*h_room; % volume of the room, m3
nrooms = length(rooms); % number of rooms

ach_inf = ones(1,nrooms)*0.05; % infiltration air change rate, 1/h
ach_vent_min = ones(1,nrooms)*0.5; % Minimum ventilation rate through
 the air handling unit, 1/h
ach_vent_whole_min = 0.5*sum(vol_room,2)*[20/35 15/35]./vol_room(1:2);
ach_vent_max = zeros(1,nrooms);
ach_vent_max(1:2) = [20 15].*3.6./vol_room(1:2);

% Heat recovery
eta_nom = 0.85;
eta = ones(N_year,nrooms).*0.85;
eta(135*N_day+1:258*N_day,:) = 0; % May 16th (136th day) to September
 15th (258th)

% Occupancy
m_adult = 70; % Assumed mass of an adult, kg
```

```
rate_occ_hr = [0.06 0.06 0.06]; % moisture release rate per adult
 person from occupancy, kg/h, (transpiration and respiration)

% Bathroom
load_shower = [0.20 0.40 0.53]; % release occurs in one time step, kg
time_1st_shower = 7; % start time of first shower, then alternates
 time steps for subsequent showers up to family size

% Kitchen
load_dish = [0.05 0.15 0.45]; % release per load, kg
time_dish = 21; % dishwasher start time;
length_dish = 60; % minutes for dishwasher

nmeals = 3; % number of meals
load_meals = [0 0 0.24; 0.45 0.57 1.33; 0.25 0.95 3.8]; % gas for
 typical scenario (middle row)
% load_meals = [0 0 0.24; 0.17 0.25 0.58; 0.25 0.95 3.8]; % electric
 for typical scenario
length_cook_meals = [0 0 20; 20 30 60; 20 40 120]; % length of cooking
 time for meal, minutes
time_meals = [8 12 18]; % hour containing meals, (7:00-8:00 is 8th
 hour)

% Constant sources
rate_plant_day = [0 0.06 0.45]; % release rate from each medium size
 plant, kg/d
m_pets = [0 6 20]; % Lack of data - Use mass, kg, with human release
 rate [None Dog+Cat/2 2Dogs]

% Clothes drying - THREE TIMES per week (Monday, Thursday, Saturday)
load_clothes = [0 1.67 2.9]; % release per, kg
length_clothes = 600; % minutes to evaporate into air at assumed
 constant rate, minutes
start_clothes = 21;

% Floor mopping - ONCE per week (Tuesday)
load_mop_m2 = [0.005 0.005 0.15]; % release per unit area of floor,
 kg/m2
mop_coverage = 0.8; % factor to account for covered areas with
 furniture, carpets, rugs, etc., -
length_mop_dry = [10 10 100]; % minutes to evaporate into air at
 assumed constant rate, minutes
start_wkly_mop = 15;

% Placeholders and calculation parameters

% Calculation constants
alpha = 6.1094;
beta = 17.625;
lambda = 243.04;
press_atm = 1013.25; % assumed constant pressure, hPa

% Simulation placeholders
e_amb = zeros(N_year,1);
```

```
x_amb = zeros(N_year,1);
rh_room = zeros(N_year,nrooms);
dp_room = zeros(N_year,nrooms);
M = zeros(N_year,nrooms);
t_exh = zeros(N_year,1);
e_sat_exh = zeros(N_year,1);
x_exh = zeros(N_year,nrooms);
x_supply = zeros(N_year,nrooms);
x_room = zeros(N_year,nrooms);
x_mixed_dry = zeros(N_year,1);
x_mixed_exh = zeros(N_year,1);
x_mixed_wet = zeros(N_year,1);
rh_mixed_wet = zeros(N_year,1);
dp_mixed_wet = zeros(N_year,1);

% Room indices
kitchen = find(strcmp(rooms,'Kitchen'));
bathroom = find(strcmp(rooms,'Bathroom'));
bedroom1 = find(strcmp(rooms,'Bedroom1'));
bedroom2 = find(strcmp(rooms,'Bedroom2'));
living = find(strcmp(rooms,'Living'));

% Input -  Occupancy schedule
occ = zeros(N_year,nrooms);
occ_sched.kitchen = [7 8; 12 13; 17 20]; % occupancy intervals
 separated into columns
occ_sched.bathroom = [7 9];
occ_sched.sleep = [22 7];
occ_sched.liv_wkday = [16 22];
occ_sched.liv_wkend = [9 22];

% Calculations - Indeces for occupied hours
i_bathroom = dayhr >= occ_sched.bathroom(1) & dayhr <
 occ_sched.bathroom(2);
i_sleep = dayhr >= occ_sched.sleep(1) | dayhr < occ_sched.sleep(2);
i_kitchen = false(N_year,1);
for meal = 1:size(occ_sched.kitchen,1) %nmeals
    i_kitchen = i_kitchen | (dayhr >= occ_sched.kitchen(meal,1) &
 dayhr < occ_sched.kitchen(meal,2));
end
i_liv_wkday = i_wkday & dayhr >= occ_sched.liv_wkday(1) & dayhr <
 occ_sched.liv_wkday(2);
i_liv_wkend = i_wkend & dayhr >= occ_sched.liv_wkend(1) & dayhr <
 occ_sched.liv_wkend(2);
i_living = i_liv_wkday | i_liv_wkend;

% Input - Room occupancy
% Average adults during occupied hours (assumed 0.5 for children)
occ(i_kitchen,kitchen) = 1;
occ(i_bathroom,bathroom) = 1;
occ(i_sleep,bedroom1) = 2;
occ(i_sleep,bedroom2) = 0.5; % number of adults, 0.5 for children
occ(i_living,living) = 1;
```

```
% Calculations - Moisture Addition
% Calculated shower index
shower_day = zeros(N_day,1);
start_shower_ts = time_1st_shower*(60/length_ts)+1;
shower_day(start_shower_ts:2:start_shower_ts+2*(family-1)) =
 load_shower(scen);
shower = repmat(shower_day,365,1);

% Calculated parameters
rate_occ_ts = rate_occ_hr(scen)/(60/length_ts); % moisture rate from
 occupancy (transpiration and respiration) per time step, kg/(time
 step)
rate_dish_ts = load_dish(scen)/(length_dish/length_ts);
nts_cook_meals = length_cook_meals(scen,:)/length_ts; % length of
 cooking meals in number of time steps, -
rate_pets_ts = rate_occ_ts/m_adult; % release rate per kilogram, based
 off human release rate, kg/(kg*time_step)
rate_plant_ts = rate_plant_day(scen)/(24*60/length_ts); % release per
 time step per plants, kg/(time step)
nts_mop = length_mop_dry(scen)/(length_ts);
load_mop_room = a_room(1:5)*load_mop_m2(scen)*mop_coverage; % 0.15 L/
m2
rate_mop_room_ts = load_mop_room/nts_mop;

% Calculated coooking and dishwasher indeces
cooking_day = zeros(N_day,1);
start_cooking_ts = time_meals*(60/length_ts)+1;
for meal = 1:nmeals
    cooking_day(start_cooking_ts(meal):start_cooking_ts(meal)...
        +nts_cook_meals(meal)-1) = load_meals(scen,meal)/
nts_cook_meals(meal);
end
cooking = repmat(cooking_day,365,1);
dish_day = zeros(N_day,1);
start_dish_ts = time_dish*(60/length_ts)+1;
dish_day(start_dish_ts:start_dish_ts+length_dish/(length_ts)) =
 rate_dish_ts;
dish = repmat(dish_day,365,1);

mopping = zeros(N_year,nrooms);
mopping_day = zeros(N_day,nrooms);
nts_mop = length_mop_dry/length_ts;
start_mop_ts = start_wkly_mop*(60/length_ts)+1;
if (nts_mop > 1)
    fill_mop = repmat(rate_mop_room_ts,nts_mop-1,1);
else
    fill_mop = rate_mop_room_ts;
end
mopping_day(start_mop_ts:start_mop_ts+nts_mop-1,:) = fill_mop;
for week = 1:52
    mopping((7*(week-1)+1)*N_day+1:(7*(week-1)+2)*N_day,:) =
 mopping_day;
end
```

```
clothes = zeros(N_year,1);
nts_clothes = length_clothes/length_ts;
rate_clothes = flip(1:nts_clothes)*load_clothes(scen)/
sum(1:nts_clothes);
start_clothes_ts = start_clothes*(60/length_ts)+1;
for week = 1:52
    for d = 1:3
        clothes((7*(week-1)+2*d-1)*N_day+start_clothes_ts:...
        (7*(week-1)+2*d-1)*N_day+start_clothes_ts+nts_clothes-1) =
 rate_clothes;
    end
end

% Moisture addition in mass
add_m_rooms = zeros(N_year,nrooms);
x_add_kgkg = zeros(N_year,nrooms);
add_m_occ = occ*rate_occ_ts; % mass of moisture added from occupancy,
 kg
add_m_rooms = add_m_rooms + add_m_occ;
add_m_shower = shower; % mass of moisture added from occupancy, kg
add_m_clothes = clothes;
add_m_rooms(:,bathroom) = add_m_rooms(:,bathroom) +
 add_m_shower(1:end-1) + add_m_clothes;
add_m_cooking = cooking;
add_m_dish = dish;
add_m_mopping = mopping;
add_m_rooms(:,kitchen) = add_m_rooms(:,kitchen) +
 add_m_cooking(1:end-1);
add_m_plants = ones(N_year,1)*rate_plant_ts;
add_m_pets = ones(N_year,1)*m_pets(scen)*rate_pets_ts;
add_m_rooms(:,living) = add_m_rooms(:,living) + add_m_plants +
 add_m_pets;
add_m_rooms = add_m_rooms + add_m_mopping;

for room = 1:nrooms
    x_add_kgkg(:,room) = add_m_rooms(:,room)/
(vol_room(room)*rho_room);
end
x_add = x_add_kgkg*1000; % g/kg

% Simulations with parameter variations
npar = 20;
nsim = 12;
nlim = 3;

x_data = zeros(N_year,nrooms,npar,nsim,nlim);
rh_data = zeros(N_year,nrooms,npar,nsim,nlim);

ach_vent_min_ts = ach_vent_min./(60/length_ts);
ach_vent_whole_min_ts = ach_vent_whole_min./(60/length_ts);
ach_vent_max_ts = ach_vent_max./(60/length_ts);
ach_inf_ts = ach_inf./(60/length_ts);

% Initials equations
```

```
a_total = sum(a_room);
e_sat_room = alpha*exp(beta*t_room/(lambda+t_room)); % saturation
 vapour pressure, hPa
x_sat_room = 621.98*e_sat_room/(press_atm-e_sat_room); % saturation
 moiture content, g/kg
for i = 1:(N_year-1)
    e_amb(i) = alpha*(rh_amb(i)/100)*exp(beta*t_amb(i)/(lambda
+t_amb(i))); % vapour pressure
    x_amb(i) = 621.98*e_amb(i)/(press(i)-e_amb(i)); % ambient moisture
 content
end

% Parameter Variation of Infiltration - Calculated variables
param_inf = 0.02:0.01:0.17; % infiltration air change rate, 1/h
npar_inf = length(param_inf);
param_inf_ts = param_inf./(60/length_ts);

% Regenerative
hr_above_limit_inf = zeros(npar_inf,nrooms);
hr_above_limit_inf_ref = zeros(npar_inf,nrooms);

% Single-room ventilation iterations
for sensit = 1:npar_inf
    ach_vent_ts = repmat(ach_vent_min_ts,N_year,1);
    % Intial equations
    rh_room(1,:) = rh_room_init; % initial relative humidity, %
    e_room(1,:) = alpha*(rh_room(1,:)/100)*exp(beta*t_room/(lambda
+t_room)); % vapour pressure, hPa
    x_room(1,:) = 621.98*e_room(1,:)./(press_atm-e_room(1,:)); % room
 moisture content after time step, g/kg
    % Iterations
    for room = 1:nrooms
        for i = 1:(N_year-1)
            % Step 1
            rh_room(i,room) = min(100*x_room(i,room)/x_sat_room,100);
            term_dp_room = log(rh_room(i,room)/100)+(beta*t_room)/
(lambda+t_room);
            dp_room(i,room) = lambda*term_dp_room/(beta-term_dp_room);
            % Step 2
            t_exh(i) = min(max(t_room-(t_room-
t_amb(i))*eta(i,room),0.5),t_room);
            e_sat_exh(i) = alpha*exp(beta*t_exh(i)/(lambda
+t_exh(i))); % saturation vapour pressure
            if t_exh(i) <= dp_room(i,room)
                x_exh(i,room) = 621.98*e_sat_exh(i)/(press_atm-
e_sat_exh(i));
                x_supply(i,room) =
 x_amb(i)+min(x_sat_room,x_room(i,room))-x_exh(i,room);
            else
                x_exh(i,room) = min(x_sat_room,x_room(i,room));
                x_supply(i,room) = x_amb(i);
            end
            % Step 3
            if (room == 1 || room == 2)
```

```
                ach_vent_ts(i,room) =
 ach_vent_ts(i,room) + (ach_vent_max_ts(room)-
ach_vent_min_ts(room))*min(1,max(rh_room(i,room)-rh_Pctrl_low,0)/
(rh_Pctrl_high-rh_Pctrl_low));
            end
            % Step 4
            x_room(i+1,room) =
 x_room(i,room)+x_add(i,room)+ach_vent_ts(i,room)*(x_supply(i,room)-
min(x_sat_room,x_room(i,room)))...
                +param_inf_ts(sensit)*(x_amb(i)-
min(x_sat_room,x_room(i,room)));
        end
    end
    % Store data
    x_data(:,:,sensit,1,1) = x_room;
    rh_data(:,:,sensit,1,1) = rh_room;
    hr_above_limit_inf(sensit,:) =
 (sum(rh_room(1:135*N_day,:)>rh_limit,1)...
        +sum(rh_room(258*N_day:end,:)>rh_limit,1))./6;
    pct_above_limit_inf = hr_above_limit_inf*100/(24*(365-
(258-135))); % only for heating season
end

% Whole-dwelling ventilation iterations
for sensit = 1:npar_inf
    ach_vent_ts = repmat(ach_vent_whole_min_ts,N_year,1);
    % Initial equations
    rh_room(1,:) = rh_room_init; % initial relative humidity, %
    e_room(1,:) = alpha*(rh_room(1,:)/100)*exp(beta*t_room/(lambda
+t_room)); % vapour pressure, hPa
    x_room(1,:) = 621.98*e_room(1,:)./(press_atm-e_room(1,:)); % room
 moisture content after time step, g/kg
    % Iterations
    for i = 1:(N_year-1)
        % Step 1
        rh_room(i,room) = min(100*x_room(i,room)/x_sat_room,100);
        % Step 2
        x_mixed_dry(i) = sum(vol_room(3:5).*x_room(i,3:5))/
sum(vol_room(3:5));
        % Step 3
        for room = 1:2
            term_dp_room = log(rh_room(i,room)/100)+(beta*t_room)/
(lambda+t_room);
            dp_room(i,room) = lambda*term_dp_room/(beta-term_dp_room);

            ach_vent_ts(i,room) = ach_vent_ts(i,room) +
 (ach_vent_max_ts(room)-
ach_vent_whole_min_ts(room))*min(1,max(rh_room(i,room)-
rh_Pctrl_low,0)/(rh_Pctrl_high-rh_Pctrl_low));
            x_supply(i,room) = x_mixed_dry(i);
        end
        % Step 4
        t_exh(i) = min(max(t_room-(t_room-
t_amb(i))*eta(1,1),0.5),t_room);
```

```
        e_sat_exh(i) = alpha*exp(beta*t_exh(i)/(lambda+t_exh(i))); %
 saturation vapour pressure
        x_mixed_wet(i) = sum(ach_vent_ts(i,1:2).*x_room(i,1:2))./
sum(ach_vent_ts(i,1:2));
        rh_mixed_wet(i) = min(100*x_mixed_wet(i)/x_sat_room,100);
        term_dp_room = log(rh_mixed_wet(i)/100)+(beta*t_room)/(lambda
+t_room);
        dp_mixed_wet(i) = lambda*term_dp_room/(beta-term_dp_room);
        if t_exh(i) <= dp_mixed_wet(i)
            x_mixed_exh(i) = 621.98*e_sat_exh(i)/(press_atm-
e_sat_exh(i));
        else
            x_mixed_exh(i) = min(x_sat_room,x_mixed_wet(i));
        end
        % Step 5
        for room = 3:5
            if t_exh(i) < dp_mixed_wet(i)
                x_supply(i,room) =
 x_amb(i)+min(x_sat_room,x_mixed_wet(i))-x_mixed_exh(i);
            else
                x_supply(i,room) = x_amb(i);
            end
            ach_vent_ts(i,room) = vol_room(room)./
sum(vol_room(3:5)).*sum(ach_vent_ts(i,1:2));
        end
        % Step 6
        for room = 1:nrooms
            x_room(i+1,room) =
 x_room(i,room)+x_add(i,room)+ach_vent_ts(i,room)*(x_supply(i,room)-
min(x_sat_room,x_room(i,room)))...
            +param_inf_ts(sensit)*(x_amb(i)-
min(x_sat_room,x_room(i,room)));
        end
    end
    % Store data
    x_data(:,:,sensit,2,1) = x_room;
    rh_data(:,:,sensit,2,1) = rh_room;
    hr_above_limit_inf_ref(sensit,:) =
 (sum(rh_room(1:135*N_day,:)>rh_limit,1)...
        +sum(rh_room(258*N_day:end,:)>rh_limit,1))./6;
    pct_above_limit_inf_ref = hr_above_limit_inf_ref*100/(24*(365-
(258-135))); % only for heating season
end

% Recuperative
hr_above_limit_inf_rec = zeros(length(param_inf),nrooms);
hr_above_limit_inf_ref_rec = zeros(npar_inf,nrooms);

% Single-room ventilation iterations
for sensit = 1:npar_inf
    ach_vent_ts = repmat(ach_vent_min_ts,N_year,1);
    % Intial equations
    rh_room(1,:) = rh_room_init; % initial relative humidity, %
```

```
    e_room(1,:) = alpha*(rh_room(1,:)/100)*exp(beta*t_room/(lambda
+t_room)); % vapour pressure, hPa
    x_room(1,:) = 621.98*e_room(1,:)./(press_atm-e_room(1,:)); % room
 moisture content after time step, g/kg
    % Iterations
    for room = 1:nrooms
        for i = 1:(N_year-1)
            % Step 1
            rh_room(i,room) = min(100*x_room(i,room)/x_sat_room,100);
            term_dp_room = log(rh_room(i,room)/100)+(beta*t_room)/
(lambda+t_room);
            dp_room(i,room) = lambda*term_dp_room/(beta-term_dp_room);
            % Step 2
            t_exh(i) = min(max(t_room-(t_room-
t_amb(i))*eta(i,room),0.5),t_room);
            e_sat_exh(i) = alpha*exp(beta*t_exh(i)/(lambda
+t_exh(i))); % saturation vapour pressure
            x_exh(i,room) = min(x_sat_room,x_room(i,room));
            x_supply(i,room) = x_amb(i);
            % Step 3
            if (room == 1 || room == 2)
                ach_vent_ts(i,room) =
 ach_vent_ts(i,room) + (ach_vent_max_ts(room)-
ach_vent_min_ts(room))*min(1,max(rh_room(i,room)-rh_Pctrl_low,0)/
(rh_Pctrl_high-rh_Pctrl_low));
            end
            % Step 4
            x_room(i+1,room) =
 x_room(i,room)+x_add(i,room)+ach_vent_ts(i,room)*(x_supply(i,room)-
min(x_sat_room,x_room(i,room)))...
                +param_inf_ts(sensit)*(x_amb(i)-
min(x_sat_room,x_room(i,room)));
        end
    end
    % Store data
    x_data(:,:,sensit,3,1) = x_room;
    rh_data(:,:,sensit,3,1) = rh_room;
    hr_above_limit_inf_rec(sensit,:) =
 (sum(rh_room(1:135*N_day,:)>rh_limit,1)...
        +sum(rh_room(258*N_day:end,:)>rh_limit,1))./6;
    pct_above_limit_inf_rec = hr_above_limit_inf_rec*100/(24*(365-
(258-135))); % only for heating season
end

% Whole-dwelling ventilation iterations
for sensit = 1:npar_inf
    ach_vent_ts = repmat(ach_vent_whole_min_ts,N_year,1);
    % Initial equations
    rh_room(1,:) = rh_room_init; % initial relative humidity, %
    e_room(1,:) = alpha*(rh_room(1,:)/100)*exp(beta*t_room/(lambda
+t_room)); % vapour pressure, hPa
    x_room(1,:) = 621.98*e_room(1,:)./(press_atm-e_room(1,:)); % room
 moisture content after time step, g/kg
    % Iterations
```

```
    for i = 1:(N_year-1)
        % Step 1
        rh_room(i,room) = min(100*x_room(i,room)/x_sat_room,100);
        % Step 2
        x_mixed_dry(i) = sum(vol_room(3:5).*x_room(i,3:5))/
sum(vol_room(3:5));
        % Step 3
        for room = 1:2
            term_dp_room = log(rh_room(i,room)/100)+(beta*t_room)/
(lambda+t_room);
            dp_room(i,room) = lambda*term_dp_room/(beta-term_dp_room);

            ach_vent_ts(i,room) = ach_vent_ts(i,room) +
 (ach_vent_max_ts(room)-
ach_vent_whole_min_ts(room))*min(1,max(rh_room(i,room)-
rh_Pctrl_low,0)/(rh_Pctrl_high-rh_Pctrl_low));
            x_supply(i,room) = x_mixed_dry(i);
        end
        % Step 4
        t_exh(i) = min(max(t_room-(t_room-
t_amb(i))*eta(1,1),0.5),t_room);
        e_sat_exh(i) = alpha*exp(beta*t_exh(i)/(lambda+t_exh(i))); %
 saturation vapour pressure
        x_mixed_wet(i) = sum(ach_vent_ts(i,1:2).*x_room(i,1:2))./
sum(ach_vent_ts(i,1:2));
        rh_mixed_wet(i) = min(100*x_mixed_wet(i)/x_sat_room,100);
        term_dp_room = log(rh_mixed_wet(i)/100)+(beta*t_room)/(lambda
+t_room);
        dp_mixed_wet(i) = lambda*term_dp_room/(beta-term_dp_room);
        x_mixed_exh(i) = min(x_sat_room,x_mixed_wet(i));
        % Step 5
        for room = 3:5
            x_supply(i,room) = x_amb(i);
            ach_vent_ts(i,room) = vol_room(room)./
sum(vol_room(3:5)).*sum(ach_vent_ts(i,1:2));
        end
        % Step 6
        for room = 1:nrooms
            x_room(i+1,room) =
 x_room(i,room)+x_add(i,room)+ach_vent_ts(i,room)*(x_supply(i,room)-
min(x_sat_room,x_room(i,room)))...
            +param_inf_ts(sensit)*(x_amb(i)-
min(x_sat_room,x_room(i,room)));
        end
    end
    % Store data
    x_data(:,:,sensit,4,1) = x_room;
    rh_data(:,:,sensit,4,1) = rh_room;
    hr_above_limit_inf_ref_rec(sensit,:) =
 (sum(rh_room(1:135*N_day,:)...
        >rh_limit,1)+sum(rh_room(258*N_day:end,:)>rh_limit,1))./6;
    pct_above_limit_inf_ref_rec = hr_above_limit_inf_ref_rec*100/
(24*(365-(258-135))); % only for heating season
end
```

```
% Parameter Variation of Heat Exchanger Efficiency - Calculated
 variables
param_eta = repmat(0.6:0.02:0.94,N_year,1);
npar_eta = size(param_eta,2);
param_eta(135*N_day+1:258*N_day,:) = 0;

% Regenerative
hr_above_limit_eta = zeros(npar_eta,nrooms);
hr_above_limit_eta_ref = zeros(npar_eta,nrooms);

% Single-room ventilation iterations
for sensit = 1:npar_eta
    ach_vent_ts = repmat(ach_vent_min_ts,N_year,1);
    % Initial equations
    rh_room(1,:) = rh_room_init; % initial relative humidity, %
    e_room(1,:) = alpha*(rh_room(1,:)/100)*exp(beta*t_room/(lambda
+t_room)); % vapour pressure, hPa
    x_room(1,:) = 621.98*e_room(1,:)./(press_atm-e_room(1,:)); % room
 moisture content after time step, g/kg
    % Iterations
    for room = 1:nrooms
        for i = 1:(N_year-1)
            % Step 1
            rh_room(i,room) = min(100*x_room(i,room)/x_sat_room,100);
            term_dp_room = log(rh_room(i,room)/100)+(beta*t_room)/
(lambda+t_room);
            dp_room(i,room) = lambda*term_dp_room/(beta-term_dp_room);
            % Step 2
            t_exh(i) = min(max(t_room-(t_room-
t_amb(i))*param_eta(i,sensit),0.5),t_room);
            e_sat_exh(i) = alpha*exp(beta*t_exh(i)/(lambda
+t_exh(i))); % saturation vapour pressure
            if t_exh(i) <= dp_room(i,room)
                x_exh(i,room) = 621.98*e_sat_exh(i)/(press_atm-
e_sat_exh(i));
                x_supply(i,room) =
 x_amb(i)+min(x_sat_room,x_room(i,room))-x_exh(i,room);
            else
                x_exh(i,room) = min(x_sat_room,x_room(i,room));
                x_supply(i,room) = x_amb(i);
            end
            % Step 3
            if (room == 1 || room == 2)
                ach_vent_ts(i,room) =
 ach_vent_ts(i,room) + (ach_vent_max_ts(room)-
ach_vent_min_ts(room))*min(1,max(rh_room(i,room)-rh_Pctrl_low,0)/
(rh_Pctrl_high-rh_Pctrl_low));
            end
            % Step 4
            x_room(i+1,room) =
 x_room(i,room)+x_add(i,room)+ach_vent_ts(i,room)*(x_supply(i,room)-
min(x_sat_room,x_room(i,room)))...
```

```
                +ach_inf_ts(1,room)*(x_amb(i)-
min(x_sat_room,x_room(i,room)));
        end
    end
    % Store data
    x_data(:,:,sensit,5,1) = x_room;
    rh_data(:,:,sensit,5,1) = rh_room;
    hr_above_limit_eta(sensit,:) =
 (sum(rh_room(1:135*N_day,:)>rh_limit,1)...
        +sum(rh_room(258*N_day:end,:)>rh_limit,1))./6;
    pct_above_limit_eta = hr_above_limit_eta*100/(24*(365-
(258-135))); % only for heating season
end

% Whole-dwelling ventilation iterations
for sensit = 1:npar_eta
    ach_vent_ts = repmat(ach_vent_whole_min_ts,N_year,1);
    % Initial equations
    rh_room(1,:) = rh_room_init; % initial relative humidity, %
    e_room(1,:) = alpha*(rh_room(1,:)/100)*exp(beta*t_room/(lambda
+t_room)); % vapour pressure, hPa
    x_room(1,:) = 621.98*e_room(1,:)./(press_atm-e_room(1,:)); % room
 moisture content after time step, g/kg
    % Iterations
    for i = 1:(N_year-1)
        % Step 1
        rh_room(i,room) = min(100*x_room(i,room)/x_sat_room,100);
        % Step 2
        x_mixed_dry(i) = sum(vol_room(3:5).*x_room(i,3:5))/
sum(vol_room(3:5));
        % Step 3
        for room = 1:2
            term_dp_room = log(rh_room(i,room)/100)+(beta*t_room)/
(lambda+t_room);
            dp_room(i,room) = lambda*term_dp_room/(beta-term_dp_room);

            ach_vent_ts(i,room) = ach_vent_ts(i,room) +
 (ach_vent_max_ts(room)-
ach_vent_whole_min_ts(room))*min(1,max(rh_room(i,room)-
rh_Pctrl_low,0)/(rh_Pctrl_high-rh_Pctrl_low));
            x_supply(i,room) = x_mixed_dry(i);
        end
        % Step 4
        t_exh(i) = min(max(t_room-(t_room-
t_amb(i))*param_eta(i,sensit),0.5),t_room);
        e_sat_exh(i) = alpha*exp(beta*t_exh(i)/(lambda+t_exh(i))); %
 saturation vapour pressure
        x_mixed_wet(i) = sum(ach_vent_ts(i,1:2).*x_room(i,1:2))./
sum(ach_vent_ts(i,1:2));
        rh_mixed_wet(i) = min(100*x_mixed_wet(i)/x_sat_room,100);
        term_dp_room = log(rh_mixed_wet(i)/100)+(beta*t_room)/(lambda
+t_room);
        dp_mixed_wet(i) = lambda*term_dp_room/(beta-term_dp_room);
        if t_exh(i) <= dp_mixed_wet(i)
```

```
            x_mixed_exh(i) = 621.98*e_sat_exh(i)/(press_atm-
e_sat_exh(i));
        else
            x_mixed_exh(i) = min(x_sat_room,x_mixed_wet(i));
        end
        % Step 5
        for room = 3:5
            if t_exh(i) < dp_mixed_wet(i)
                x_supply(i,room) =
 x_amb(i)+min(x_sat_room,x_mixed_wet(i))-x_mixed_exh(i);
            else
                x_supply(i,room) = x_amb(i);
            end
            ach_vent_ts(i,room) = vol_room(room)./
sum(vol_room(3:5)).*sum(ach_vent_ts(i,1:2));
        end
        % Step 6
        for room = 1:nrooms
            x_room(i+1,room) =
 x_room(i,room)+x_add(i,room)+ach_vent_ts(i,room)*(x_supply(i,room)-
min(x_sat_room,x_room(i,room)))...
            +ach_inf_ts(1,room)*(x_amb(i)-
min(x_sat_room,x_room(i,room)));
        end
    end
    % Store data
    x_data(:,:,sensit,6,1) = x_room;
    rh_data(:,:,sensit,6,1) = rh_room;
    hr_above_limit_eta_ref(sensit,:) =
 (sum(rh_room(1:135*N_day,:)>rh_limit,1)...
        +sum(rh_room(258*N_day:end,:)>rh_limit,1))./6;
    pct_above_limit_eta_ref = hr_above_limit_eta_ref*100/(24*(365-
(258-135))); % only for heating season
end

% Recuperative
hr_above_limit_eta_rec = zeros(npar_eta,nrooms);
hr_above_limit_eta_ref_rec = zeros(npar_eta,nrooms);

% Single-room ventilation iterations
for sensit = 1:npar_eta
    ach_vent_ts = repmat(ach_vent_min_ts,N_year,1);
    % Initial equations
    rh_room(1,:) = rh_room_init; % initial relative humidity, %
    e_room(1,:) = alpha*(rh_room(1,:)/100)*exp(beta*t_room/(lambda
+t_room)); % vapour pressure, hPa
    x_room(1,:) = 621.98*e_room(1,:)./(press_atm-e_room(1,:)); % room
 moisture content after time step, g/kg
    % Iterations
    for room = 1:nrooms
        for i = 1:(N_year-1)
            % Step 1
            rh_room(i,room) = min(100*x_room(i,room)/x_sat_room,100);
```

```
            term_dp_room = log(rh_room(i,room)/100)+(beta*t_room)/
(lambda+t_room);
            dp_room(i,room) = lambda*term_dp_room/(beta-term_dp_room);
            % Step 2
            t_exh(i) = min(max(t_room-(t_room-
t_amb(i))*param_eta(i,sensit),0.5),t_room);
            e_sat_exh(i) = alpha*exp(beta*t_exh(i)/(lambda
+t_exh(i))); % saturation vapour pressure
            x_exh(i,room) = min(x_sat_room,x_room(i,room));
            x_supply(i,room) = x_amb(i);
            % Step 3
            if (room == 1 || room == 2)
                ach_vent_ts(i,room) =
 ach_vent_ts(i,room) + (ach_vent_max_ts(room)-
ach_vent_min_ts(room))*min(1,max(rh_room(i,room)-rh_Pctrl_low,0)/
(rh_Pctrl_high-rh_Pctrl_low));
            end
            % Step 4
            x_room(i+1,room) =
 x_room(i,room)+x_add(i,room)+ach_vent_ts(i,room)*(x_supply(i,room)-
min(x_sat_room,x_room(i,room)))...
                +ach_inf_ts(1,room)*(x_amb(i)-
min(x_sat_room,x_room(i,room)));
        end
    end
    % Store data
    x_data(:,:,sensit,7,1) = x_room;
    rh_data(:,:,sensit,7,1) = rh_room;
    hr_above_limit_eta_rec(sensit,:) =
 (sum(rh_room(1:135*N_day,:)>rh_limit,1)...
        +sum(rh_room(258*N_day:end,:)>rh_limit,1))./6;
    pct_above_limit_eta_rec = hr_above_limit_eta_rec*100/(24*(365-
(258-135))); % only for heating season
end

% Whole-dwelling ventilation iterations
for sensit = 1:npar_eta
    ach_vent_ts = repmat(ach_vent_whole_min_ts,N_year,1);
    % Initial equations
    rh_room(1,:) = rh_room_init; % initial relative humidity, %
    e_room(1,:) = alpha*(rh_room(1,:)/100)*exp(beta*t_room/(lambda
+t_room)); % vapour pressure, hPa
    x_room(1,:) = 621.98*e_room(1,:)./(press_atm-e_room(1,:)); % room
 moisture content after time step, g/kg
    % Iterations
    for i = 1:(N_year-1)
        % Step 1
        rh_room(i,room) = min(100*x_room(i,room)/x_sat_room,100);
        % Step 2
        x_mixed_dry(i) = sum(vol_room(3:5).*x_room(i,3:5))/
sum(vol_room(3:5));
        % Step 3
        for room = 1:2
            rh_room(i,room) = min(100*x_room(i,room)/x_sat_room,100);
```

```
            term_dp_room = log(rh_room(i,room)/100)+(beta*t_room)/
(lambda+t_room);
            dp_room(i,room) = lambda*term_dp_room/(beta-term_dp_room);

            ach_vent_ts(i,room) = ach_vent_ts(i,room) +
 (ach_vent_max_ts(room)-
ach_vent_whole_min_ts(room))*min(1,max(rh_room(i,room)-
rh_Pctrl_low,0)/(rh_Pctrl_high-rh_Pctrl_low));
            x_supply(i,room) = x_mixed_dry(i);
        end
        % Step 4
        t_exh(i) = min(max(t_room-(t_room-
t_amb(i))*param_eta(i,sensit),0.5),t_room);
        e_sat_exh(i) = alpha*exp(beta*t_exh(i)/(lambda+t_exh(i))); %
 saturation vapour pressure
        x_mixed_wet(i) = sum(ach_vent_ts(i,1:2).*x_room(i,1:2))./
sum(ach_vent_ts(i,1:2));
        rh_mixed_wet(i) = min(100*x_mixed_wet(i)/x_sat_room,100);
        term_dp_room = log(rh_mixed_wet(i)/100)+(beta*t_room)/(lambda
+t_room);
        dp_mixed_wet(i) = lambda*term_dp_room/(beta-term_dp_room);
        x_mixed_exh(i) = min(x_sat_room,x_mixed_wet(i));
        % Step 5
        for room = 3:5
            rh_room(i,room) = min(100*x_room(i,room)/x_sat_room,100);
            x_supply(i,room) = x_amb(i);
            ach_vent_ts(i,room) = vol_room(room)./
sum(vol_room(3:5)).*sum(ach_vent_ts(i,1:2));
        end
        % Step 6
        for room = 1:nrooms
            x_room(i+1,room) =
 x_room(i,room)+x_add(i,room)+ach_vent_ts(i,room)*(x_supply(i,room)-
min(x_sat_room,x_room(i,room)))...
            +ach_inf_ts(1,room)*(x_amb(i)-
min(x_sat_room,x_room(i,room)));
        end
    end
    % Store data
    x_data(:,:,sensit,8,1) = x_room;
    rh_data(:,:,sensit,8,1) = rh_room;
    hr_above_limit_eta_ref_rec(sensit,:) =
 (sum(rh_room(1:135*N_day,:)>...
        rh_limit,1)+sum(rh_room(258*N_day:end,:)>rh_limit,1))./6;
    pct_above_limit_eta_ref_rec = hr_above_limit_eta_ref_rec*100/
(24*(365-(258-135))); % only for heating season
end

% Parameter Variation of Room Temperature - Calculated variables
param_tem = 17:0.5:26;
npar_tem = size(param_tem,2);

% Regenerative
hr_above_limit_tem = zeros(npar_tem,nrooms);
```

```
hr_above_limit_tem_ref = zeros(npar_tem,nrooms);

% Single-room ventilation iterations
for sensit = 1:npar_tem
    ach_vent_ts = repmat(ach_vent_min_ts,N_year,1);
    % Initial equations
    rh_room(1,:) = rh_room_init; % initial relative humidity, %
    e_room(1,:) = alpha*(rh_room(1,:)/100)*exp(beta*param_tem(sensit)/
(lambda+param_tem(sensit))); % vapour pressure, hPa
    x_room(1,:) = 621.98*e_room(1,:)./(press_atm-e_room(1,:)); % room
 moisture content after time step, g/kg
    % Calculate new saturation conditions
    e_sat_room = alpha*exp(beta*param_tem(sensit)/(lambda
+param_tem(sensit))); % saturation vapour pressure, hPa
    x_sat_room = 621.98*e_sat_room/(press_atm-e_sat_room); %
 saturation moiture content, g/kg
    % Iterations
    for room = 1:nrooms
        for i = 1:(N_year-1)
            % Step 1
            rh_room(i,room) = min(100*x_room(i,room)/x_sat_room,100);
            term_dp_room =
 log(rh_room(i,room)/100)+(beta*param_tem(sensit))/(lambda
+param_tem(sensit));
            dp_room(i,room) = lambda*term_dp_room/(beta-term_dp_room);
            % Step 2
            t_exh(i) = min(max(param_tem(sensit)-(param_tem(sensit)-
t_amb(i))*eta(i,1),0.5),param_tem(sensit));
            e_sat_exh(i) = alpha*exp(beta*t_exh(i)/(lambda
+t_exh(i))); % saturation vapour pressure
            if t_exh(i) <= dp_room(i,room)
                x_exh(i,room) = 621.98*e_sat_exh(i)/(press_atm-
e_sat_exh(i));
                x_supply(i,room) =
 x_amb(i)+min(x_sat_room,x_room(i,room))-x_exh(i,room);
            else
                x_exh(i,room) = min(x_sat_room,x_room(i,room));
                x_supply(i,room) = x_amb(i);
            end
            % Step 3
            if (room == 1 || room == 2)
                ach_vent_ts(i,room) =
 ach_vent_ts(i,room) + (ach_vent_max_ts(room)-
ach_vent_min_ts(room))*min(1,max(rh_room(i,room)-rh_Pctrl_low,0)/
(rh_Pctrl_high-rh_Pctrl_low));
            end
            % Step 4
            x_room(i+1,room) =
 x_room(i,room)+x_add(i,room)+ach_vent_ts(i,room)*(x_supply(i,room)-
min(x_sat_room,x_room(i,room)))...
                +ach_inf_ts(1,room)*(x_amb(i)-
min(x_sat_room,x_room(i,room)));
        end
    end
```

```
    % Store data
    x_data(:,:,sensit,9,1) = x_room;
    rh_data(:,:,sensit,9,1) = rh_room;
    hr_above_limit_tem(sensit,:) =
 (sum(rh_room(1:135*N_day,:)>rh_limit,1)...
        +sum(rh_room(258*N_day:end,:)>rh_limit,1))./6;
    pct_above_limit_tem = hr_above_limit_tem*100/(24*(365-
(258-135))); % only for heating season

end

% Whole-dwelling ventilation iterations
for sensit = 1:npar_tem
    ach_vent_ts = repmat(ach_vent_whole_min_ts,N_year,1);
    % Initial equations
    rh_room(1,:) = rh_room_init; % initial relative humidity, %
    e_room(1,:) = alpha*(rh_room(1,:)/100)*exp(beta*param_tem(sensit)/
(lambda+param_tem(sensit))); % vapour pressure, hPa
    x_room(1,:) = 621.98*e_room(1,:)./(press_atm-e_room(1,:)); % room
 moisture content after time step, g/kg
    % Calculate new saturation conditions
    e_sat_room = alpha*exp(beta*param_tem(sensit)/(lambda
+param_tem(sensit))); % saturation vapour pressure, hPa
    x_sat_room = 621.98*e_sat_room/(press_atm-e_sat_room); %
 saturation moiture content, g/kg
    % Iterations
    for i = 1:(N_year-1)
        % Step 1
        rh_room(i,room) = min(100*x_room(i,room)/x_sat_room,100);
        % Step 2
        x_mixed_dry(i) = sum(vol_room(3:5).*x_room(i,3:5))/
sum(vol_room(3:5));
        % Step 3
        for room = 1:2
            rh_room(i,room) = min(100*x_room(i,room)/x_sat_room,100);
            term_dp_room =
 log(rh_room(i,room)/100)+(beta*param_tem(sensit))/(lambda
+param_tem(sensit));
            dp_room(i,room) = lambda*term_dp_room/(beta-term_dp_room);
            ach_vent_ts(i,room) = ach_vent_ts(i,room) +
 (ach_vent_max_ts(room)-
ach_vent_whole_min_ts(room))*min(1,max(rh_room(i,room)-
rh_Pctrl_low,0)/(rh_Pctrl_high-rh_Pctrl_low));
            x_supply(i,room) = x_mixed_dry(i);
        end
        % Step 4
        t_exh(i) = min(max(param_tem(sensit)-(param_tem(sensit)-
t_amb(i))*eta(i,1),0.5),param_tem(sensit));
        e_sat_exh(i) = alpha*exp(beta*t_exh(i)/(lambda+t_exh(i))); %
 saturation vapour pressure
        x_mixed_wet(i) = sum(ach_vent_ts(i,1:2).*x_room(i,1:2))./
sum(ach_vent_ts(i,1:2));
        rh_mixed_wet(i) = min(100*x_mixed_wet(i)/x_sat_room,100);
```

```
        term_dp_room =
 log(rh_mixed_wet(i)/100)+(beta*param_tem(sensit))/(lambda
+param_tem(sensit));
        dp_mixed_wet(i) = lambda*term_dp_room/(beta-term_dp_room);
        if t_exh(i) <= dp_mixed_wet(i)
            x_mixed_exh(i) = 621.98*e_sat_exh(i)/(press_atm-
e_sat_exh(i));
        else
            x_mixed_exh(i) = min(x_sat_room,x_mixed_wet(i));
        end
        % Step 5
        for room = 3:5
            rh_room(i,room) = min(100*x_room(i,room)/x_sat_room,100);
            if t_exh(i) < dp_mixed_wet(i)
                x_supply(i,room) =
 x_amb(i)+min(x_sat_room,x_mixed_wet(i))-x_mixed_exh(i);
            else
                x_supply(i,room) = x_amb(i);
            end
            ach_vent_ts(i,room) = vol_room(room)./
sum(vol_room(3:5)).*sum(ach_vent_ts(i,1:2));
        end
        % Step 6
        for room = 1:nrooms
            x_room(i+1,room) =
 x_room(i,room)+x_add(i,room)+ach_vent_ts(i,room)*(x_supply(i,room)-
min(x_sat_room,x_room(i,room)))...
            +ach_inf_ts(1,room)*(x_amb(i)-
min(x_sat_room,x_room(i,room)));
        end
    end
    % Store data
    x_data(:,:,sensit,10,1) = x_room;
    rh_data(:,:,sensit,10,1) = rh_room;
    hr_above_limit_tem_ref(sensit,:) =
 (sum(rh_room(1:135*N_day,:)>rh_limit,1)...
        +sum(rh_room(258*N_day:end,:)>rh_limit,1))./6;
    pct_above_limit_tem_ref = hr_above_limit_tem_ref*100/(24*(365-
(258-135))); % only for heating season

end

% Recuperative
hr_above_limit_tem_rec = zeros(npar_tem,nrooms);
hr_above_limit_tem_ref_rec = zeros(npar_tem,nrooms);

% Single-room ventilation iterations
for sensit = 1:npar_tem
    ach_vent_ts = repmat(ach_vent_min_ts,N_year,1);
    % Initial equations
    rh_room(1,:) = rh_room_init; % initial relative humidity, %
    e_room(1,:) = alpha*(rh_room(1,:)/100)*exp(beta*param_tem(sensit)/
(lambda+param_tem(sensit))); % vapour pressure, hPa
```

```
    x_room(1,:) = 621.98*e_room(1,:)./(press_atm-e_room(1,:)); % room
 moisture content after time step, g/kg
    % Calculate new saturation conditions
    e_sat_room = alpha*exp(beta*param_tem(sensit)/(lambda
+param_tem(sensit))); % saturation vapour pressure, hPa
    x_sat_room = 621.98*e_sat_room/(press_atm-e_sat_room); %
 saturation moiture content, g/kg
    % Iterations
    for room = 1:nrooms
        for i = 1:(N_year-1)
            % Step 1
            rh_room(i,room) = min(100*x_room(i,room)/x_sat_room,100);
            term_dp_room =
 log(rh_room(i,room)/100)+(beta*param_tem(sensit))/(lambda
+param_tem(sensit));
            dp_room(i,room) = lambda*term_dp_room/(beta-term_dp_room);
            % Step 2
            t_exh(i) = min(max(param_tem(sensit)-(param_tem(sensit)-
t_amb(i))*eta(i,1),0.5),param_tem(sensit));
            e_sat_exh(i) = alpha*exp(beta*t_exh(i)/(lambda
+t_exh(i))); % saturation vapour pressure
            x_exh(i,room) = min(x_sat_room,x_room(i,room));
            x_supply(i,room) = x_amb(i);
            % Step 3
            if (room == 1 || room == 2)
                ach_vent_ts(i,room) =
 ach_vent_ts(i,room) + (ach_vent_max_ts(room)-
ach_vent_min_ts(room))*min(1,max(rh_room(i,room)-rh_Pctrl_low,0)/
(rh_Pctrl_high-rh_Pctrl_low));
            end
            % Step 4
            x_room(i+1,room) =
 x_room(i,room)+x_add(i,room)+ach_vent_ts(i,room)*(x_supply(i,room)-
min(x_sat_room,x_room(i,room)))...
                +ach_inf_ts(1,room)*(x_amb(i)-
min(x_sat_room,x_room(i,room)));
        end
    end
    % Store data
    x_data(:,:,sensit,11,1) = x_room;
    rh_data(:,:,sensit,11,1) = rh_room;
    hr_above_limit_tem_rec(sensit,:) =
 (sum(rh_room(1:135*N_day,:)>rh_limit,1)...
        +sum(rh_room(258*N_day:end,:)>rh_limit,1))./6;
    pct_above_limit_tem_rec = hr_above_limit_tem_rec*100/(24*(365-
(258-135))); % only for heating season
end

% Whole-dwelling ventilation iterations
for sensit = 1:npar_tem
    ach_vent_ts = repmat(ach_vent_whole_min_ts,N_year,1);
    % Initial equations
    rh_room(1,:) = rh_room_init; % initial relative humidity, %
```

```
    e_room(1,:) = alpha*(rh_room(1,:)/100)*exp(beta*param_tem(sensit)/
(lambda+param_tem(sensit))); % vapour pressure, hPa
    x_room(1,:) = 621.98*e_room(1,:)./(press_atm-e_room(1,:)); % room
 moisture content after time step, g/kg
    % Calculate new saturation conditions
    e_sat_room = alpha*exp(beta*param_tem(sensit)/(lambda
+param_tem(sensit))); % saturation vapour pressure, hPa
    x_sat_room = 621.98*e_sat_room/(press_atm-e_sat_room); %
 saturation moiture content, g/kg
    % Iterations
    for i = 1:(N_year-1)
        % Step 1
        rh_room(i,room) = min(100*x_room(i,room)/x_sat_room,100);
        % Step 2
        x_mixed_dry(i) = sum(vol_room(3:5).*x_room(i,3:5))/
sum(vol_room(3:5));
        % Step 3
        for room = 1:2
            rh_room(i,room) = min(100*x_room(i,room)/x_sat_room,100);
            term_dp_room =
 log(rh_room(i,room)/100)+(beta*param_tem(sensit))/(lambda
+param_tem(sensit));
            dp_room(i,room) = lambda*term_dp_room/(beta-term_dp_room);

            ach_vent_ts(i,room) = ach_vent_ts(i,room) +
 (ach_vent_max_ts(room)-
ach_vent_whole_min_ts(room))*min(1,max(rh_room(i,room)-
rh_Pctrl_low,0)/(rh_Pctrl_high-rh_Pctrl_low));
            x_supply(i,room) = x_mixed_dry(i);
        end
        % Step 4
        t_exh(i) = min(max(param_tem(sensit)-(param_tem(sensit)-
t_amb(i))*eta(i,1),0.5),param_tem(sensit));
        e_sat_exh(i) = alpha*exp(beta*t_exh(i)/(lambda+t_exh(i))); %
 saturation vapour pressure
        x_mixed_wet(i) = sum(ach_vent_ts(i,1:2).*x_room(i,1:2))./
sum(ach_vent_ts(i,1:2));
        rh_mixed_wet(i) = min(100*x_mixed_wet(i)/x_sat_room,100);
        term_dp_room =
 log(rh_mixed_wet(i)/100)+(beta*param_tem(sensit))/(lambda
+param_tem(sensit));
        dp_mixed_wet(i) = lambda*term_dp_room/(beta-term_dp_room);
        x_mixed_exh(i) = min(x_sat_room,x_mixed_wet(i));
        % Step 5
        for room = 3:5
            rh_room(i,room) = min(100*x_room(i,room)/x_sat_room,100);
            x_supply(i,room) = x_amb(i);
            ach_vent_ts(i,room) = vol_room(room)./
sum(vol_room(3:5)).*sum(ach_vent_ts(i,1:2));
        end
        % Step 6
        for room = 1:nrooms
```

```
            x_room(i+1,room) =
 x_room(i,room)+x_add(i,room)+ach_vent_ts(i,room)*(x_supply(i,room)-
min(x_sat_room,x_room(i,room)))...
            +ach_inf_ts(1,room)*(x_amb(i)-
min(x_sat_room,x_room(i,room)));
        end
    end
    % Store data
    x_data(:,:,sensit,12,1) = x_room;
    rh_data(:,:,sensit,12,1) = rh_room;
    hr_above_limit_tem_ref_rec(sensit,:) =
 (sum(rh_room(1:135*N_day,:)...
        >rh_limit,1)+sum(rh_room(258*N_day:end,:)>rh_limit,1))./6;
    pct_above_limit_tem_ref_rec = hr_above_limit_tem_ref_rec*100/
(24*(365-(258-135))); % only for heating season
end

% Plots of results

% Regenerative only
figure;

subplot(2,3,1);
plot(repmat(param_inf(1,:),nrooms,1)',pct_above_limit_inf(:,1:5),...
    'LineWidth',2)
hold on, grid on
line([0.05 0.05],[0 100],'Linestyle','--','Color','k')
title('Single-room'),
axis([0.02 0.17 0 100])
ylabel('Duration >70% RH [%]')

subplot(2,3,2);
plot(repmat(param_eta(1,:),nrooms,1)',pct_above_limit_eta(:,1:5),...
    'LineWidth',2)
hold on, grid on
line([0.85 0.85],[0 100],'Linestyle','--','Color','k')
h = fill([0.8 0.8 1 1],[0 100 100 0],'g');
set(h,'facealpha',0.1)
title('Single-room'),
axis([0.7 0.94 0 100])

subplot(2,3,3);
plot(repmat(param_tem(1,:),nrooms,1)',pct_above_limit_tem(:,1:5),...
    'LineWidth',2)
hold on, grid on
line([22 22],[0 100],'Linestyle','--','Color','k')
title('Single-room'),
axis([17 26 0 100])

subplot(2,3,4);
plot(repmat(param_inf(1,:),nrooms,1)',...
    pct_above_limit_inf_ref(:,1:5),'LineWidth',2);
hold on, grid on
line([0.05 0.05],[0 100],'Linestyle','--','Color','k')
```

```
title('Whole Dwelling'),
axis([0.02 0.17 0 100])
xlabel('Infiltration [h^{-1}]'), ylabel('Duration >70% RH [%]')

subplot(2,3,5);
ax4 = plot(repmat(param_eta(1,:),nrooms,1)',...
    pct_above_limit_eta_ref(:,1:5),'LineWidth',2);
hold on, grid on
line([0.85 0.85],[0 100],'Linestyle','--','Color','k')
h = fill([0.8 0.8 1 1],[0 100 100 0],'g');
set(h,'facealpha',0.1)
title('Whole Dwelling'),
xlabel('Temperature Eff. [-]'),
axis([0.7 0.94 0 100])

subplot(2,3,6);
ax4 = plot(repmat(param_tem(1,:),nrooms,1)',...
    pct_above_limit_tem_ref(:,1:5),'LineWidth',2);
hold on, grid on
line([22 22],[0 100],'Linestyle','--','Color','k')
title('Whole Dwelling'),
xlabel('Room Temperature [^{\circ}C]'),
axis([17 26 0 100])
legend('Kitchen','Bathroom','Big Bedroom','Small Bedroom','Living
 Room','Orientation','Horizontal')

% Recuperative only
figure;

subplot(2,3,1);
plot(repmat(param_inf(1,:),nrooms,1)',...
    pct_above_limit_inf_rec(:,1:5),'LineWidth',2)
hold on, grid on
line([0.05 0.05],[0 100],'Linestyle','--','Color','k')
title('Single-room'),
axis([0.02 0.17 0 100])
ylabel('Duration >70% RH [%]')

subplot(2,3,2);
plot(repmat(param_eta(1,:),nrooms,1)',...
    pct_above_limit_eta_rec(:,1:5),'LineWidth',2)
hold on, grid on
line([0.85 0.85],[0 100],'Linestyle','--','Color','k')
h = fill([0.8 0.8 1 1],[0 100 100 0],'g');
set(h,'facealpha',0.1)
title('Single-room'),
axis([0.7 0.94 0 100])

subplot(2,3,3);
plot(repmat(param_tem(1,:),nrooms,1)',...
    pct_above_limit_tem_rec(:,1:5),'LineWidth',2)
hold on, grid on
line([22 22],[0 100],'Linestyle','--','Color','k')
title('Single-room'),
```

```
axis([17 26 0 100])

s4 = subplot(2,3,4);
plot(repmat(param_inf(1,:),nrooms,1)',...
    pct_above_limit_inf_ref_rec(:,1:5),'LineWidth',2);
hold on, grid on
line([0.05 0.05],[0 100],'Linestyle','--','Color','k')
title('Whole Dwelling'),
axis([0.02 0.17 0 100])
xlabel('Infiltration [h^{-1}]'), ylabel('Duration >70% RH [%]')

s5 = subplot(2,3,5);
ax4 = plot(repmat(param_eta(1,:),nrooms,1)',...
    pct_above_limit_eta_ref_rec(:,1:5),'LineWidth',2);
hold on, grid on
line([0.85 0.85],[0 100],'Linestyle','--','Color','k')
h = fill([0.8 0.8 1 1],[0 100 100 0],'g');
set(h,'facealpha',0.1)
title('Whole Dwelling'),
xlabel('Temperature Eff. [-]'),
axis([0.7 0.94 0 100])

s6 = subplot(2,3,6);
ax4 = plot(repmat(param_tem(1,:),nrooms,1)',...
    pct_above_limit_tem_ref_rec(:,1:5),'LineWidth',2);
hold on, grid on
line([22 22],[0 100],'Linestyle','--','Color','k')
title('Whole Dwelling'),
xlabel('Room Temperature [^{\circ}C]'),
axis([17 26 0 100])


% ASHRAE 160 Evaluation - Testing only the nominal case for faster
% calculations

% limits = [99.99 89 80]-10;
lim_span = [1 7 30];
ma_rh_data = zeros(N_year,nrooms,4,3);
min_ma_rh_data = zeros(nrooms,4,3);
max_ma_rh_data = zeros(nrooms,4,3);
% test_ma_rh_data = false(nrooms-1,npar,nsim,nlim);

for lim = 1:3
    for sim = 1:4
        par = 4;
        for room = 1:(nrooms)
            ma_rh_data(:,room,sim,lim) =
 smooth(rh_data(:,room,par,sim,1)...
                ,lim_span(lim)*24*6);
            max_ma_rh_data(room,sim,lim) = ...

 max(max(ma_rh_data(10*N_day:135*N_day,room,sim,lim)),...
                max(ma_rh_data(258*N_day:355*N_day-1,room,sim,lim)));
            min_ma_rh_data(room,sim,lim) = ...
```

```
 min(min(ma_rh_data(10*N_day:135*N_day,room,sim,lim)),...
                min(ma_rh_data(258*N_day:355*N_day-2,room,sim,lim)));
%           test_ma_rh_data(room,par,sim,lim) = ...
%
 or(any(ma_rh_data(1*N_day:135*N_day,room,par,sim,lim)>=...
%
 limits(lim),1),any(ma_rh_data(258*N_day:365*N_day-1,...
%               room,par,sim,lim)>=limits(lim),1));
        end
    end
end

% ASHRAE 160 Evaluation for all parameter variations (for reference)

% % limits = [99.99 89 80]-10;
% lim_span = [1 7 30];
% ma_rh_data = zeros(N_year,nrooms-1,npar,nsim);
% min_ma_rh_data = zeros(nrooms,npar,nsim);
% max_ma_rh_data = zeros(nrooms,npar,nsim);
% test_ma_rh_data = false(nrooms,npar,nsim,nlim);
%
% for lim = 1:nlim
% for sim = 1:nsim
% for par = 1:npar
% for room = 1:nrooms
% ma_rh_data(:,room,par,sim) = ...
%   smooth(rh_data(:,room,par,sim,1),lim_span(lim)*24*6);
% max_ma_rh_data(room,par,sim) = ...
%   max(max(ma_rh_data(10*N_day:135*N_day,room,par,sim)),...
%   max(ma_rh_data(258*N_day:355*N_day-1,room,par,sim)));
% min_ma_rh_data(room,par,sim) = ...
%   min(min(ma_rh_data(10*N_day:135*N_day,room,par,sim)),...
%   min(ma_rh_data(258*N_day:355*N_day-2,room,par,sim)));
% test_ma_rh_data(room,par,sim,lim) = ...
%     or(any(ma_rh_data(1*N_day:135*N_day,room,par,sim,...
%     lim)>=limits(lim),1),any(ma_rh_data(258*N_day:...
%     365*N_day-1,room,par,sim,lim)>=limits(lim),1));
% end
% end
% end
% end

% Cumulative Distribution Plots

% Heating Season
figure;
for i=1:5
cdfplot(rh_data([1:135*N_day 258*N_day:end],i,4,1,1))
hold on
end
title('Heating Season Cumulative Distribution'),
xlabel('Relative Humidity [%]'), ylabel('Fraction below [-]')
```

```
% legend('Kitchen','Bathroom','Big Bedroom','Small Bedroom','Living
 Room','Orientation','Horizontal')

% November 1st to March 31st
figure;
for i=1:5
cdfplot(rh_data([1:90*N_day (304*N_day+1):end],i,4,1,1))
hold on
end
title('Nov-Mar Cumulative Distribution'),
xlabel('Relative Humidity [%]'), ylabel('Fraction below [-]')
axis([10 100 0 1])
% legend('Kitchen','Bathroom','Big Bedroom','Small Bedroom','Living
 Room','Orientation','Horizontal')

% October
figure;
for i=1:5
cdfplot(rh_data(273*N_day:304*N_day,i,4,1,1))
hold on
end
title('October Cumulative Distribution'),
xlabel('Relative Humidity [%]'), ylabel('Fraction below [-]')
axis([10 100 0 1])
% legend('Kitchen','Bathroom','Big Bedroom','Small Bedroom','Living
 Room','Orientation','Horizontal')

% January
figure;
for i=1:5
cdfplot(rh_data(1:31*N_day,i,4,1,1))
hold on
end
title('January Cumulative Distribution'),
xlabel('Relative Humidity [%]'), ylabel('Fraction below [-]')
% legend('Kitchen','Bathroom','Big Bedroom','Small Bedroom','Living
 Room','Orientation','Horizontal')

% April
figure;
for i=1:5
cdfplot(rh_data(90*N_day:120*N_day,i,4,1,1))
hold on
end
title('April Cumulative Distribution'),
xlabel('Relative Humidity [%]'), ylabel('Fraction below [-]')
% legend('Kitchen','Bathroom','Big Bedroom','Small Bedroom','Living
 Room','Orientation','Horizontal')
```

Published with MATLAB® R2015a

Dette forskningsprojekt udviklede og analyserede to enkeltrums ventilationsenheder. Den ene med en ny kort roterende plastik varmeveksler, den anden med en ny oprullet spiral modstrøms varmeveksler af plastik folie. Nærværende afhandling har inkluderet teori, litteratur, design kriterier, hurtig udvikling af prototyper samt simuleringer for succesfuldt at kunne udvikle og analysere enkeltrumsventilation med varmegenvinding og behovstyring.

DTU Civil Engineering
Technical University of Denmark

Brovej, Bygning 118
2800 Kongens Lyngby

www.byg.dtu.dk

ISBN 9788778774286
ISSN 1601-2917